

Investigation of New Mild Routes to Substituted and Unsubstituted 1,2-Cycloheptadienes and Their Trapping Reactions

by

Yaseen Ahmed Almeahmadi

A thesis submitted in partial fulfillment of the requirements for the degree of

Master of Science

Department of Chemistry
University of Alberta

© Yaseen Ahmed Almeahmadi, 2019

Abstract

Strained cyclic allenes are one of many reactive intermediates. They are rare and underutilized chemical species, and their use in the formation of strategic bonds in organic chemistry is limited. Strained cyclic allenes have a unique reactivity that allows useful bond-forming processes to be feasible under mild reaction conditions. In this thesis, I dedicated my time and knowledge to investigate the synthetic potential of these strained, reactive intermediates. We took advantage of the unique reactivity of cyclic allenes to synthesize heterocyclic compounds.

Chapter 1 provides fundamentals of strained intermediates, especially cyclic allenes. It also presents the most recent advances in the field of strained cyclic allenes whose rings contain eight atoms or fewer. The potential of these reactive species to provide access to useful complex scaffolds in a single step from readily available precursors is discussed.

Chapter 2 focuses on seven-membered cyclic allenes. 1,2-Cycloheptadiene has been far less-studied when compared to 1,2-cyclohexadienes and six-membered-ring heterocyclic allenes. Medium ring cyclic allenes, composed of seven or eight atoms, are known to undergo rapid dimerization once generated. I report the first trapping processes of 1,2-cycloheptadiene with 1,3-dipoles via mild conditions. These allenes have been generated via a fluoride-mediated desilylative elimination, as reported previously by our group and others. Moreover, I proposed one of the shortest approaches to access seven-membered cyclic allenes from feasible starting materials by a well-established chemistry. This approach tolerates several 1,3-dipolar trapping partners, such as nitrile oxides, nitrones, and

azomethine imines, allowing rapid access to fused heterocyclic compounds with high regioselectivity and diastereoselectivity.

Chapter 3 investigates a new approach through the metal–halogen exchange reactions to generate six-, seven-, and eight-membered cyclic allenes. We also examined the trapping process of this new generation. Using this new method, we successfully isolated several cycloadducts with good yields. The advantage of this approach is that readily available precursors are used and can be accessed on a large scale.

Preface

Chapter 2 of this thesis will be published as Almehmadi, Y. A.; West, F. G., “A Mild Method for the Generation and Trapping of 1,2-Cycloheptadiene with 1,3-Dipoles”; this manuscript is in preparation. I was responsible for all the experimental work, data collection, and characterization of the compounds, as well as the manuscript preparation and data analysis. F. G. West was my supervisor and corresponding author, who contributed to the project planning and guidance for the manuscript contents.

Chapter 3 of this thesis will be published as Almehmadi, Y. A.; Constantin, M. G.; Liu, X.; Soueidan, O. M.; West, F. G., “Generation of Reactive Cyclic Allenes Through Metal-Halogen Exchange Promoted Elimination”; this manuscript is in preparation. M. G. Constantin and I contributed equally to this work, and we were responsible for all the experimental work, data collection, and characterization of the compounds. M. G. Constantin and I were responsible for the manuscript preparation and data analysis. F. G. West was my supervisor and corresponding author, who contributed to the project planning and guidance for the manuscript contents.

Acknowledgements

I would like to begin by expressing my sincere gratitude to my supervisor, Dr. F. G. West, for his endless patience, guidance, support, and mentorship. I also would like to thank you for accommodating me in your lab and for the freedom you gave me to manage my project; this influenced my way of thinking and self-confidence during my graduate studies. Without your support, I would not be here today, defending my thesis for a master's degree. I cannot thank you enough as you are the one who has been always here for me to get support from and to ask for advice regarding science and personal life.

I am truly thankful to my Supervisory Committee Members, Dr. John Vederas and Dr. Rylan Lundgren, for their support and willingness to help during my graduate studies. I am also grateful to Dr. Derrick Clive for his time and willingness to be my arm's length examiner. These people have been selected to examine each facet of my dissertation and broad knowledge in the discipline. For that, I would like to express my deepest sincere appreciation to them.

I would like to thank the current and previous members of the West group for creating such a fantastic environment to conduct research. Working with current and former group members was a great pleasure for me, and I have learnt so many things from you all, not only in chemistry but also about your amazing cultures. I will always remember all of you (Ahmed Oraby, Marius, Shorena Marwa, Kyle, Natasha, Xinghai, James, Jenny, Luna, Tom, Yury, Claudia, Shaohui, Maxwell, Peter). I want to single out two people who helped me the most, not only in chemistry but also during my stay in Edmonton from the start. Firstly, I am very grateful to my mentor, Dr. Olivier Soueidan, (and his amazing family) who taught me so many things (I cannot even count). Secondly, I am thankful to my spiritual brother, Ahmed Elmenoufy, for all the support and help he offered me. You are seriously a couple of the best people I have met at the University of Alberta. From outside the university, I would like to acknowledge my close friends, Rizwan Jehee and Britney Jennison, for their endless support and help.

I am also very thankful to the staff members of the NMR, IR, Mass Spectroscopy facility labs, and X-ray services. Many thanks also go to the staff members of the glass and

machine shops. My research would not have been possible without your support. I am also grateful to Dr. Anna D. Jordan for reading my thesis and providing me with her valuable feedback and comments. All these people deserve my special gratitude for their readiness to help and for their time. Thank you very much to every single one of you for being so approachable.

I am also grateful to the Department of Chemistry, Rabigh–College of Science and Arts at King Abdulaziz University and the Saudi Cultural Bureau in Ottawa for the very generous postgraduate scholarship during my MSc studies. I am greatly indebted to all the chemistry staff at my university back home, especially to my undergraduate mentors, Dr. Mohamed Elhefnawy and Dr. Abdulmuniem Elmasry. I also would like to express my profound gratitude to Dr. Mohamed Aljahdali, former Dean of Rabigh–College of Science and Arts for his encouragement and strong support during and after my undergraduate studies.

Last but not least, words cannot express how grateful and thankful I am to my family and friends. My special thanks go to my beloved mother and father, as well as my sisters and brothers. These people always have encouraged and supported me during my studies, and I would like to thank them for being there, not only in the good times but also in the difficult moments. Without their never-ending support, unlimited love, and care, I would not have been able to accomplish what I have achieved today. In fact, I would like to dedicate this thesis to my beloved family.

Table of Contents

1. Introduction to The Generation, Trapping and Mechanism of Strained Cyclic Allenes	1
1.1. Why Reactive Intermediates?	1
1.2. Sources of Strain in Small Rings.....	1
1.2.1. Strained Cyclic Alkynes	3
1.2.2. Benzyne and Pyridynes	5
1.3. Cyclic Allenes	7
1.3.1. Dimerization and Trapping Reactions of Cyclic Allenes in Comparison to Cyclic Alkynes	8
1.4. Three-, Four-, and Five-Membered Cyclic Allenes	11
1.5. Six-Membered Cyclic Allenes	14
1.5.1. 1,2-Cyclohexadienes.....	14
1.5.2. Azacyclic Allene 101 and Oxacyclic allene 102	19
1.5.3. Intramolecular Trapping of 1,2-Cyclohexadienes	21
1.6. Seven-Membered Cyclic Allenes	24
1.7. Eight-Membered Cyclic Allenes	26
1.8. Conclusions and Thesis Objective	27
1.9. References:.....	29
2. A Mild Method for the Generation and Intermolecular Trapping of 1,2-Cycloheptadiene with 1,3-Dipoles.....	32
2.1. 1,3-Dipolar Cycloadditions	32
2.2. Reactions of Acyclic Allenes with 1,3-Dipoles	32
2.3. Background and Experimental Design.....	34
2.4. Results and Discussion.....	36

2.5. Conclusion.....	47
2.6. Future Directions.....	48
2.7. Experimental and General Information.....	50
2.8. References.....	69
3. A Novel Method for the Generation of Reactive Cyclic Allenes via Metal–Halogen Exchange Promoted Elimination.....	71
3.1. Background.....	71
3.2. Results and Discussion.....	73
3.3. Conclusion.....	85
3.4. Future Directions.....	86
3.5. Experimental and General Information.....	87
3.6. References.....	91
Compiled References.....	92
Appendix I: Selected NMR Spectra.....	97
Appendix II: X-ray Crystallographic Data for Compound 25 (Chapter 2).....	150
Appendix III: X-ray Crystallographic Data for Compound 27 (Chapter 2).....	163
Appendix IV: X-ray Crystallographic Data for Compound 38a (Chapter 2).....	178
Appendix V: X-ray Crystallographic Data for Compound 39 (Chapter 2).....	191

List of Figures

Chapter 1

- Figure 1.1. General structures of strained cyclic intermediates..... 1
- Figure 1.2. Possible regio- and diastereoselectivities of the reaction between six-membered cyclic allene and nitrones..... 18
- Figure 1.3. Proposed mechanism of cycloaddition reaction of cyclic allene with nitrene 1,3-dipole..... 18

Chapter 2

- Figure 2.1. Possible regiochemical outcomes associated with 1,3-dipolar cycloaddition of acyclic allenes. 33
- Figure 2.2. Generalized examples of strained cyclic intermediates..... 34
- Figure 2.3. X-ray crystal structure of **25**..... 37
- Figure 2.4. X-ray crystal structure of the endo cycloadduct **27**..... 38
- Figure 2.5. X-ray crystal structure of the endo cycloadduct **38a** and TROESY correlations strongly suggesting the relative stereochemistry of cycloadduct **38a**..... 43
- Figure 2.6. X-ray crystal structure of **39**..... 44
- Figure 2.7. TROESY correlations strongly suggesting the relative stereochemistry of cycloadduct **41**. 45

List of Tables

Chapter 3

Table 3.1. Optimization of the Dimerization Process of 1,2-Cyclohexadiene Using Li–Br Exchange Promoted Elimination. ^[a]	77
Table 3.2. Optimization of Trapping Six-membered Cyclic Allene with Furan. ^[a]	81
Table 3.3. Isolated Yields of 1,2-Cyclohexadiene Cycloadducts Using Several Conditions at 1 mmol scale.	82

List of Schemes

Chapter 1

Scheme 1.1. Examples of useful epoxide reactions.	2
Scheme 1.2. Common approach to generate strained cyclic alkynes.	3
Scheme 1.3. Application of a strained cyclic system to the in vivo labeling of cellular structure.....	4
Scheme 1.4. Examples of strained cyclic alkynes in total synthesis.....	5
Scheme 1.5. Common approaches to generate benzyne.....	6
Scheme 1.6. Examples of strained benzyne and pyridynes in total synthesis.	7
Scheme 1.7. Trimerization and dimerization of cyclohexyne and 1,2-cyclohexadiene.	9
Scheme 1.8. Interception of the dimerization process of cyclic allenes by nitroxide radicals.	9
Scheme 1.9. Temperature effects on the dimerization processes of cyclic allenes.	10
Scheme 1.10. Trapping reactions of cyclohexyne and 1,2-cyclohexadiene with DPIBF.	11
Scheme 1.11. Photochemical isomerization of conjugated enynes believed to proceed through 1,2-cyclobutadiene intermediates.	12
Scheme 1.12. Synthesis of four-membered-ring allene 62 and its stabilization by coordination to the rhodium complex.	12
Scheme 1.13. First evidence for generation of a 1,2-cyclopentadiene via DMS method.	13
Scheme 1.14. Known generations and trapping processes of 1,2-cyclohexadienes in [2+2] and [4+2] fashion.	15
Scheme 1.15. Synthesis of allenes 83 and 84 and their [4+2] cycloaddition with DPIBF by Quintana et al.	16
Scheme 1.16. Trapping reactions of 1,2-cyclohexadienes with 1,3-dipoles.....	17

Scheme 1.17. DMS reactions to generate six-membered heterocyclic allenes.....	19
Scheme 1.18. Route to synthesis substituted and unsubstituted cyclic allene (101 , 102 , and 121) precursors.....	20
Scheme 1.19. Trapping reactions of six-membered heterocyclic allenes with several trapping partners.	21
Scheme 1.20. Strategies to trap cyclic allenes intramolecularly.....	22
Scheme 1.21. Synthesis of allylic silanes 139 and 141	23
Scheme 1.22. Tethered allene and its intramolecular Diels-Alder trapping.	24
Scheme 1.23. Known methods to generate seven-membered cyclic allenes.....	25
Scheme 1.24. Efforts to generate substituted and unsubstituted 1,2-cycloheptadienes via DMS rearrangement.....	26
Scheme 1.25. Known generation, dimerization, and trapping processes of 1,2-cyclooctadiene in [4+2] cycloaddition with DPIBF.	27
Scheme 1.26. Isolation of 1,2-cyclooctadienes.....	27
 Chapter 2	
Scheme 2.1. [3+2] Cycloaddition of nitrile oxide and acyclic allene.....	34
Scheme 2.2. Retrosynthesis of 1,2-cycloheptadiene precursors.	35
Scheme 2.3. Synthesis of acetoxy-substituted 1,2-cycloheptadiene precursor.....	36
Scheme 2.4. Dimerization process of acetoxy-substituted 1,2-cycloheptadiene 23 and hydrolysis of dimer 24 to diketone 25	36
Scheme 2.5. [4+2] Cycloaddition of 1-acetoxy-1,2-cycloheptadiene with DPIBF.	37
Scheme 2.6. a. Possible regiochemical outcomes of the reaction between allene 23 and 1,3-Dipoles. b. Proposed Mechanisms.	40
Scheme 2.7. Reaction of cyclic allene 23 with nitrile oxide 35	41

Scheme 2.8. Trapping processes of cyclic allene 23 with azomethine imines. ^[a] the reaction was run at room temperature.....	42
Scheme 2.9. Hydrolysis of the acetate of cycloadduct 38a to ketone 39	43
Scheme 2.10. Reaction of cyclic allene 23 with nitrene 40	45
Scheme 2.11. Attempts to synthesize allylic silane 45	46
Scheme 2.12. Synthesis of precursor 45 to generate unsubstituted 1,2-cycloheptadiene.....	46
Scheme 2.13. Dimerization process of unsubstituted cyclic allene 16 and trapping process with azomethine imine 37a	47
Scheme 2.14. Proposed synthesis of monosubstituted 1,2-cycloheptadienes.....	49
Scheme 2.15. Possible intramolecular trapping of cyclic allenes with azide.	50
 Chapter 3	
Scheme 3.1. The most commonly used methods to generate cyclic allenes.....	72
Scheme 3.2. Unexpected dimerization process.....	74
Scheme 3.3. Ichikawa's work and proposed generation of cyclic allenes.	75
Scheme 3.4. General route to synthesis of allylic esters 29a–d	75
Scheme 3.5. Synthesis of seven- and eight-membered ring carbonates 36 and 37	78
Scheme 3.6. Dimerization of 1,2-cycloheptadiene 9 and 1,2-cyclooctadiene 10	78
Scheme 3.7. Synthesis of allylic iodo-carbonates 42 and 43	79
Scheme 3.8. Dimerization processes of strained cyclic allenes 4 and 5 generated via magnesium–halogen exchange reactions.	80
Scheme 3.9. Dimerization and trapping reactions of six-membered cyclic allene 4 via magnesium–halogen exchange promoted elimination. ^[a] It was necessary to run the reaction at rt to obtain optimized yields.....	83
Scheme 3.10. Undesired reaction between <i>i</i> -PrMgCl and the 1,3-dipole 45	84

Scheme 3.11. Dimerization and attempted trapping reactions of seven-membered cyclic allene via magnesium–halogen exchange promoted elimination. [a] It was necessary to run the reaction at rt to obtain optimized yields.	85
Scheme 3.12. Possible generation of cyclic allenes via vinyl tin reagents with allylic carbonate.	86

List of Symbols and Abbreviations

^1H	proton
Ac	acetyl
Ac_2O	acetic anhydride
CH_3CN	acetonitrile
app.	apparent (spectral)
aq	aqueous solution
Ar	aryl
DPIBF	1,3-diphenylisobenzofuran
Bn	benzyl
Boc	<i>tert</i> -butyloxycarbonyl
Br	broad (spectral)
<i>n</i> -Bu	butyl
Calcd	calculated
cm^{-1}	wave numbers
COSY	H-H correlation spectroscopy
TESCl	chlorotriethylsilane
conc.	concentrated
d	day(s); doublet (spectral)
DFT	density functional theory
DABCO	1,4-diazabicyclo[2.2.2]octane
DCM	dichloromethane
DPIBF	1,3-diphenylisobenzofuran
DMS	Doering–Moore–Skattebøl
dd	doublet of doublets (spectral)
ddd	doublet of doublets of doublets (spectral)
dddd	doublet of doublets of doublets of doublets (spectral)
DMAP	4-dimethylamino pyridine
DMSO	dimethyl sulfoxide

de	diastereomeric excess
dq	doublet of quartets (spectral)
d.r.	diastereomeric ratio
dt	doublet of triplets (spectral)
EDG	electron-donating group
ee	enantiomeric excess
EI	electron impact (mass spectrometry)
<i>endo</i>	endocyclic
equiv	equivalent(s)
e.r.	enantiomeric ratio
ESI	electrospray ionization (mass spectrometry)
Et	ethyl
EtOAc	ethyl acetate
EWG	electron-withdrawing group
<i>exo</i>	exocyclic
FT-IR	Fourier-transform infrared spectroscopy
HMBC	heteronuclear multiple bond coherence (spectral)
HOMO	highest occupied molecular orbital
HSQC	heteronuclear single quantum coherence (spectral)
HRMS	high resolution mass spectrometry
<i>hν</i>	light
<i>i</i> -Bu	isobutyl
<i>i</i> -Pr	isopropyl
<i>J</i>	coupling constant
L	liter(s); unspecified ligand
LDA	lithium diisopropylamide
LUMO	lowest unoccupied molecular orbital
m	multiplet (spectral)
M ⁺	molecular ion
Me	methyl
MHz	megahertz

mp	melting point
MS	molecular sieves
Ms	methanesulfonyl
m/z	mass to charge ratio
nm	nanometer(s)
NMR	nuclear magnetic resonance
NOE	nuclear Overhauser enhancement
<i>n</i> -Pr	propyl
Ph	phenyl
ppm	parts per million
Py	pyridine
q	quartet (spectral)
qt	quartet of triplet
quint	quintet
R	generalized alkyl group of substituents
R_f	retention factor (in chromatography)
rt	room temperature
s	singlet (spectral)
SM	starting material
S_N	nucleophilic substitution
t	triplet (spectral)
T	temperature
<i>t</i> -Bu	<i>tert</i> -butyl
tet	tetrahedral
Tf	trifluoromethanesulfonyl
THF	tetrahydrofuran
TLC	thin layer chromatography
TMS	trimethylsilyl
Tq	triplet of quartet
TROESY	transverse rotating-frame overhauser enhancement spectroscopy
Ts	<i>p</i> -toluenesulfonyl

p-TsOH (pTSA)	<i>p</i> -toluenesulfonic acid
UV	ultraviolet light
wt.	weight
δ	chemical shift
λ	wavelength

Chapter 1

Introduction to the Generation, Trapping and Mechanism of Strained Cyclic Allenes

1.1. Why Reactive Intermediates?

Reactive intermediates are short-lived species, which are generated in reactions and react rapidly with other species or with themselves. These intermediates have been an interesting area of study for organic chemists and have been used to afford significant transformations.¹ For instance, they have been used to form carbon–carbon, carbon–nitrogen, carbon–oxygen bonds. Moreover, there are mainly two types of reactive intermediates, and each type gains its reactivity from its source of instability. The reactivity of the first type, which includes cations, radicals, and carbenes, is driven by the fact that all these classes of compounds have an incomplete valence shell of electrons. The second type of reactive intermediates, which this thesis will be focusing on, obtain their reactivity from the non-ideal bond angles in cyclic systems that would result in strain, including hetarynes, benzyne, cyclic alkynes, and cyclic allenes (Figure 1.1).

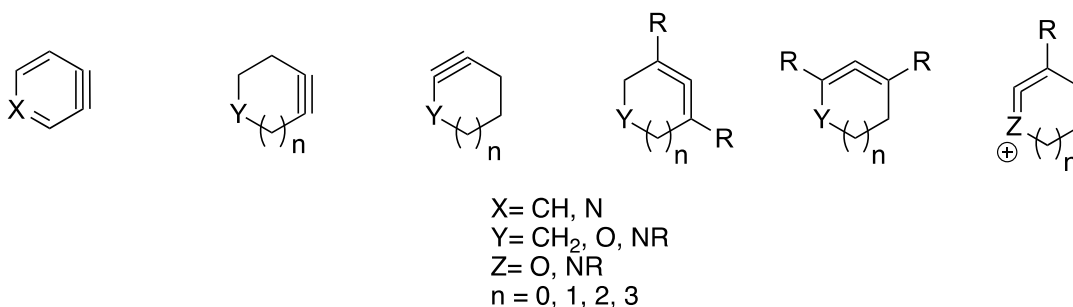
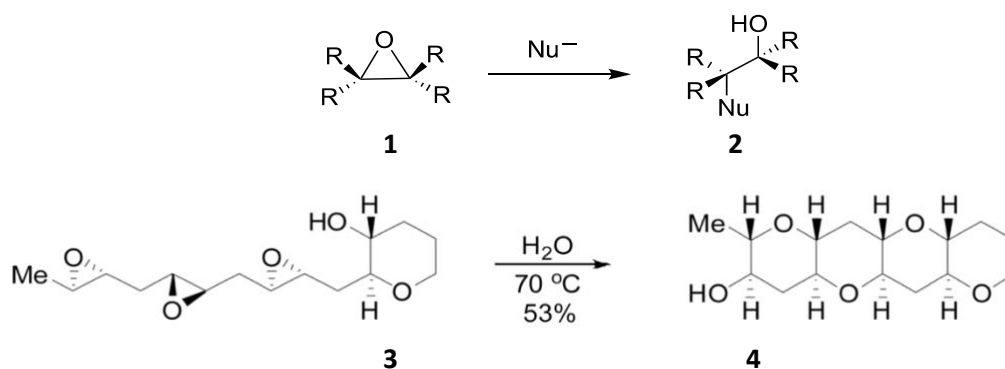


Figure 1.1. General structures of strained cyclic intermediates.

1.2. Sources of Strain in Small Rings

Based on the valence shell electron pair repulsion (VSEPR) theory, the ideal bond angles of sp^3 , sp^2 , and sp hybridized carbons are approximately 109.5, 120, and 180°, respectively.² One method to introduce strain and, therefore, reactivity into a cyclic system is by changing

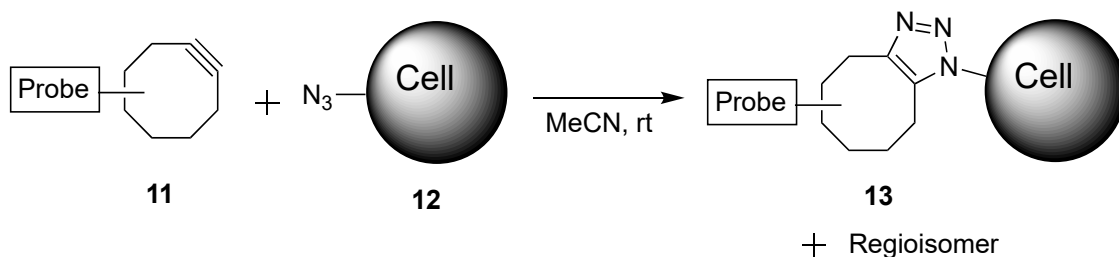
the bond angles of these atoms. For example, a *trans* alkene can be used to introduce strain when incorporated into small-size rings, fewer than eight atoms, or when an olefin is placed on a bridgehead position in a bridged small-ring system. This empirical observation is known among organic chemists as Bredt's rule, which states that placing a double bond at a bridgehead of a bridged cyclic system is not favorable and results in introducing strain as the system would be equivalent to having a *trans* alkene on a small ring, fewer than eight atoms.³ Another method to introduce strain is by decreasing the size of the ring, which forces the system to rehybridize and results in a system with non-ideal angles. For instance, in the case of cyclopropane, the p-orbitals of the carbons are overlapped due to constrained angles, as postulated by Walsh.⁴ It also has been shown that as a result of the strain in cyclopropane, the protons in this system are more acidic compared with a normal sp^3 system and the length of the carbon–hydrogen bonds are shortened because of the increase in s-character. An additional example of a strained system is epoxide **1**. The opening of an epoxide with a variety of nucleophiles under mild conditions has been used for decades among the scientific community, as shown in Scheme 1.1.⁵ The driving force of these reactions is the release of strain from the system. These strained classes of compounds also have been used in many total syntheses,⁶⁻⁷ such as in the synthesis of subunit **4** found in polyether natural products.⁴



Scheme 1.1. Examples of useful epoxide reactions.

There are many other strained cyclic systems known in the chemical literature. In this Chapter, I will concentrate on providing a brief overview of strained unsaturated cyclic compounds, first with benzyne and cyclic alkynes, focusing on their generation and

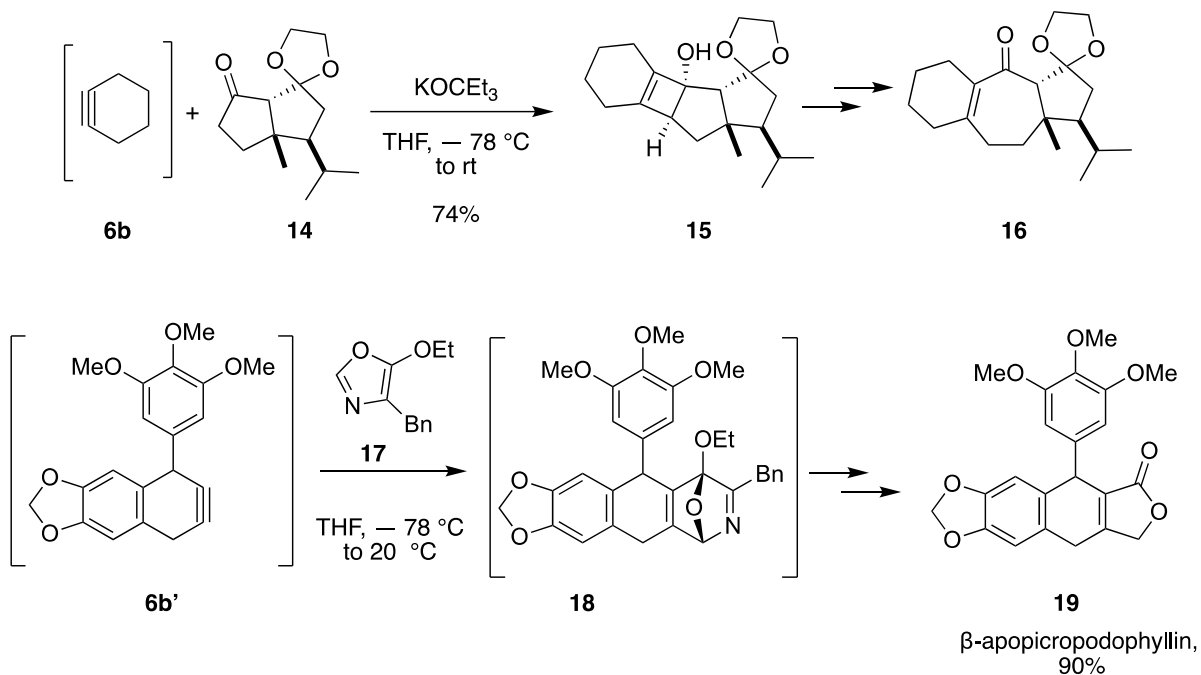
reactivity and trapping processes,^{6,9-10} and a recent computational study showed that the angle of cycloptyne is bent to 116° instead of 180°. ¹¹ Moreover, in 1957, the existence of cyclohexyne **6b** was reported first by Roberts,¹² followed by further studies by Caubere and Gross to examine the reactivity and trapping processes of **6b**.^{6, 13-14} Cyclooctyne **6d** is a reactive compound for the same reason as well, but it can be isolated. In 1960, Wittig illustrated that cyclic alkyne **6d** can undergo cycloaddition with 1,3-diphenylisobenzofuran (DPBF).¹⁵ A year later, Wittig¹⁶ and Huisgen^{17,18} reported that a strained alkyne can undergo [3+2]cycloaddition with azide. In the development of “click” reactions,¹⁹ Bertozzi and coworkers developed a very mild condition to perform the cycloaddition of azide with strained alkyne **6d** and applied this method in vivo labeling of cellular structures,^{20, 21} as shown in Scheme 1.3.



Scheme 1.3. Application of a strained cyclic system to the in vivo labeling of cellular structure.

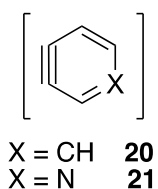
Within the context of the useful applications of strained cyclic alkynes, intermediate **6b** was used by Carreira and his coworkers as a key intermediate in the total synthesis of guanacastapenes N and O.²² They took advantage of the reactive intermediate to perform [2+2] cycloaddition of **6b** to the enolate form of **14**. This resulted in the formation of strained cyclobutanol **16**, which can undergo ring opening to give larger rings in the presence of a Lewis base or acid, resulting in the formation of **17**, which is a key precursor in the synthesis of guanacastapenes N and O (Scheme 1.4).²³ Moreover, in 2018, Park and coworkers showed another useful application of **6b**, which was used in the synthesis of β -apopicropodophyllin, an anticancer compound with activity against non-small cell lung cancer cells with IC₅₀ values of 16.9, 13.1, and 17.1 nM.²⁴ They successfully made cyclic alkyne **6d'** and trapped it with **17** to form reactive intermediate **18**.²⁵ This intermediate can eliminate benzonitrile to

give the corresponding substituted furan, which can be transferred to furanone **19** upon treatment with aqueous HBr (Scheme 1.4).²⁴



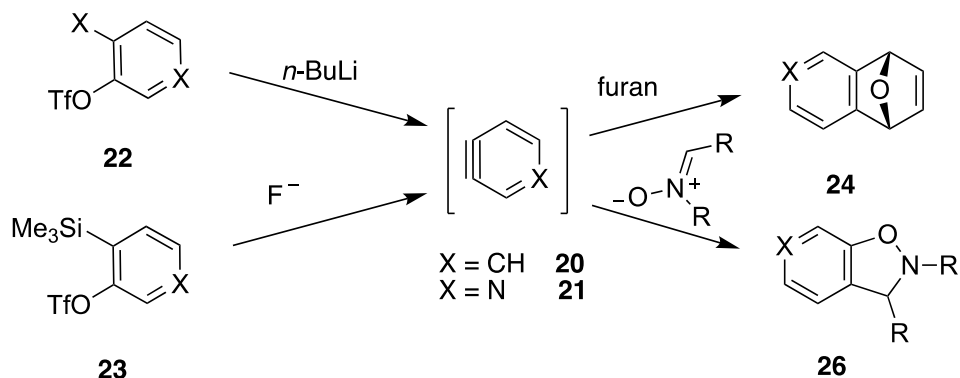
Scheme 1.4. Examples of strained cyclic alkynes in total synthesis.

1.2.2. Benzyne and Pyridynes



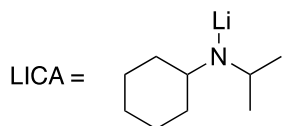
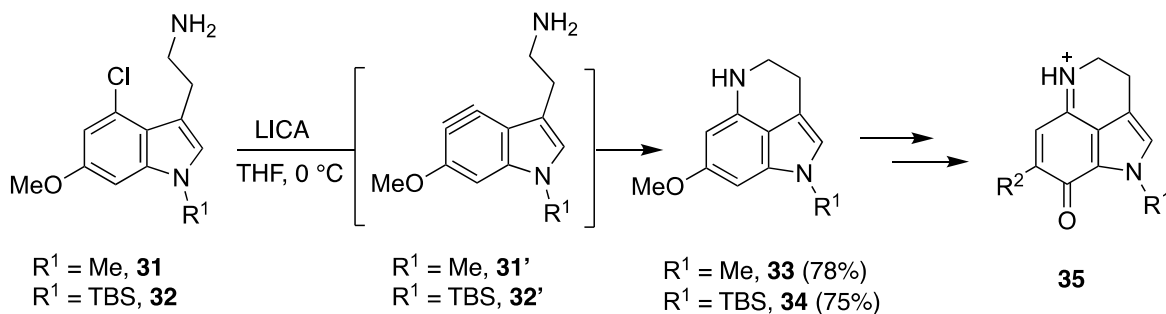
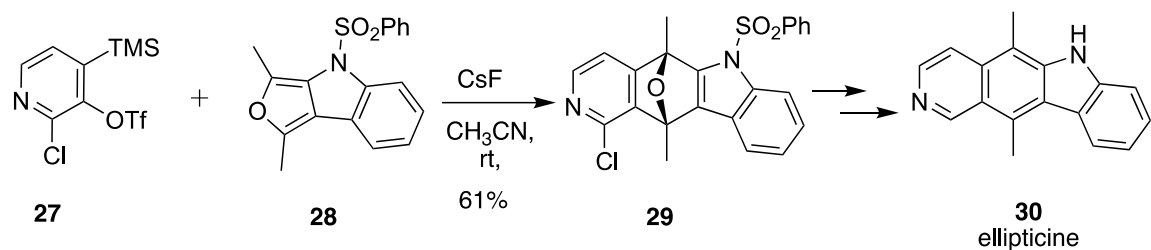
The structure of the reactive intermediate aryne **20** was proposed first by Roberts in 1953.²⁶ This important class of highly reactive compounds and their substituted derivatives has intrigued the scientific community for decades. Moreover, a computational study showed that 1,2-pyridyne and 2,3-pyridyne are less favourable than 3,4-pyridyne **21**²⁷ due to the introduction of great distortions when the triple bond is closer to N. This class of compounds has been shown to create interesting transformations once generated. They have, for example, been used to form carbon–carbon, carbon–nitrogen, and carbon–oxygen bonds.²⁷

There are several methods used to generate and trap this class of useful intermediates, as shown in Scheme 1.5.



Scheme 1.5. Common approaches to generate benzyne.

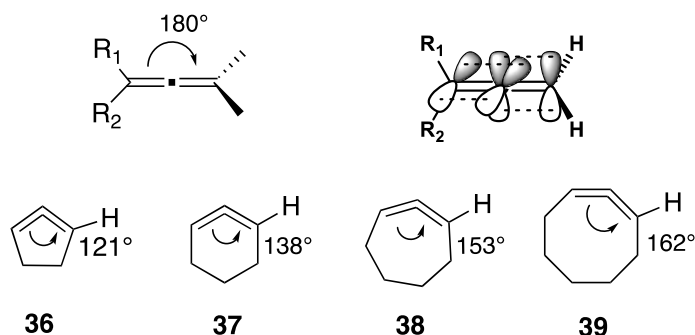
Benzyne and 3,4-pyridynes also have been used in the total synthesis of natural products and bioactive compounds. Guitián and coworkers showed an application of **21** when they used it in the synthesis of ellipticine **30** (Scheme 1.6), which had been investigated previously by several groups.^{28, 29} They treated **27** with CsF in the presence of **28**, resulting in the [4+2] cycloaddition product **29** with the desired regioisomer as the major product.³⁰ Moreover, another application of this reactive intermediate was showcased in the total synthesis reported by Iwao and his coworkers in 1998 when they produced makaluvamines A, I, K, and D (**35a–d**).³¹ They used 4,5-indolyne **31'** and **32'** derived from **31** and **32** as a key step in the synthesis of these compounds. After the formation of 4,5-indolyne **31'** and **32'**, as shown in Scheme 1.6, intramolecular nucleophilic addition of the primary amine formed **33** and **34**, which are key precursors in the synthesis of makaluvamines A, I, K, and D (**35a–d**).



- 35a**, $\text{R}^1 = \text{Me, R}^2 = \text{NH}_2$ (makaluvamine A)
35b, $\text{R}^1 = \text{H, R}^2 = \text{NH}_2$ (makaluvamine I)
35c, $\text{R}^1 = \text{Me, R}^2 = 4\text{-Hydroxyphenylethylamine}$ (makaluvamine K)
35d, $\text{R}^1 = \text{H, R}^2 = 4\text{-Hydroxyphenylethylamine}$ (makaluvamine D)

Scheme 1.6. Examples of strained benzyne and pyridynes in total synthesis.

1.3. Cyclic Allenes

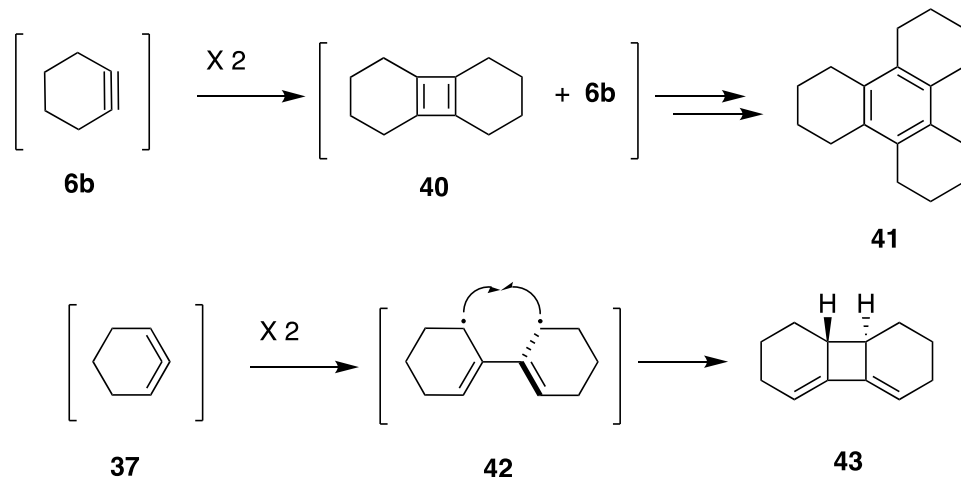


Unlike arynes, pyridynes, and cyclic alkynes, cyclic allenes are cumulene molecules, which are defined as having two or more consecutive C=C bonds. The reactivity of cyclic cumulenes arises from the fact that the cumulated system of allenes ordinarily assumes a linear C=C=C geometry of 180° . However, when encased within a medium or small ring (8-

members or less), there is substantial distortion of this idealized geometry, raising the ground state energy of the allene system, which makes these species reactive.³² These intermediates have been shown to participate in a variety of interesting reactions, both concerted pericyclic and stepwise.³³⁻³⁴ A number of approaches to generate these transient intermediates have been explored, including base-catalyzed elimination, zinc elimination of dihalides, the Doering–Moore–Skatebøl reaction (DMS), and photolysis of halocycloalkenes. I wish to focus on this strained class of cyclic intermediates, and my intention in this chapter is to provide an overview to all reactive cyclic allenes. I will focus mainly on three different ring sizes of cyclic allenes, 1,2-cyclohexadiene, 1,2-cycloheptadiene, 1,2-cyclooctadiene.

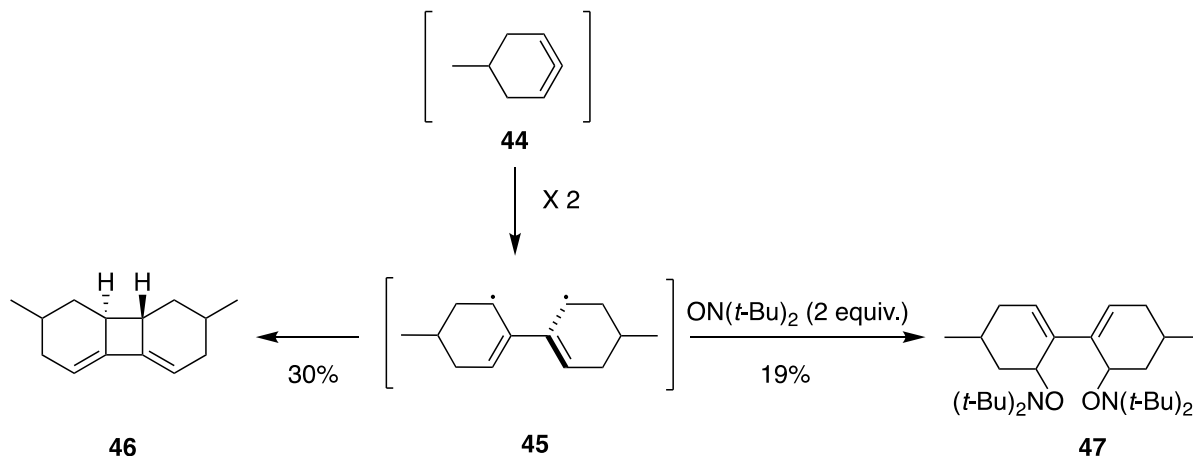
1.3.1. Dimerization and Trapping Reactions of Cyclic Allenes in Comparison to Cyclic Alkynes

The reactivity of strained carbocyclic allenes and alkynes vary and result in different cycloadducts. The first main difference between cyclic allenes and cyclic alkynes is the dimerization processes observed in allene reactions. For example, the dimerization of cyclohexyne **6b** and 1,2-cyclohexadiene **37** results in different products, as shown in Scheme 1.7. The dimerization of **6b** furnished the antiaromatic cyclobutadiene **40**, which underwent further reactions to release the high-energy system to form **41**.³⁵ Many research groups have reported the dimerization of cyclic allenes, which is an unavoidable and rapid reaction. Once strained cyclic allenes are formed, they dimerize easily, and as such there are a few factors that should be considered when generating these reactive intermediates. For instance, the 6-membered cyclic allene will react with itself to release the strain energy to produce the diradical **42**, which is believed to be more stable than the strained carbocyclic allene **37**. This diradical intermediate **42** can undergo further radical-radical coupling to form **43**. The *trans*-isomer conjugated diene **42**, is favored kinetically due to the twisted bis(allyl) biradical and due to the less sterically hindered structure compared to the *cis* isomers.



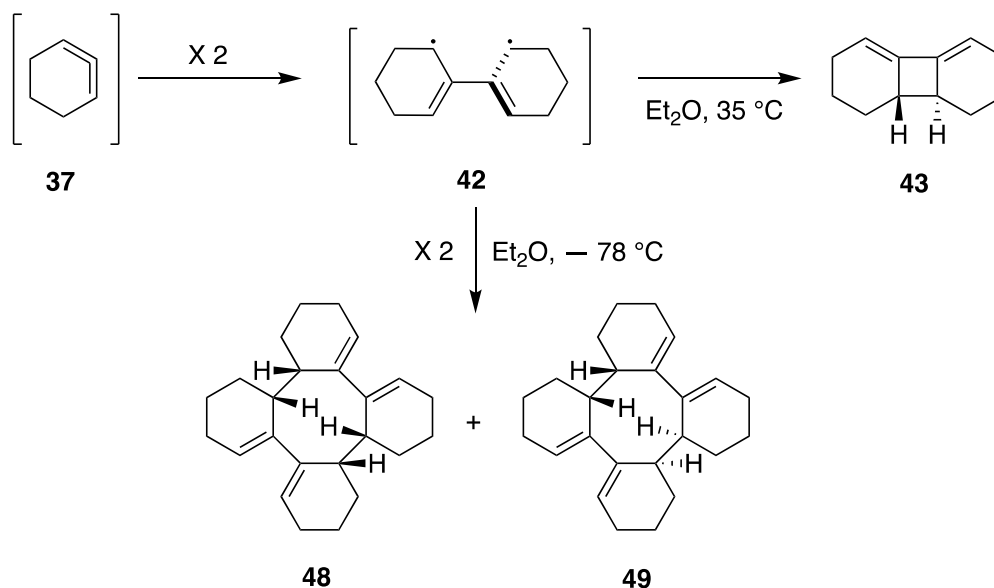
Scheme 1.7. Trimerization and dimerization of cyclohexyne and 1,2-cyclohexadiene.

It also was shown that the diradical intermediate **45** can be trapped with nitroxides (di-*t*-butylnitroxide specifically), as reported by Bottini in 1977.³⁶ In this report, **45** was trapped with a radical scavenger. Upon the generation of methyl branched cyclic allene **44** in the presence of 2 equiv. di-*t*-butylnitroxide, the diradical intermediate **45** was intercepted to provide **47** in 19% yield and the dimer **46** in 30%, as shown in Scheme 1.8. This indicates the radical character of the dimerization processes of cyclic allenes, which suggests a closed-shell cyclic allene **44**. In contrast, it was found that allene **44** has no diradical character due to the absence of any reaction between **44** and di-*t*-butylnitroxide.



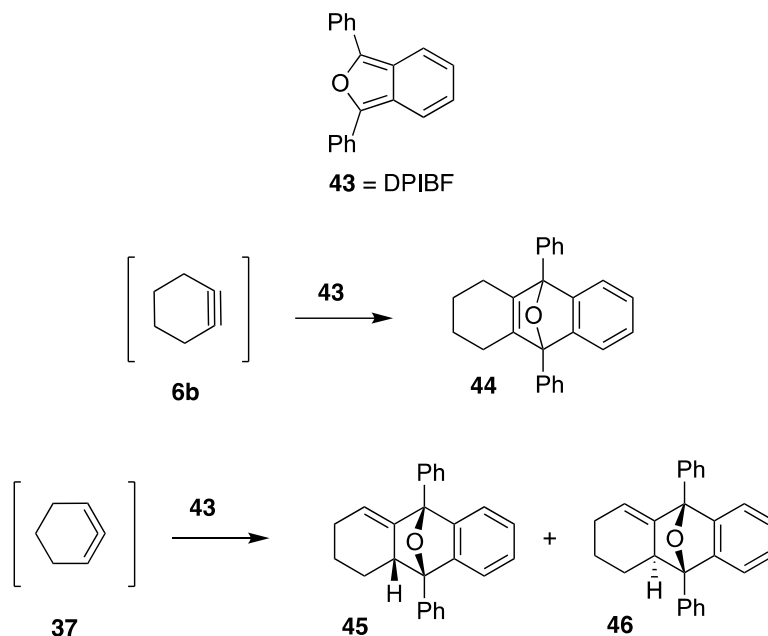
Scheme 1.8. Interception of the dimerization process of cyclic allenes by nitroxide radicals.

The dimerization and oligomerization of cyclic allenes can be controlled by the reaction temperature. In an early study done by Moore and Moser, for example, both dimer and tetramers of 1,2-cyclohexadiene were isolated by changing the reaction temperature.³⁷ It was reported in this study that at $-78\text{ }^{\circ}\text{C}$ 1,2-cyclohexadiene formed the tetramers **48** and **49** mainly, while at $35\text{ }^{\circ}\text{C}$ the dimer **43** was predominant. This different behaviour can be explained by the fact that the formation of the cyclobutane ring in **43**, with two sp^2 carbons, requires some amount of energy due to the fact that **42** has a different half-life at $-78\text{ }^{\circ}\text{C}$ and $35\text{ }^{\circ}\text{C}$. At low temperature, intermediate **42** has a longer half-life, which leads to a reaction of two molecules of **42**, intermolecularly. However, at $35\text{ }^{\circ}\text{C}$, a faster reaction occurs intramolecularly between the diradical to form cyclobutane ring **43**.



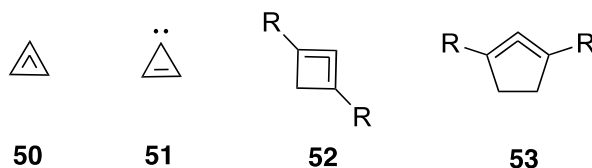
Scheme 1.9. Temperature effects on the dimerization processes of cyclic allenes.

Strained cyclic alkynes and cyclic allenes also can furnish different cycloadducts via trapping of the reactive intermediate. For example, when trapping these two classes of highly reactive intermediates with 1,3-diphenylisobenzofuran (DPIBF), different cycloadducts are formed. The position of the olefin and the reaction of a trap with a $\text{C}=\text{C}$ bond instead of a triple bond, which would result in the possibility of endo and exo isomers, are the main differences in the resulting cycloadducts, as shown in Scheme 1.10.^{16, 38}



Scheme 1.10. Trapping reactions of cyclohexyne and 1,2-cyclohexadiene with DPIBF.

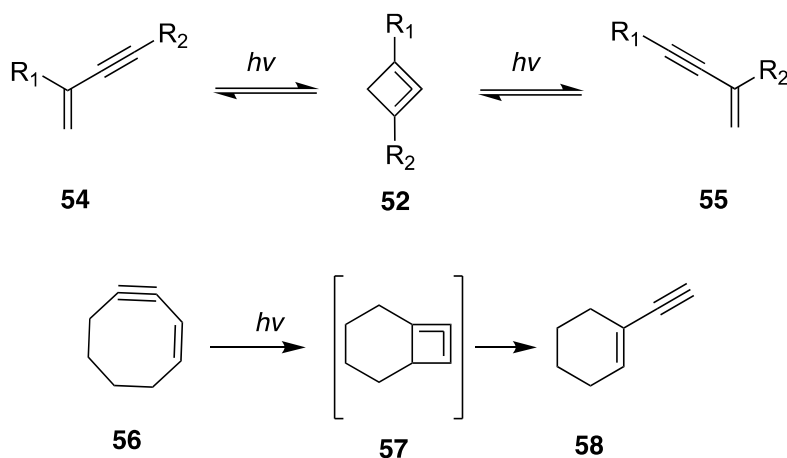
1.4. Three-, Four-, and Five-Membered Cyclic Allenes



These three classes of cyclic allenes are less-studied when compared with larger size strained cyclic allenes (six-membered and larger). Cyclopropadiene **50** is the smallest possible allene-containing ring system. Using a computational study, it was shown that the most stable isomer of **50** is cyclopropylidene **51**.³⁹

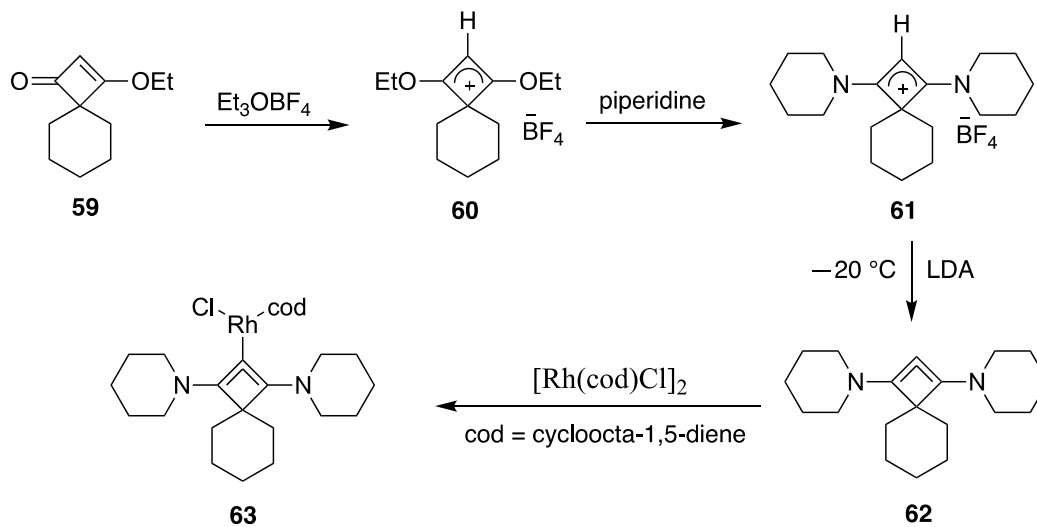
The existence of the 1,2-cyclobutadienes **52** was reported first by experimental evidence when Meier and König observe equilibration between isomeric enynes **54** and **55**, and postulate that the equilibrium occurred via transient **52**.⁴⁰ These reactions are in equilibrium, as shown in Scheme 1.11. It is believed that, upon treating enynes **54** and **55** with a light source, **52** is formed and can reopen in one of two possible pathways to regenerate **54** and **55**. Another transformation, which appears to go through the formation of 1,2-cyclobutadienes, is the photoisomerization of cyclooctenyne **56**.⁴⁰ It was proposed that

this transformation would be a result of the formation of a strained cyclic allene **57**, followed by ring opening to **58**.



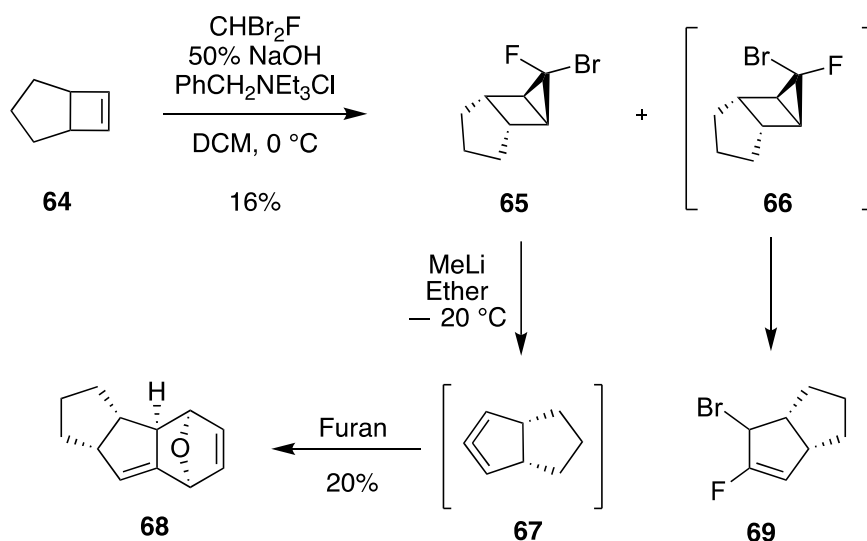
Scheme 1.11. Photochemical isomerization of conjugated enynes believed to proceed through 1,2-cyclobutadiene intermediates.

In 2009, Bertrand and his coworkers reported that by stabilizing 1,2-cyclobutadienes **52** with piperidines at both termini, as shown in Scheme 1.12, the allene **62** was stable enough at $-20\text{ }^{\circ}\text{C}$ to permit its characterization.⁴¹ However, this compound readily decomposed when the temperature is raised above $-5\text{ }^{\circ}\text{C}$. To avoid this decomposition, allene **62** was stabilized by its coordination (as a ligand) to a rhodium complex and gave **63** in 76% yield.



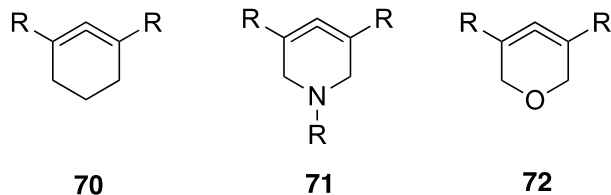
Scheme 1.12. Synthesis of four-membered-ring allene **62** and its stabilization by coordination to the rhodium complex.

A number of attempts to generate 1,2-cyclopentadiene **53** were carried out. Favorskii and coworkers attempted first to access this reactive intermediate via base-mediated elimination.^{42, 45} In this study, 1,2-dibromocyclopentene was treated with metallic sodium; however, 1,3-cyclopentadiene was isolated instead of the desired allene. Another attempt to generate 1,2-cyclopentadiene via fluoride promoted elimination was reported by Balci. However, in this report, 2-bromo-3-trimethylsilylcyclopentene was subjected to a fluoride ion source and furnished a Wurtz-like dimer.⁴³ In 2002, Balci and his coworkers reported the first successful example of the generation of five-membered cyclic allenes via a Doering–Moore–Skattebøl (DMS) reaction, as shown in Scheme 1.13.⁴⁴ Surprisingly, *exo,exo*-fluorobromocyclopropane **65** underwent ring-opening to give allene **67**, which was trapped with furan to give the [4+2] cycloadduct **68**. Alternately, *exo,endo*-isomer **66** rearranged to **69**. These results can be explained by the fact that the C–Br bond of the *exo,endo*-isomer **66** proceeded through a heterolytic simultaneous cleavage with the disrotatory opening of the cyclopropane resulting in **69**. However, when the C–F bond, which is a stronger bond than C–Br, is placed inside the ring as in **65**, the rearrangement would not take place. This would result in an isolable compound **65**, which can be treated with MeLi to generate cyclic allene **67** via DMS rearrangement.



Scheme 1.13. First evidence for generation of a 1,2-cyclopentadiene via DMS method.

1.5. Six-Membered Cyclic Allenes



The six-membered cyclic allenes have been the subject of the largest amount of work. In this chapter, only the most recent work related to this class of compounds is covered. This subsection will include the following subsections: unsubstituted 1,2-cyclohexadiene **36**, substituted 1,2-cyclohexadienes **70**, six-membered azacyclic **71**, and six-membered oxacyclic **72**.

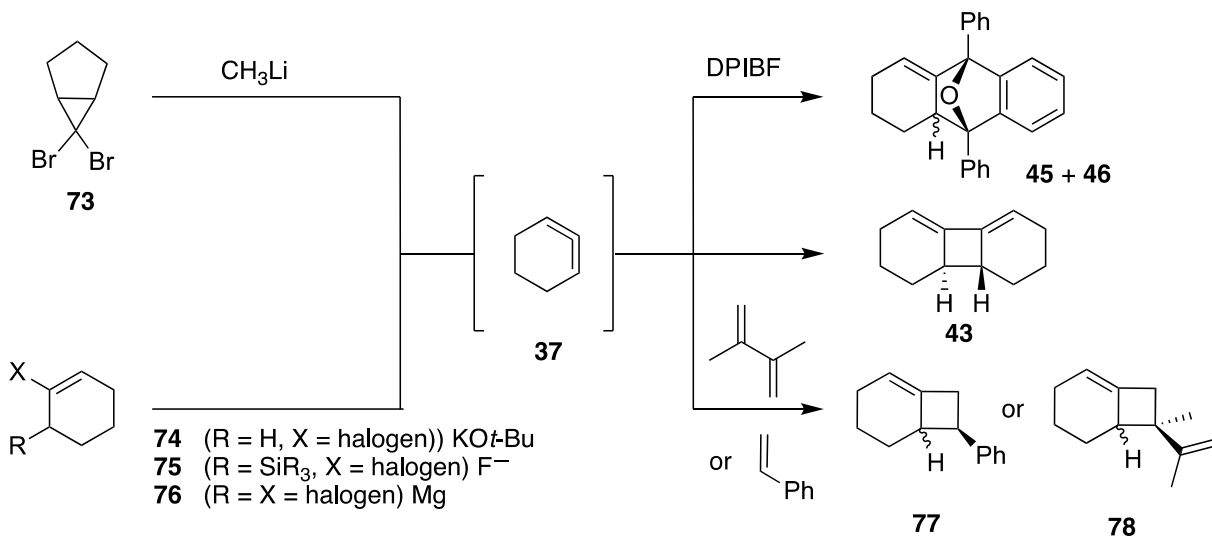
1.5.1. 1,2-Cyclohexadienes



37

1,2-Cyclohexadiene **37** is one of the most studied cyclic allenes. In 1935, Favorskii made the first attempt to synthesize this reactive intermediate.⁴⁵ In 1940, Dominin reported the second attempt to synthesize allene **37**. The method, which was used in this report, was the treatment of 1,6-dichlorocyclohexene with sodium in Et₂O;^{46, 47} this resulted in the formation of oligomers **48** and **49**. Two decades later, a study done by Ball and Landor showed that upon dehydrohalogenation of 1-chlorocyclohexene, oligomers resulting from the formation of allene **37** were isolated.⁴⁸⁻⁴⁹ In 1966, the first clear illustration of the existence of allene **37** was demonstrated by Wittig and Fritze.³⁸ 1-Bromocyclohexene **74** was treated with *t*-BuOK in DMSO with and without trapping partner (DPIBF), and both the [2+2] dimer and the [4+2] cycloadduct with DPIBF were isolated. This was the first example illustrating that **37** can be trapped. In addition to these two generation methods for 1,2-cyclohexadiene **37**, there are

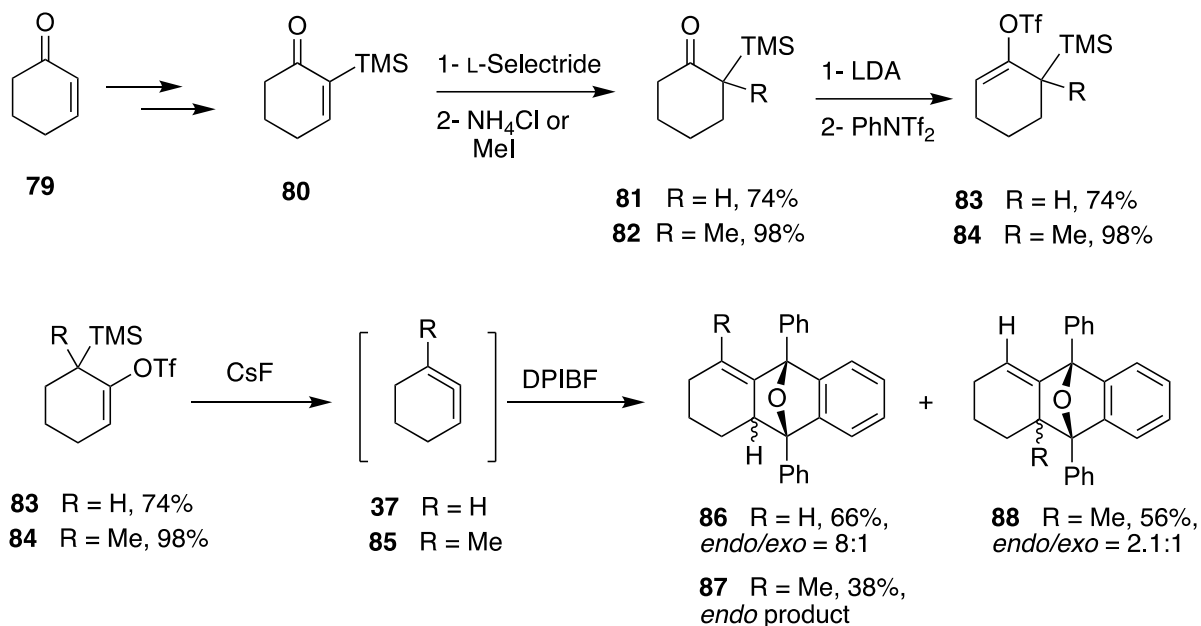
other known methods, which are summarized in Scheme 1.14. These studies traditionally have relied upon trapping the cyclic allenes by a large excess of in situ trapping partners, such as DPIBF, styrene, various 1,3-dienes, and enolates. This stoichiometry, with excess trapping agent, is required to overcome the propensity for dimerization by cyclic allenes.³²



Scheme 1.14. Known generations and trapping processes of 1,2-cyclohexadienes in [2+2] and [4+2] fashion.

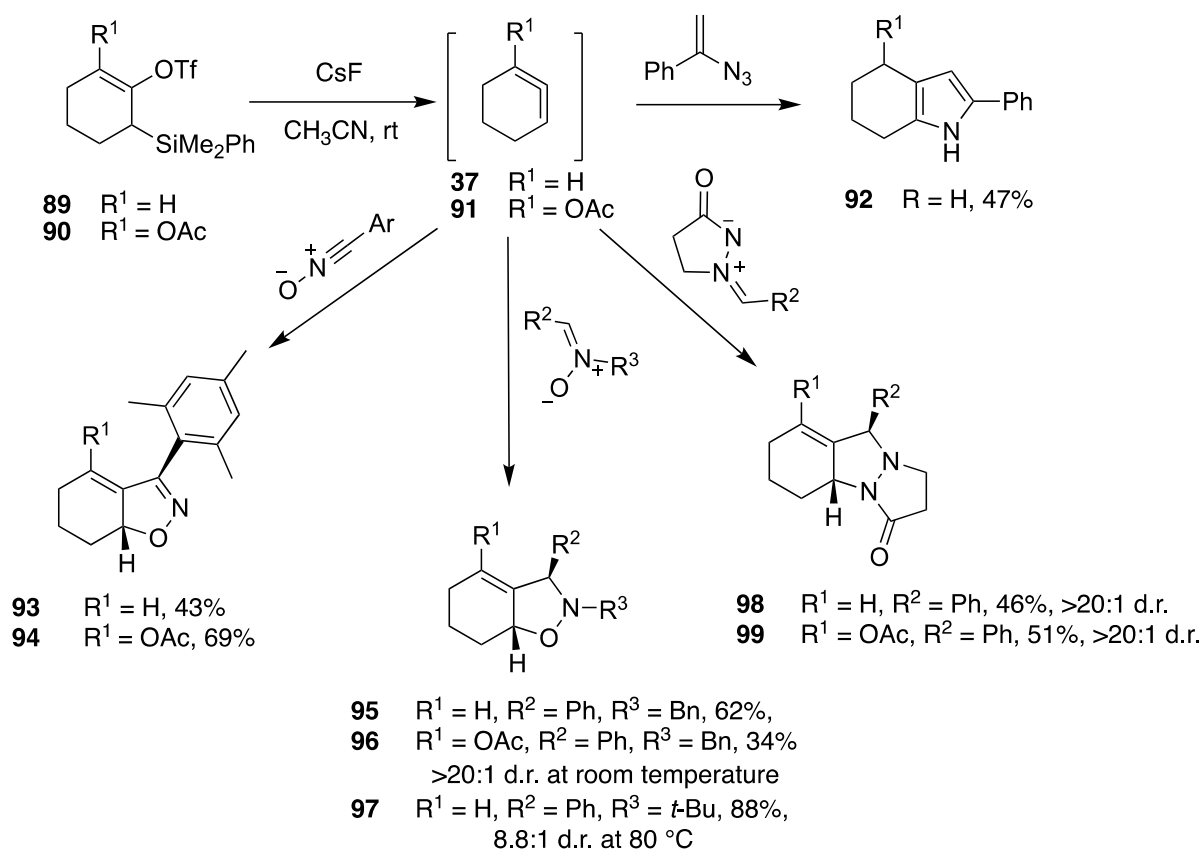
The most efficient method of generating cyclic allenes, which has been used recently by the Guitián group,⁵⁰ Garg group,³⁴ and our group,³³ is the fluoride-mediated desilylative elimination. This generation was first introduced by Johnson and Shakespeare in 1990,⁵¹ and this methodology is preferred due to its mild conditions and high functional group tolerance. To generate cyclic allenes via the fluoride-mediated desilylative elimination, the preparation of allylic silanes with a leaving group on a sp² hybridized carbon atom is required. In 2009, it was reported by Quintana et al. that the use of an alkenyl triflate as a leaving group showed an improvement in this allene generation approach.⁵⁰ In this study, allylic silanes with an sp² triflate were synthesized from 2-(trimethylsilyl)cyclohexanone **80**, which was subjected to reduction with L-Selectride. This results in hydride conjugate addition to enone **80** to form **81** and **82**, depending on workup conditions. Next, treatment of **81** and **82** with LDA furnished the kinetically favored enolate, and reaction with N-phenyltrifluoromethanesulfonimide afforded the enol triflates **83** or **84**. This enolate was capped with N-phenyltrifluoromethanesulfonimide, resulting in the formation of **83** and **84**. Using this

approach, both precursors needed to access the allene precursors, either unsubstituted or substituted with methyl, were made in good yields, as shown in Scheme 1.15.



Scheme 1.15. Synthesis of allenes **83** and **84** and their [4+2] cycloaddition with DPIBF by Quintana et al.

The desilylative elimination study by the Guitián group (Scheme 1.15) served as a starting point for the investigation of trapping of 1,2-cyclohexadienes with 1,3-dipoles.^{33, 34} The Garg group focused on the synthesis of unsubstituted 1,2-cyclohexadiene and trapping this reactive intermediate with nitrones at 80 °C. The West group focused on two cyclic allene substrates, the unsubstituted allene **37** as well as the acetoxy-substituted 1,2-cyclohexadiene **91**. The West group also studied the trapping of these two allenes with nitrile oxides, nitrones, azomethine imines, and organoazides as 1,3-dipoles at room temperature. In these studies, it was found that raising the temperature to 80 °C increases the yield of the reaction but decreases diastereoselectivity, as shown in cycloadduct **97** when compared with cycloadducts **91–96** and **98–99**. It also is believed that substituting the allene with an acetoxy group may result in an increased yield of the cycloadducts in several cases.³³ Selected examples are shown in Scheme 1.16 from these two studies, which were published in 2016.



Scheme 1.16. Trapping reactions of 1,2-cyclohexadienes with 1,3-dipoles.

DFT calculations were carried out to study mechanistic aspects of trapping the unsubstituted 1,2-cyclohexadiene with nitrones.³⁴ Both the regioselectivity and diastereoselectivity of the cycloaddition were investigated. Different pathways, which could furnish either of the four possible regioisomers and stereoisomers, were assessed, as shown in Figure 1.2. Computational studies demonstrated that Pathway 1 (Figure 1.2) is disfavored for the reaction of **37** with nitrone **100**. The lower energy process (Pathway 2) requires attack of the central carbon of allene **36** on the carbon terminus of nitrone **100**. This results in the formation of a new C—C bond, and complete regioselectivity will be obtained in the formation of the C—N or C—O bonds between the heteroatom of the 1,3-dipoles and the terminus carbon of the allene.

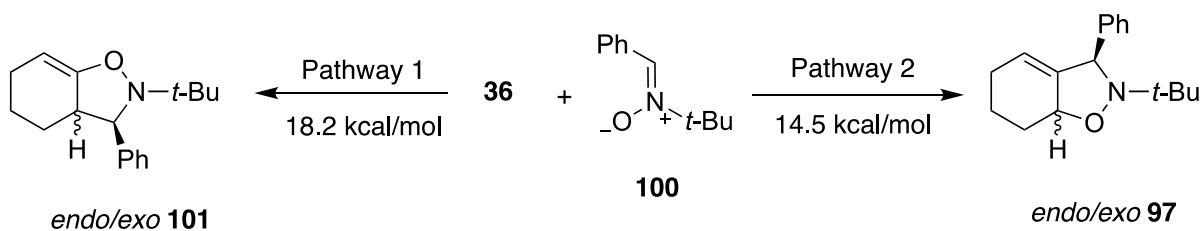
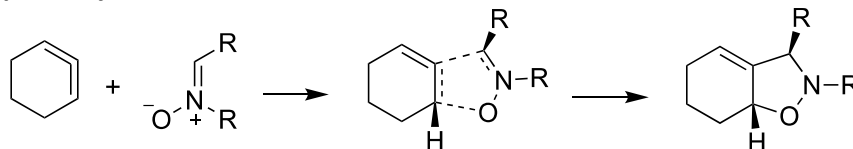


Figure 1.2. Possible regio- and diastereoselectivities of the reaction between six-membered cyclic allene and nitrones.

Moreover, it was observed that in all the trapping processes attempted by the Garg and West groups the endo products were predominant. It has been reported that the transition states of the endo products in these processes are more energetically favorable by 1.2 kcal/mol when compared with the transition states of exo products.^{34, 52} The mechanisms of these transformations are believed to be in competition between both a stepwise process and an asynchronous concerted pericyclic process, as shown in Figure 1.3.

Concerted pathway



Stepwise pathway

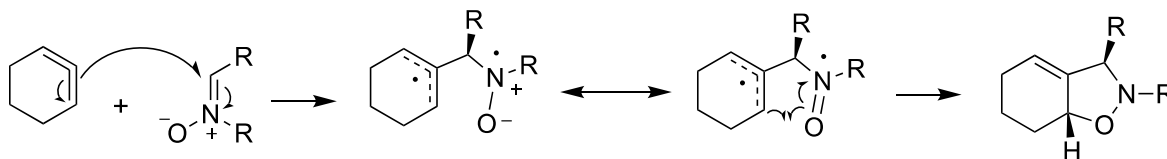


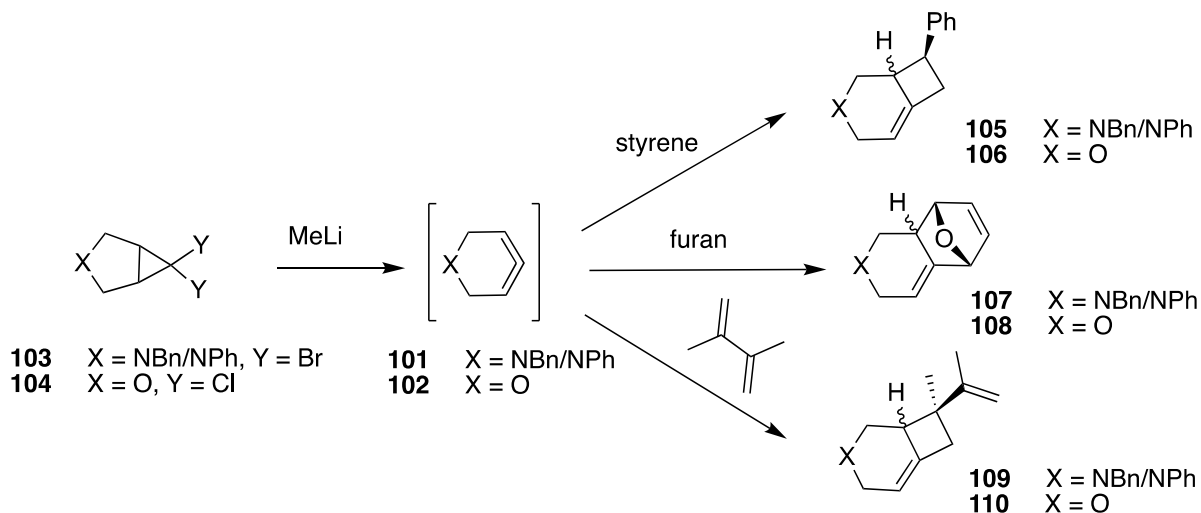
Figure 1.3. Proposed mechanism of cycloaddition reaction of cyclic allene with nitrone 1,3-dipole.

1.5.2. Azacyclic Allene **101** and Oxacyclic allene **102**



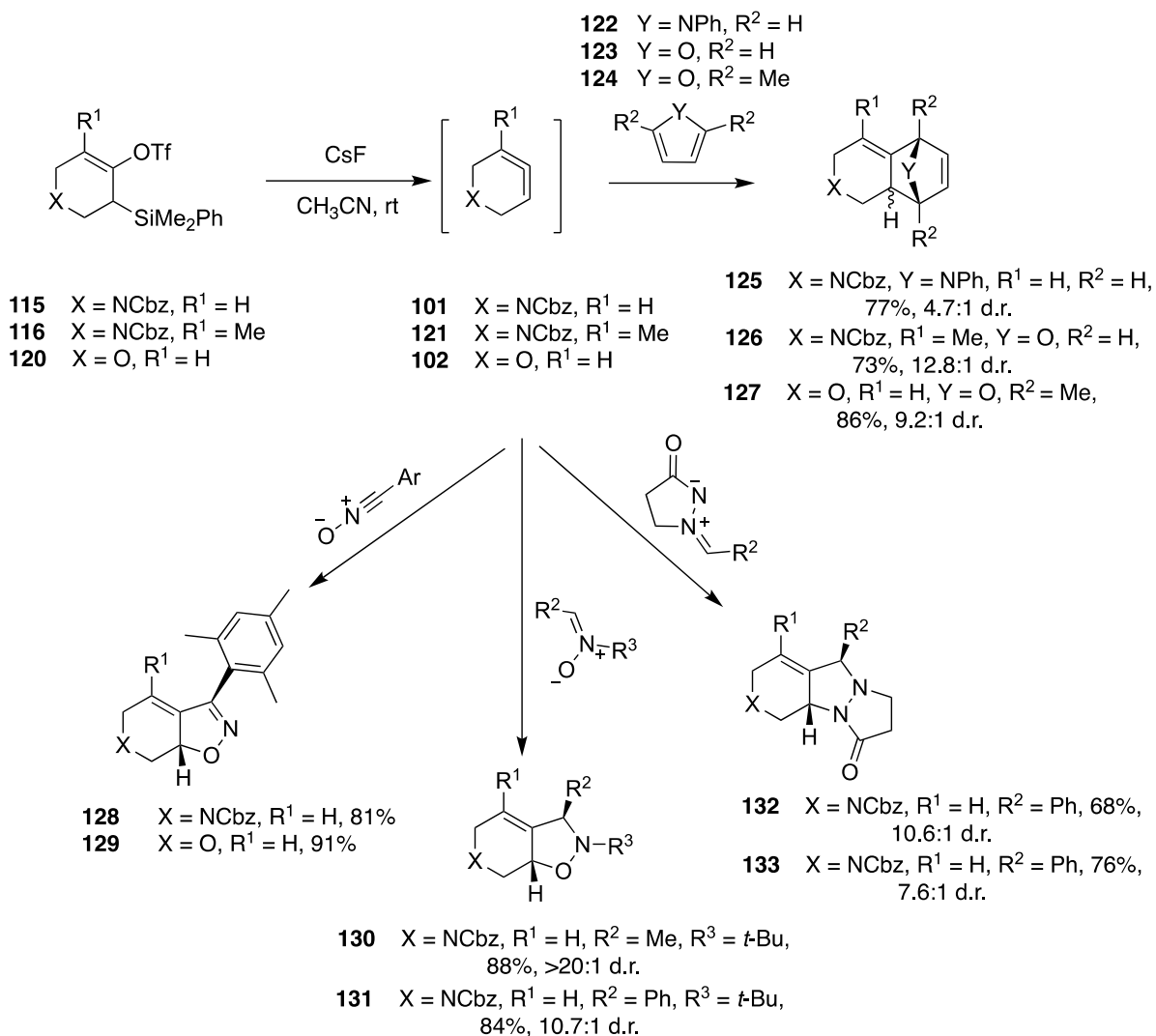
101 X = NCbz
102 X = O

The cyclic allenes described in this subsection differ from 1,2-cyclohexadiene **37** by the replacement of one sp^3 methylene carbon by heteroatoms such as oxygen and nitrogen. Incorporating a nitrogen atom in this strained system instead of a methylene group results in 1-aza-3,4-cyclohexadiene **101**, while replacement of the methylene group with oxygen results in 1-oxa-3,4-cyclohexadiene **102**. Allenes **101**⁵² and **102**⁵³⁻⁵⁴ were reported first by Christl using the methyllithium-promoted DMS rearrangement. In addition to their generation, allenenes **101** and **102** were trapped successfully in Diels–Alder reactions and [2+2] cycloadditions, as shown in Scheme 1.17.



Scheme 1.17. DMS reactions to generate six-membered heterocyclic allenenes.

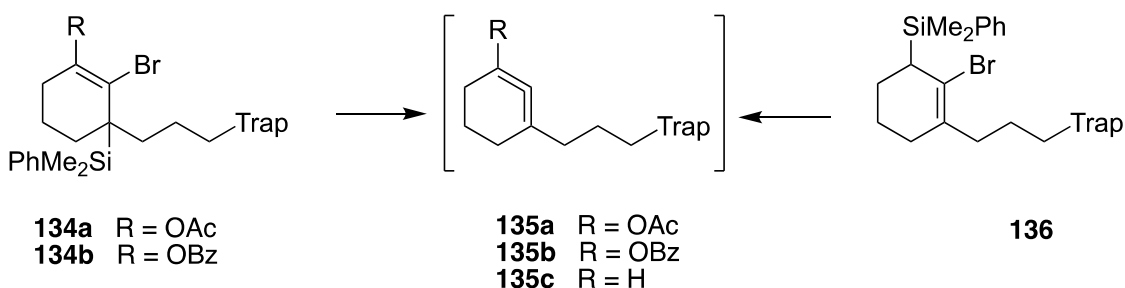
In recent reports, the Garg group studied the two reactive intermediates **101**⁵⁵ and **102**⁵⁶ and reported calculation studies and trapping reactions of these strained intermediates with 1,3-dipoles. These reactive intermediates were accessed using the fluoride-promoted elimination at room temperature. In order to use this generation method to access cyclic



Scheme 1.19. Trapping reactions of six-membered heterocyclic allenes with several trapping partners.

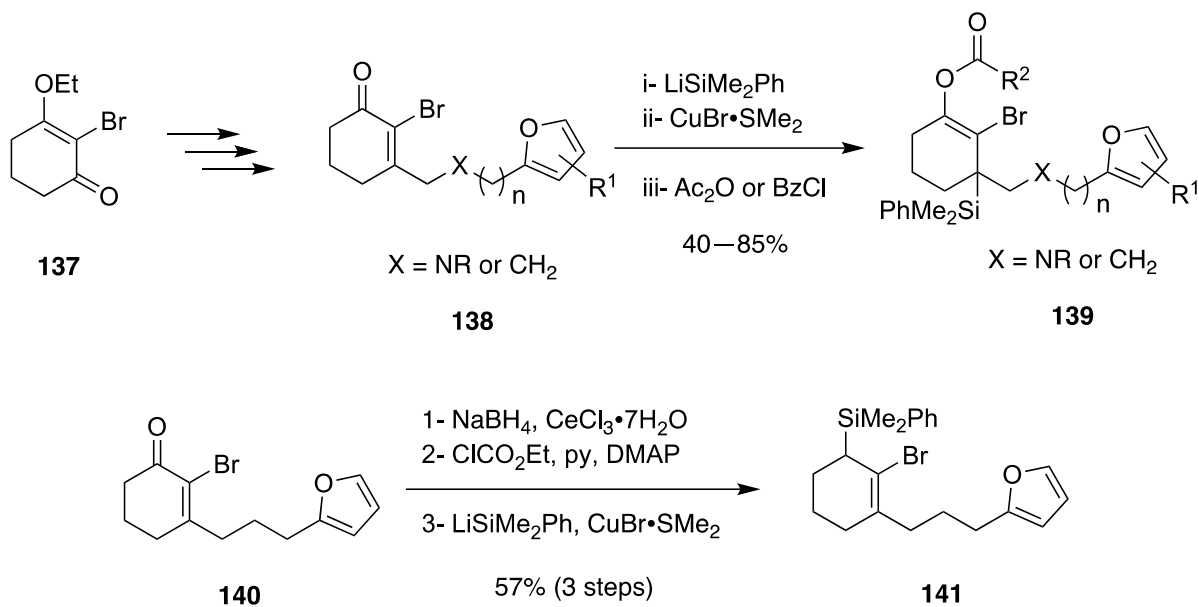
1.5.3. Intramolecular Trapping of 1,2-Cyclohexadienes

The West group has investigated the challenge associated with these methodologies employing several trapping partners to capture the reactive intermediates in an intramolecular trapping reaction.⁵⁷ In the first report, it was shown that 6-membered cyclic allenes can be trapped with a Diels–Alder cycloaddition via pendent furans in an intramolecular reaction. To study the intramolecular trapping, it was envisioned that a trap with a tether of suitable length (Scheme 1.20), such as in **134** and **136**, could be intercepted intramolecularly by cyclic allene **135** once generated.



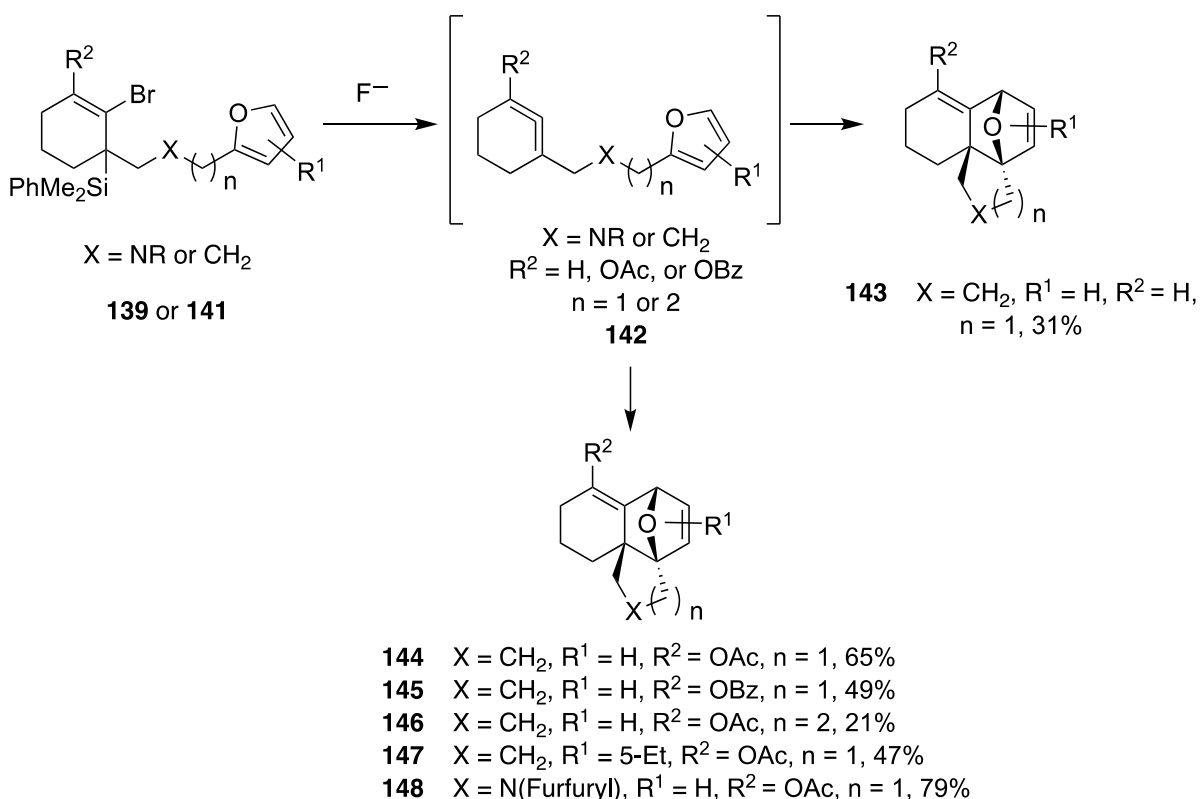
Scheme 1.20. Strategies to trap cyclic allenes intramolecularly.

The West group started examining this idea by the tethering of cyclic allene **135** with a pendent furan group, known to function effectively as a trap for cyclic allenes in intermolecular reactions. To synthesize derivatives of **134**, Stork–Danheiser-type transpositions were used to install the furan-bearing tether starting from 2-bromo-3-ethoxycyclohexanone **137** (Scheme 1.21). This results in functionalized cyclohexenones **138**, which were treated with silylcuprate in a 1,4-conjugate addition reaction, followed by capturing the enolate oxygen with an acetyl or a benzoyl group to form allylic silane derivatives **139**. Moreover, to synthesize allylic silane **136**, which would result in the allene precursor without an oxygen substitution on the allene, enone **140** was subjected to Luche reduction conditions to form the corresponding alcohol. This was converted to the corresponding carbonate, and the allylic carbonate was displaced directly with silylcuprate to afford **141**.



Scheme 1.21. Synthesis of allylic silanes **139** and **141**.

Next, allylic silanes **139** and **141** were subjected to desilylation conditions using 5 equiv. *tetra*-*n*-butylammonium fluoride (TBAF) in acetonitrile at room temperature. This resulted in the formation of allene **142**, followed by a Diels–Alder cycloaddition to form cycloadducts **143–148** in moderate to good yields. All cycloadducts were formed with complete diastereoselectivity and regioselectivity, as determined by NMR analysis. The reaction was evaluated with respect to different functionalizations on the furan moiety as well as various tethers, as shown in Scheme 1.22.



Scheme 1.22. Tethered allene and its intramolecular Diels-Alder trapping.

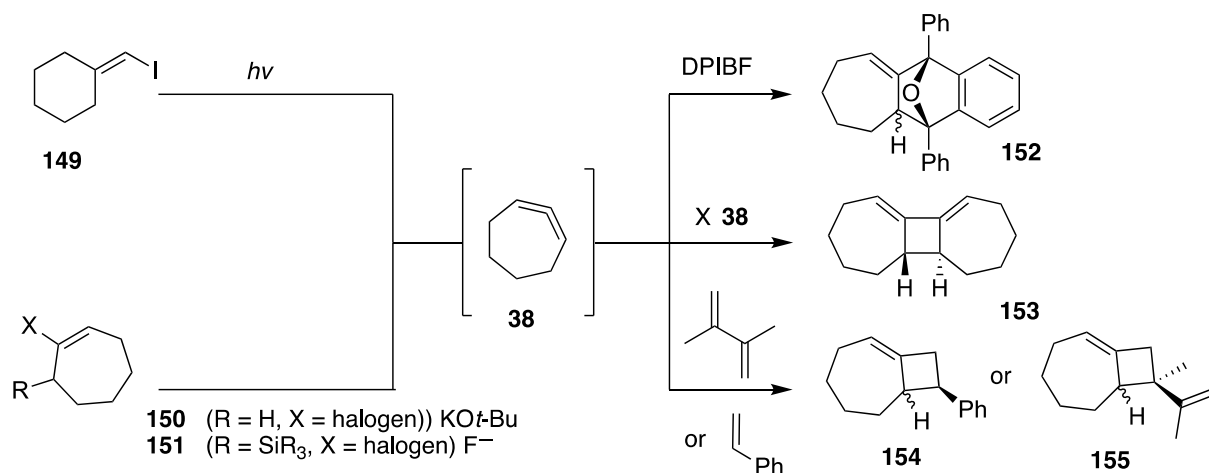
1.6. Seven-Membered Cyclic Allenes



38

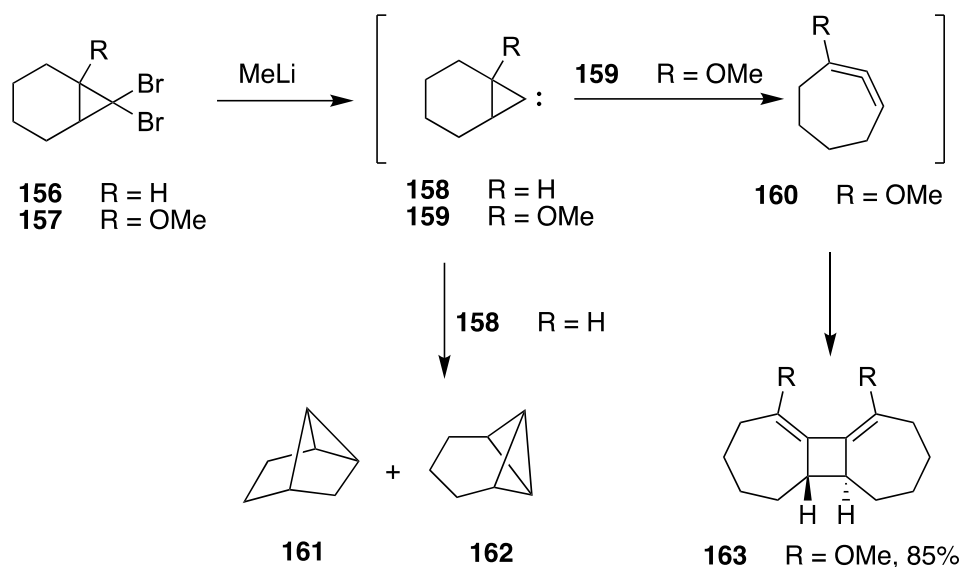
1,2-Cycloheptadiene **38** is a less-studied cyclic allene when compared with its six-membered counterpart. This subsection and Chapter 2 focus on cyclic allene **38**. The most common generation methods used to access **38** are base-mediated elimination in an E2-like fashion,^{15, 48, 58-59} photolysis of a vinyl iodide,⁶⁰ a modified Doering–Moore–Skattebøl reaction,⁶¹ and fluoride-mediated elimination.⁶² These studies have relied traditionally upon trapping the cyclic allenes via the same methods as 6-membered allenes (Scheme 1.23). After an erroneous report by Favorskii on the isolation of 1,2-cycloheptadiene,⁴⁵ the existence of 1,2-cycloheptadiene was proven first by Ball and Landor where E2 elimination of HCl from 1-

chloro-1-cycloheptene, by the treatment with $\text{KO}t\text{-Bu}$, was used as the method to generate 1,2-cycloheptadiene.⁴⁸ Subsequent studies showed that 1,2-cycloheptadiene can be trapped with 1,3-diphenylisobenzofuran,¹⁵ dienes, and styrene.⁶³ There are a few examples where 1,2-cycloheptadiene **38** was trapped in [4+2] and [2+2] cycloadditions. Chapter 2 will focus on the work that the West group has contributed in studying reactive intermediate **38** and its trapping reactions with 1,3-dipoles.



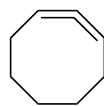
Scheme 1.23. Known methods to generate seven-membered cyclic allenes.

To generate cyclic allenes, the DMS reaction commonly is used. However, in the case of unsubstituted 1,2-cyclohexadiene **38**, the DMS method cannot be employed. When this method was applied to generate allene **38**, tricycloheptanes **161** and **162** were isolated as a mixture in a ratio of 1:23 (**161**:**162**), as shown in Scheme 1.24.⁶⁴ These transformations are proposed to result from transannular insertion reactions of carbene intermediate **158**. In contrast to the unsubstituted example, 1-methoxy-1,2-cycloheptadiene **160** can be generated via the DMS reaction and was shown to undergo [2+2] trapping to furnish **163** in high yield.⁶¹



Scheme 1.24. Efforts to generate substituted and unsubstituted 1,2-cycloheptadienes via DMS rearrangement.

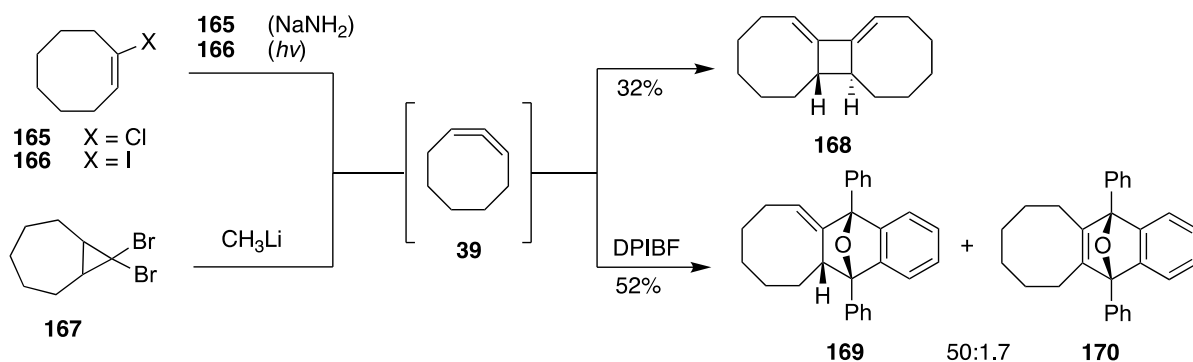
1.7. Eight-Membered Cyclic Allenes



39

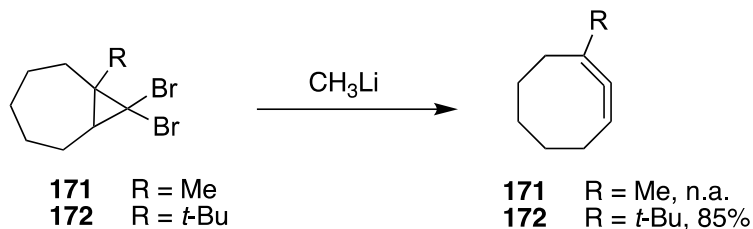
The existence of 1,2-cyclooctadiene **39** was described first by Ball and Landor in 1961.⁴⁸ Upon the treatment of 1-chlorocyclooctene with strong base (NaNH_2), a dehydrohalogenation process occurred and afforded dimer **168**, which is believed to derive from transient allene **39**, as shown in Scheme 1.25. Several years later, Wittig and his co-workers generated 1,2-cyclooctadiene **39** using similar reaction conditions to those used by Ball and Landor. Wittig was the first to succeed in trapping allene **39** with 1,3-diphenylisobenzofuran.⁶⁵

Marquis and Gardner were the first to report that allene **39** can be accessed via the DMS rearrangement using precursor **167** (Scheme 1.25).⁶⁶ Allene **39** readily undergoes dimerization. However, cold and dilute reaction conditions enabled the detection of this compound through carbon NMR and IR analysis.⁶⁷



Scheme 1.25. Known generation, dimerization, and trapping processes of 1,2-cyclooctadiene in [4+2] cycloaddition with DPIBF.

Substitution of cyclic allene **39** leads to a sufficiently stable compound for isolation. For example, substitution with a C1-methyl group results in greater kinetic stability and increases the half-life of **39** to approximately 10–15 min at ambient temperature.³² After this limited time, dimerization products were obtained. The first report of the only isolable 1,2-cyclooctadiene was reported by Johnson when substitution of a 1-*t*-butyl group on allene **172** was added.⁶⁸ This report illustrated that **172** was stable at room temperature, and it was purified by preparative gas liquid chromatography (GLC) and characterized.



Scheme 1.26. Isolation of 1,2-cyclooctadienes.

1.8. Conclusions and Thesis Objective

The generation and trapping processes of reactive intermediates, such as cyclic allenes, have been an area of interest to chemists for decades due to their high reactivity. These reactive intermediates enable the formation of complex polycyclic organic frameworks, which would be hard to form by other means. They also proceed through novel and interesting

mechanisms. In the past few decades, several methods have been designed and studied to generate cyclic allene intermediates. These approaches have focused on a variety of complementary reaction conditions. Once these reactive intermediates are generated, they often can be intercepted by trapping partners to form novel cycloadducts. Having found a number of highly efficient trapping processes employing derivatives of 1,2-cyclohexadiene, as illustrated in Section 1.5, we now have turned our attention to the larger homologue, 1,2-cycloheptadiene. Our aim is to seek an entry into the 1,2-cycloheptadiene system in order to gain some perspective on the behaviour of this strained intermediate.

In Chapter 2, a mild approach to generate substituted and unsubstituted 1,2-cycloheptadiene is described. This approach uses fluoride-mediated elimination reactions from the precursor containing an allylic silane with an adjacent sp^2 leaving group, which was synthesized by copper mediated nucleophilic silylation. The routes to access this cyclic allene precursor are considered to be one of the shortest methods toward the synthesis of 1,2-cycloheptadiene and its derivatives. Once these reactive intermediates are formed, they can undergo intermolecular cycloadditions in the presence of 1,3-dipoles with high regio- and diastereoselectivity.

In Chapter 3, a new approach to generate six-membered and seven-membered cyclic allenes through the metal–halogen exchange reaction is reported. This new approach relies on simple starting materials and occurs under complementary conditions to those already reported in this field. This chapter gives a report on how this approach was designed and shows the trapping transformations that have been carried out on the generation of these reactive intermediates. As a result, 6- and 7-membered cyclic allenes were generated through this method, which we call a metal–halogen exchange promoted elimination.

1.9. References:

1. Moss, R. A.; Platz, M.; Jones, M., *Reactive Intermediate Chemistry*. Wiley Online Library: 2004.
2. Gillespie, R. J., *J. Chem. Educ.* **1963**, *40* (6), 295.
3. Bredt, J.; Houben, J.; Levy, P., *Ber. Dtsch. Chem. Ges.* **1902**, *35* (2), 1286-1292.
4. Walsh, A. D., *Nature* **1947**, *159* (4031), 165.
5. Huang, C.-Y.; Doyle, A. G., *Chem. Rev.* **2014**, *114* (16), 8153-8198.
6. He, J.; Ling, J.; Chiu, P., *Chem. Rev.* **2014**, *114* (16), 8037-8128.
7. Vilotijevic, I.; Jamison, T. F., *Angew. Chem. Int. Ed.* **2009**, *48* (29), 5250-5281.
8. Wittig, G.; Krebs, A.; Pohlke, R., *Angew. Chem.* **1960**, *72* (9), 324-324.
9. Montgomery, L. K.; Applegate, L. E., *J. Am. Chem. Soc.* **1967**, *89* (20), 5305-5307.
10. Chapman, O. L.; Gano, J.; West, P. R.; Regitz, M.; Maas, G., *J. Am. Chem. Soc.* **1981**, *103* (23), 7033-7036.
11. Medina, J. M.; McMahon, T. C.; Jimenez-Osuna, G.; Houk, K. N.; Garg, N. K., *J. Am. Chem. Soc.* **2014**, *136* (42), 14706-14709.
12. Scardiglia, F.; Roberts, J. D., *Tetrahedron* **1957**, *1* (4), 343-344.
13. Fixari, B.; Brunet, J. J.; Caubere, P., *Tetrahedron* **1976**, *32* (8), 927-934.
14. Wentrup, C.; Blanch, R.; Briehl, H.; Gross, G., *J. Am. Chem. Soc.* **1988**, *110* (6), 1874-1880.
15. Wittig, G.; Meske-Schüller, J., *Justus Liebigs Ann. Chem.* **1968**, *711* (1), 76-81.
16. Wittig, G.; Krebs, A., *Chem. Ber.* **1961**, *94* (12), 3260-3275.
17. Huisgen, R., *Proc. Chem. Soc.* **1961**, 357-396.
18. Huisgen, R., *Angew. Chem. Int. Ed.* **1963**, *2* (10), 565-598.
19. Kolb, H. C.; Finn, M. G.; Sharpless, K. B., *Angew. Chem. Int. Ed.* **2001**, *40* (11), 2004-2021.
20. Baskin, J. M.; Prescher, J. A.; Laughlin, S. T.; Agard, N. J.; Chang, P. V.; Miller, I. A.; Lo, A.; Codelli, J. A.; Bertozzi, C. R., *Proc. Natl. Acad. Sci. U.S.A.* **2007**, *104* (43), 16793-16797.
21. Agard, N. J.; Prescher, J. A.; Bertozzi, C. R., *J. Am. Chem. Soc.* **2004**, *126* (46), 15046-15047.
22. Gampe, C. M.; Carreira, E. M., *Angew. Chem. Int. Ed.* **2011**, *50* (13), 2962-2965.
23. Gampe, C. M.; Boulos, S.; Carreira, E. M., *Angew. Chem. Int. Ed.* **2010**, *49* (24), 4092-4095.
24. Kim, J. Y.; Cho, J. H.; Choi, J.-R.; Shin, H.-J.; Song, J.-Y.; Hwang, S.-G.; Um, H.-D.; Do Yoo, Y.; Kim, J.; Park, J. K., *Toxicol. Appl. Pharmacol.* **2018**, *357*, 39-49.
25. Lee, C. J.; Swain, M.; Kwon, O., *Org. Lett.* **2018**, *20* (17), 5474-5477.
26. Roberts, J. D.; Simmons Jr, H. E.; Carlsmith, L. A.; Vaughan, C. W., *J. Am. Chem. Soc.* **1953**, *75* (13), 3290-3291.
27. Goetz, A. E.; Bronner, S. M.; Cisneros, J. D.; Melamed, J. M.; Paton, R. S.; Houk, K. N.; Garg, N. K., *Angew. Chem. Int. Ed.* **2012**, *51* (11), 2758-2762.
28. Díaz, M. T.; Cobas, A.; Guitián, E.; Castedo, L., *Synlett* **1998**, *1998* (2), 157-158.
29. May, C.; Moody, C. J., *J. Chem. Soc., Perkin Trans. 1* **1988**, (2), 247-250.

30. Díaz, M.; Cobas, A.; Guitián, E.; Castedo, L., *Eur. J. Org. Chem.* **2001**, 2001 (23), 4543-4549.
31. Iwao, M.; Motoi, O.; Fukuda, T.; Ishibashi, F., *Tetrahedron* **1998**, 54 (31), 8999-9010.
32. Johnson, R. P., *Chem. Rev.* **1989**, 89 (5), 1111-1124.
33. Lofstrand, V. A.; West, F. G., *Chem. Eur. J.* **2016**, 22 (31), 10763-10767.
34. Barber, J. S.; Styduhar, E. D.; Pham, H. V.; McMahon, T. C.; Houk, K. N.; Garg, N. K., *J. Am. Chem. Soc.* **2016**, 138 (8), 2512-5.
35. Wittig, G.; Mayer, U., *Chem. Ber.* **1963**, 96 (1), 342-348.
36. Bottini, A. T.; Cabral, L. J.; Dev, V., *Tetrahedron Lett.* **1977**, 18 (7), 615-618.
37. Moore, W. R.; Moser, W. R., *J. Am. Chem. Soc.* **1970**, 92 (18), 5469-5474.
38. Wittig, G.; Fritze, P., *Angew. Chem. Int. Ed.* **1966**, 5 (9), 846-846.
39. Seburg, R. A.; Patterson, E. V.; Stanton, J. F.; McMahon, R. J., *J. Am. Chem. Soc.* **1997**, 119 (25), 5847-5856.
40. H. Meier; König, P., *Nouv. J. Chim.* **1986**, 10, 437-428.
41. Melaimi, M.; Parameswaran, P.; Donnadiou, B.; Frenking, G.; Bertrand, G., *Angew. Chem.* **2009**, 121 (26), 4886-4889.
42. Balci, M.; Taskesenligil, Y., *Recent Developments in Strained Cyclic Allenes*. Wiley Online Library: 2000; Vol. 31, p 43.
43. Ceylan, M.; Seçen, H.; Sütbeyaz, Y., *J. Chem. Res. (S)* **1997**, (3), 70-71.
44. Algi, F.; Özen, R.; Balci, M., *Tetrahedron Lett.* **2002**, 43 (17), 3129-3131.
45. Favorskii, A. E., *J. Gen. Chem. (USSR) (Engl. Transl.)* **1936**, 6, 720-731.
46. Domnin, N. A., *J. Gen. Chem. (USSR) (Engl. Transl.)* **1940**, 10, 1939.
47. Domnin, N. A., *J. Gen. Chem. (USSR) (Engl. Transl.)* **1945**, 15, 461.
48. Ball, W. J.; Landor, S. R., *Proc. Chem. Soc.* **1961**, 143-144.
49. Ball, W. J.; Landor, S. R., *J. Chem. Soc.* **1962**, (0), 2298-2304.
50. Quintana, I.; Peña, D.; Pérez, D.; Guitián, E., *Eur. J. Org. Chem.* **2009**, 2009 (32), 5519-5524.
51. Shakespeare, W. C.; Johnson, R. P., *J. Am. Chem. Soc.* **1990**, 112 (23), 8578-8579.
52. Christl, M.; Braun, M.; Wolz, E.; Wagner, W., *Chem. Ber.* **1994**, 127 (6), 1137-1142.
53. Schreck, M.; Christl, M., *Angew. Chem.* **1987**, 99 (7), 720-721.
54. Schreck, M.; Christl, M., *Angew. Chem. Int. Ed.* **1987**, 26 (7), 690-692.
55. Barber, J. S.; Yamano, M. M.; Ramirez, M.; Darzi, E. R.; Knapp, R. R.; Liu, F.; Houk, K. N.; Garg, N. K., *Nat. Chem.* **2018**, 10 (9), 953.
56. Yamano, M.; Knapp, R.; Ngamnthiporn, A.; Ramirez, M.; Houk, K.; Stoltz, B.; Garg, N. K., *Angew. Chem.* **2019**.
57. Lofstrand, V. A.; McIntosh, K. C.; Almealmadi, Y. A.; West, F. G., *In preparation* **2019**.
58. Brunet, J. J.; Fixari, B.; Caubere, P., *Tetrahedron* **1974**, 30 (16), 2931-2937.
59. Bottini, A. T.; Frost II, K. A.; Anderson, B. R.; Dev, V., *Tetrahedron* **1973**, 29 (14), 1975-1981.
60. Kropp, P. J.; McNeely, S. A.; Davis, R. D., *J. Am. Chem. Soc.* **1983**, 105 (23), 6907-6915.

61. Taylor, K. G.; Hobbs, W. E.; Clark, M. S.; Chaney, J., *J. Org. Chem.* **1972**, *37* (15), 2436-2443.
62. Sütbeyaz, Y.; Ceylan, M.; Seçen, H., *J. chem. research. (S)* **1993**, 293.
63. Bottini, A. T.; Hilton, L. L., *Tetrahedron* **1975**, *31* (17), 2003-2004.
64. Moore, W. R.; Ward, H. R.; Merritt, R. F., *J. Am. Chem. Soc.* **1961**, *83* (8), 2019-2020.
65. Wittig, G.; Dorsch, H. L.; Meske-Schüller, J., *Justus Liebigs Ann. Chem.* **1968**, *711* (1), 55-64.
66. Marquis, E. T.; Gardner, P. D., *Tetrahedron Lett.* **1966**, *7* (25), 2793-2798.
67. Wisser, J. P.; Ramakers, J. E., *J. Chem. Soc., Chem. Commun.* **1972**, 178.
68. Price, J. D.; Johnson, R. P., *Tetrahedron Lett.* **1986**, *27* (39), 4679-4682.

Chapter 2

A Mild Method for the Generation and Intermolecular Trapping of 1,2-Cycloheptadiene with 1,3-Dipoles

2.1. 1,3-Dipolar Cycloadditions

Organic chemists have been interested in dipolar cycloadditions for many years. The first examples of a 1,3-dipolar cycloaddition were done by Schönbein in 1847.¹ He used the reactive species ozone, which underwent a [3+2] cycloaddition with various alkenes. After this report, many types of 1,3-dipoles have been discovered. These include but are not limited to azides, nitrones, nitrous oxides, oxides, nitrile oxides, carbonyl ylides, and azomethine imines.² The use of 1,3-dipoles in organic synthesis has been hampered due to their instability and their inherent difficulty to isolate. Due to the high energy of these compounds, poor chemo-, regio-, and diastereoselectivity often are obtained in the dipolar cycloadditions. However, despite these challenges, they often have been used by organic chemists to access heterocyclic containing compounds efficiently in fewer steps.

As there is a limited repertoire of methods by which cycloheptane containing functionalized materials can be produced in a single step from readily available precursors, the aim of this chapter is to harness the reactivity of strained cyclic allenes and 1,3-dipoles to access a variety of polycyclic cycloheptane containing compounds. Moreover, our goal is to examine a mild entry into the 1,2-cycloheptadiene system in order to gain some perspective on the behavior of this strained intermediate. Here, we discuss our efforts to examine the trapping reaction of 1,2-cycloheptadienes with 1,3-dipoles to access heterocycles containing a cycloheptane moiety.

2.2. Reactions of Acyclic Allenes with 1,3-Dipoles

1,3-Dipoles are known to undergo [3+2] cycloaddition with unsymmetrical olefins and alkynes with two possible regiochemical outcomes. 1,3-Dipoles also are known to react with

acyclic allenes. This reaction, however, can produce four possible regiochemical outcomes, as a result of reaction of either allene C=C bond in one of two orientations with the dipole. This regioselectivity depends greatly on the substitution pattern of the allene. The regiochemical diversity that is associated with these types of reactions is illustrated in Figure 2.1.

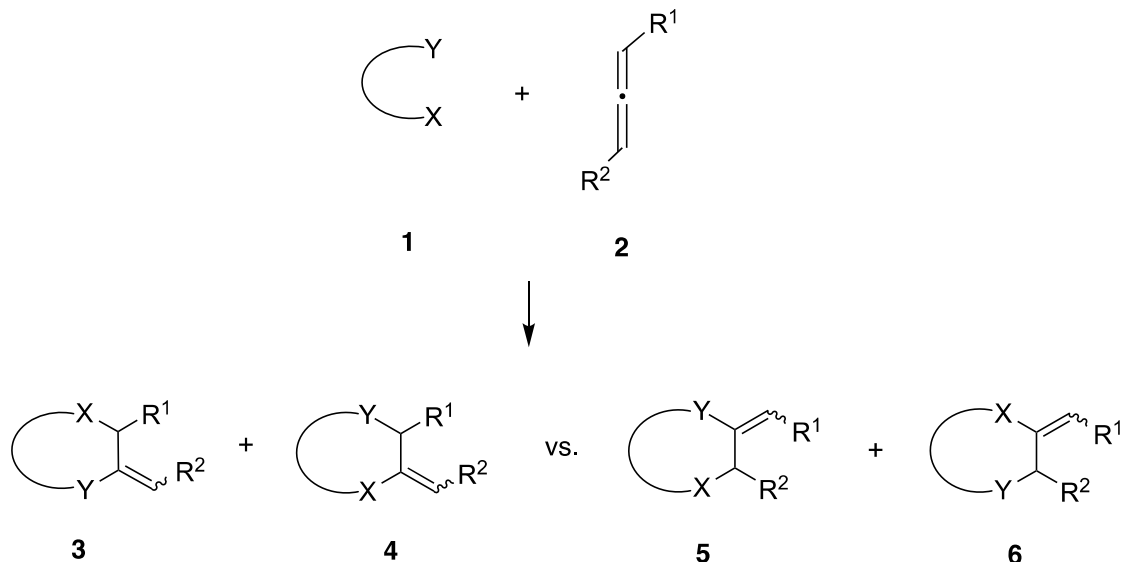
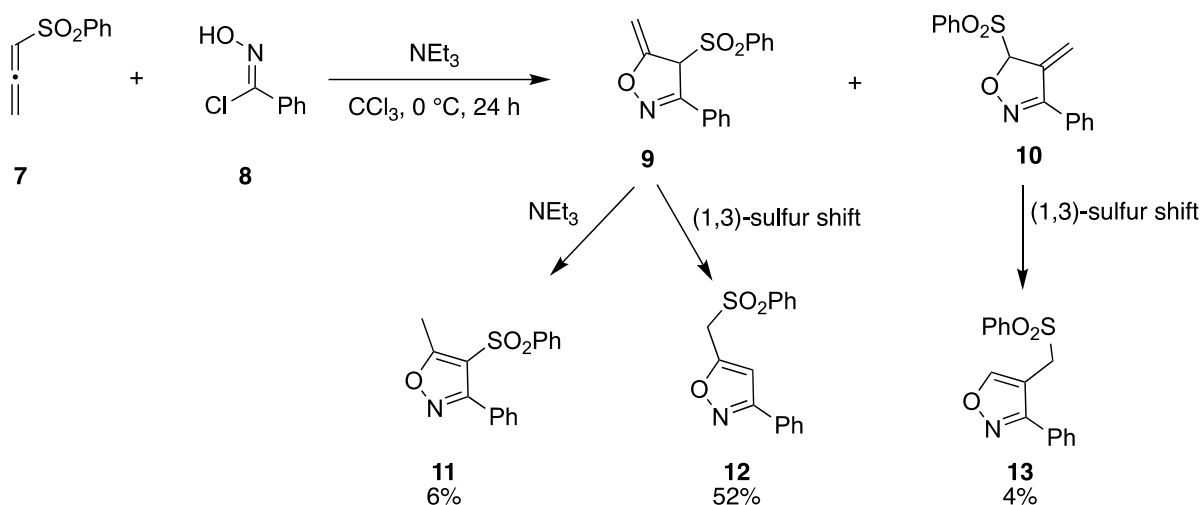


Figure 2.1. Possible regiochemical outcomes associated with 1,3-dipolar cycloaddition of acyclic allenes.

There are many examples in the chemical literature where 1,3-dipolar compounds are used to react with acyclic allenes. Mild reaction conditions have been used in the case of several 1,3-dipoles. For instance, it was reported by Padwa and coworkers that the nitrile oxide formed from α -chlorobenzaldoxime **8** under basic conditions underwent [3+2] cycloaddition with allene **7** under mild reaction conditions (Scheme 2.1).³ This example also demonstrates that the substitution pattern of allenes is important to the regioselectivity of the reaction, as mentioned previously. In this report, although regioisomers **11**, **12**, and **13** were reported, **12** was the major product. The authors' rationale for these results is that the [3+2] cycloaddition took place on the more reactive allene bond, which is conjugated to sulfonyl group to form **9**, followed by 1,3-allylic sulfonyl and hydrogen shifts, resulting in rearomatization to form **12**.



Scheme 2.1. [3+2] Cycloaddition of nitrile oxide and acyclic allene.

2.3. Background and Experimental Design

Utilizing the inherently high reactivity found in strained intermediates, such as hetarynes, benzyne, and cyclic alkynes, has been a vital method to drive novel bond-forming processes. These processes have allowed for the rapid construction of complex scaffolds, which have numerous applications in natural product synthesis and in pharmaceutical, material, and organometallic chemistry.⁴⁻¹⁶ These intermediates (Figure 2.2) have intrigued chemists for decades, and a noticeable body of literature has been assembled from studies of these intermediates, as previously summarized in Chapter 1. Unlike hetarynes, benzyne, and cyclic alkynes, cyclic allenes are a less well-studied class of highly reactive intermediates.

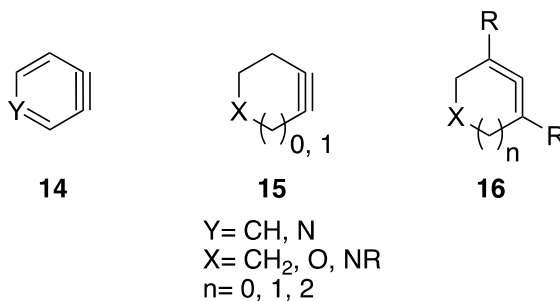
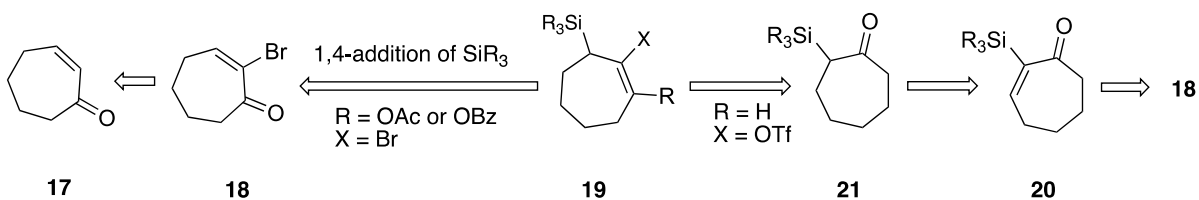


Figure 2.2. Generalized examples of strained cyclic intermediates.

This chapter presents the result of work designed to investigate the behavior of 1,2-cycloheptadiene, which has received relatively less attention than other cyclic allenes.

Previous studies in this area have focused principally on several methods to generate these highly reactive, strained intermediates. As described in Section 1.6, the most common generation methods used in prior work include base-mediated elimination in an E₂ like fashion,¹⁷⁻¹⁸ photolysis of a vinyl iodide,¹⁹ a modified DMS reaction,²⁰ and fluoride-mediated elimination.²¹

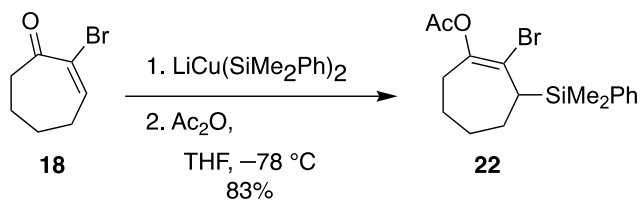
The mild method for generation of 1,2-cycloheptadiene that we chose to investigate is the fluoride-mediated desilylative elimination, rather than other methods, due to its high functional group tolerance. The generation of a cyclic allene via the fluoride-mediated desilylative elimination was introduced first by Johnson and Shakespeare²² to generate 1,2-cyclohexadiene, and was recently studied by our group²³ and the Garg group.²⁴ These studies were summarized in Chapter 1.5.1. This generation requires the preparation of allylic silanes with a leaving group on a sp² hybridized carbon atom. To access these key precursors, we proposed the route shown in Scheme 2.2. The substituted 1,2-cycloheptadiene precursors were hypothesized to be available by the 1,4-conjugate addition of SiMe₂Ph to the well preceded starting material, enone **18**, and the enolate was capped with acetic anhydride or benzoyl chloride. To access the unsubstituted 1,2-cycloheptadiene precursors, we envisioned that enone **18** could be protected with a ketal, followed by lithium-halogen exchange and reaction with silyl chloride, and finally acid work-up to remove the ketal. This would result in the formation of enone **20**, which can be converted to **21** with hydride conjugate addition using L-Selectride. Generation of the kinetic enolate by treatment of compound **21** with LDA at low temperature, and trapping of the enolate with a triflyl source, would lead to a suitable precursor for the unsubstituted 1,2-cycloheptadiene.



Scheme 2.2. Retrosynthesis of 1,2-cycloheptadiene precursors.

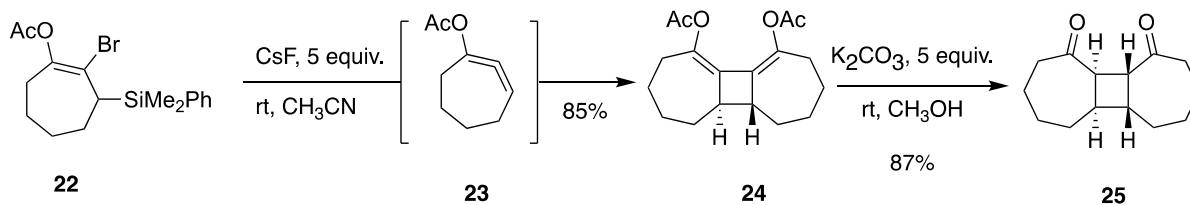
2.4. Results and Discussion

With the retrosynthesis in mind, I focused on the preparation of acetoxy-allylic silanes with a bromine atom installed as a leaving group on the adjacent sp^2 carbon with the general structure of **22**. This key starting material is used to form the acetoxy-substituted 1,2-cycloheptadiene after fluoride-initiated elimination, which can then be intercepted by trapping partners. Allylic silane **22** was accessed by the 1,4-conjugate addition of SiMe_2Ph anion to the common starting material, enone **18**, and the intermediate enolate was capped with acetic anhydride (Scheme 2.3). It is of note that performing the reaction at low temperature ($-78\text{ }^\circ\text{C}$) was very important in order to avoid undesired products, such the displacement of the bromine with SiMe_2Ph .



Scheme 2.3. Synthesis of acetoxy-substituted 1,2-cycloheptadiene precursor.

Next, I started investigating the reactivity of 1-acetoxy-1,2-cycloheptadiene. Allylic silane **22** was firstly treated with CsF in acetonitrile at room temperature, in the absence of traps, to examine the dimerization process of the seven-membered cyclic allene, as illustrated in Scheme 2.4. This reaction resulted in the formation of dimer **24** in high yield. We also showed that dimer **24** can be hydrolyzed to the diketone **25** under mild conditions. The stereochemistry of **25** was confirmed via X-ray crystallographic analysis, as shown in Figure 2.3.



Scheme 2.4. Dimerization process of acetoxy-substituted 1,2-cycloheptadiene **23** and hydrolysis of dimer **24** to diketone **25**.

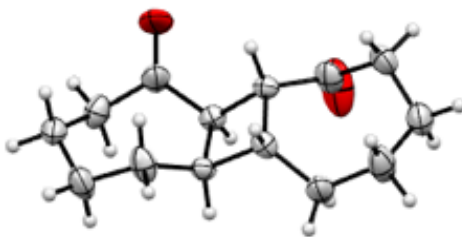
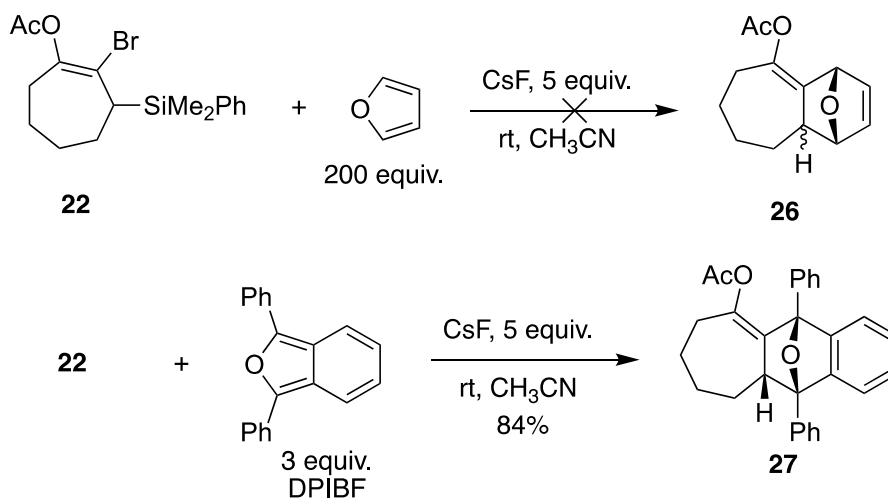


Figure 2.3. X-ray crystal structure of **25**.

In further reactions, trapping the cyclic allene **23** via a Diels–Alder reaction using furan failed to furnish **26** (Scheme 2.5), in contrast to 1-acetoxy-1,2-cyclohexadiene, which was successfully intercepted by furan in previous work by our group.²³ This might be due to the low reactivity of 1,2-cycloheptadiene as dienophile, with insufficient strain energy released to overcome the loss of aromaticity of furan. However, trapping allene **23** with a much more reactive furan, 1,3-diphenylisobenzofuran (DPIBF), furnished the corresponding *endo* [4+2]-cycloadduct **27** in high yield. We were not able to isolate any *exo* product, and if it was present, it was formed only in trace amounts. The stereochemistry of the *endo* [4+2]-cycloadduct **27** was confirmed by single crystal X-ray diffraction analysis, as illustrated in Figure 2.4.



Scheme 2.5. [4+2] Cycloaddition of 1-acetoxy-1,2-cycloheptadiene with DPIBF.

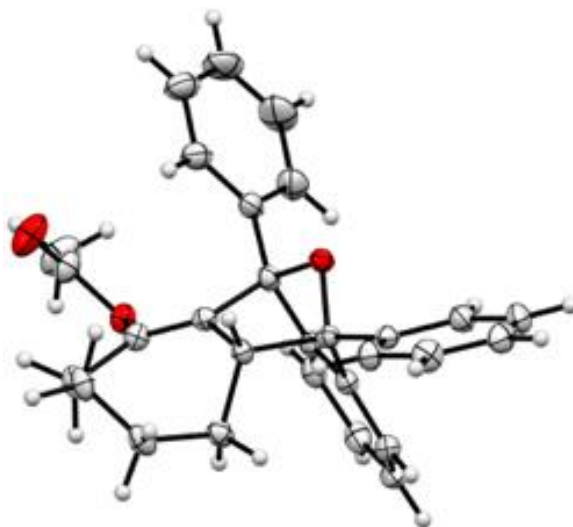
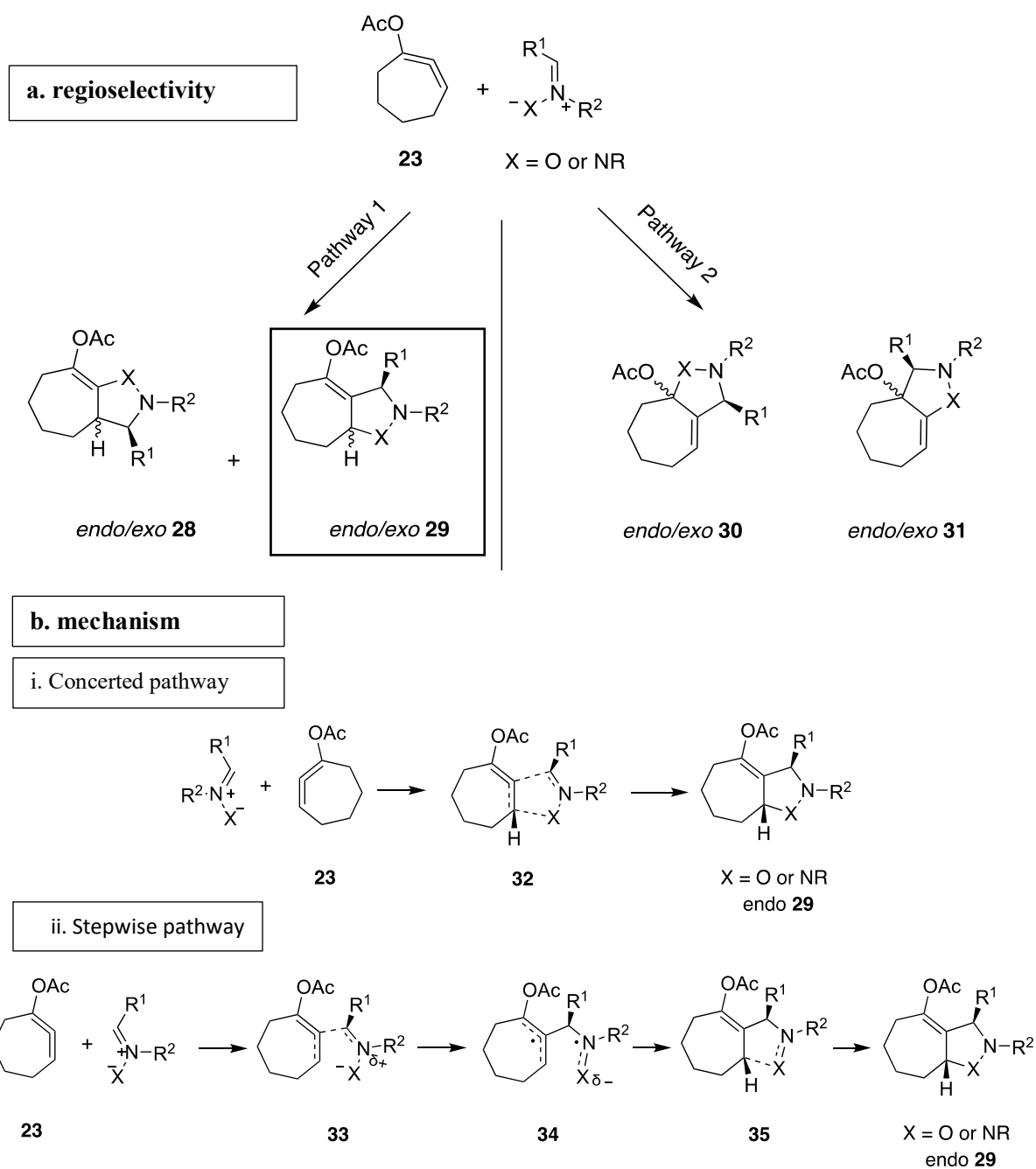


Figure 2.4. X-ray crystal structure of the endo cycloadduct **27**.

These preliminary experiments demonstrated that the functionalized 1,2-cycloheptadiene **23** could be generated in two steps from a simple bromoenone precursor and underwent efficient conversion to dimer or a Diels–Alder cycloadduct. Next, we sought to examine the trapping processes of this reactive intermediate with a variety of 1,3-dipoles that could produce polycyclic fused heterocycles. Upon addition of CsF (3 equiv.) to a stirred solution of allylic silane **22** and various 1,3-dipoles (5 equiv.) in acetonitrile at 80 °C (unless otherwise specified), the corresponding cycloadducts were obtained in good yields. We found that decreasing the stoichiometry of CsF (from 5 to 3 equiv.) and increasing the equivalents of 1,3-dipoles (from 3 to 5 equiv.) led to better yields. These changes also resulted in less dimerization processes. All cycloadducts resulting from the reaction of acetoxy-substituted 1,2-cycloheptadiene were formed as a single regioisomer **29** (Scheme 2.6, part a), as determined by NMR analysis, rather than as other regioisomers, **28**, **30**, and **31**. This would support previous reports stating that the central carbon of cyclic allenes acts as a weak nucleophile to the electron deficient carbon of 1,3-dipoles.²³⁻²⁵ Scheme 2.6, part a illustrates the regiochemical diversity of [3+2] cycloadditions of cyclic allene **23** with 1,3-dipoles. This results in the formation of a new C—C bond, and complete regioselectivity was obtained in the formation of the C—N or C—O bonds between the heteroatom of the 1,3-dipole and the nonoxygenated alkene carbon of the allene.²³ This complete regioselectivity might be due to

the fact that there is a significant raising of the LUMO of the allene double bond conjugated with the acetoxy. This would result in

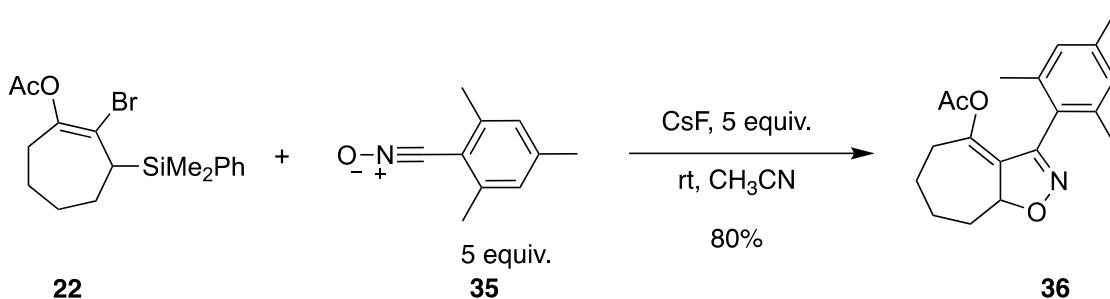
It also was observed that in all the trapping processes of the acetoxy-substituted 1,2-cycloheptadiene with 1,3-dipoles, the endo products were predominant. Preferential endo product formation is not surprising as it has been reported that the endo products of cyclic allenes are the most thermodynamically stable products.²⁶ The mechanism of these transformations is believed to be in competition between both a biradical stepwise process and an asynchronous concerted pericyclic process (Scheme 2.6, part b).²³⁻²⁵



Scheme 2.6. a. Possible regiochemical outcomes of the reaction between allene **23** and 1,3-Dipoles. b. Proposed Mechanisms.

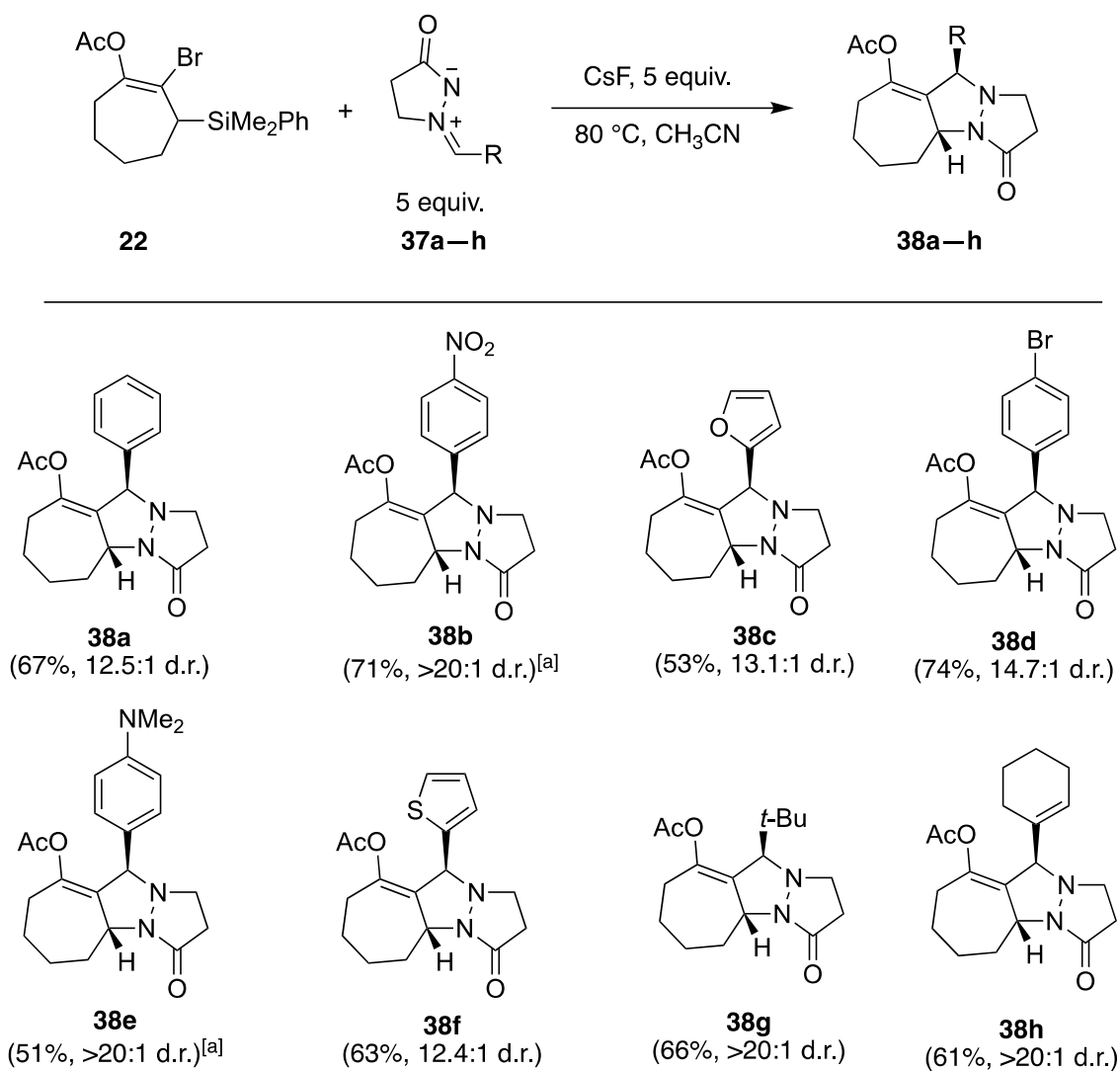
Three classes of 1,3-dipolar traps were used in trapping reactions of 1-acetoxy-1,2-cycloheptadiene. It was reported recently by the Garg group and by our group that nitrones, nitrile oxides, and azomethine imines can trap 1,2-cyclohexadienes and azacyclic allenes.²³⁻²⁶

These studies were summarized in Section 1.5.1. By applying similar conditions to seven-atom cyclic allenes, nitrile oxide **35** afforded **36** in high yield (80%) and as a single regioisomer using our standard conditions, as shown in Scheme 2.7. This reaction was carried out at room temperature to avoid decomposition of **35**, which was observed when the reaction was run at 80 °C.



Scheme 2.7. Reaction of cyclic allene **23** with nitrile oxide **35**.

The second class of 1,3-dipoles we examined was azomethine imines. This is a class of stable, isolable 1,3-dipoles that nonetheless retain good reactivity in [3+2]-cycloadditions. Several azomethine imines, **37a–h**, were examined and were found to produce tricyclic products, **38a–h**, in good yields (Scheme 2.8). Azomethine imines containing aliphatic or aromatic group were tolerated well in these reactions. For **38b** and **38e**, we found that it was desirable to run the reaction at room temperature due to excess decomposition of **37b** and **37e**. Unsurprisingly, trapping of cyclic allene **23** with an azomethine imine **37c**, which contains a furan moiety, occurred exclusively via a [3+2] cycloaddition reaction to form **38c**, and the furan moiety failed to react (consistent with our earlier observation of no intermolecular trapping by furan). The relative ratio of the endo and exo products of cycloadducts was determined by ¹H-NMR, and the endo products were found to be the major products as determined by NMR correlations using the TROESY (Transverse Rotating-frame Overhauser Enhancement Spectroscopy) NMR technique and further confirmed by obtaining the X-ray crystal structure for **38a**, as shown in Figure 2.5.



Scheme 2.8. Trapping processes of cyclic allene **23** with azomethine imines. ^[a] The reaction was run at room temperature.

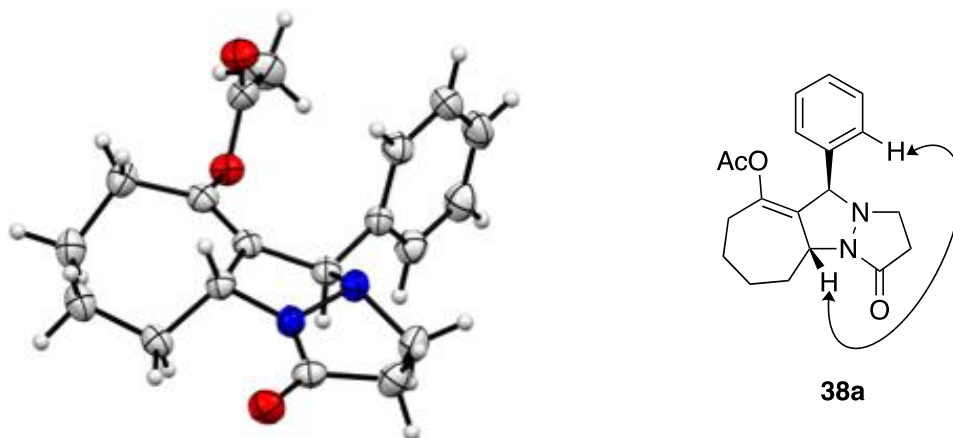
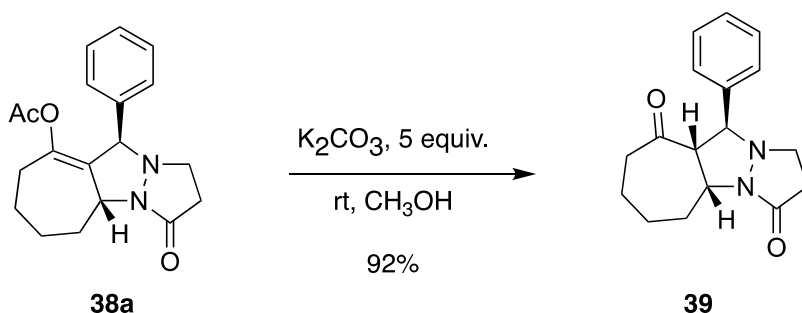


Figure 2.5. X-ray crystal structure of the endo cycloadduct **38a** and TROESY correlations strongly suggesting the relative stereochemistry of cycloadduct **38a**.

Adducts derived from acetoxy-substituted allene **23** possess enol acetate moieties potentially able to serve as handles for further structural elaboration. This would afford a unique entry toward the synthesis of multiple heterocyclic compounds using this ketone moiety as a useful synthetic handle for further functionalization. For instance, the cycloadduct **38a** was hydrolyzed to its ketone form under mild conditions to afford **39** in high yields (Scheme 2.9). To access this class of compounds, such as **39**, there is only one known method where a non-commercially available multifunctional primary amine catalyst must be used.²⁷ Here, we were able to introduce a second approach to this tricyclic compound via cyclic allenes. The relative stereochemistry of **39** was confirmed by single crystal X-ray diffraction analysis (Figure 2.6).



Scheme 2.9. Hydrolysis of the acetate of cycloadduct **38a** to ketone **39**.

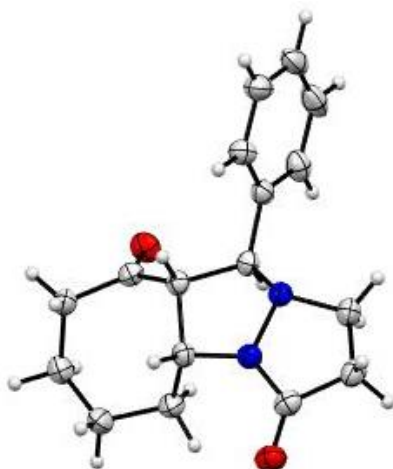
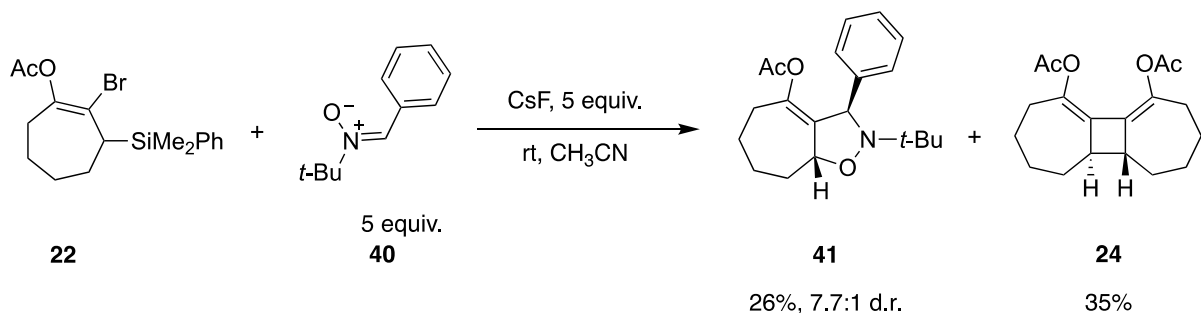


Figure 2.6. X-ray crystal structure of **39**.

The third and final class of 1,3-dipoles we have examined is the nitrone **40**. It was found that nitrones also can undergo [3+2] cycloaddition with 1-acetoxy-1,2-cycloheptadiene, although the yield is slightly lower when compared with the nitrile oxide and azomethine imine examples and with our previous work on six-membered cyclic allenes. Trapping 1-acetoxy-1,2-cycloheptadiene with nitrone **40** allowed for the formation of an isoxazolidine cycloheptane containing compound such as **41**. In the course of trapping cyclic allene **23** with nitrone **40**, cycloadduct **41** was formed in low yield (26%, 7.7:1 d.r.) along with 35% of dimer **24** (Scheme 2.10). Varying the temperature, diluting the reaction, and changing the addition sequence of reagents did not help to increase the yield of the trapping process using nitrone **40**. The relative stereochemistry of **41** was verified by 2D-TROESY as the following observed H–H correlation, which is illustrated by the arrow (Figure 2.7).



Scheme 2.10. Reaction of cyclic allene **23** with nitron **40**.

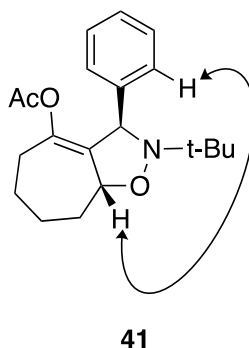
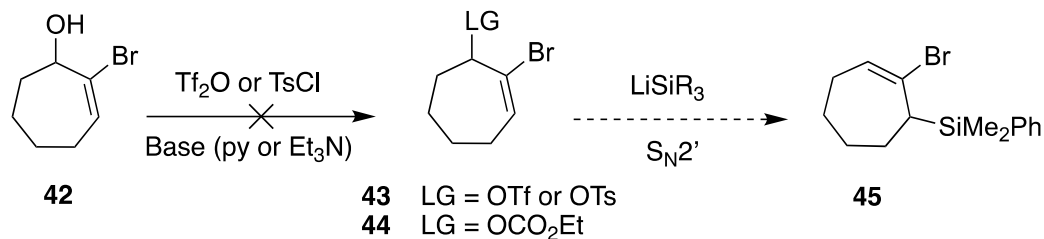


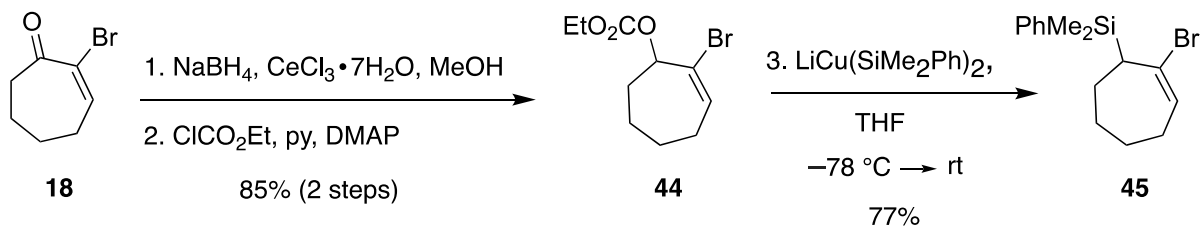
Figure 2.7. TROESY correlations strongly suggesting the relative stereochemistry of cycloadduct **41**.

In addition to the generation and trapping processes of the acetoxy-substituted 1,2-cycloheptadiene **23** with several 1,3-dipoles, we aimed to generate unsubstituted 1,2-cycloheptadiene. We hypothesized that in order to access this type of allene we needed to synthesize allylic silane **45**. To access **45**, we chose to investigate a different route from the one which was proposed in Scheme 2.2. This change in plan was to avoid a multi-step route and a low yielding reaction, which was obtained in the protection step of enone **18** with a ketal group. As a result, we envisioned that SiMe₂Ph can be added to **43** or **44** in a S_N2' reaction (Scheme 2.11). To test this hypothesis, we first attempted to synthesize **42** and **43**, where LG is a triflate and tosylate, respectively. However, these attempts were not successful, and the starting material **42** was recovered.



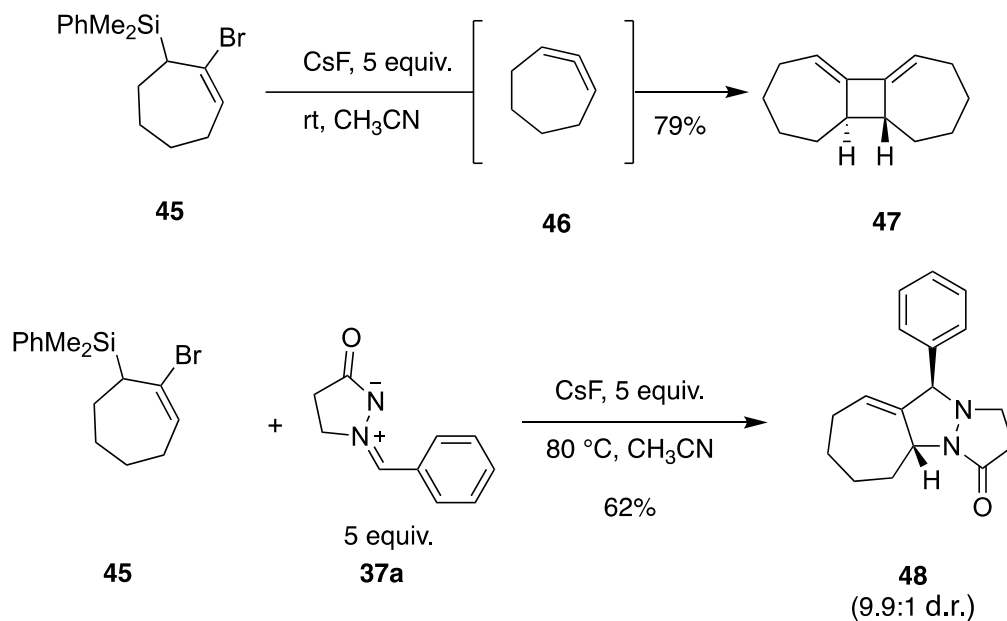
Scheme 2.11. Attempts to synthesize allylic silane **45**.

I then focused on the synthesis of carbonate **44** using well-established chemistry (Scheme 2.12). Carbonate **44** was synthesized from readily available enone **18**, which was reduced to the corresponding alcohol using Luche reduction conditions to form 2-bromocyclohept-2-en-1-ol. This was followed by conversion of alcohol to the corresponding carbonate **44**. A nucleophilic substitution reaction of SiMe_2Ph anion on carbonate **44** enabled us to access precursor **45** in good yield. Although either direct $\text{S}_{\text{N}}2$ displacement of carbonate or $\text{S}_{\text{N}}2'$ reaction with allylic transposition could afford **10**, I believe that this process occurs via the former mechanism based upon related results employing substituted cyclohexenyl carbonates.²⁹



Scheme 2.12. Synthesis of precursor **45** to generate unsubstituted 1,2-cycloheptadiene

Next, using **45**, we were able to examine the dimerization process of unsubstituted 1,2-cycloheptadiene after subjecting it to CsF in acetonitrile at room temperature, and dimer **47** was obtained in high yield. Dimer **47** is a result of the generation and [2+2] dimerization process of the unsubstituted cyclic allene **46** (Scheme 2.12). The proton and carbon NMR and mass spectrometry data of **47** matches with previous reports.^{17, 28} Furthermore, we were able to trap **46** with azomethine imine **37a** in a [3+2] cycloaddition reaction. This reaction afforded cycloadduct **48** in 62% yield (Scheme 2.12).



Scheme 2.13. Dimerization process of unsubstituted cyclic allene **16** and trapping process with azomethine imine **37a**.

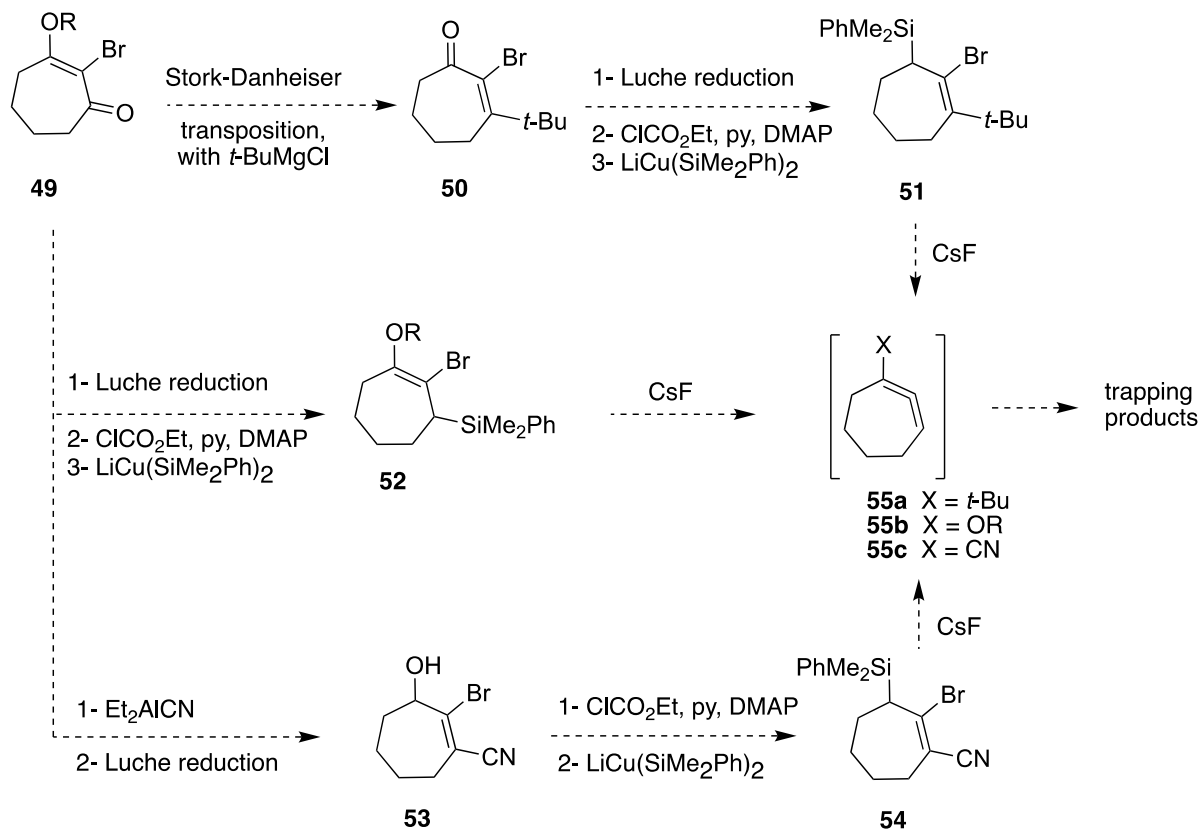
2.5. Conclusion

I successfully reported the first trapping reactions of 1,2-cycloheptadienes with 1,3-dipoles, in addition to the well-established [4+2] cycloaddition with 1,3-diphenylisobenzofuran (DPIBF), under mild conditions via fluoride-mediated elimination. I also described one of the shortest approaches to access 1,2-cycloheptadiene using a convenient route and well-established chemistry. In the case of trapping with nitrile oxide **35** and nitrene **40**, this transformation affords the formation of a new C–O bond in addition to the C–C bond to the central allene carbon. In the case of trapping with azomethine imines **37a–h**, new C–N

bonds are formed through this methodology, and a new C—C bonds are formed along with two stereogenic centres in high diastereo- and regioselectivity. We demonstrated that the acetoxy cycloadducts can be hydrolyzed to the corresponding ketone, introducing a convenient handle for further functionalization of these complex products. In this chapter, we illustrated that valuable building blocks containing cycloheptane functionalized materials for the construction of complex molecular scaffolds can be produced by utilizing the reactivity found in 1,2-cycloheptadiene.

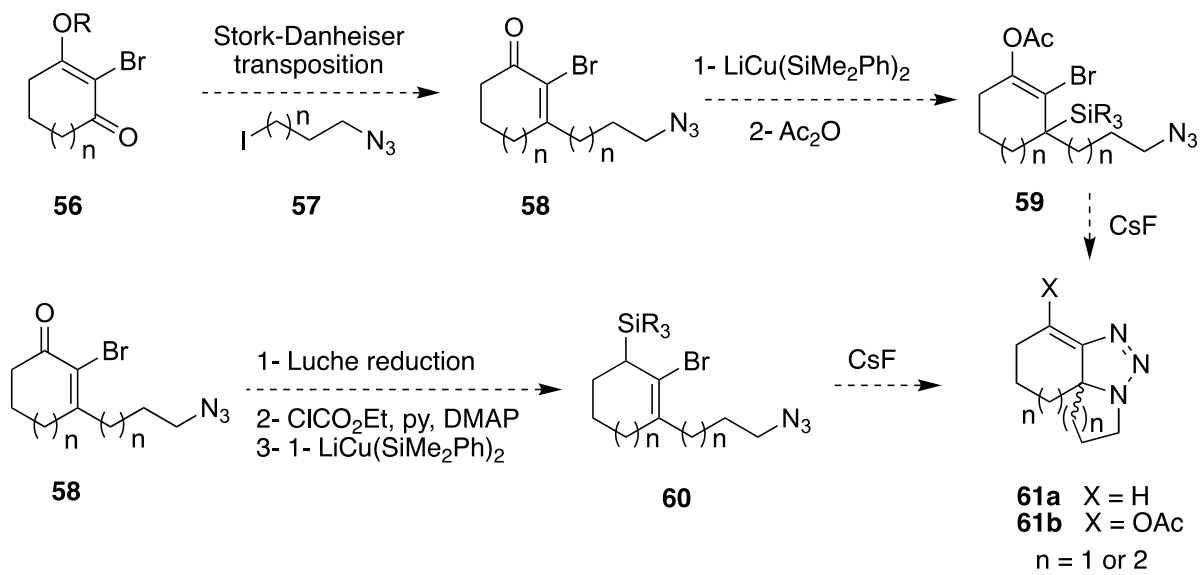
2.6. Future Directions

In this chapter, I described new synthetic methodology that demonstrated that the reactivity of strained cyclic allenes can be harnessed to produce complex scaffolds. However, further investigations are needed in this area. One possible study that could be carried out in future is to focus on varying the substitution on the allene with a sterically bulky group **55a**, electron releasing group (ERG) **55b**, and electron withdrawing group (EWG) **55c**. Via the routes shown in Scheme 2.13, it would be worthwhile to evaluate the generation of these monosubstituted 1,2-cycloheptadienes **55a–c** and their trapping reactions.



Scheme 2.14. Proposed synthesis of monosubstituted 1,2-cycloheptadienes.

The West group has successfully trapped six-membered cyclic allenes in an intramolecular fashion with pendent furan groups.²⁹ The process appears to tolerate a variety of substituents on the furan, as well as different tethers linking it to the cyclic allene. This transformation also proceeds in complete regioselectivity and diastereoselectivity, and cycloadducts were formed in good yields (Section 1.5.3). In previous work by our group, azides failed to trap 1,2-cyclohexadiene intermolecularly. Therefore, it would be valuable to investigate the intramolecular trapping reactions of both 1,2-cyclohexadienes and 1,2-cycloheptadienes with azide tethers from precursors **59** and **60**. I assume that these precursors can be synthesized possibly by using similar route to our previous method (Section 1.5.3), as shown in Scheme 2.14.



Scheme 2.15. Possible intramolecular trapping of cyclic allenes with azide.

2.7. Experimental and General Information

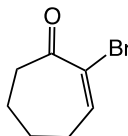
All reactions were carried out in glassware that was stored in an oven overnight or was flame-dried under a positive nitrogen atmosphere, unless otherwise specified. Transfer of anhydrous reagents was accomplished with oven-dried syringes or cannulae. Distilled water (H₂O) was used, and solvents (CH₃CN, DCM, Et₂O, THF, and PhMe) were dried using a solvent purification system, and NEt₃ was distilled before using. Thin layer chromatography was performed on glass plates pre-coated with 0.25 mm Kieselgel 60 F254 (Merck). Flash chromatography columns were packed with 230–400 mesh silica gel (Silicycle), and the stains for TLC analysis were conducted using 2.5% p-anisaldehyde in AcOH-H₂SO₄-EtOH (1:3:86) and further heating until development of color. Reagents were used as purchased from Sigma-Aldrich, Oakwood, and Alfa Aesar.

Proton nuclear magnetic resonance spectra (¹H NMR) were recorded at 400 MHz, 500 MHz, 600 MHz, or 700 MHz and coupling constants (*J*) are reported in Hertz (Hz). Carbon nuclear magnetic resonance spectra (¹³C NMR) were recorded at 100 MHz or 125 MHz. The chemical shifts are reported on the δ scale (ppm) and referenced to the residual solvent peaks (CDCl₃: s, 7.26 ppm, ¹H; t, 77.06 ppm, ¹³C) as internal standards. Standard

notation is used to describe the multiplicity of the signals observed in ^1H NMR spectra: broad (br), apparent (app), multiplet (m), singlet (s), doublet (d), triplet (t), quartet (q), pentet (p), etc. Infrared (IR) spectra were measured with a Mattson Galaxy Series FT-IR 3000 spectrophotometer. Mass spectra were recorded by using electron impact ionization (EI) measured by a Kratos MS50 instrument or electrospray ionization (ESI) measured by Agilent 6220 oaTOF instrument as specified in each case.

Nitrile oxide **35**,³⁰ and azomethine imines **37a–h**,^{31,32} and nitron **40**,³³ are all known literature compounds and were produced via the published routes. ^1H NMR and ^{13}C NMR spectral data matched those reported in the literature. 1,3-Diphenylisobenzofuran (DPIBF) is available from Sigma-Aldrich. Phenyltrimethylsilyl lithium reagent (LiSiMe_2Ph) was prepared by a procedure similar to that employed by Gilman and coworkers,³⁴ which was modified by the West group.²³

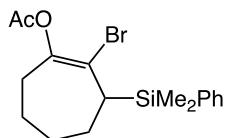
2-Bromocyclohept-2-en-1-one (**18**)



A solution of bromine (1.5 mL, 29.4 mmol) in CH_2Cl_2 (60 mL) was added dropwise to a solution of 2-cyclohepten-1-one (3.64 mL, 32.7 mmol) in CH_2Cl_2 (59 mL). After stirring for 30 min, Et_3N (5.9 mL, 42.5 mmol) was added dropwise to the mixture. The reaction mixture was stirred for 10 min and quenched with 1 M HCl (1 x 30 mL). After the phases were separated, the aqueous layer was extracted with EtOAc (3 x 40 mL), and the combined organic layers were washed successively with 1 M NaOH, an aqueous solution of $\text{Na}_2\text{S}_2\text{O}_3$, brine and dried over MgSO_4 . Filtration, concentration under reduced pressure, and purification by column chromatography on silica gel with 9:1 hexanes/EtOAc afforded 2-bromocyclohept-2-en-1-one **18** (4.7 g, 76% yield) as a slightly yellow oil: $R_f = 0.36$ (8:2, hexanes:EtOAc); ^1H NMR (400 MHz, CDCl_3) δ 7.33 (t, $J = 6.6$ Hz, 1H), 2.77–2.68 (m, 2H), 2.49–2.39 (m, 2H), 1.87–1.77 (m, 4H); ^{13}C NMR (125 MHz, CDCl_3) δ 196.2, 147.8, 126.9, 41.3, 29.3, 24.7, 21.2; IR (cast film, cm^{-1}) 3034, 2941, 2868, 1682, 1599, 1451; HRMS (EI) calcd for $[\text{M}]^+ \text{C}_7\text{H}_9\text{O}^{79}\text{Br}$: 187.9837, found: 187.9833. This compound was prepared by a

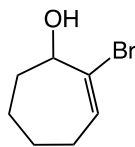
modified procedure, and all characterization data were in agreement with those previously reports.³⁵

2-Bromo-3-(dimethyl(phenyl)silyl)cyclohept-1-en-1-yl acetate (**22**)



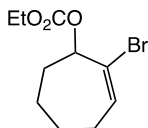
To a suspension of CuBr•DMS (411 mg, 2.0 mmol) complex in THF (13 mL) cooled to 0 °C was added a previously prepared solution of LiSiMe₂Ph (568 mg, 4.0 mmol) via cannula, giving a deep red solution. The cuprate was maintained at 0 °C for 30 min, then the reaction mixture was cooled to -78 °C, and a 0.4 M solution of enone **18** (300 mg, 1.6 mmol) in THF (4 mL) was added dropwise via cannula. This solution was stirred at -78 °C for 3 h, after which Ac₂O (0.75 mL, 8.0 mmol) was added via syringe. The solution was maintained at -78 °C for an additional 1 h, then was warmed up to room temperature for 2 h. A 30 mL portion of Et₂O and a 25 mL portion of distilled water were added. After the phases were separated, the aqueous layer was extracted carefully with Et₂O (3 x 30 mL). The combined organic layers were washed with distilled water and brine, and dried over MgSO₄. Filtration, concentration under reduced pressure, and purification by column chromatography on silica gel with 3:1 hexanes/DCM afforded the corresponding allylic silyl **22** (480 mg, 83% yield) as a colourless oil: R_f = 0.63 (9:1, hexanes:EtOAc); ¹H NMR (500 MHz, CDCl₃) δ 7.63–7.58 (m, 2H), 7.4–7.36 (m, 3H), 2.56–2.55 (m, 1H), 2.17 (s, 3H), 2.11–2.05 (m, 2H), 1.83–1.70 (m, 3H), 1.58–1.52 (m, 1H), 1.52–1.43 (m, 2H), 0.54 (s, 3H) 0.50 (s, 3H); ¹³C NMR (125 MHz, CDCl₃) δ 168.3, 147.0, 138.0, 134.1, 129.2, 127.8, 116.2, 39.2, 32.2, 28.4, 27.5, 24.9, 20.8, -1.8, -2.1; IR (cast film, cm⁻¹) 3069, 3048, 3020, 3928, 2859, 1756, 1654, 1589, 1445, 1428; HRMS (EI) calcd for [M]⁺ C₁₇H₂₃⁷⁹BrSiO₂: 366.0651, found: 366.0649.

2-Bromocyclohept-2-en-1-ol



To a solution of enone **18** (1.5 g, 7.9 mmol) and $\text{CeCl}_3 \cdot 7\text{H}_2\text{O}$ (3.5 g, 8.7 mmol) in MeOH (18 mL) was added NaBH_4 (420 mg, 11.1 mmol) portion-wise at 0 °C. The resulting mixture was then warmed and stirred at room temperature for 1 h, after which it was cooled to 0 °C and quenched with 1 M HCl (1 x 25 mL) at 0 °C. After the phases were separated, the aqueous layer was extracted with Et₂O (3 x 25 mL), and the combined organic layers were washed with brine and dried over MgSO_4 . Filtration, concentration under reduced pressure, and purification by column chromatography on silica gel with 8:2 hexanes/EtOAc afforded 2-bromocyclohept-2-en-1-ol (1.3 g, 90% yield) as a colourless oil: $R_f = 0.32$ (8:2, hexanes:EtOAc); $^1\text{H NMR}$ (500 MHz, CDCl_3) δ 6.32 (t, $J = 6.7$ Hz, 1H), 4.48–4.46 (m, 1H), 2.29–2.14 (m, 1H), 2.14–2.01 (m, 1H), 1.98–1.79 (m, 3H), 1.73–1.58 (m, 3H) [Note: the OH proton of the allylic alcohol was not detected.]; $^{13}\text{C NMR}$ (125 MHz, CDCl_3) δ 134.4, 129.9, 75.5, 32.4, 28.0, 25.9, 23.2; IR (cast film, cm^{-1}) 3400, 3035, 2930, 2861, 2690, 1637, 1445; HRMS (EI) calcd for $[\text{M}]^+ \text{C}_7\text{H}_{11}^{79}\text{BrO}$: 189.9993, found: 189.9994. All characterization data were in agreement with those previously reports.³⁶

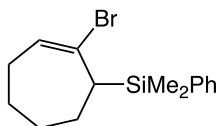
2-Bromocyclohept-2-en-1-yl ethyl carbonate (46)



To a solution of 2-bromocyclohept-2-en-1-ol (1.36 g, 7.1 mmol) and pyridine (0.85 mL, 10.7 mmol) in DCM (50 mL) was slowly added ethyl chloroformate (0.80 mL, 8.5 mmol) at 0 °C. The resulting mixture was then warmed and stirred at room temperature for 1 h after 20 mg of DMAP was added. Once the reaction was complete, as determined by TLC, the mixture was cooled to 0 °C and quenched with ice-cold 1 M HCl (1 x 35 mL). After the phases were separated, the aqueous layer was extracted with DCM (3 x 30 mL), and the combined organic layers were washed with an aqueous solution of NaHCO_3 , H_2O , brine, and dried over

MgSO₄. Filtration, concentration under reduced pressure, and purification by column chromatography on silica gel with 9:1 hexanes/EtOAc afforded 2-bromocyclohept-2-en-1-yl ethyl carbonate **46** (1.7 g, 88% yield) as a pale yellow oil: $R_f = 0.65$ (9:1, hexanes:EtOAc); ¹H NMR (500 MHz, CDCl₃) δ 6.46 (t, $J = 6.7$ Hz, 1H), 5.45–5.43 (m, 1H), 4.26 (m, 2H), 2.34–2.24 (m, 1H), 2.19–2.01 (m, 2H), 1.98–1.87 (m, 2H), 1.79–1.68 (m, 2H), 1.68–1.59 (m, 1H), 1.36 (t, $J = 7.1$ Hz, 3H). ¹³C NMR (125 MHz, CDCl₃) δ 154.5, 137.9, 123.1, 80.8, 64.2, 29.9, 28.1, 25.7, 23.4, 14.3; IR (cast film, cm⁻¹) 3044, 2983, 2936, 2864, 1746, 1641, 1448; HRMS (ESI) calcd for [M+Na]⁺ C₁₀H₁₅⁷⁹BrNaO₃: 285.0097, found: 285.0096.

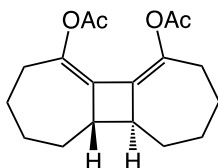
(2-Bromocyclohept-2-en-1-yl)dimethyl(phenyl)silane (**45**)



To a suspension of CuBr•DMS (350 mg, 1.7 mmol) complex in THF (11.3 mL) cooled to 0 °C was added a previously prepared solution of LiSiMe₂Ph (405 mg, 2.85 mmol) dropwise via cannula, giving a deep red solution. The cuprate solution was maintained at 0 °C for 30 min, then it was cooled to –78 °C, and a 0.4 M solution of 2-bromocyclohept-2-en-1-yl ethyl carbonate **46** (300 mg, 1.14 mmol) in THF (2.85 mL) was added dropwise via cannula. The solution was maintained at –78 °C for 3 h. After the mixture was warmed up to room temperature, a 30 mL portion of Et₂O and a 25 mL portion of distilled water were added and left to stir for 5–10 min. After the phases were separated, the aqueous layer was extracted carefully with Et₂O (3 x 30 mL). The combined organic layers were washed with distilled water and brine, and dried over MgSO₄. Filtration, concentration under reduced pressure, and purification by column chromatography on silica gel with 20:1 hexanes/DCM afforded the corresponding allylic silyl **45** (180 mg, 77% yield) as a colourless oil: $R_f = 0.78$ (9:1, hexanes:DCM); ¹H NMR (500 MHz, CDCl₃) δ 7.65–7.59 (m, 2H), 7.43–7.36 (m, 3H), 6.14 (dd, $J = 9.2, 4.3$ Hz, 1H), 2.62 (t, $J = 5.0$ Hz, 1H), 1.96–1.85 (m, 1H), 1.84–1.75 (m, 1H), 1.78–1.65 (m, 1H), 1.61–1.55 (m, 2H), 1.52–1.41 (m, 1H), 1.37–1.23 (m, 1H), 0.97–0.87 (m, 1H), 0.56 (s, 3H), 0.52 (s, 3H); ¹³C NMR (125 MHz, CDCl₃) δ 138.2, 134.1, 131.0, 129.2, 127.7, 127.6, 43.9, 29.1, 28.6, 28.3, 27.2, –1.5, –2.1; IR (cast film, cm⁻¹) 3069, 3048, 2924,

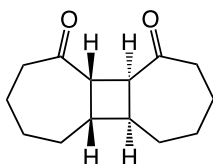
2851, 1629, 1445, 1427; HRMS (EI) calcd for $[M]^+$ $C_{15}H_{21}^{79}BrSi$: 308.0596, found: 308.0593.

2,10-Diacetoxytricyclo[7.5.0^{2,8}]tetradeca-7,9-diene (**24**)



To a dry 25 mL round-bottom flask was added allylic silane **22** (300 mg, 0.8 mmol), CsF (620 mg, 4.1 mmol), and 100 mg of 3Å molecular sieve. Then, a nitrogen atmosphere was established via a purge needle. To the flask, CH_3CN (8 mL) was added via syringe, and the reaction mixture was allowed to stir overnight at room temperature. The resulting mixture was concentrated under reduced pressure and purified by column chromatography on silica gel with 8:2 hexanes/EtOAc to afford the corresponding dimer **24** (107 mg, 85% yield) as a white solid: R_f = 0.62 (8:2, hexanes:EtOAc); mp = 109.2–110.0 °C; 1H NMR (700 MHz, $CDCl_3$) δ 2.48–2.41 (m, 4H), 2.14–2.08 (m, 8H), 1.91–1.84 (m, 4H), 1.78–1.71 (m, 2H), 1.61–1.55 (m, 2H), 1.48–1.33 (m, 4H); ^{13}C NMR (175 MHz, $CDCl_3$) δ 169.0, 143.4, 127.1, 44.9, 34.3, 32.8, 28.9, 25.5, 21.0; IR (cast film, cm^{-1}) 2925, 2851, 17501, 1710, 1680, 1444; HRMS (EI) calcd for $[M]^+$ $C_{18}H_{24}O_4$: 304.1675, found: 304.1678.

Tricyclo[7.5.0^{2,8}]tetradeca-3,14-dione (**25**)

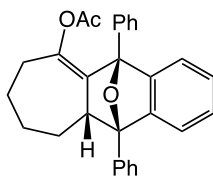


To a stirred solution of dimer **24** (90 mg, 0.3 mmol) in CH_3OH (10 mL) was added K_2CO_3 (210 mg, 1.5 mmol) at room temperature. The reaction vessel was sealed, allowed to stir for 2 h, then filtered, concentrated under reduced pressure, and purified by column chromatography on silica gel with 7:3 hexanes/EtOAc to afford **25** as a white crystalline solid (57 mg, 87% yield): R_f = 0.41 (7:3, hexanes:EtOAc); mp = 78.5–79.4 °C; 1H NMR (700 MHz, $CDCl_3$) δ 3.76–3.72 (m, 2H), 2.45–2.40 (m, 4H), 2.07–2.01 (m, 2H), 1.89–1.78

(m, 6H), 1.49–1.41 (m, 2H), 1.38–1.30 (m, 2H), 1.30–1.22 (m, 2H); ^{13}C NMR (175 MHz, CDCl_3) δ 211.4, 45.7, 43.1, 39.3, 32.4, 27.6, 24.7; IR (cast film, cm^{-1}) 2926, 2855, 1699, 1446; HRMS (EI) calcd for $[\text{M}]^+$ $\text{C}_{14}\text{H}_{20}\text{O}_2$: 220.1463, found: 220.1461.

X-ray quality crystals were grown via slow evaporation from a solution of **25** in EtOAc. Relative stereochemistry was determined by X-ray crystallography (Appendix II).

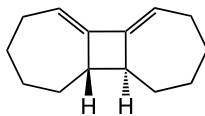
(5S,10aR,11R)-5,11-Diphenyl-7,8,9,10,10a,11-hexahydro-5H-5,11-epoxycyclohepta[b]naphthalen-6-yl acetate (27)



To a dry flask was added allylic silane **22** (150 mg, 0.41 mmol), 1,3-diphenylisobenzofuran (DPIBF) (324 mg, 1.2 mmol), CsF (311 mg, 2.1 mmol), and 100 mg of 3Å molecular sieve. Then, a nitrogen atmosphere was established via a purge needle. To the flask, CH_3CN (20.5 mL) was added via syringe, and the reaction mixture was allowed to stir overnight at room temperature. The resulting mixture was concentrated under reduced pressure and purified by column chromatography on silica gel with 9:1 hexanes/EtOAc to afford the endo product **27** (146 mg, 84% yield) as a pale yellow solid: $R_f = 0.75$ (8:2, hexanes:EtOAc); mp = 174.1–175.0 °C; ^1H NMR (500 MHz, CDCl_3) δ 7.90–7.79 (m, 2H), 7.73–7.56 (m, 3H), 7.51–7.30 (m, 6H), 7.26–6.20 (m, 2H), 7.13 (d, $J = 7.3$ Hz, 1H), 3.56 (d, $J = 11.4$ Hz, 1H), 2.69–2.59 (m, 1H), 2.07–1.99 (m, 2H), 1.80–1.73 (m, 2H), 1.6–1.53 (m, 1H), 1.37 (s, 3H), 1.31–1.18 (m, 1H), 0.38–0.22 (m, 1H); ^{13}C NMR (100 MHz, CDCl_3) δ 168.5, 146.6, 143.7, 142.9, 136.1, 135.5, 134.1, 128.7, 128.7, 128.5, 128.4, 128.3, 128.2, 127.3, 126.2, 122.2, 120.6, 90.3, 90.3, 48.2, 33.6, 30.6, 28.3, 24.5, 19.9; IR (cast film, cm^{-1}) 3062, 3030, 2928, 2854, 1750, 1705, 1603, 1500, 1458, 1447; HRMS (EI) calcd for $[\text{M}]^+$ $\text{C}_{29}\text{H}_{26}\text{O}_3$: 422.1882, found: 422.1889.

X-ray quality crystals were grown via slow evaporation from a solution of cycloadduct **27** in EtOAc. Relative stereochemistry was determined by X-ray crystallography (Appendix III).

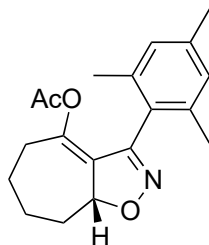
***trans*-Tricyclo[7.5.0.0^{2,8}]tetradeca-7,9-diene (**47**)**



To a dry flask was added allylic silane **45** (300 mg, 1.0 mmol), CsF (740 mg, 4.9 mmol) and 100 mg of 3Å molecular sieve. Then, a nitrogen atmosphere was established via a purge needle. To the flask, CH₃CN (10 mL) was added via syringe, and the reaction mixture was allowed to stir overnight at room temperature. The resulting mixture was concentrated under reduced pressure and purified by column chromatography on silica gel with hexanes to afford the corresponding dimer **47** (72 mg, 79% yield): *R_f* = 0.63 (hexanes); ¹H NMR (600 MHz, CDCl₃) δ 5.84–5.78 (m, 2H), 2.50–2.44 (m, 2H), 2.25–2.17 (m, 2H), 2.13–2.04 (m, 2H), 2.04–1.95 (m, 2H), 1.93–1.90 (m, 2H), 1.87–1.79 (m, 2H), 1.46–1.36 (m, 2H), 1.34–1.22 (m, 4H); ¹³C NMR (150 MHz, CDCl₃) δ 145.8, 118.4, 48.5, 33.2, 30.9, 29.6, 28.8; IR (cast film, cm⁻¹) 3419, 2919, 2848, 2684, 1713, 1673, 1445; HRMS (EI) calcd for [M]⁺ C₁₄H₂₀: 188.1564, found: 188.1563.

Optimized Procedure for Initial Cyclic Allene Cycloaddition of Acetoxy-Substituted 1,2-Cycloheptadiene **23 with Nitrile Oxide **35****

3-Mesityl-6,7,8,8a-tetrahydro-5H-cyclohepta[d]isoxazol-4-yl acetate (36**)**



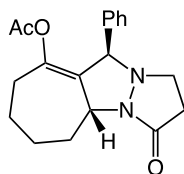
To a dry flask was added allylic silane **22** (190 mg, 0.5 mmol), nitrile oxide **35** (417 mg, 2.5 mmol), CsF (380 mg, 2.5 mmol), and 100 mg of 3Å molecular sieve. Then, a nitrogen atmosphere was established via a purge needle. To the flask, CH₃CN (25.0 mL) was added via syringe, and the reaction mixture was allowed to stir overnight at room temperature. The resulting mixture was concentrated under reduced pressure and purified by column chromatography on silica gel with 9:1 hexanes/EtOAc to afford the corresponding

cycloadduct **36** (130 mg, 80% yield) as a colourless oil: $R_f = 0.22$ (9:1, hexanes:EtOAc); ^1H NMR (700 MHz, CDCl_3) δ 6.86 (s, 2H), 5.35–5.33 (m, 1H), 2.55–2.53 (m, 1H), 2.25 (s, 3H), 2.16–2.11 (m, 7H), 2.04–1.99 (m, 1H), 1.82–1.66 (m, 5H), 1.22 (s, 3H); ^{13}C NMR (175 MHz, CDCl_3) δ 168.4, 154.5, 145.4, 138.3, 137.4, 137.3, 131.5, 127.9, 127.8, 126.3, 83.9, 35.3, 32.2, 27.1, 25.6, 21.0, 19.6, 19.4, 18.9; IR (cast film, cm^{-1}) 2930, 2858, 1762, 1684, 1612, 1580, 1545, 1485, 1444; HRMS (EI) calcd for $[\text{M}]^+$ $\text{C}_{19}\text{H}_{23}\text{NO}_3$: 313.1678, found: 313.1677.

General and Optimized Procedure for Initial Cyclic Allene Cycloaddition of 1,2-Cycloheptadienes **23** and **46** with Azomethine Imines (**37a–h**)

To a dry flask was added allylic silane **22** (1 equiv.), the appropriate azomethine imine **37a–h** (5 equiv.), CsF (3 equiv.), and 100 mg of 3Å molecular sieve. Then, a nitrogen atmosphere was established via a purge needle. To the flask, CH_3CN was added to achieve substrate concentration of 0.02 M, and the reaction was heated to 80 °C and stirred for 2 h, unless otherwise specified. The resulting mixture was cooled to room temperature, concentrated under reduced pressure, and purified by column chromatography on silica gel with 80:20:1 EtOAc/hexanes/ NEt_3 to afford the corresponding cycloadducts **38a–h**.

(4aR,10R)-3-Oxo-10-phenyl-2,3,4a,5,6,7,8,10-octahydro-1H-cyclohepta[c]pyrazolo[1,2-a]pyrazol-9-yl acetate (**38a**)

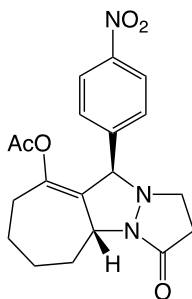


The general procedure was followed using allyl silane **22** (182 mg, 0.50 mmol), azomethine imine **37a** (435 mg, 2.50 mmol), and CsF (227 mg, 1.50 mmol) in CH_3CN (25.0 mL) to furnish 109 mg of **38a** (67%) as a white solid: $R_f = 0.25$ (EtOAc); mp = 114.1–114.9 °C; ^1H NMR (400 MHz, CD_3OD , 60 °C) δ 7.34–7.25 (m, 3H), 7.21–7.14 (m, 2H), 4.65–4.57 (m, 1H), 4.46 (app d, $J = 3.5$ Hz, 1H), 3.28–3.26 (m, 1H), 3.03–2.94 (m, 2H), 2.64–2.52 (m, 2H), 2.52–2.42 (m, 1H), 2.29–2.16 (m, 1H), 2.12–1.98 (m, 2H), 1.80–1.48 (m, 6H); ^{13}C NMR

(100 MHz, CD₃OD, 60 °C) δ 168.3, 168.2, 146.4, 136.5, 133.5, 128.8, 128.2, 128.0, 69.6, 56.6, 45.7, 34.2, 33.3, 30.0, 27.6, 24.3, 18.4; IR (cast film, cm⁻¹) 3063, 2929, 2855, 1754, 1682, 1602, 1496, 1454, 1434, 1418; HRMS (ESI) calcd for [M+H]⁺ C₁₉H₂₃N₂O₃: 327.1703, found: 327.1701.

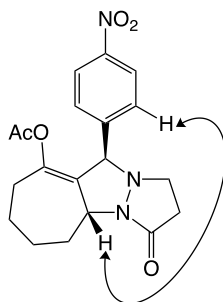
X-ray quality crystals were grown via slow evaporation from a solution of **38a** in EtOAc. Relative stereochemistry was determined by X-ray crystallography (Appendix IV).

(4aR,10R)-10-(4-Nitrophenyl)-3-oxo-2,3,4a,5,6,7,8,10-octahydro-1H-cyclohepta[c]pyrazolo[1,2-a]pyrazol-9-yl acetate (38b)

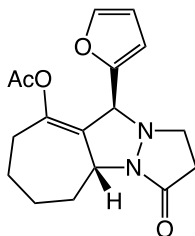


The general procedure was followed using allyl silane **22** (218 mg, 0.59 mmol), azomethine imine **37b** (650 mg, 2.96 mmol), and CsF (270 mg, 1.78 mmol) in CH₃CN (29.5 mL) to furnish 156 mg of **38b** (71%) as a yellow solid. It was necessary to run the reaction overnight (ca. 10 h) at rt to obtain optimized yields: R_f = 0.33 (EtOAc); mp = 129.4–130.2 °C; ¹H NMR (400 MHz, CDCl₃, 60 °C) δ 8.22–8.14 (m, 2H), 7.45–7.37 (m, 2H), 4.61–4.53 (m, 1H), 4.33 (s, 1H), 3.06–3.01 (m, 1H), 2.97–2.85 (m, 2H), 2.60–2.53 (m, 2H), 2.52–2.41 (m, 1H), 2.12–2.02 (m, 2H), 1.82–1.68 (m, 2H), 1.68–1.51 (m, 5H); ¹³C NMR (100 MHz, CDCl₃, 60 °C) δ 167.3, 166.3, 148.0, 146.8, 144.7, 133.7, 129.8, 123.5, 69.8, 56.7, 47.6, 35.3, 33.8, 29.7, 27.7, 24.4, 19.7; IR (cast film, cm⁻¹) 3106, 3075, 2931, 2856, 17.55, 1683, 1604, 1523, 1419; HRMS (ESI) calcd for [M+H]⁺ C₁₉H₂₂N₃O₅: 372.1554, found: 372.1567.

The relative configuration of **38b** was assigned via the 2D TROESY correlation illustrated below:

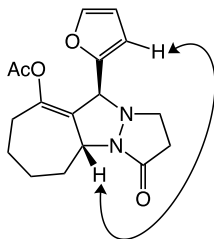


(4aR,10S)-10-(Furan-2-yl)-3-oxo-2,3,4a,5,6,7,8,10-octahydro-1H-cyclohepta[c]pyrazolo[1,2-a]pyrazol-9-yl acetate (38c)

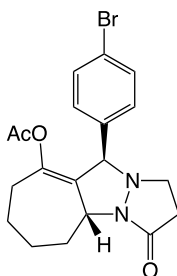


The general procedure was followed using allyl silane **22** (172 mg, 0.47 mmol), azomethine imine **37c** (385 mg, 2.34 mmol), and CsF (214 mg, 1.41 mmol) in CH₃CN (23.5 mL) to furnish 81 mg of **38c** (54%) as a white solid: $R_f = 0.29$ (EtOAc); mp = 111.1–112.0 °C; ¹H NMR (600 MHz, CDCl₃, 60 °C) δ 7.40 (br s, 1H), 6.33 (br s, 1H), 6.17 (br s, 1H), 4.74–4.66 (m, 2H), 3.30 (dt, $J = 11.6, 9.5$ Hz, 1H), 3.12 (ddd, $J = 11.7, 10.0, 4.3$ Hz, 1H), 2.65–2.60 (m, 1H), 2.37–2.32 (m, 1H), 2.19–2.11 (m, 1H), 2.09–2.04 (m, 1H), 1.90 (s, 3H), 1.88–1.68 (m, 5H), 1.66–1.56 (m, 1H); ¹³C NMR (151 MHz, CDCl₃, 60 °C) δ 172.3, 167.8, 150.2, 146.7, 143.1, 131.5, 110.7, 110.0, 61.4, 56.1, 43.7, 33.9, 32.3, 31.8, 28.0, 24.8, 20.0; IR (cast film, cm⁻¹) 3114, 2932, 2857, 1755, 1698, 1497, 1444, 1370; HRMS (ESI) calcd for [M+Na]⁺ C₁₇H₂₀N₂NaO₄: 339.1315, found: 339.1315.

The relative configuration of **38c** was assigned via the 2D TROESY correlation illustrated below:

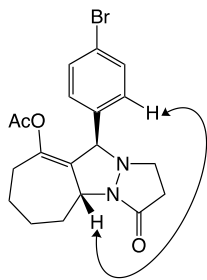


(4aR,10R)-10-(4-Bromophenyl)-3-oxo-2,3,4a,5,6,7,8,10-octahydro-1H-cyclohepta[c]pyrazolo[1,2-a]pyrazol-9-yl acetate (38d**)**

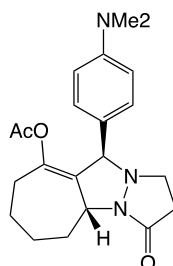


The general procedure was followed using allyl silane **22** (167 mg, 0.45 mmol), azomethine imine **37d** (574 mg, 2.27 mmol), and CsF (205 mg, 1.35 mmol) in CH₃CN (22.5 mL) to furnish 135 mg of **38d** (74%) as a pale yellow solid: *R_f* = 0.25 (EtOAc); mp = 122.1–123.4 °C; ¹H NMR (600 MHz, CDCl₃, 60 °C) δ 7.50–7.45 (m, 2H), 7.12–7.07 (m, 2H), 4.57 (app d, *J* = 11.1 Hz, 1H), 4.26 (br s, 1H), 3.07–3.03 (m, 1H), 2.92 (app q, *J* = 9.8 Hz, 1H), 2.85–2.79 (m, 1H), 2.61–2.51 (m, 2H), 2.41–2.38 (m, 1H), 2.13–2.04 (m, 2H), 1.81–1.67 (m, 2H), 1.67–1.51 (m, 5H); ¹³C NMR (150 MHz, CDCl₃, 60 °C) δ 167.5, 167.0, 146.3, 136.1, 133.8, 131.7, 130.5, 122.3, 69.9, 56.7, 47.0, 35.0, 33.9, 30.0, 27.9, 24.5, 19.7; IR (cast film, cm⁻¹) 2930, 2855, 1754, 1683, 1590, 1488, 1435, 1419, 1369; HRMS (ESI) calcd for [M+H]⁺ C₁₉H₂₂⁷⁹BrN₂O₃: 405.0808, found: 405.0798.

The relative configuration of **38d** was assigned via the 2D TROESY correlation illustrated below:

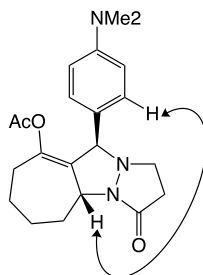


(4aR,10R)-10-(4-(Dimethylamino)phenyl)-3-oxo-2,3,4a,5,6,7,8,10-octahydro-1H-cyclohepta[c]pyrazolo[1,2-a]pyrazol-9-yl acetate (38e**)**

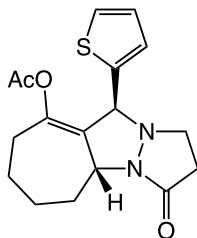


The general procedure was followed using allyl silane **22** (207 mg, 0.56 mmol), azomethine imine **37e** (611 mg, 2.82 mmol), and CsF (255 mg, 1.68 mmol) in CH₃CN (28.0 mL) to furnish 105 mg of **38e** (51%) as a yellow solid. It was necessary to run the reaction overnight (ca. 10 h) at rt to obtain optimized yields: $R_f = 0.50$ (EtOAc); mp = 131.7–132.9 °C; ¹H NMR (600 MHz, CDCl₃, 60 °C) δ 7.03–6.98 (m, 2H), 6.70–6.65 (m, 2H), 4.64 (d, $J = 10.9$ Hz, 1H), 4.36 (s, 1H), 3.04–3.00 (m, 2H), 2.95 (s, 6H), 2.65–2.60 (m, 2H), 2.43–2.40 (m, 1H), 2.21 (m, 1H), 2.15–2.05 (m, 2H), 1.81–1.55 (m, 7H); ¹³C NMR (150 MHz, CDCl₃, 60 °C) δ 168.8, 168.0, 150.7, 145.8, 134.4, 129.8, 124.0, 112.5, 69.7, 56.7, 45.6, 40.4, 34.5, 34.1, 30.9, 28.3, 24.9, 20.0; IR (cast film, cm⁻¹) 3452, 3357, 2974, 2942, 2912, 2972, 2853, 2804, 1741, 1687, 1611, 1524, 1487, 1448; HRMS (ESI) calcd for [M+H]⁺ C₂₁H₂₈N₃O₃: 370.2125, found: 370.2121.

The relative configuration of **38e** was assigned via the 2D TROESY correlation illustrated below:

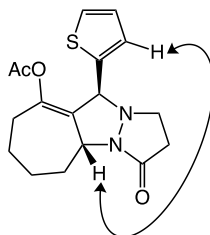


(4aR,10S)-3-Oxo-10-(thiophen-2-yl)-2,3,4a,5,6,7,8,10-octahydro-1H-cyclohepta[c]pyrazolo[1,2-a]pyrazol-9-yl acetate (38f)

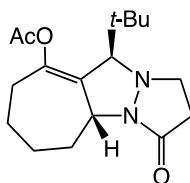


The general procedure was followed using allyl silane **22** (178 mg, 0.48 mmol), azomethine imine **37f** (432 mg, 2.40 mmol), and CsF (219 mg, 1.44 mmol) in CH₃CN (24.0 mL) to furnish 101 mg of **38f** (63%) as a faintly red solid: $R_f = 0.25$ (EtOAc); mp = 104–105 °C; ¹H NMR (400 MHz, CDCl₃, 60 °C) δ 7.28 (app dd, $J = 5.1, 1.2$ Hz, 1H), 6.96 (app dd, $J = 5.1, 3.5$ Hz, 1H), 6.87 (br s, 1H), 4.81 (br s, 1H), 4.67–4.65 (m, 1H), 3.16–3.13 (m, 1H), 3.10–2.99 (m, 1H), 2.64–2.51 (m, 1H), 2.47–2.40 (m, 2H), 2.21–2.00 (m, 3H), 1.85–1.51 (m, 7H); ¹³C NMR (100 MHz, CDCl₃, 60 °C) δ 169.1, 167.7, 146.7, 139.0, 133.8, 127.2, 126.9, 126.3, 63.6, 55.7, 44.3, 33.9, 31.1, 29.6, 27.9, 24.7, 19.9; IR (cast film, cm⁻¹) 3070, 2929, 2855, 1753, 1683, 1418, 1369; HRMS (EI) calcd for [M]⁺ C₁₇H₂₀N₂SO₃: 332.1195, found: 332.1194.

The relative configuration of **38f** was assigned via the 2D TROESY correlation illustrated below:

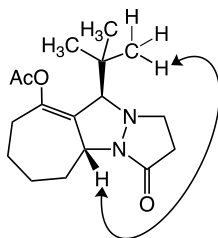


(4aR,10R)-10-(*tert*-Butyl)-3-oxo-2,3,4a,5,6,7,8,10-octahydro-1H-cyclohepta[*c*]pyrazolo[1,2-*a*]pyrazol-9-yl acetate (38g**)**

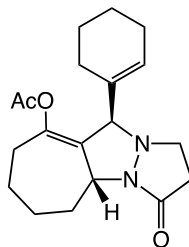


The general procedure was followed using allyl silane **22** (200 mg, 0.54 mmol), azomethine imine **37g** (416 mg, 2.70 mmol), and CsF (246 mg, 1.62 mmol) in CH₃CN (27.0 mL) to furnish 109 mg of **38g** (66%) as a white solid: $R_f = 0.41$ (EtOAc); mp = 88.5–89.4 °C; ¹H NMR (600 MHz, CDCl₃, 60 °C) δ 4.06–4.02 (m, 1H), 3.48–3.40 (m, 2H), 2.94 (m, 1H), 2.79–2.70 (m, 2H), 2.56–2.51 (m, 1H), 2.49–2.38 (m, 1H), 2.22–2.17 (m, 1H), 2.09 (s, 3H), 1.96–1.89 (m, 1H), 1.89–1.83 (m, 1H), 1.75–1.62 (m, 3H), 0.92 (s, 9H); ¹³C NMR (150 MHz, CDCl₃, 60 °C) δ 167.8, 165.2, 148.3, 129.9, 75.1, 57.3, 55.4, 37.7, 36.3, 29.8, 27.1, 25.2, 24.0, 23.3, 21.1; IR (cast film, cm⁻¹) 2949, 2866, 1756, 1678, 1463, 1416; HRMS (ESI) calcd for [M+H]⁺ C₁₇H₂₇N₂O₃: 307.2016, found: 307.2011.

The relative configuration of **38g** was assigned via the 2D TROESY correlation illustrated below:

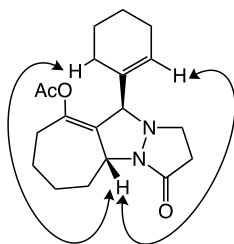


(4aR,10R)-10-(Cyclohex-1-en-1-yl)-3-oxo-2,3,4a,5,6,7,8,10-octahydro-1H-cyclohepta[c]pyrazolo[1,2-a]pyrazol-9-yl acetate (38h)

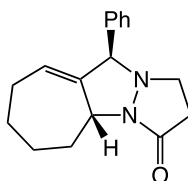


The general procedure was followed using allyl silane **22** (212 mg, 0.58 mmol), azomethine imine **37h** (516 mg, 2.90 mmol), and CsF (264 mg, 1.74 mmol) in CH₃CN (29.0 mL) to furnish 117 mg of **38h** (61%) as a white solid: $R_f = 0.44$ (EtOAc); mp = 95.2–95.9 °C; ¹H NMR (400 MHz, CDCl₃, 60 °C) δ 5.64–5.57 (m, 1H), 4.26 (app d, $J = 10.9$ Hz, 1H), 3.65 (s, 1H), 3.29–3.18 (m, 1H), 2.84–2.72 (m, 2H), 2.72–2.59 (m, 2H), 2.54–2.47 (m, 1H), 2.08–1.82 (m, 9H), 1.72–1.45 (m, 8H); ¹³C NMR (100 MHz, CDCl₃, 60 °C) δ 167.8, 165.0, 145.1, 134.5, 132.5, 128.0, 72.9, 56.2, 47.4, 35.8, 33.7, 29.5, 27.6, 25.5, 24.5, 24.3, 22.4, 22.2, 20.1; IR (cast film, cm⁻¹) 2928, 2856, 1753, 1680, 1437, 1418; HRMS (ESI) calcd for [M+H]⁺ C₁₉H₂₇N₂O₃: 331.2016, found: 331.2014.

The relative configuration of **38h** was assigned via the 2D TROESY correlations illustrated below:

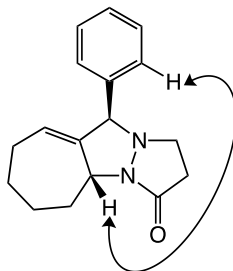


(4aR,10R)-10-Phenyl-1,2,4a,5,6,7,8,10-octahydro-3H-cyclohepta[c]pyrazolo[1,2-a]pyrazol-3-one (48)

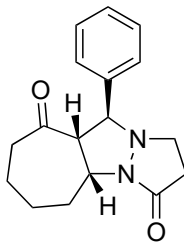


The general procedure was followed using allyl silane **45** (180 mg, 0.58 mmol), azomethine imine **37a** (505 mg, 2.90 mmol), and CsF (264 mg, 1.74 mmol) in CH₃CN (29.0 mL) to furnish 97 mg of **48** (62%) as a colourless oil: *R_f* = 0.38 (EtOAc); ¹H NMR (600 MHz, CDCl₃) δ 7.40–7.30 (m, 5H), 5.36–5.26 (m, 1H), 4.43 (d, *J* = 11.4 Hz, 1H), 4.03 (s, 1H), 3.31 (td, *J* = 8.7, 2.3 Hz, 1H), 3.07–2.99 (m, 1H), 2.83–2.60 (m, 3H), 2.21–2.01 (m, 3H), 1.83–1.66 (m, 2H), 1.44–1.41 (m, 1H), 1.30–1.25 (m, 1H); ¹³C NMR (151 MHz, CDCl₃) δ 165.4, 150.4, 137.3, 128.8, 128.5, 128.2, 125.0, 73.6, 58.7, 49.6, 36.0, 29.1, 28.9, 28.0, 26.6; IR (cast film, cm⁻¹) 3028, 2925, 2850, 1681, 1497, 1441, 1417; HRMS (ESI) calcd for [M+H]⁺ C₁₇H₂₁N₂O: 269.1648, found: 269.1645.

The relative configuration of **48** was assigned via the 2D TROESY correlation illustrated below:



(4aR,9aS,10S)-10-Phenyloctahydro-3H-cyclohepta[c]pyrazolo[1,2-a]pyrazole-3,9(4aH)-dione (39)

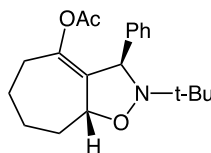


To a stirred solution of **38a** (100 mg, 0.3 mmol) in CH₃OH (10 mL) was added K₂CO₃ (212 mg, 1.5 mmol) at room temperature. The reaction vessel was sealed, , allowed to stir for 2 h, then filtered, concentrated under reduced pressure, and purified by column chromatography on silica gel with 100:2 EtOAc/NEt₃ to afford **39** (80 mg, 92% yield); R_f = 0.32 (EtOAc); mp = 110.9–110.1 °C; ¹H NMR (700 MHz, CDCl₃) δ 7.48–7.44 (m, 2H), 7.33 (d, *J* = 7.2 Hz, 2H), 7.31–7.26 (m, 1H), 4.23 (t, *J* = 11.1 Hz, 1H), 3.96 (app d, *J* = 9.1 Hz, 1H), 3.77 (t, *J* = 9.6 Hz, 1H), 3.30–3.25 (m, 1H), 3.09 (d, *J* = 14.7 Hz, 1H), 2.81–2.76 (m, 1H), 2.73–2.66 (m, 1H), 2.66–2.60 (m, 1H), 2.42–2.37 (m, 2H), 1.91–1.86 (m, 2H), 1.67–1.54 (m, 2H), 1.32–1.23 (m, 1H); ¹³C NMR (125 MHz, CDCl₃) δ 207.4, 164.2, 137.0, 128.6, 128.2, 128.1, 68.2, 67.3, 53.8, 50.0, 43.2, 36.9, 27.92, 25.6, 24.9; ; IR (cast film, cm⁻¹) 3059, 3031, 2931, 2859, 1709, 1681, 1495, 1416; HRMS (ESI) calcd for [M+H]⁺ C₁₇H₂₁N₂O₂: 285.1598, found: 285.1593.

X-ray quality crystals were grown via slow evaporation from a solution of **39** in EtOAc. Relative stereochemistry was determined by X-ray crystallography (Appendix III).

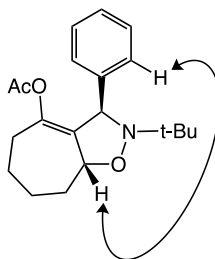
Optimized Procedure for Initial Cyclic Allene Cycloaddition of Acetoxy-Substituted 1,2-Cycloheptadiene **23 with Nitron **40**.**

(3R,8aR)-2-(*tert*-Butyl)-3-phenyl-3,5,6,7,8,8a-hexahydro-2H-cyclohepta[d]isoxazol-4-yl acetate (41**)**



To a dry flask was added allylic silane **22** (200 mg, 0.54 mmol), nitron **40** (483 mg, 2.7 mmol), CsF (414 mg, 2.7 mmol), and 100 mg of 3Å molecular sieve. Then, a nitrogen atmosphere was established via a purge needle. To the flask, CH₃CN (27.0 mL) was added via syringe, and the reaction mixture was allowed to stir overnight at room temperature. The resulting mixture was concentrated under reduced pressure and purified by column chromatography on silica gel with 8:2 hexanes/EtOAc to afford the corresponding cycloadduct **41** (46 mg, 26% yield) as a pale yellow oil: *R_f* = 0.46 (8:2, hexanes:EtOAc); ¹H NMR (500 MHz, CDCl₃) δ 7.40–7.37 (m, 2H), 7.28–7.25 (m, 2H), 7.23–7.18 (m, 1H), 4.73–4.67 (m, 1H), 4.65–4.60 (m, 1H), 2.39–2.37 (m, 1H), 2.17–2.08 (m, 2H), 1.87–1.79 (m, 1H), 1.71 (s, 3H), 1.66–1.56 (m, 4H), 1.01 (s, 9H); ¹³C NMR (125 MHz, CDCl₃) δ 167.9, 142.9, 142.7, 137.8, 129.0, 127.9, 127.0, 67.2, 58.4, 36.6, 32.9, 30.7, 26.2, 25.2, 24.7, 20.3; IR (cast film, cm⁻¹) 3085, 3064, 3028, 2972, 2933, 2859, 1754, 1714, 1683, 1602, 1454; HRMS (ESI) calcd for [M+H]⁺ C₂₀H₂₈NO₃: 330.2064, found: 330.2059.

The relative configuration of **41** was assigned via the 2D TROESY correlation illustrated below:



2.8. References

1. Schönbein, C. F., *Ber. Verh. Nat. Ges. Basel* **1847**, 7, 4-6.
2. Gothelf, K. V.; Jørgensen, K. A., *Chem. Rev.* **1998**, 98 (2), 863-910.
3. Padwa, A.; Craig, S. P.; Chiacchio, U.; Kline, D. N., *J. Org. Chem.* **1988**, 53 (10), 2232-2238.
4. Pellissier, H.; Santelli, M., *Tetrahedron* **2003**, 59 (6), 701-730.
5. Wenk, H. H.; Winkler, M.; Sander, W., *Angew. Chem. Int. Ed.* **2003**, 42 (5), 502-528.
6. Tadross, P. M.; Stoltz, B. M., *Chem. Rev.* **2012**, 112 (6), 3550-3577.
7. Wu, C.; Shi, F., *Asian J. Org. Chem.* **2013**, 2 (2), 116-125.
8. Bhunia, A.; Yetra, S. R.; Biju, A. T., *Chem. Soc. Rev.* **2012**, 41 (8), 3140-3152.
9. Sanz, R., *Org. Prep. Proced. Int.* **2008**, 40 (3), 215-291.
10. Gampe, C. M.; Carreira, E. M., *Angew. Chem. Int. Ed.* **2012**, 51 (16), 3766-3778.
11. Yoshida, H.; Takaki, K., *Synlett* **2012**, 23 (12), 1725-1732.
12. Dubrovskiy, A. V.; Markina, N. A.; Larock, R. C., *Org. Biomol. Chem.* **2013**, 11 (2), 191-218.
13. Hoffmann, R. W.; Suzuki, K., *Angew. Chem. Int. Ed.* **2013**, 52 (10), 2655-2656.
14. Goetz, A. E.; Garg, N. K., *J. Org. Chem.* **2014**, 79 (3), 846-851.
15. Moss, R. A.; Platz, M. S.; Jones Jr, M., *Reactive Intermediate Chemistry*. John Wiley & Sons: 2004.
16. Sary, I.; Stara, I. G.; Dodziuk, H., *Strained Hydrocarbons: Beyond the van't Hoff and Le Bel Hypothesis*. Wiley-VCH, Weinheim: 2009.
17. Ball, W. J.; Landor, S. R., *Proc. Chem. Soc.* **1961**, 143-144.
18. Bottini, A. T.; Frost II, K. A.; Anderson, B. R.; Dev, V., *Tetrahedron* **1973**, 29 (14), 1975-1981.
19. Kropp, P. J.; McNeely, S. A.; Davis, R. D., *J. Am. Chem. Soc.* **1983**, 105 (23), 6907-6915.
20. Taylor, K. G.; Hobbs, W. E.; Clark, M. S.; Chaney, J., *J. Org. Chem.* **1972**, 37 (15), 2436-2443.
21. Sütbeyaz, Y.; Ceylan, M.; Seçen, H., *J. Chem. Res. (S)* **1993**, 293.
22. Shakespeare, W. C.; Johnson, R. P., *J. Am. Chem. Soc.* **1990**, 112 (23), 8578-8579.
23. Lofstrand, V. A.; West, F. G., *Chem. Eur. J.* **2016**, 22 (31), 10763-10767.
24. Barber, J. S.; Yamano, M. M.; Ramirez, M.; Darzi, E. R.; Knapp, R. R.; Liu, F.; Houk, K. N.; Garg, N. K., *Nat. Chem.* **2018**, 10 (9), 953-960.
25. Werstiuk, N. H.; Roy, C. D.; Ma, J., *Can. J. Chem.* **1996**, 74 (10), 1903-1905.
26. Barber, J. S.; Styduhar, E. D.; Pham, H. V.; McMahan, T. C.; Houk, K. N.; Garg, N. K., *J. Am. Chem. Soc.* **2016**, 138 (8), 2512-5.
27. Chen, W.; Du, W.; Duan, Y. Z.; Wu, Y.; Yang, S. Y.; Chen, Y. C., *Angew. Chem.* **2007**, 119 (40), 7811-7814.
28. Laycock, D. E.; Wain, R. J.; Wightman, R. H., *Can. J. Chem.* **1977**, 55 (1), 21-23.
29. Lofstrand, V. A.; McIntosh, K. C.; Almealmadi, Y. A.; West, F. G., *In preparation* **2019**.
30. Bode, J. W.; Hachisu, Y.; Matsuura, T.; Suzuki, K., *Tetrahedron Letters* **2003**, 44 (17), 3555-3558.
31. Shintani, R.; Fu, G. C., *J. Am. Chem. Soc.* **2003**, 125 (36), 10778-10779.

32. Shen, S.; Yang, Y.; Duan, J.; Jia, Z.; Liang, J., *Org. Biomol. Chem.* **2018**, *16* (7), 1068-1072.
33. Canterbury, D. P.; Herrick, I. R.; Um, J.; Houk, K. N.; Frontier, A. J., *Tetrahedron* **2009**, *65* (16), 3165-3179.
34. George, M. V.; Peterson, D. J.; Gilman, H., *J. Am. Chem. Soc.* **1960**, *82* (2), 403-406.
35. Li, K.; Alexakis, A., *Angew. Chem. Int. Ed.* **2006**, *45* (45), 7600-7603.
36. Ramadhar, T. R.; Kawakami, J.-i.; Batey, R. A., *Synlett* **2017**, *28* (20), 2865-2870.

Chapter 3

A Novel Method for the Generation of Reactive Cyclic Allenes via Metal–Halogen Exchange Promoted Elimination

3.1. Background

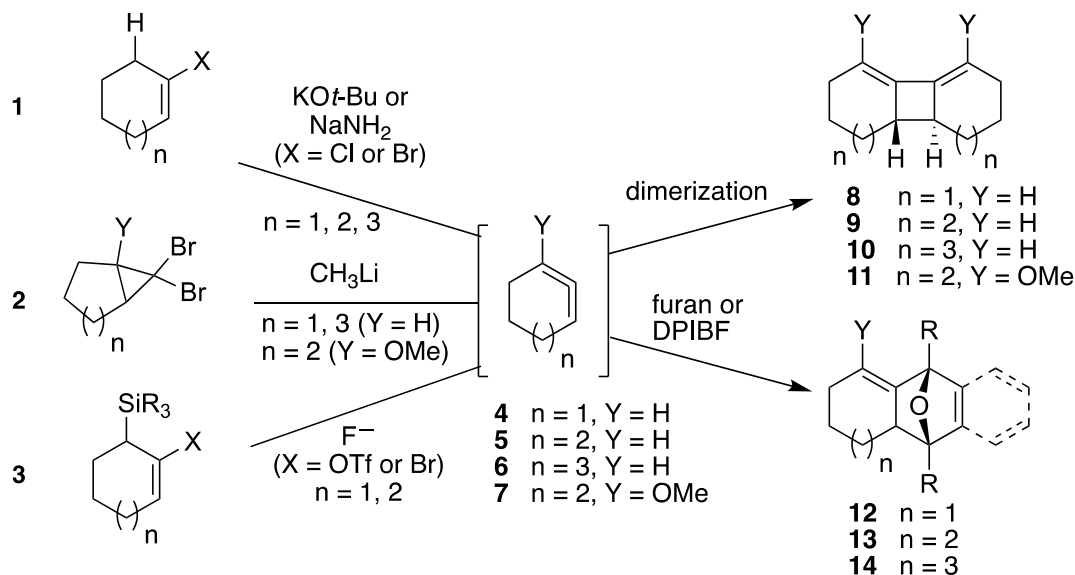
In the first two chapters, I focused on the importance of cyclic allenes and how they have afforded novel transformations upon their generation and trapping with 1,3-dipoles.¹⁻³ The recent work done in this area has focused on the generation of cyclic allenes by three main methods (*vide infra*).

In 1961, Ball and Landor produced the first generation of cyclic allenes when they carried out the dehydrohalogenations of 1-chlorocycloheptene and 1-chlorocyclooctene with NaNH_2 (Scheme 3.1). These processes allowed the formation of 1,2-cycloheptadiene **5** and 1,2-cyclooctadiene **6**.⁴ Later in the same decade, Wittig and Fritze were the first to show the existence of 1,2-cyclohexadiene **4**, using similar processes to those applied to generate 7- and 8-membered-ring allenes.⁵ They demonstrated that 1-bromocyclohexene can undergo dehydrohalogenation upon treatment with potassium *tert*-butoxide ($\text{KO}t\text{-Bu}$) to form 1,2-cyclohexadiene **4**. However, this method, known as base-induced elimination, requires the use of strongly basic conditions, which can limit the generality of this method due to functional group incompatibilities.

Moreover, in 1970 a new method to generate cyclic allenes, via the Doering–Moore–Skattebøl (DMS) reaction, was reported by Moore and Moser (Scheme 3.1).⁶ Generating cyclic allenes using the DMS reaction requires the preparation of *gem*-dihalocyclopropanes fused to a ring of size $n-1$ (with n being the desired cyclic allene ring size). Upon treatment with organolithium reagents, the cyclopropane undergoes ring expansion, resulting in the formation of the cyclic allene. This method is capable of furnishing 1,2-cyclohexadiene **4** and 1,2-cyclooctadiene **6**. However, the generation of 1,2-cycloheptadiene **5** was not observed using this method, and tricycloheptanes⁷ were obtained instead, as shown in Section 1.6. The apparent inability to access 1,2-cycloheptadienes, along with limited functional group

tolerance to alkyllithium reagents would limit the use of this method. The only reported example of the DMS reaction being successfully used to generate seven membered cyclic allenes was Chaney and co-workers' synthesis of substituted 1,2-cycloheptadiene **7** using 1-methoxy-7,7-dibromobicyclo[4.1.0]heptane as their starting material.⁸

Another commonly used method to generate cyclic allenes, which has been recently studied by the West group¹ and the Garg group,^{2,3} is the fluoride-mediated desilylative elimination, which was reported first by Johnson and Shakespeare.⁹ Fluoride-mediated desilylative elimination requires the synthesis of allylic silanes with an adjacent sp^2 leaving group (LG). Upon subjecting the allylic silane to a fluoride source, an E2 elimination of bromide occurs to form the cyclic allenes.



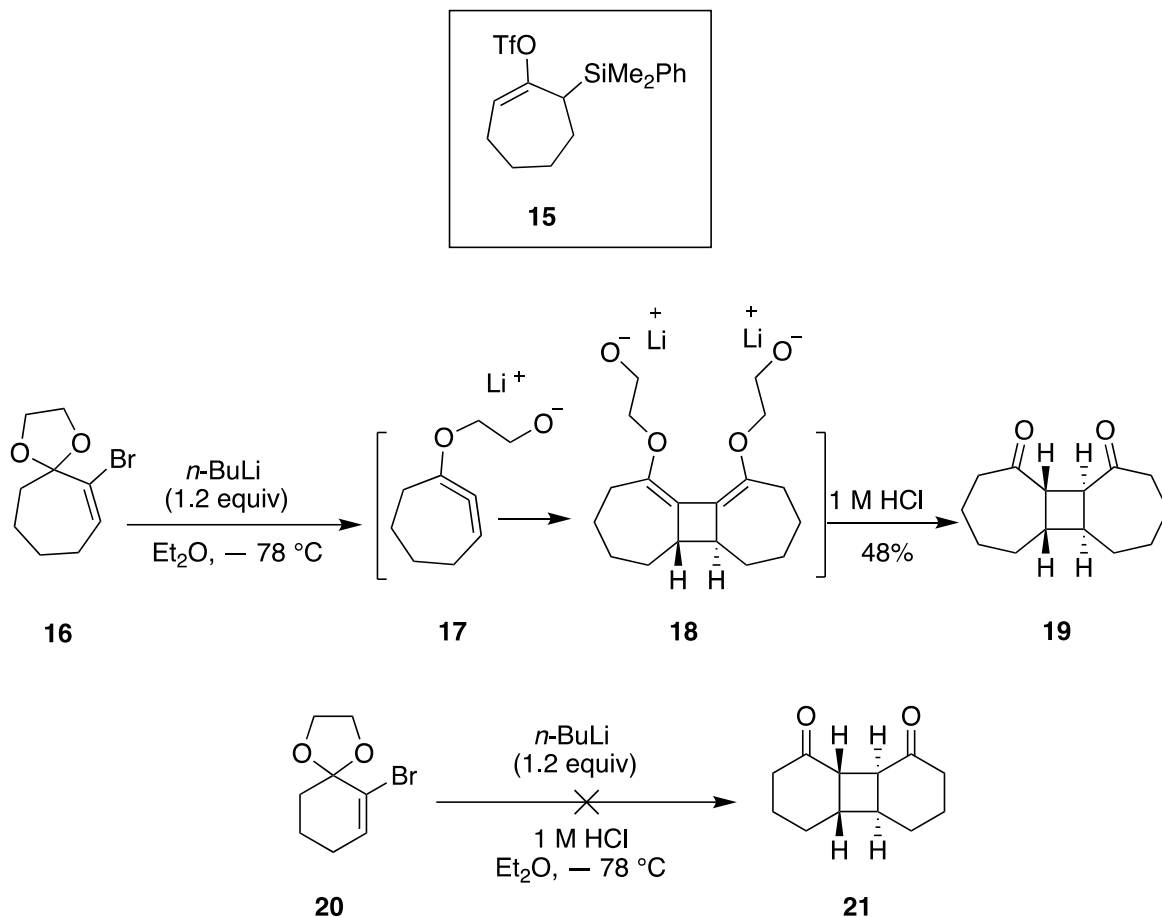
Scheme 3.1. The most commonly used methods to generate cyclic allenes.

There is value in designing and investigating alternative methods to generate these reactive intermediates, especially if a new method proceeds under complementary conditions to the other approaches and relies on readily available starting materials. With this in mind, I describe here our efforts to generalize an alternative elimination strategy involving an sp^2 carbanion with a leaving group present on an adjacent sp^3 centre.

3.2. Results and Discussion

During the course of our initial studies of fluoride-mediated desilylative elimination, which required the synthesis of allylic silane **15**, functionalization of bromocycloheptenone ketal **16** was required. To our surprise, we found that upon treatment of **16** with *n*-BuLi at -78 °C, we isolated the dimeric cyclobutane product **19**. Optimization of this process allowed for the formation of **19** in 48% yield (Scheme 3.2).

The NMR analysis and mass spectrum of this product matched our previous report in Chapter 2 when we obtained the same product using fluoride-mediated desilylative elimination. The NMR and mass spectrometry data of **19** match with the one which was confirmed previously by single crystal X-ray diffraction analysis. The most likely source of this product is an allene dimerization process involving two molecules of the cyclic allene **17** resulting from lithium–halogen exchange and eliminative opening of the cyclic ketal. [2+2]-Cycloaddition through the unsubstituted termini of the allenes **17** would afford the bis(enol ether) **18**, which could undergo hydrolysis on work-up to afford the observed diketone **19**. In a further experiment, we attempted to carry out the analogous transformation on the corresponding bromocyclohexene **20**, but this experiment was not fruitful. Complete decomposition to an uncharacterizable mixture was obtained.

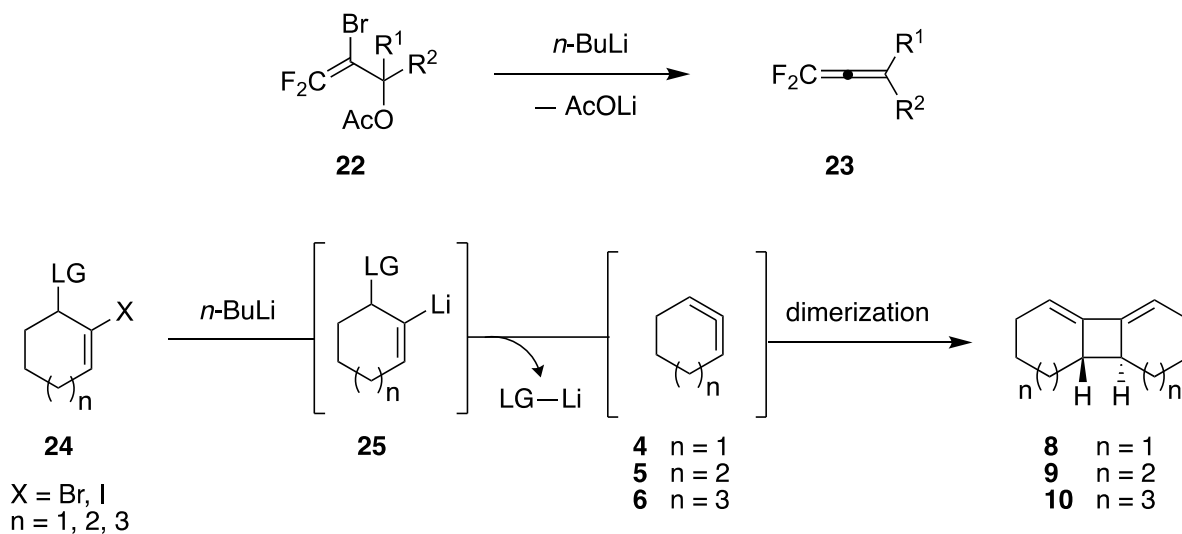


Scheme 3.2. Unexpected dimerization process.

Assuming this proposed mechanism was correct, we then attempted to intercept diene **18** with electrophilic reagents, such as MeI, ClSiMe_3 , and Ac_2O . However, these experiments failed, and complete decomposition to an uncharacterizable mixture was observed. Moreover, we tried to trap cyclic allene **17** with reactive trapping partners, such as 1,3-diphenylisobenzofuran (DPIBF) and styrene, but this did not yield the desired products. In all these trapping attempts of allene **17**, dimer **19** was obtained.

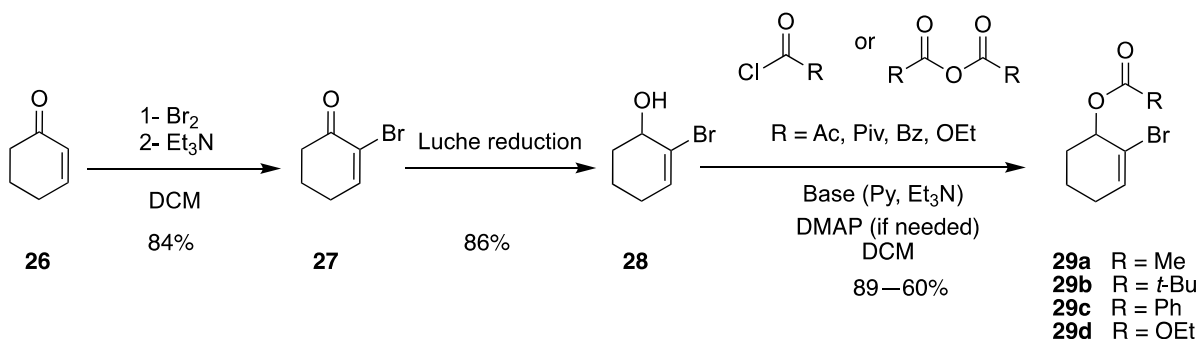
In a study from Ichikawa's group, it was documented that acyclic allenes can be generated via lithium-halogen exchange promoted elimination, as shown in Scheme 3.3.¹⁰ This study showed that upon lithiation of 2-bromo-1,1-difluoroalkenes with allylic leaving groups **22**, 1,1-difluoroallenes **23** were obtained in high yields. In light of the unexpected dimerization shown in Scheme 3.2 and Ichikawa's findings, M.-G. Constantin, a PhD candidate in the West group, and I worked together to develop a new methodology to access

cyclic allenes by similar means. We hypothesized that lithiation of **24** could result in a concerted 1,2-elimination of the vicinal leaving group, resulting in the formation of cyclic allenes **4–6**, which could dimerize to form **8–10** or, alternatively, be trapped with furan or other trapping partners. The attractiveness of this approach is the simplicity and ready availability of the starting substrates **24**.



Scheme 3.3. Ichikawa's work and proposed generation of cyclic allenes.

We first focused on the synthesis of the allylic leaving groups seen in compounds **29a–d**. These compounds were synthesized using the readily available starting material **26** and well-established chemistry.¹¹ Enone **26** was alpha-brominated and subjected to Luche reduction conditions to form alcohol **28**, which was then converted to compounds **29a–d** using standard conditions, as summarized in Scheme 3.4.

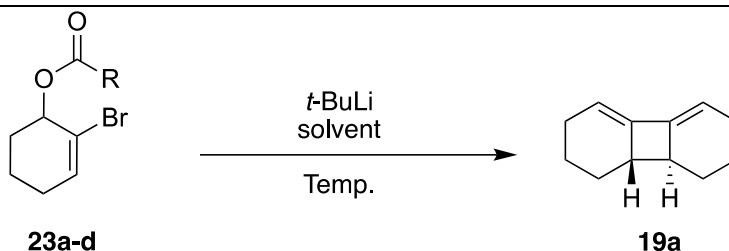


Scheme 3.4. General route to synthesis of allylic esters **29a–d**.

We then subjected **29a–d** to organolithium reagents to examine our aforementioned hypothesis that cyclic allenes could be generated using lithium–halogen exchange promoted elimination. In the process of screening organolithium reagents, we found that *t*-BuLi was best suited to give the desired transformation. We started by treating acetate **29a** (Entry 1, Table 3.1) with 2.2 equivalents of *t*-BuLi at low temperature in hexane. As a result, traces of dimer **4** were visible in the crude ¹H NMR spectrum despite obtaining a complex mixture of products in this experiment. In a further two experiments, we treated pivalate **29b** and benzoate **29c** with *t*-BuLi under the same reaction conditions used for acetate **29a**. In the case of pivalate, we obtained dimer **4** in a very small amount, while in the case of benzoate, we were not able to see any evidence of dimer formation.

Upon applying the same reaction conditions at – 78 °C to carbonate **29d**, we obtained traces of the expected dimer in a reaction mixture that was less complex than that obtained with the acetate and pivalate containing compounds. However, when the reaction was carried out at room temperature, the isolated yield of the dimer increased significantly to 23% when compared with low temperature (– 78 °C) experiments. We also screened other solvents, such as THF and Et₂O, but observed no improvement in the yield of the reaction. As a result of this optimization, we found that treatment of carbonate **29d** with *t*-BuLi (2.2 equiv) at room temperature in hexane produced the best result.

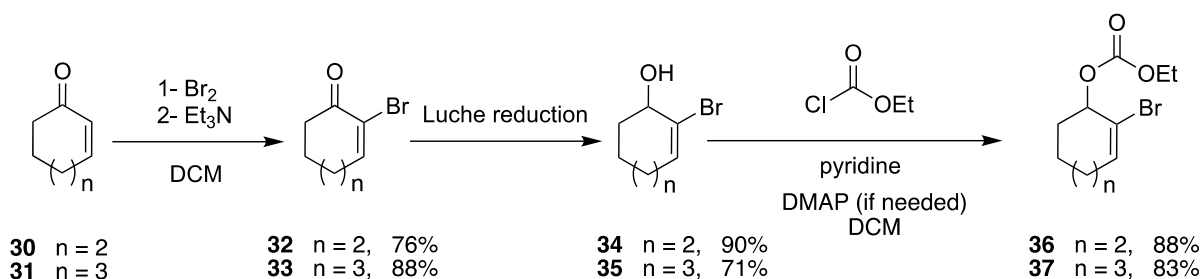
Table 3.1. Optimization of the Dimerization Process of 1,2-Cyclohexadiene Using Li-Br Exchange Promoted Elimination.^[a]



Entry	Starting Material	Solvent	Temp. (° C)	Observation
1	23a R = Me	Hexane	-78	Traces of 19a in complex mixture
2	23b R = <i>t</i> -Bu	Hexane	-78	Traces of 19a in complex mixture
3	23c R = Ph	Hexane	-78	No product observed
4	23d R = OEt	Hexane	-78	Traces of 19a in complex mixture
5	23d R = OEt	Hexane	rt	23% isolated yield
6	23d R = OEt	Et ₂ O	rt	Traces of 19a in complex mixture
7	23d R = OEt	THF	rt	Traces of 19a in complex mixture
8	23d R = OEt	Et ₂ O	-78	Traces of 19a in complex mixture
9	23d R = OEt	THF	-78	Traces of 19a in complex mixture

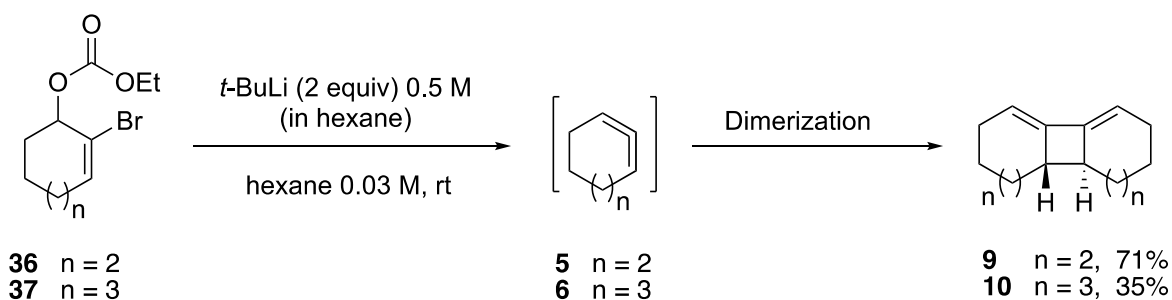
[a] This optimization mainly was done by M.-G. Constantin.

M.-G. Constantin and I further examined this method to generate cyclic allenes of other ring sizes, such as 1,2-cycloheptadiene and 1,2-cyclooctadiene. The synthetic route used to synthesize allylic carbonates **36** and **37** paralleled that used for **29d**, starting with cyclic enones **30** and **31** (Scheme 3.5).



Scheme 3.5. Synthesis of seven- and eight-membered ring carbonates **36** and **37**.

Carbonates **36** and **37** were treated with *t*-BuLi (2.2 equiv) to examine the generation and subsequent dimerization of 1,2-cycloheptadiene and 1,2-cyclooctadiene using this new method. 1,2-Cycloheptadiene dimer **9** was obtained in high yield (71%), whilst the 1,2-cyclooctadiene dimer **10** was obtained in 35% yield. Unfortunately, our attempts to trap the reactive intermediates **4–6** with furan, styrene, or dienes failed. Unsurprisingly, in the case of trapping 1,2-cycloheptadiene with furan, dimer **9** was obtained instead of the desired [4+2] cycloadduct. This result is consistent with our earlier observation in Section 2.4, where trapping 1,2-cycloheptadiene with furan using the fluoride-mediated desilylative elimination failed. Until now, we are not certain why these trapping attempts were not successful. Further investigations are ongoing and will be reported upon in due course.

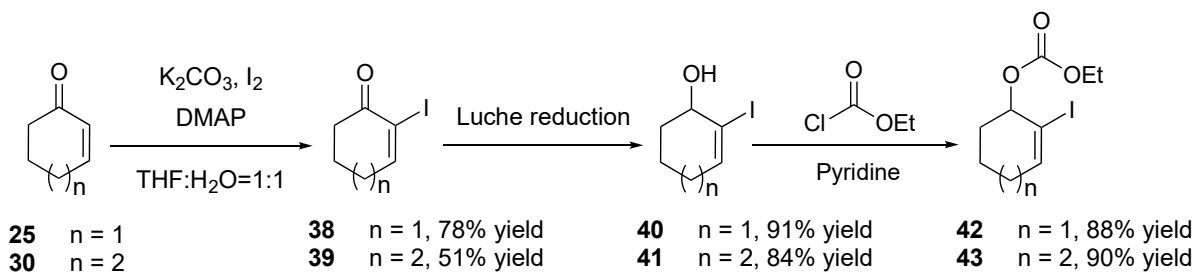


Scheme 3.6. Dimerization of 1,2-cycloheptadiene **9** and 1,2-cyclooctadiene **10**.

Given our success in generating cyclic allenes via lithium–halogen exchange promoted elimination, we turned our attention to the question of whether the corresponding magnesiation reaction could be used to generate these reactive intermediates under milder

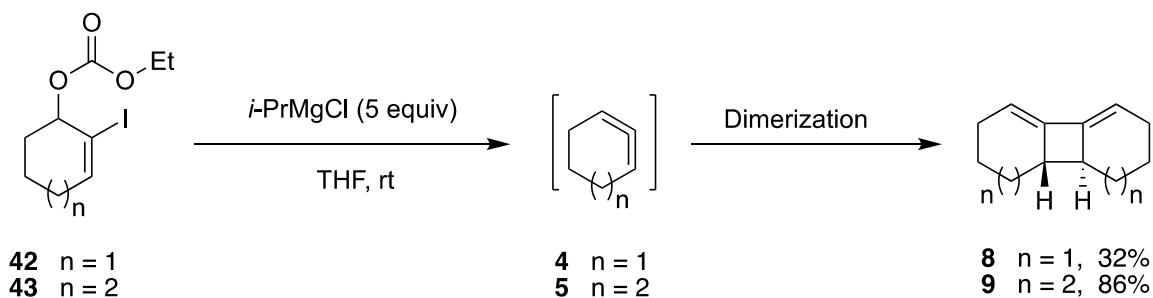
conditions than those of the lithiation process. Therefore, we started investigating new reaction conditions to generate cyclic allenes through magnesium–halogen exchange promoted elimination and exposing the generated reactive intermediates to trapping reagents to form useful cycloadducts. Initial attempts using the magnesiation process with bromo-carbonate **29d** were not productive, and the starting material was recovered. Therefore, we chose to try this process on the corresponding iodo-carbonates instead. It has been shown that iodides undergo the magnesium–halogen exchange reaction more readily.^{12,13} This new approach was explored further by us, together with an undergraduate student, X. Liu, as part of a CHEM 401/403 project.

We first successfully synthesized the target iodo-carbonates **42** and **43** in three steps from readily available starting materials, enones **25** and **30**, respectively, using well-established chemistry. Enones **25** and **30** were converted to iodo-enones **38** and **39** under mild conditions in good yields. Next, the iodo-enones were subjected to Luche reduction conditions to form alcohols **40** and **41**, followed by conversion of these alcohols to the corresponding carbonates **42** and **43** in high yields, as shown in Scheme 3.7.



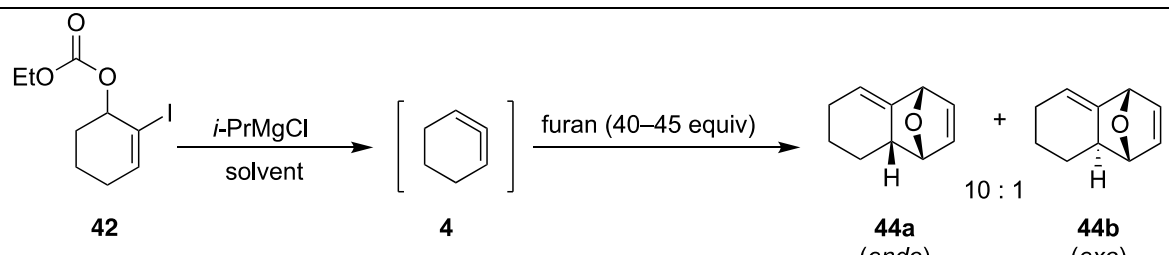
Scheme 3.7. Synthesis of allylic iodo-carbonates **42** and **43**.

With carbonates **42** and **43** in hand, we examined the magnesiation process to determine whether this approach would result in 1,2-elimination of carbonate and permit the formation of the desired cyclic allenes. Upon the treatment of carbonates **42** and **43** with *i*-PrMgCl, dimers derived from **4** and **5** were obtained in better yield compared with the lithiation process, as shown in Scheme 3.8. Characterization data of the obtained compounds matches well with previous reports.^{4,5}



Scheme 3.8. Dimerization processes of strained cyclic allenes **4** and **5** generated via magnesium–halogen exchange reactions.

We then attempted to trap the generated 1,2-cyclohexadiene **4** with furan. We were pleased to confirm that this generation method, using the magnesium–halogen exchange reaction, results in cyclic allenes which can be trapped with furan unlike those generated using the lithium–halogen exchange reaction. Given this result, we optimized the reaction conditions by treating the starting material **42** with several organomagnesium reagents in the presence of furan as a trapping partner. This reaction also was performed at different temperatures, solvents, and concentrations, as summarized in Table 3.1. A very low yield was obtained when hexane was used as a solvent; this could be due to the low solubility of *i*-PrMgCl in hexane (Entry 2, Table 3.2). Running the reaction in Et₂O or furan (Entries 3–4, Table 3.2) did not improve the yield. Then, we examined more reaction conditions by varying the reaction temperature, the stoichiometry, and the rate of addition of the organomagnesium reagent. As a result of this optimization, we found that slow addition (over 30 min) of 4 equivalents of 0.4 M *i*-PrMgCl in THF at 50 °C gave the best result, with a 43% NMR yield and a 10:1 (*endo:exo*) ratio of [4+2]-cycloadducts **44a** (*endo*-) and **44b** (*exo*-) (Entry 12, Table 3.2).

Table 3.2. Optimization of Trapping Six-membered Cyclic Allene with Furan.^[a]

The reaction scheme shows the conversion of iodo-carbonate **42** to cyclohexene **4** using *i*-PrMgCl in a solvent. Cyclohexene **4** then reacts with furan (40–45 equiv) to produce a 10:1 ratio of *endo* (**44a**) and *exo* (**44b**) bicyclic cycloadducts.

Entry	Solvent	T, °C	Slow addition	Conc. (M) ^[b]	Equiv of <i>i</i> -PrMgCl	NMR Yield ^[c]
1	THF	RT	no	0.03	3 equiv	28%
2	Hexane	RT	no	0.03	3 equiv	3%
3	Et ₂ O	RT	no	0.03	3 equiv	20%
4	Furan	RT	no	0.03	3 equiv	25%
5	THF	RT	yes	0.03	3 equiv	24%
6	THF	RT	yes	0.03	5 equiv	39%
7	THF	RT	no	0.03	5 equiv	18%
8	THF	0 °C	no	0.03	5 equiv	0%
9	THF	RT	no	0.01	5 equiv	8%
10	THF	50 °C	no	0.03	5 equiv	33%
11	THF	RT	no	0.1	5 equiv	26%
12	THF	50 °C	yes	0.03	5 equiv	43%

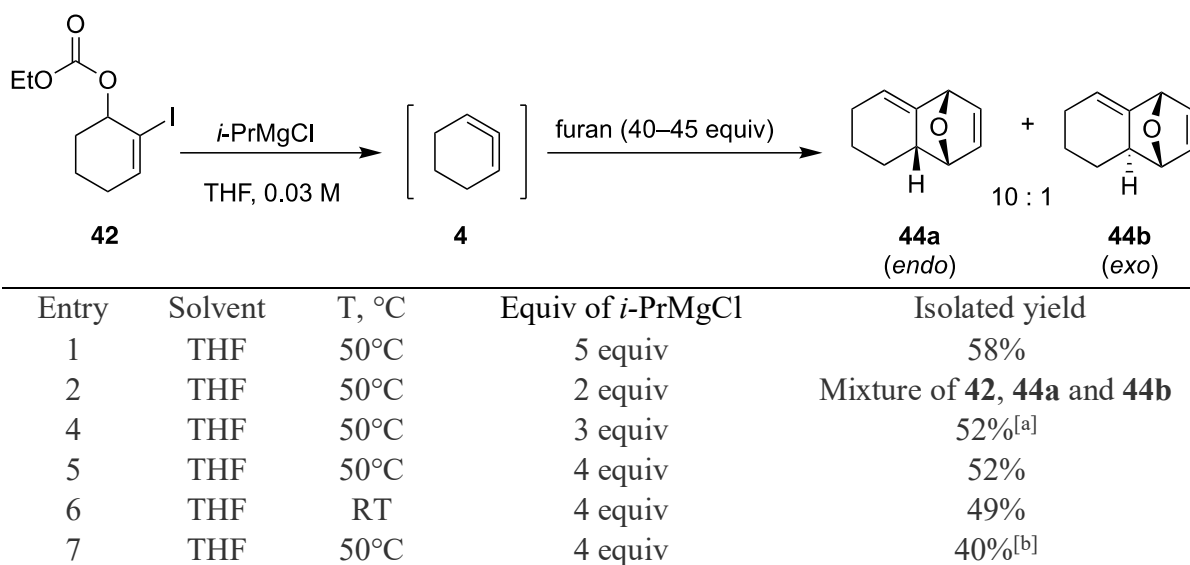
[a] Iodo-carbonate **42** (0.1 mmol) and furan (40–45 equiv) was added to a dry flask, and then a nitrogen atmosphere was established via a purge needle. To this flask, THF (0.03 M) was added, and the reaction mixture was heated to 50 °C. To this flask, 0.5 M *i*-PrMgCl (4 equiv) in THF was added slowly over 1 h using a syringe pump. The reaction mixture was allowed to stir at the same temperature for 30 min. [b] Starting concentration of **42**. [c] All yields reported were measured by NMR methods using mesitylene as an internal standard, 0.034 mmol (5μL). The integration of the mesitylene aromatic proton signal at 6.8 ppm was compared with integrals for alkene signals in **28a,b** at 6.3 and 6.0 ppm, respectively.

As all the yields in Table 3.2 were calculated from reactions carried out on a small scale (0.1 mmol), we were concerned about potential measuring errors in their determination. Therefore, we scaled up the same reaction to 1 mmol instead of 0.1 mmol and used the optimized reaction conditions (Entry 12, Table 3.2). We obtained 58% isolated yield of a mixture of 10:1 *endo* and *exo* cycloadducts, as shown in Table 3.3.

To establish whether 5 equivalents of *i*-PrMgCl are required to produce the same result, we explored further variations of the reaction conditions. We first reduced the equivalents of *i*-PrMgCl from 5 to 2–4 equivalents, as shown in Entries 2–5 (Table 3.2). We found that to drive the reaction to completion in 60 min, we needed at least 4 equivalents of

organomagnesium reagent. We can, alternatively, achieve the same result by the addition of 3 equivalents of *i*-PrMgCl, but with significantly longer reaction times (up to 18 h). However, using 4 equivalents of *i*-PrMgCl results in a slight increase in the yield of the reaction but also a decrease in reaction time to 1 h. Varying the reaction temperature and inverting the addition order by slowly adding the starting material **42** to a mixture of *i*-PrMgCl and furan in THF did not improve the yield of the reaction. As a result of these optimizations, we found that the conditions in Entry 5 (Table 3.3) gave the best results, and these conditions were used for other trapping processes of cyclic allenes **44a** and **44b**.

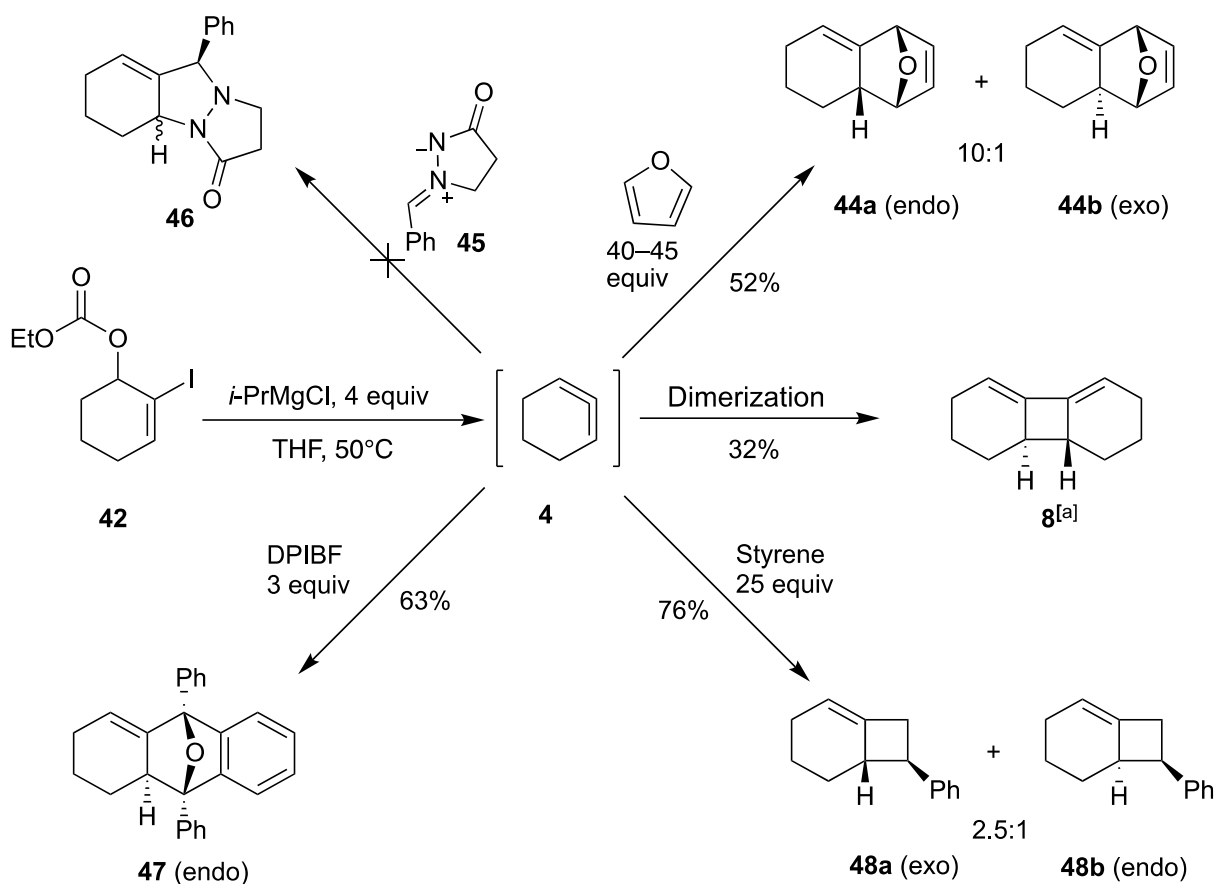
Table 3.3. Isolated Yields of 1,2-Cyclohexadiene Cycloadducts Using Several Conditions at 1 mmol scale.



[a] The reaction was completed after 18 h. [b] Slow addition of **36** to a stirred solution of furan and 0.5 M *i*-PrMgCl in THF.

These preliminary experiments demonstrated that the functionalized unsubstituted cyclic allenes **4** could be generated by magnesium–halogen exchange promoted elimination in two steps from the simple iodoenone precursor **25** and underwent efficient conversion to dimers **8**. Next, we sought to examine several cycloaddition reactions under the optimized reaction conditions. We were able to trap 1,2-cyclohexadiene **4** with furan, 1,3-diphenylisobenzofuran (DPIBF), and styrene (Scheme 3.9). As already noted, trapping of **4** with furan produced a 10:1 mixture of diastereomeric cycloadducts **44a** and **44b**, the endo- and exo- products, respectively, in 58% yield. In addition, we were able to trap 1,2-

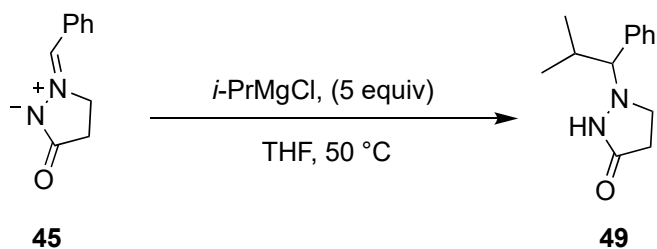
cyclohexadiene with DPIBF in 63% yield, but only the *endo*- product **47** was isolated successfully. We were not able to isolate any *exo* product and, if it was present, it was formed only in trace amounts. In a further reaction, the cycloaddition with styrene furnished the *exo*- and *endo*- cycloadducts **48a** and **48b** (2.5:1) in 76% yield.



Scheme 3.9. Dimerization and trapping reactions of six-membered cyclic allene **4** via magnesium–halogen exchange promoted elimination. ^[a] It was necessary to run the reaction at rt to obtain optimized yields.

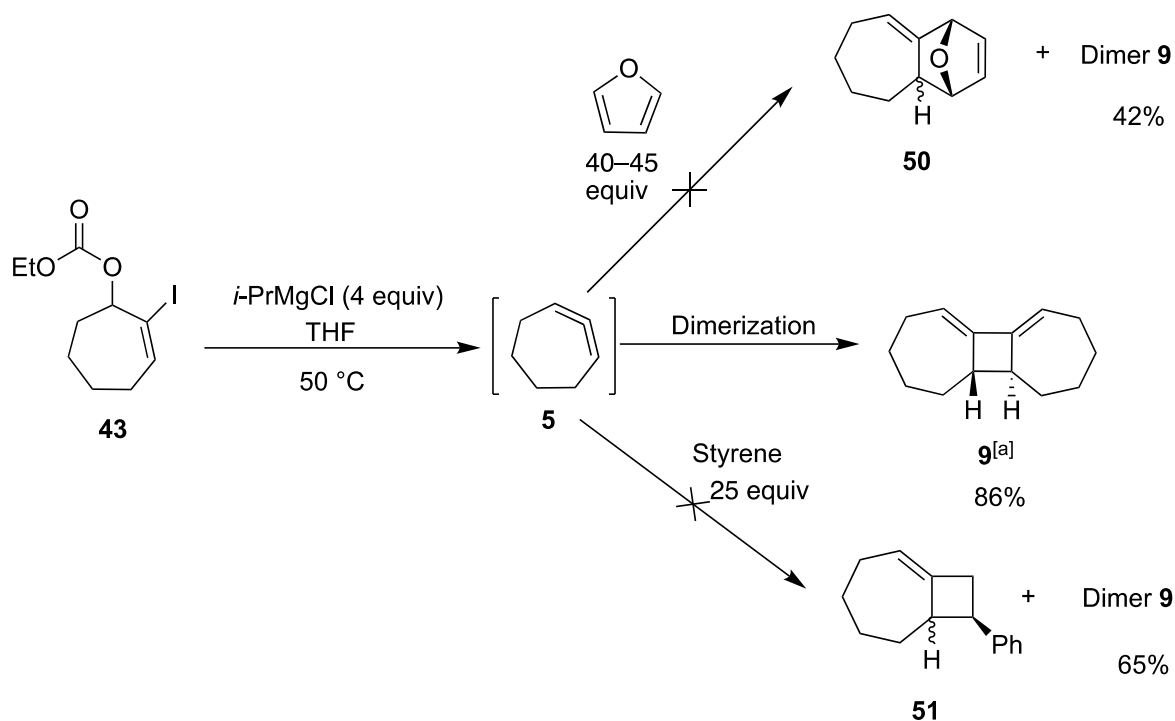
Trapping cyclic allene **4** via a [3+2] cycloaddition reaction using azomethine imine 1,3-dipole failed. This could be due to the undesired reaction between the reactive 1,3-dipole and *i*-PrMgCl.¹⁴ Therefore, we conducted a control experiment, where we subjected **45** to *i*-PrMgCl (5 equiv) and found from the initial evaluation of crude ¹H NMR data that 1,3-dipole **45** was consumed completely and produced **49** (Scheme 3.10). Unfortunately, this class of traps may not be tolerated in this new generation method using magnesium–halogen

exchange promoted elimination due to a competing reaction between the organomagnesium reagent and the 1,3-dipole.



Scheme 3.10. Undesired reaction between *i*-PrMgCl and the 1,3-dipole **45**.

With our success in trapping the six-membered cyclic allene **4** with furan, DPIBF, and styrene by this new generation method, we aimed to examine this method to access the seven-membered cyclic allene and trap it with the same trapping partners we used to trap 1,2-cyclohexadiene. We first evaluated the dimerization of 1,2-cycloheptadiene **5**, as illustrated previously, and obtained 86% yield of dimer product **9** (Scheme 3.11). We also examined the [4+2]-cycloaddition with furan and the [2+2]-cycloaddition with styrene; however, these attempts were not fruitful. We obtained 42% yield (in the case of furan) and 65% yield (in the case of styrene) of dimer **9** after purification by column chromatography. We theorized that this change in trapping behavior results from diminished reactivity due to decreased ring strain. The bond angle of the central allene carbon in the six-membered cyclic allene **4** is 138°, while in the seven-membered cyclic allene it is 153°, significantly closer to the ideal 180°. ¹⁵ This leads to a decrease in strain energy of ~18 kcal/mol. Thus, the seven-membered cyclic allene is less reactive than the six-membered cyclic allene due to its larger ring size. Unsurprisingly, trapping 1,2-cycloheptadiene with furan failed; this result aligned with the previous observation in Chapter 2. The much more reactive furan-based trap, DPIBF, will be examined in the future.



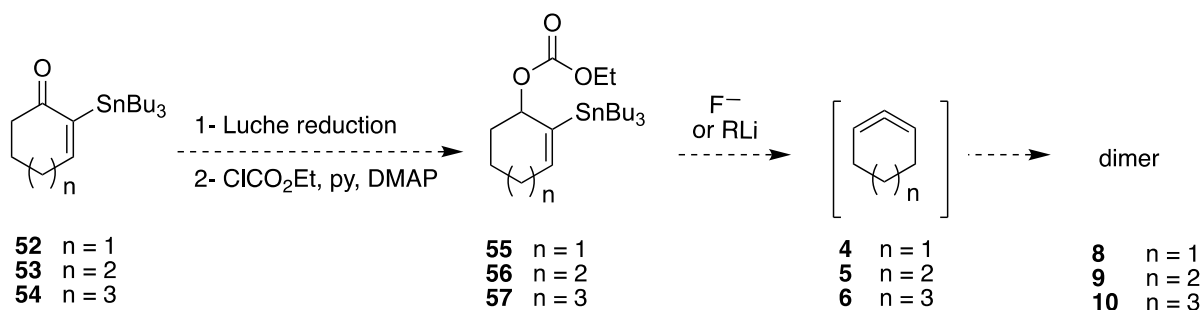
Scheme 3.11. Dimerization and attempted trapping reactions of seven-membered cyclic allene via magnesium–halogen exchange promoted elimination. [a] It was necessary to run the reaction at rt to obtain optimized yields.

3.3. Conclusion

In this chapter, I have described the preliminary results of work carried out in collaboration with M.-G. Constantin to develop new methods to generate and trap cyclic allenes via metal–halogen exchange promoted elimination. These methods involve the preparation of an acyclic carbonate with an adjacent sp^2 leaving group and treating of these compounds with an alkyllithium or alkylmagnesium reagent. We documented that both organolithium and organomagnesium reagents can be used to generate cyclic allenes via these methods. However, trapping the six-membered cyclic allene with furan, DPIBF, styrene failed; only a dimer was obtained in the case of using organolithium reagents to access these reactive intermediates. On the other hand, the generation of 1,2-cyclohexadiene by magnesium–halogen exchange promoted elimination, and its trapping reaction was successful. We were able to show a couple of examples where we used this new method to access 1,2-cyclohexadiene and trap with furan, DPIBF, and styrene.

3.4. Future Directions

The ability to generate cyclic allenes under mild reaction conditions is highly sought-after. For example, where the known generation of cyclic allenes failed or showed attenuated yields, a different approach could be taken using the corresponding carbonates **55**, **56**, or **57**. Enones **52–54** can be reduced to the corresponding alcohols using Luche reduction, followed by conversion of alcohols to the corresponding carbonates **55–57**. These carbonates may undergo a concerted E2 mechanism to eliminate the carbonates upon the treatment with a fluoride source, such as TBAF or CsF, or organolithium reagents, as shown in Scheme 3.11. This proposed route to synthesize cyclic allenes takes advantage of the weak C–Sn bond.



Scheme 3.11. Possible generation of cyclic allenes via vinyl tin reagents with allylic carbonate.

3.5. Experimental and General Information

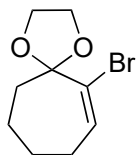
All reactions were carried out in glassware that was stored in an oven overnight or was flame-dried under a positive nitrogen atmosphere, unless otherwise specified. Transfer of anhydrous reagents was accomplished with oven-dried syringes or cannulae. Distilled water (H₂O) was used, and solvents (DCM, Et₂O, THF, and PhMe) were used from a solvent purification system. Hexane was distilled from calcium hydride, and benzene (C₆H₆) was dried over 4 Å molecular sieves overnight. Thin layer chromatography was performed on glass plates pre-coated with 0.25 mm Kieselgel 60 F254 (Merck). Flash chromatography columns were packed with 230–400 mesh silica gel (Silicycle), and the stains for TLC analysis were conducted using 2.5% *p*-anisaldehyde in AcOH-H₂SO₄-EtOH (1:3:86) and further heating until development of color. Reagents were used as purchased from Sigma-Aldrich, Oakwood, and Alfa Aesar.

Proton nuclear magnetic resonance spectra (¹H NMR) were recorded at 400 MHz or 500 MHz, and coupling constants (*J*) are reported in Hertz (Hz). Carbon nuclear magnetic resonance spectra (¹³C NMR) were recorded at 100 MHz or 125 MHz. The chemical shifts are reported on the δ scale (ppm) and referenced to the residual solvent peaks (CDCl₃: s, 7.26 ppm, ¹H; t, 77.06 ppm, ¹³C) as internal standards. Standard notation is used to describe the multiplicity of the signals observed in ¹H NMR spectra: broad (br), apparent (app), multiplet (m), singlet (s), doublet (d), triplet (t), quartet (q), pentet (p), etc. Infrared (IR) spectra were measured with a Mattson Galaxy Series FT-IR 3000 spectrophotometer. Mass spectra were recorded by electron impact ionization (EI) measured by a Kratos MS50 instrument or by electrospray ionization (ESI) measured by an Agilent 6220 oaTOF instrument, as specified in each case.

Azomethine imines **45**,^{17,18} is a known literature compound and was produced via the published routes; ¹H NMR and ¹³C NMR spectral data matched those reported in the literature. 1,3-Diphenylisobenzofuran (DPIBF) is available from Sigma-Aldrich. Bromo-carbonate **29d**,¹¹ 2-iodo-2-cyclohexen-1-ol **40**,¹⁹ and 2-iodo-2-cyclohepten-1-ol **41**,²⁰ was prepared according to known literature procedures. Compounds **29a–d** and **37**, iodo-carbonates **42** and **43**, and compound **49** were synthesized by M.-G. Constantin. Therefore,

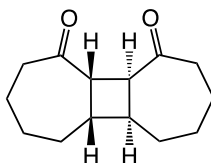
experimental data are not included in my chapter. Compounds **32**, **34**, and **36** were prepared according to the previous procedures, which were reported in Section 2.7.

2-Bromo-2-cycloheptenone ethylene ketal (**16**)



To a solution of enone **26** (1.93 g, 10.2 mmol) and HOCH₂CH₂OH (3.17 g, 51.0 mmol) in benzene (60 mL) were added *p*-TsOH (527 mg, 3.1 mmol). The reaction mixture was heated at reflux for 24 h under a Dean–Stark setup. Concentration under reduced pressure and purification by column chromatography on silica gel with 9:1 hexanes/ethyl acetate afforded **16** (1.0 g, 42%) as a colorless oil: *R_f* = 0.69 (9:1, hexane:EtOAc); ¹H NMR (500 MHz, CDCl₃) δ 6.51 (t, *J* = 6.8 Hz, 1H), 4.24–4.13 (m, 2H), 4.04–3.94 (m, 2H), 2.25–2.15 (m, 2H), 2.01–1.95 (m, 2H), 1.81–1.71 (m, 2H), 1.71–1.62 (m, 2H); ¹³C NMR (125 MHz, CDCl₃) δ 136.8, 129.6, 109.3, 76.8, 65.6, 34.7, 27.3, 24.7, 21.4; IR (cast film, cm⁻¹) 3033, 2937, 2890, 1629, 1473, 1452; HRMS (EI) calcd for [M]⁺ C₉H₁₃O₂⁷⁹Br: 232.0099, found: 232.0096. This procedure was adapted from the published synthesis of 2-bromo-2-cyclohexenone ethylene ketal from 2-bromo-2-cyclohexenone.²¹

Tricyclo[7.5.0.0^{2,8}]tetradeca-3,14-dione (**19**)



To a stirred solution of ketal **11** (255 mg, 1.1 mmol) in THF (11.0 mL) under N₂ atmosphere was added 0.6 M *n*-BuLi (2.2 mL, 1.3 mmol) dropwise at –78 °C. The reaction mixture was allowed to stir for 4 h, after which the reaction was quenched with 1 M HCl. After separating the phases, the aqueous layer was extracted with EtOAc (3 x 30 mL), and the combined organic layers were dried over MgSO₄. Filtration, concentration under reduced pressure, and

purification by column chromatography on silica gel with 7:3 hexanes/ethyl acetate afforded **13** (58 mg, 48% yield).

Notes: Relative stereochemistry was determined by X-Ray Crystallography for the same compound in Chapter 2. ^1H and ^{13}C spectral data also match those reported in Chapter 2.

General Protocol for the Dimerization Process of Cyclic Allenes via Lithium–Halogen Exchange Promoted Elimination.

To a stirred solution of a particular bromo-carbonate **29a**, **36**, or **37** (1 equiv) in hexane (0.1 M) under a N_2 atmosphere was added 0.5 M *t*-BuLi (2.2 equiv) in hexane dropwise at room temperature. The reaction mixture was allowed to stir for 20 min, after which it was quenched with water. After separating the phases, the aqueous layer was extracted with Et_2O (3 x 30 mL), and the combined organic layers were dried over MgSO_4 . Filtration, concentration under reduced pressure, and purification by column chromatography on silica gel with hexanes afforded the corresponding dimers **4** (23 %), **5** (71 %), **6** (35 %).

General Protocol for the Dimerization Process of Cyclic Allenes via Magnesium–Halogen Exchange Promoted Elimination

To a dry flask was added the appropriate iodo-carbonate **42–43** (1 equiv), then a N_2 atmosphere was established via a purge needle, and THF (0.1 M) was added to the flask at room temperature. To this flask, 0.5 M *i*-PrMgCl (4 equiv) in THF was added slowly over 1 h using a syringe pump at the same temperature, and the reaction mixture was allowed to stir for 30 min, after which the mixture was quenched with water. After separating the phases, the aqueous layer was extracted with Et_2O (3 x 30 mL), and the combined organic layers were dried over MgSO_4 . Filtration, concentration under reduced pressure, and purification by column chromatography on silica gel with hexanes afforded the corresponding dimers **4** (32%) and **5** (86%).

General Protocol for Trapping Reactions of Cyclic Allenes (18a–b) with Furan, DPIBF, and Styrene via Magnesium–Halogen Exchange Promoted Elimination

To a dry flask was added the appropriate iodo-carbonate **42–43** (1 equiv) and the appropriate trapping partner [furan (40-45 equiv), DPIBF (3 equiv), or styrene (25 equiv)], then a N₂ atmosphere was established via a purge needle. To this flask, THF (0.03 M) was added, the reaction mixture was heated to 50 °C, and 0.5 M *i*-PrMgCl (4 equiv) in THF was added slowly over 1 h using a syringe pump. The reaction mixture was allowed to stir at the same temperature for 30 min, then it was cooled to room temperature and quenched with water. After separating the phases, the aqueous layer was extracted with Et₂O (3 x 30 mL), and the combined organic layers were dried over MgSO₄. Filtration, concentration under reduced pressure, and purification by column chromatography on silica gel with hexanes/EtOAc afforded the corresponding cycloadducts **44a–b** (58%), **47** (63%), or **48a–b** (76%).

Dimers **4**,^{5, 22} **5** and **6**,⁴ and cycloadducts **44a–b**,²² **48**,²²⁻²³ **49a–b**⁶ are all known literature compounds. ¹H and ¹³C NMR spectral data are in agreement with those previously reported in the chemical literature.

3.6. References

1. Lofstrand, V. A.; West, F. G., *Chem. Eur. J.* **2016**, *22* (31), 10763-10767.
2. Barber, J. S.; Yamano, M. M.; Ramirez, M.; Darzi, E. R.; Knapp, R. R.; Liu, F.; Houk, K. N.; Garg, N. K., *Nat. Chem.* **2018**, *10* (9), 953-960.
3. Barber, J. S.; Styduhar, E. D.; Pham, H. V.; McMahon, T. C.; Houk, K.; Garg, N. K., *J. Am. Chem. Soc.* **2016**, *138* (8), 2512-2515.
4. Ball, W. J.; Landor, S. R., *Proc. Chem. Soc.* **1961**, 143-144.
5. Wittig, G.; Fritze, P., *Angew. Chem. Int. Ed.* **1966**, *5* (9), 846-846.
6. Moore, W. R.; Moser, W. R., *J. Am. Chem. Soc.* **1970**, *92* (18), 5469-5474.
7. Moore, W. R.; Ward, H. R.; Merritt, R. F., *J. Am. Chem. Soc.* **1961**, *83* (8), 2019-2020.
8. Taylor, K. G.; Hobbs, W. E.; Clark, M. S.; Chaney, J., *J. Org. Chem.* **1972**, *37* (15), 2436-2443.
9. Shakespeare, W. C.; Johnson, R. P., *J. Am. Chem. Soc.* **1990**, *112* (23), 8578-8579.
10. Yokota, M.; Fuchibe, K.; Ueda, M.; Mayumi, Y.; Ichikawa, J., *Org. Lett.* **2009**, *11* (17), 3994-3997.
11. Nwokogu, G. C., *J. Org. Chem.* **1985**, *50* (20), 3900-3908.
12. Barl, N. M.; Werner, V.; Samann, C.; Knochel, P., *Heterocycles* **2014**, *88* (2), 827-844.
13. Knochel, P.; Dohle, W.; Gommermann, N.; Kneisel, F. F.; Kopp, F.; Korn, T.; Sapountzis, I.; Vu, V. A., *Angew. Chem. Int. Ed.* **2003**, *42* (36), 4302-4320.
14. Dorn, H.; Graubaum, H., *J. Prakt. Chem.* **1976**, *318* (2), 253-260.
15. Johnson, R. P., *Chem. Rev.* **1989**, *89* (5), 1111-1124.
16. Yoshida, S.; Karaki, F.; Uchida, K.; Hosoya, T., *Chem. Commun.* **2015**, *51* (42), 8745-8748.
17. Shintani, R.; Fu, G. C., *J. Am. Chem. Soc.* **2003**, *125* (36), 10778-10779.
18. Shen, S.; Yang, Y.; Duan, J.; Jia, Z.; Liang, J., *Org. Biomol. Chem.* **2018**, *16* (7), 1068-1072.
19. Nugent, J.; Matousov, E. K.; Banwell, M. G.; Willis, A. C., *J. Org. Chem.* **2017**, *82* (23), 12569-12589.
20. Praveen, C.; Perumal, P. T., *Chin. J. Catal.* **2016**, *37* (2), 288-299.
21. Zhang, J.-T.; Qi, X.-L.; Chen, J.; Li, B.-S.; Zhou, Y.-B.; Cao, X.-P., *J. Org. Chem.* **2011**, *76* (10), 3946-3959.
22. Quintana, I.; Peña, D.; Pérez, D.; Guitián, E., *Eur. J. Org. Chem.* **2009**, *2009* (32), 5519-5524.
23. Wittig, G.; Meske-Schüller, J., *Liebigs Ann. Chem.* **1968**, *711* (1), 76-81.

Compiled References

Chapter 1

1. Moss, R. A.; Platz, M.; Jones, M., *Reactive Intermediate Chemistry*. Wiley Online Library: 2004.
2. Gillespie, R. J., *J. Chem. Educ.* **1963**, *40* (6), 295.
3. Bredt, J.; Houben, J.; Levy, P., *Ber. Dtsch. Chem. Ges.* **1902**, *35* (2), 1286-1292.
4. Walsh, A. D., *Nature* **1947**, *159* (4031), 165.
5. Huang, C.-Y.; Doyle, A. G., *Chem. Rev.* **2014**, *114* (16), 8153-8198.
6. He, J.; Ling, J.; Chiu, P., *Chem. Rev.* **2014**, *114* (16), 8037-8128.
7. Vilotijevic, I.; Jamison, T. F., *Angew. Chem. Int. Ed.* **2009**, *48* (29), 5250-5281.
8. Wittig, G.; Krebs, A.; Pohlke, R., *Angew. Chem.* **1960**, *72* (9), 324-324.
9. Montgomery, L. K.; Applegate, L. E., *J. Am. Chem. Soc.* **1967**, *89* (20), 5305-5307.
10. Chapman, O. L.; Gano, J.; West, P. R.; Regitz, M.; Maas, G., *J. Am. Chem. Soc.* **1981**, *103* (23), 7033-7036.
11. Medina, J. M.; McMahon, T. C.; Jimenez-Osuna, G.; Houk, K. N.; Garg, N. K., *J. Am. Chem. Soc.* **2014**, *136* (42), 14706-14709.
12. Scardiglia, F.; Roberts, J. D., *Tetrahedron* **1957**, *1* (4), 343-344.
13. Fixari, B.; Brunet, J. J.; Caubere, P., *Tetrahedron* **1976**, *32* (8), 927-934.
14. Wentrup, C.; Blanch, R.; Briehl, H.; Gross, G., *J. Am. Chem. Soc.* **1988**, *110* (6), 1874-1880.
15. Wittig, G.; Meske-Schüller, J., *Justus Liebigs Ann. Chem.* **1968**, *711* (1), 76-81.
16. Wittig, G.; Krebs, A., *Chem. Ber.* **1961**, *94* (12), 3260-3275.
17. Huisgen, R., *Proc. Chem. Soc.* **1961**, 357-396.
18. Huisgen, R., *Angew. Chem. Int. Ed.* **1963**, *2* (10), 565-598.
19. Kolb, H. C.; Finn, M. G.; Sharpless, K. B., *Angew. Chem. Int. Ed.* **2001**, *40* (11), 2004-2021.
20. Baskin, J. M.; Prescher, J. A.; Laughlin, S. T.; Agard, N. J.; Chang, P. V.; Miller, I. A.; Lo, A.; Codelli, J. A.; Bertozzi, C. R., *Proc. Natl. Acad. Sci. U.S.A.* **2007**, *104* (43), 16793-16797.
21. Agard, N. J.; Prescher, J. A.; Bertozzi, C. R., *J. Am. Chem. Soc.* **2004**, *126* (46), 15046-15047.
22. Gampe, C. M.; Carreira, E. M., *Angew. Chem. Int. Ed.* **2011**, *50* (13), 2962-2965.
23. Gampe, C. M.; Boulos, S.; Carreira, E. M., *Angew. Chem. Int. Ed.* **2010**, *49* (24), 4092-4095.
24. Kim, J. Y.; Cho, J. H.; Choi, J.-R.; Shin, H.-J.; Song, J.-Y.; Hwang, S.-G.; Um, H.-D.; Do Yoo, Y.; Kim, J.; Park, J. K., *Toxicol. Appl. Pharmacol.* **2018**, *357*, 39-49.
25. Lee, C. J.; Swain, M.; Kwon, O., *Org. Lett.* **2018**, *20* (17), 5474-5477.
26. Roberts, J. D.; Simmons Jr, H. E.; Carlsmith, L. A.; Vaughan, C. W., *J. Am. Chem. Soc.* **1953**, *75* (13), 3290-3291.
27. Goetz, A. E.; Bronner, S. M.; Cisneros, J. D.; Melamed, J. M.; Paton, R. S.; Houk, K. N.; Garg, N. K., *Angew. Chem. Int. Ed.* **2012**, *51* (11), 2758-2762.

28. Díaz, M. T.; Cobas, A.; Guitián, E.; Castedo, L., *Synlett* **1998**, 1998 (02), 157-158.
29. May, C.; Moody, C. J., *J. Chem. Soc., Perkin Trans. 1* **1988**, (2), 247-250.
30. Díaz, M.; Cobas, A.; Guitián, E.; Castedo, L., *Eur. J. Org. Chem.* **2001**, 2001 (23), 4543-4549.
31. Iwao, M.; Motoi, O.; Fukuda, T.; Ishibashi, F., *Tetrahedron* **1998**, 54 (31), 8999-9010.
32. Johnson, R. P., *Chem. Rev.* **1989**, 89 (5), 1111-1124.
33. Lofstrand, V. A.; West, F. G., *Chem. Eur. J.* **2016**, 22 (31), 10763-10767.
34. Barber, J. S.; Styduhar, E. D.; Pham, H. V.; McMahon, T. C.; Houk, K. N.; Garg, N. K., *J. Am. Chem. Soc.* **2016**, 138 (8), 2512-5.
35. Wittig, G.; Mayer, U., *Chem. Ber.* **1963**, 96 (1), 342-348.
36. Bottini, A. T.; Cabral, L. J.; Dev, V., *Tetrahedron Lett.* **1977**, 18 (7), 615-618.
37. Moore, W. R.; Moser, W. R., *J. Am. Chem. Soc.* **1970**, 92 (18), 5469-5474.
38. Wittig, G.; Fritze, P., *Angew. Chem. Int. Ed.* **1966**, 5 (9), 846-846.
39. Seburg, R. A.; Patterson, E. V.; Stanton, J. F.; McMahon, R. J., *J. Am. Chem. Soc.* **1997**, 119 (25), 5847-5856.
40. H. Meier; König, P., *Nouv. J. Chim.* **1986**, 10, 437-428.
41. Melaimi, M.; Parameswaran, P.; Donnadiou, B.; Frenking, G.; Bertrand, G., *Angew. Chem.* **2009**, 121 (26), 4886-4889.
42. Balci, M.; Taskesenligil, Y., *Recent Developments in Strained Cyclic Allenes*. Wiley Online Library: 2000; Vol. 31, p 43.
43. Ceylan, M.; Seçen, H.; Sütbeyaz, Y., *J. Chem. Res. (S)* **1997**, (3), 70-71.
44. Algi, F.; Özen, R.; Balci, M., *Tetrahedron Lett.* **2002**, 43 (17), 3129-3131.
45. Favorskii, A. E., *J. Gen. Chem. (USSR) (Engl. Transl.)* **1936**, 6, 720-731.
46. Domnin, N. A., *J. Gen. Chem. (USSR) (Engl. Transl.)* **1940**, 10, 1939.
47. Domnin, N. A., *J. Gen. Chem. (USSR) (Engl. Transl.)* **1945**, 15, 461.
48. Ball, W. J.; Landor, S. R., *Proc. Chem. Soc.* **1961**, 143-144.
49. Ball, W. J.; Landor, S. R., *J. Chem. Soc* **1962**, (0), 2298-2304.
50. Quintana, I.; Peña, D.; Pérez, D.; Guitián, E., *Eur. J. Org. Chem.* **2009**, 2009 (32), 5519-5524.
51. Shakespeare, W. C.; Johnson, R. P., *J. Am. Chem. Soc.* **1990**, 112 (23), 8578-8579.
52. Christl, M.; Braun, M.; Wolz, E.; Wagner, W., *Chem. Ber.* **1994**, 127 (6), 1137-1142.
53. Schreck, M.; Christl, M., *Angew. Chem.* **1987**, 99 (7), 720-721.
54. Schreck, M.; Christl, M., *Angew. Chem. Int. Ed.* **1987**, 26 (7), 690-692.
55. Barber, J. S.; Yamano, M. M.; Ramirez, M.; Darzi, E. R.; Knapp, R. R.; Liu, F.; Houk, K. N.; Garg, N. K., *Nat. Chem.* **2018**, 10 (9), 953.
56. Yamano, M.; Knapp, R.; Ngamnthiporn, A.; Ramirez, M.; Houk, K.; Stoltz, B.; Garg, N. K., *Angew. Chem.* **2019**, 131 (17), 5809-5713.
57. Lofstrand, V. A.; McIntosh, K. C.; Almeahmadi, Y. A.; West, F. G., *In preparation* **2019**.
58. Brunet, J. J.; Fixari, B.; Caubere, P., *Tetrahedron* **1974**, 30 (16), 2931-2937.

59. Bottini, A. T.; Frost Ii, K. A.; Anderson, B. R.; Dev, V., *Tetrahedron* **1973**, 29 (14), 1975-1981.
60. Kropp, P. J.; McNeely, S. A.; Davis, R. D., *J. Am. Chem. Soc.* **1983**, 105 (23), 6907-6915.
61. Taylor, K. G.; Hobbs, W. E.; Clark, M. S.; Chaney, J., *J. Org. Chem.* **1972**, 37 (15), 2436-2443.
62. Sütbeyaz, Y.; Ceylan, M.; Seçen, H., *J. chem. research (S)* **1993**, 293.
63. Bottini, A. T.; Hilton, L. L., *Tetrahedron* **1975**, 31 (17), 2003-2004.
64. Moore, W. R.; Ward, H. R.; Merritt, R. F., *J. Am. Chem. Soc.* **1961**, 83 (8), 2019-2020.
65. Wittig, G.; Dorsch, H. L.; Meske-Schüller, J., *Justus Liebigs Ann. Chem.* **1968**, 711 (1), 55-64.
66. Marquis, E. T.; Gardner, P. D., *Tetrahedron Lett.* **1966**, 7 (25), 2793-2798.
67. Wisser, J. P.; Ramakers, J. E., *J. Chem. Soc., Chem. Commun.* **1972**, 178.
68. Price, J. D.; Johnson, R. P., *Tetrahedron Lett.* **1986**, 27 (39), 4679-4682.

Chapter 2

1. Schönbein, C. F., *Ber. Verh. Nat. Ges. Basel.* **1847**, 7, 4-6.
2. Gothelf, K. V.; Jørgensen, K. A., *Chem. Rev.* **1998**, 98 (2), 863-910.
3. Padwa, A.; Craig, S. P.; Chiacchio, U.; Kline, D. N., *J. Org. Chem.* **1988**, 53 (10), 2232-2238.
4. Pellissier, H.; Santelli, M., *Tetrahedron* **2003**, 59 (6), 701-730.
5. Wenk, H. H.; Winkler, M.; Sander, W., *Angew. Chem. Int. Ed.* **2003**, 42 (5), 502-528.
6. Tadross, P. M.; Stoltz, B. M., *Chem. Rev.* **2012**, 112 (6), 3550-3577.
7. Wu, C.; Shi, F., *Asian J. Org. Chem.* **2013**, 2 (2), 116-125.
8. Bhunia, A.; Yetra, S. R.; Biju, A. T., *Chem. Soc. Rev.* **2012**, 41 (8), 3140-3152.
9. Sanz, R., *Org. Prep. Proced. Int.* **2008**, 40 (3), 215-291.
10. Gampe, C. M.; Carreira, E. M., *Angew. Chem. Int. Ed.* **2012**, 51 (16), 3766-3778.
11. Yoshida, H.; Takaki, K., *Synlett* **2012**, 23 (12), 1725-1732.
12. Dubrovskiy, A. V.; Markina, N. A.; Larock, R. C., *Org. Biomol. Chem.* **2013**, 11 (2), 191-218.
13. Hoffmann, R. W.; Suzuki, K., *Angew. Chem. Int. Ed.* **2013**, 52 (10), 2655-2656.
14. Goetz, A. E.; Garg, N. K., *J. Org. Chem.* **2014**, 79 (3), 846-851.
15. Moss, R. A.; Platz, M. S.; Jones Jr, M., *Reactive Intermediate Chemistry*. John Wiley & Sons: 2004.
16. Sary, I.; Stara, I. G.; Dodziuk, H., *Strained Hydrocarbons: Beyond the van't Hoff and Le Bel Hypothesis*. Wiley-VCH, Weinheim: 2009.
17. Ball, W. J.; Landor, S. R., *Proc. Chem. Soc.* **1961**, 143-144.
18. Bottini, A. T.; Frost Ii, K. A.; Anderson, B. R.; Dev, V., *Tetrahedron* **1973**, 29 (14), 1975-1981.
19. Kropp, P. J.; McNeely, S. A.; Davis, R. D., *J. Am. Chem. Soc.* **1983**, 105 (23), 6907-6915.
20. Taylor, K. G.; Hobbs, W. E.; Clark, M. S.; Chaney, J., *J. Org. Chem.* **1972**, 37 (15), 2436-2443.
21. Sütbeyaz, Y.; Ceylan, M.; Seçen, H., *J. Chem. Res. (S)* **1993**, 293.
22. Shakespeare, W. C.; Johnson, R. P., *J. Am. Chem. Soc.* **1990**, 112 (23), 8578-8579.
23. Lofstrand, V. A.; West, F. G., *Chem. Eur. J.* **2016**, 22 (31), 10763-10767.

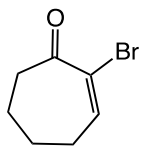
24. Barber, J. S.; Yamano, M. M.; Ramirez, M.; Darzi, E. R.; Knapp, R. R.; Liu, F.; Houk, K. N.; Garg, N. K., *Nat. Chem.* **2018**, *10* (9), 953-960.
25. Werstiuk, N. H.; Roy, C. D.; Ma, J., *Can. J. Chem.* **1996**, *74* (10), 1903-1905.
26. Barber, J. S.; Styduhar, E. D.; Pham, H. V.; McMahon, T. C.; Houk, K. N.; Garg, N. K., *J. Am. Chem. Soc.* **2016**, *138* (8), 2512-5.
27. Chen, W.; Du, W.; Duan, Y. Z.; Wu, Y.; Yang, S. Y.; Chen, Y. C., *Angew. Chem.* **2007**, *119* (40), 7811-7814.
28. Laycock, D. E.; Wain, R. J.; Wightman, R. H., *Can. J. Chem.* **1977**, *55* (1), 21-23.
29. Lofstrand, V. A.; McIntosh, K. C.; Almealmadi, Y. A.; West, F. G., *In preparation* **2019**.
30. Bode, J. W.; Hachisu, Y.; Matsuura, T.; Suzuki, K., *Tetrahedron Letters* **2003**, *44* (17), 3555-3558.
31. Shintani, R.; Fu, G. C., *J. Am. Chem. Soc.* **2003**, *125* (36), 10778-10779.
32. Shen, S.; Yang, Y.; Duan, J.; Jia, Z.; Liang, J., *Org. Biomol. Chem.* **2018**, *16* (7), 1068-1072.
33. Canterbury, D. P.; Herrick, I. R.; Um, J.; Houk, K. N.; Frontier, A. J., *Tetrahedron* **2009**, *65* (16), 3165-3179.
34. George, M. V.; Peterson, D. J.; Gilman, H., *J. Am. Chem. Soc.* **1960**, *82* (2), 403-406.

Chapter 3

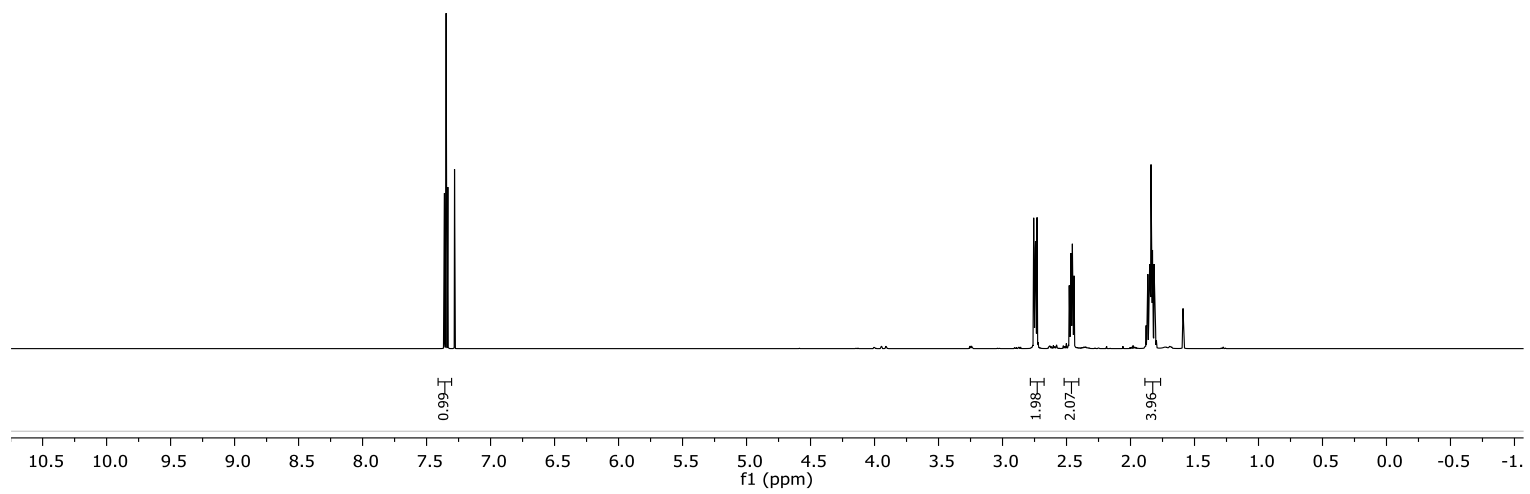
1. Lofstrand, V. A.; West, F. G., *Chem. Eur. J.* **2016**, *22* (31), 10763-10767.
2. Barber, J. S.; Yamano, M. M.; Ramirez, M.; Darzi, E. R.; Knapp, R. R.; Liu, F.; Houk, K. N.; Garg, N. K., *Nat. Chem.* **2018**, *10* (9), 953-960.
3. Barber, J. S.; Styduhar, E. D.; Pham, H. V.; McMahon, T. C.; Houk, K.; Garg, N. K., *J. Am. Chem. Soc.* **2016**, *138* (8), 2512-2515.
4. Ball, W. J.; Landor, S. R., *Proc. Chem. Soc.* **1961**, 143-144.
5. Wittig, G.; Fritze, P., *Angew. Chem. Int. Ed.* **1966**, *5* (9), 846-846.
6. Moore, W. R.; Moser, W. R., *J. Am. Chem. Soc.* **1970**, *92* (18), 5469-5474.
7. Moore, W. R.; Ward, H. R.; Merritt, R. F., *J. Am. Chem. Soc.* **1961**, *83* (8), 2019-2020.
8. Taylor, K. G.; Hobbs, W. E.; Clark, M. S.; Chaney, J., *J. Org. Chem.* **1972**, *37* (15), 2436-2443.
9. Shakespeare, W. C.; Johnson, R. P., *J. Am. Chem. Soc.* **1990**, *112* (23), 8578-8579.
10. Yokota, M.; Fuchibe, K.; Ueda, M.; Mayumi, Y.; Ichikawa, J., *Org. Lett.* **2009**, *11* (17), 3994-3997.
11. Nwokogu, G. C., *J. Org. Chem.* **1985**, *50* (20), 3900-3908.
12. Barl, N. M.; Werner, V.; Samann, C.; Knochel, P., *Heterocycles* **2014**, *88* (2), 827-844.
13. Knochel, P.; Dohle, W.; Gommermann, N.; Kneisel, F. F.; Kopp, F.; Korn, T.; Sapountzis, I.; Vu, V. A., *Angew. Chem. Int. Ed.* **2003**, *42* (36), 4302-4320.
14. Dorn, H.; Graubau, H., *J. Prakt. Chem.* **1976**, *318* (2), 253-260.
15. Johnson, R. P., *Chem. Rev.* **1989**, *89* (5), 1111-1124.
16. Yoshida, S.; Karaki, F.; Uchida, K.; Hosoya, T., *Chem. Commun.* **2015**, *51* (42), 8745-8748.

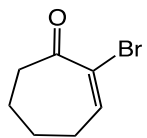
17. Shintani, R.; Fu, G. C., *J. Am. Chem. Soc.* **2003**, *125* (36), 10778-10779.
18. Shen, S.; Yang, Y.; Duan, J.; Jia, Z.; Liang, J., *Org. Biomol. Chem.* **2018**, *16* (7), 1068-1072.
19. Nugent, J.; Matousov, E. K.; Banwell, M. G.; Willis, A. C., *J. Org. Chem.* **2017**, *82* (23), 12569-12589.
20. Praveen, C.; Perumal, P. T., *Chin. J. Catal.* **2016**, *37* (2), 288-299.
21. Zhang, J.-T.; Qi, X.-L.; Chen, J.; Li, B.-S.; Zhou, Y.-B.; Cao, X.-P., *J. Org. Chem.* **2011**, *76* (10), 3946-3959.
22. Quintana, I.; Peña, D.; Pérez, D.; Guitián, E., *Eur. J. Org. Chem.* **2009**, *2009* (32), 5519-5524.
23. Wittig, G.; Meske-Schüller, J., *Liebigs Ann. Chem.* **1968**, *711* (1), 76-81.

**Appendix I: Selected NMR Spectra
(Chapter 2)**

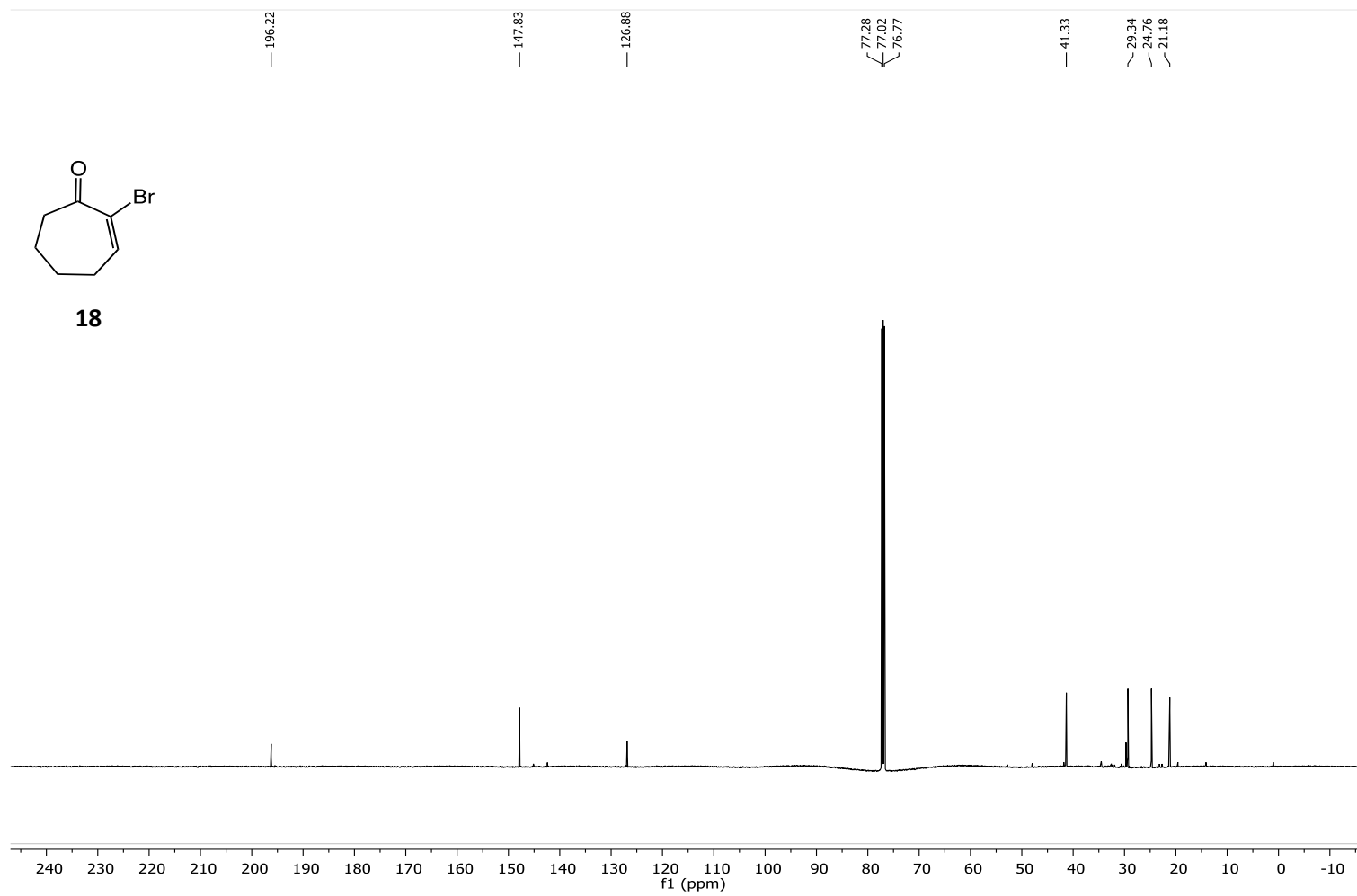


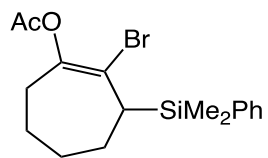
18



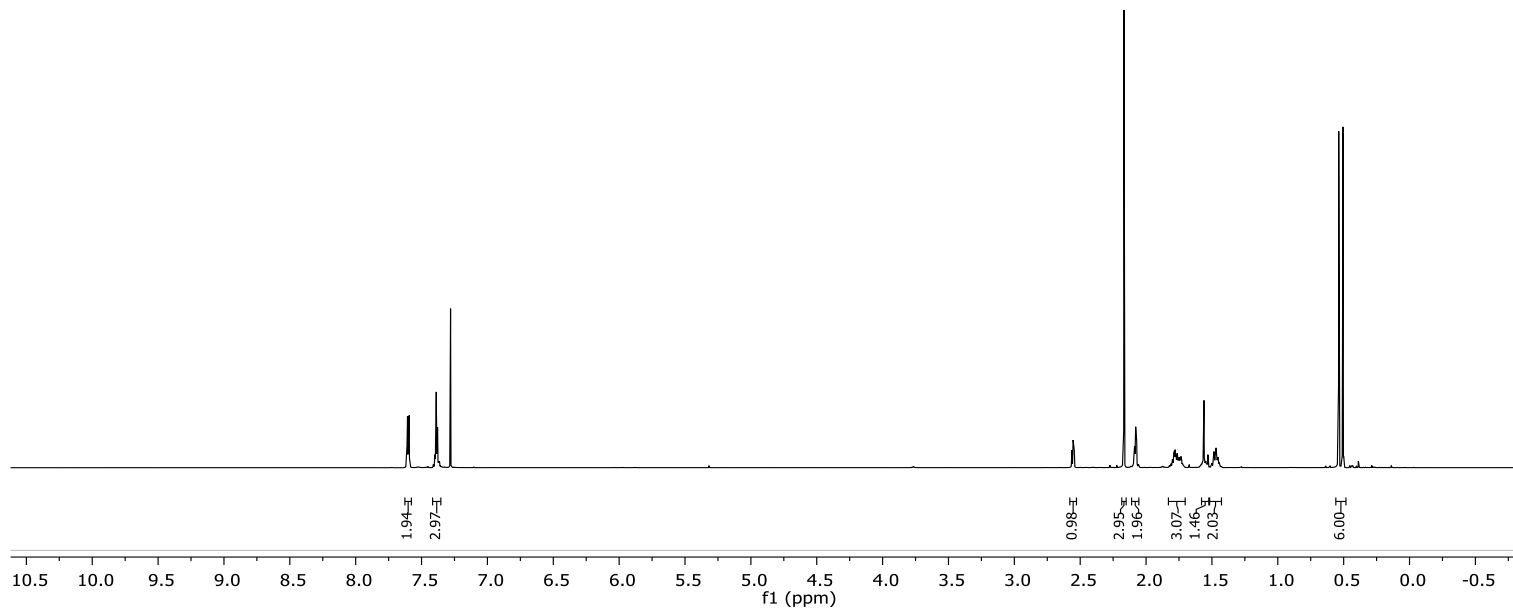


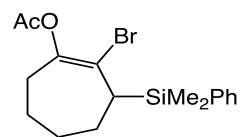
18



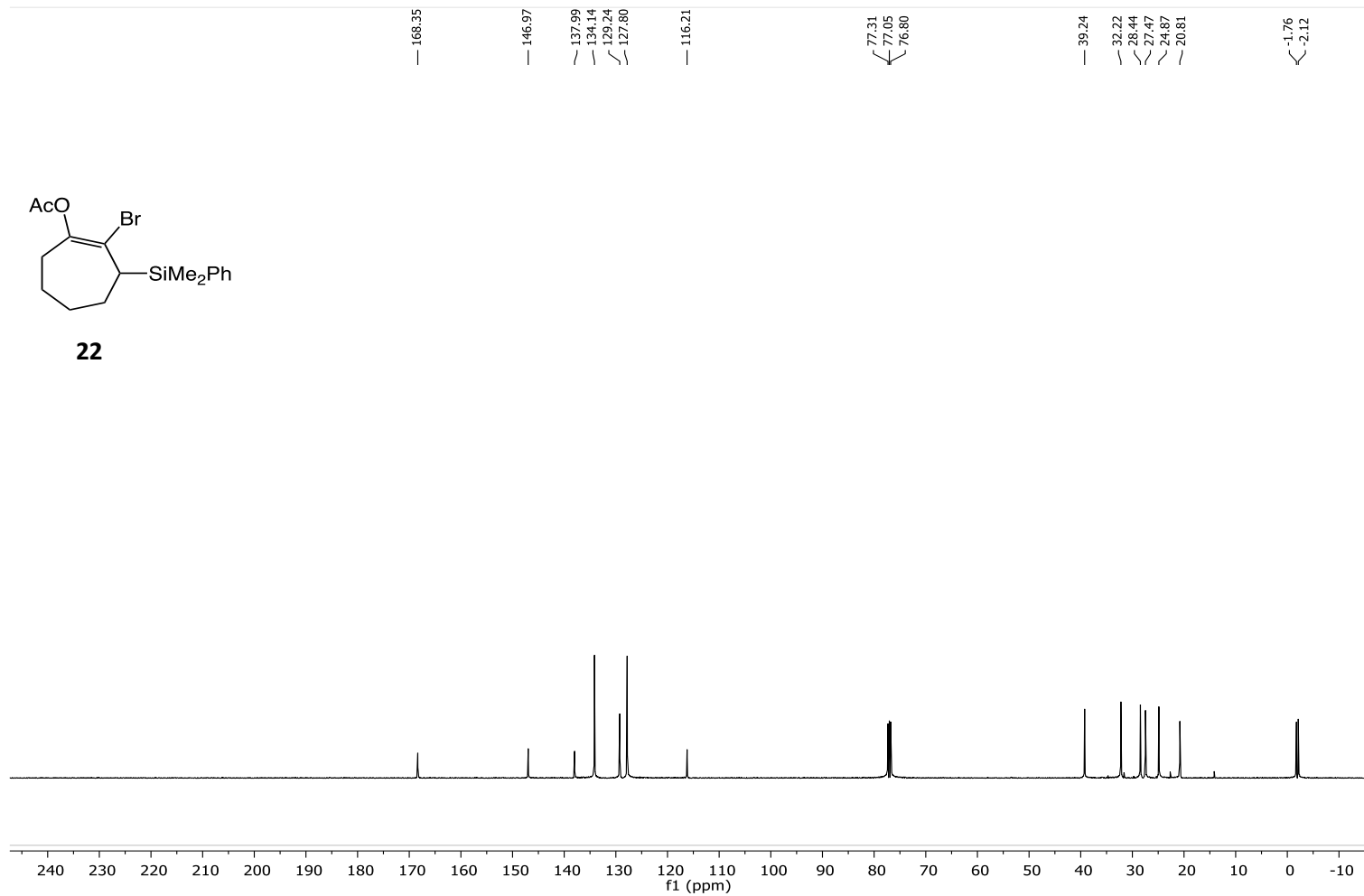


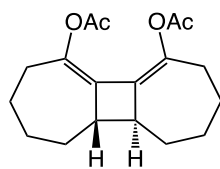
22



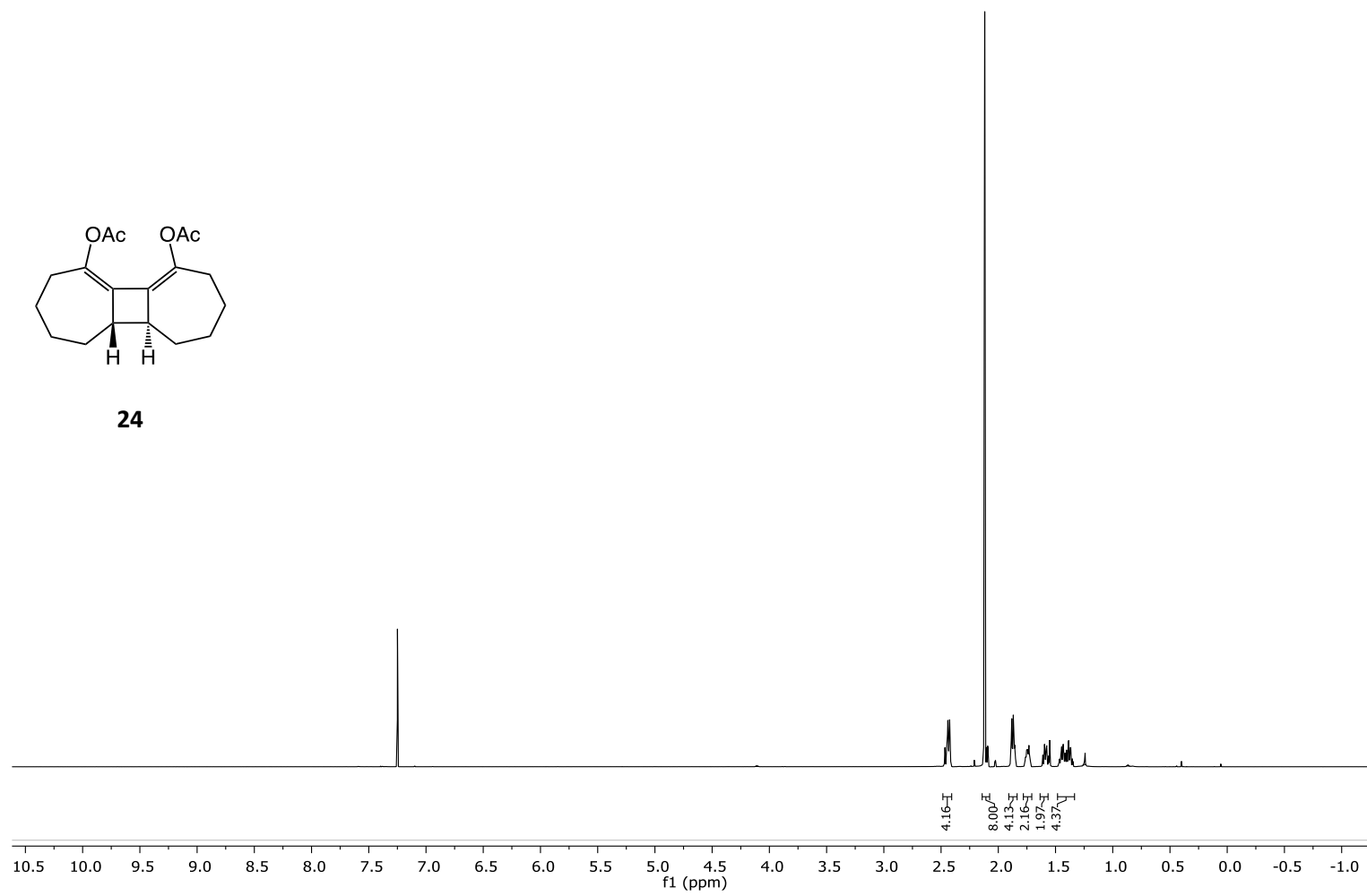


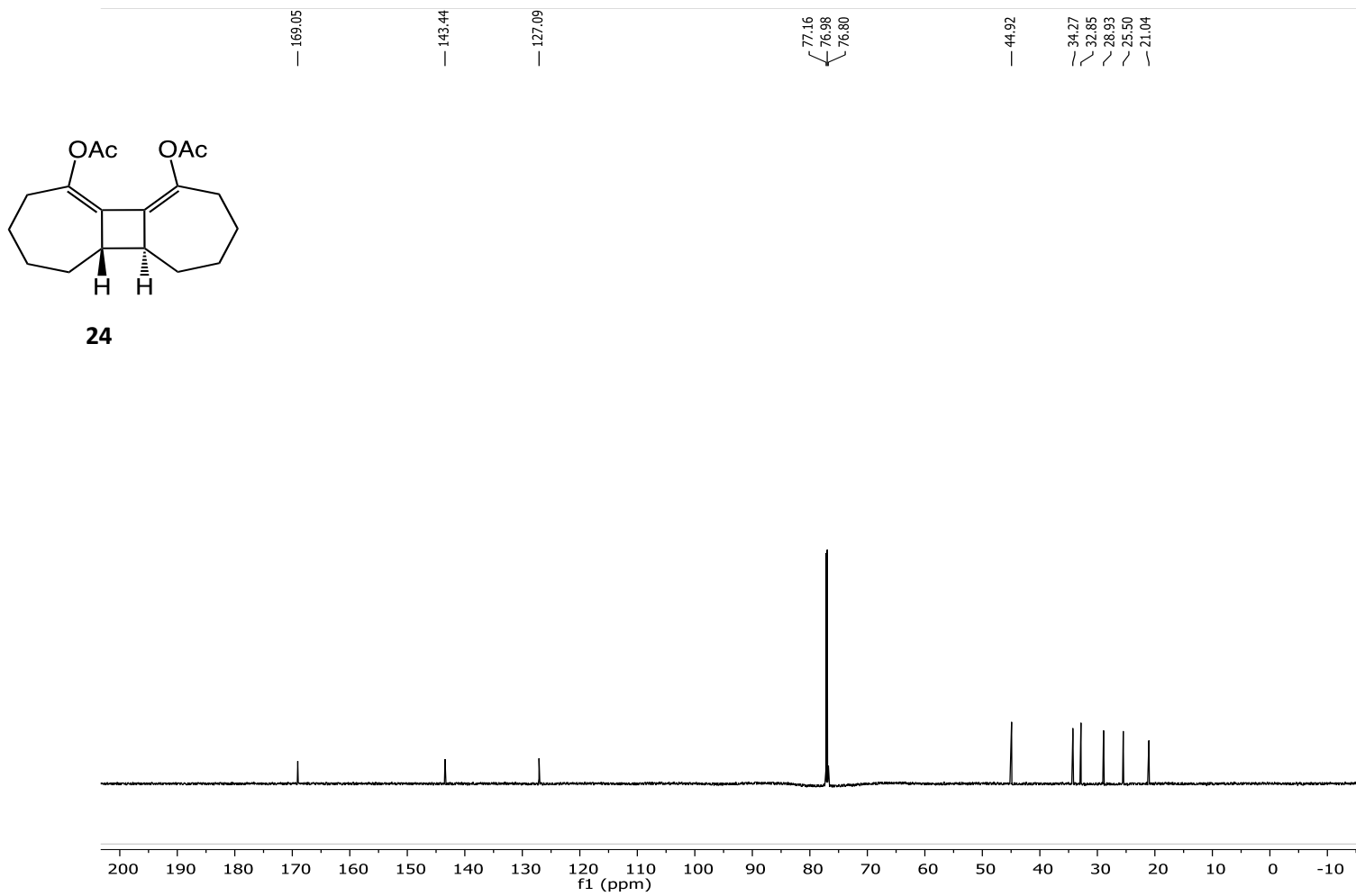
22

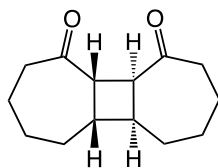




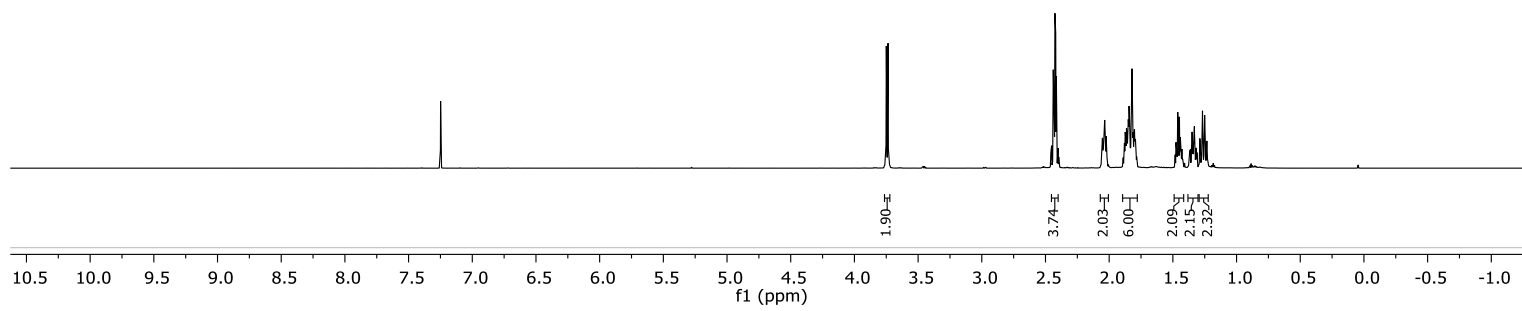
24







25

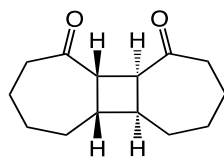


— 211.43

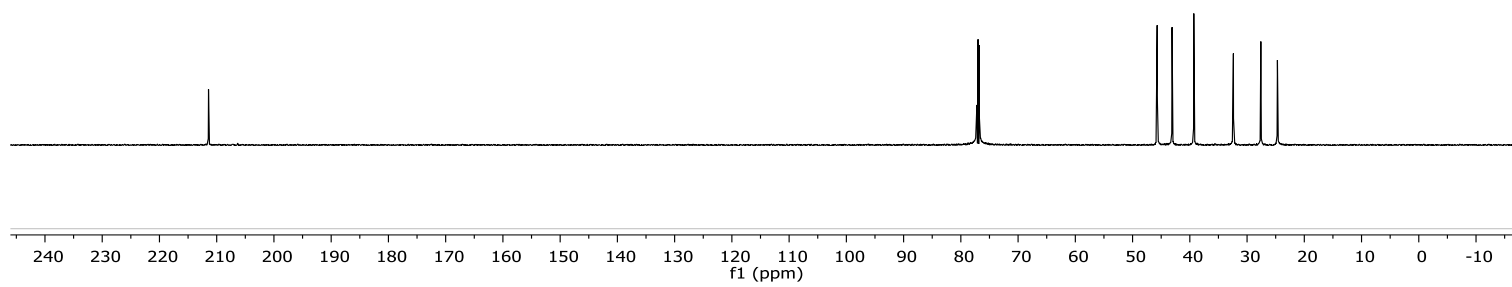
77.18
76.99
76.81

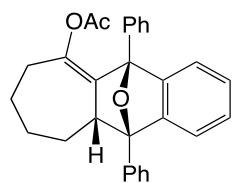
45.70
43.10
39.31

32.39
27.59
24.69

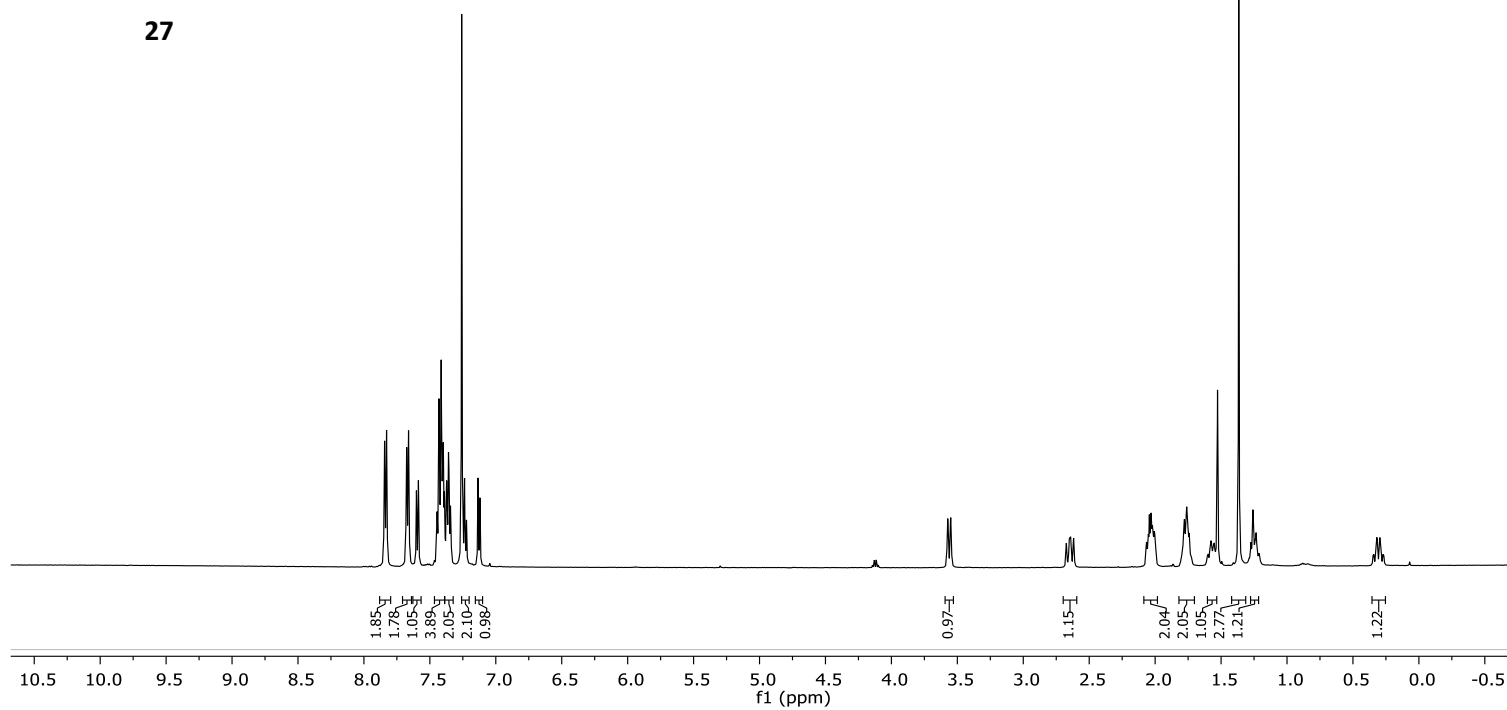


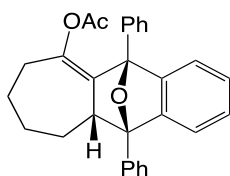
25



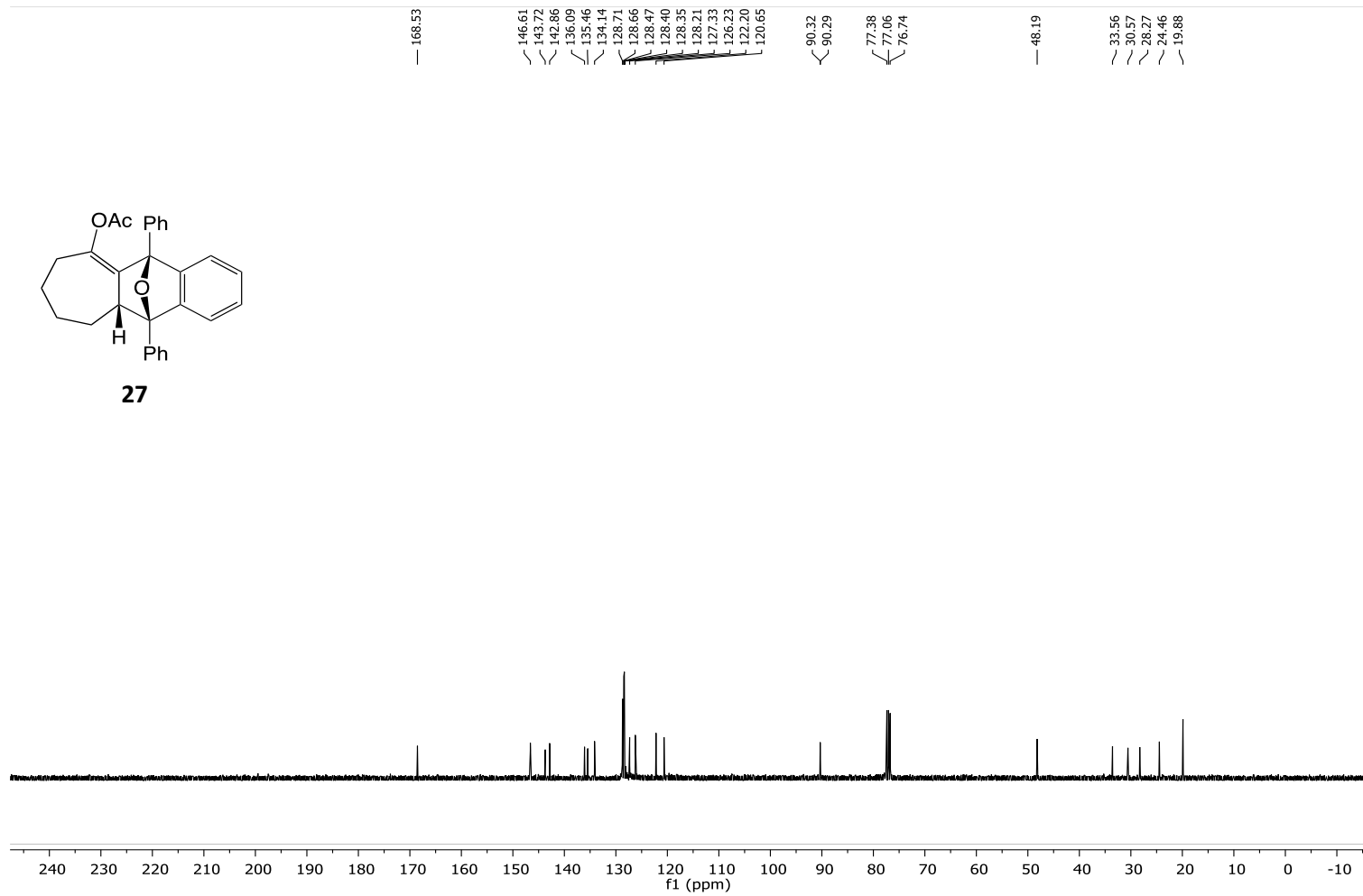


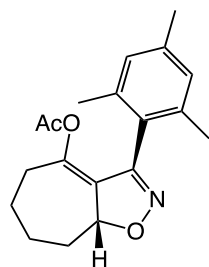
27



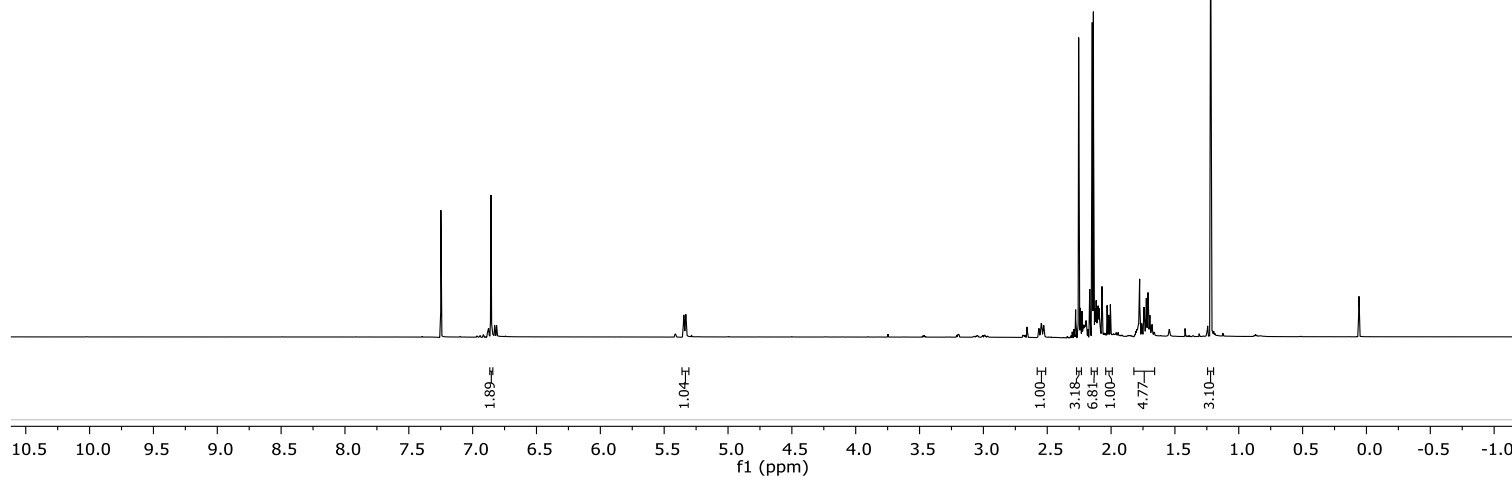


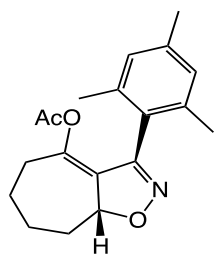
27



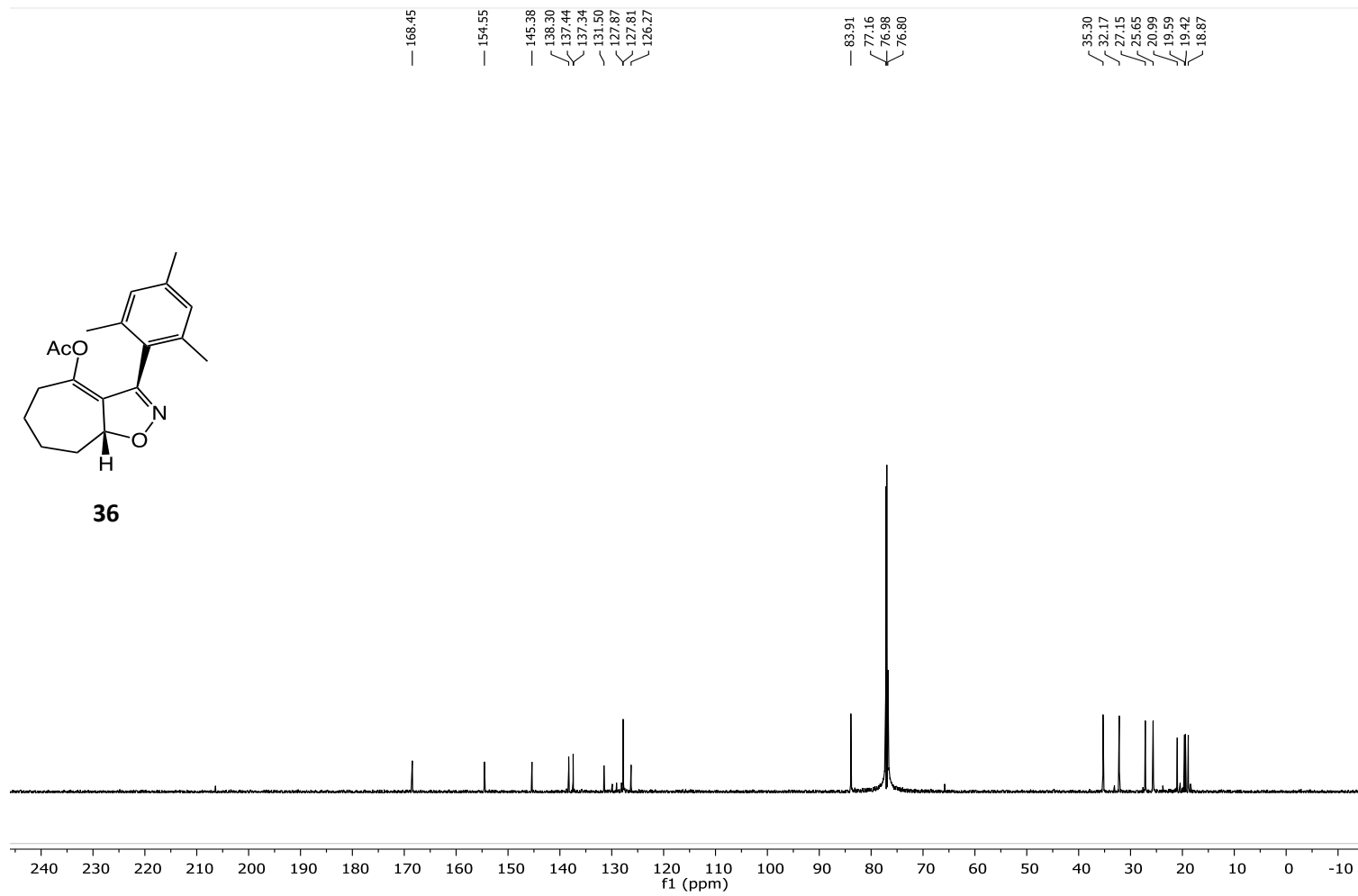


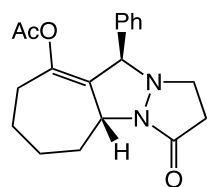
36



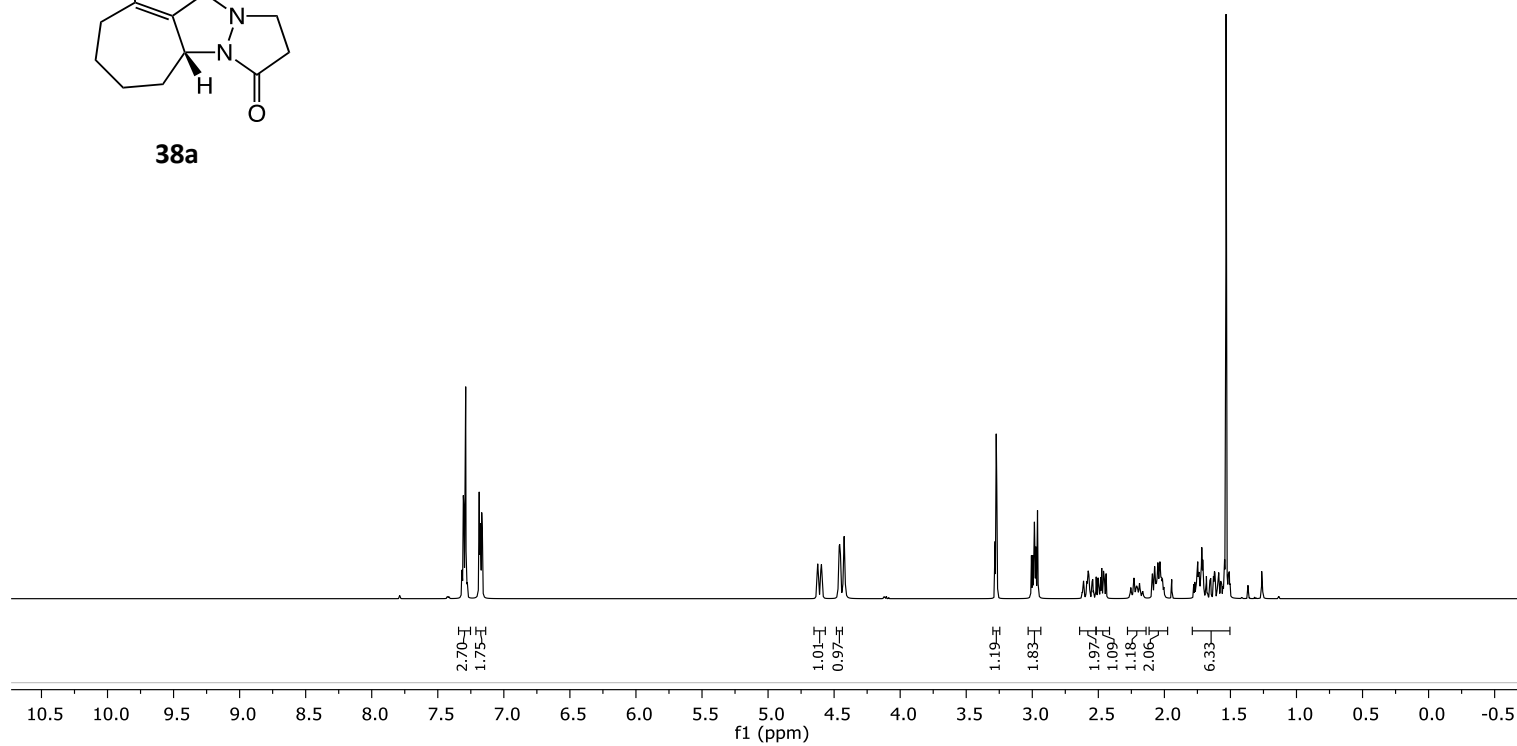


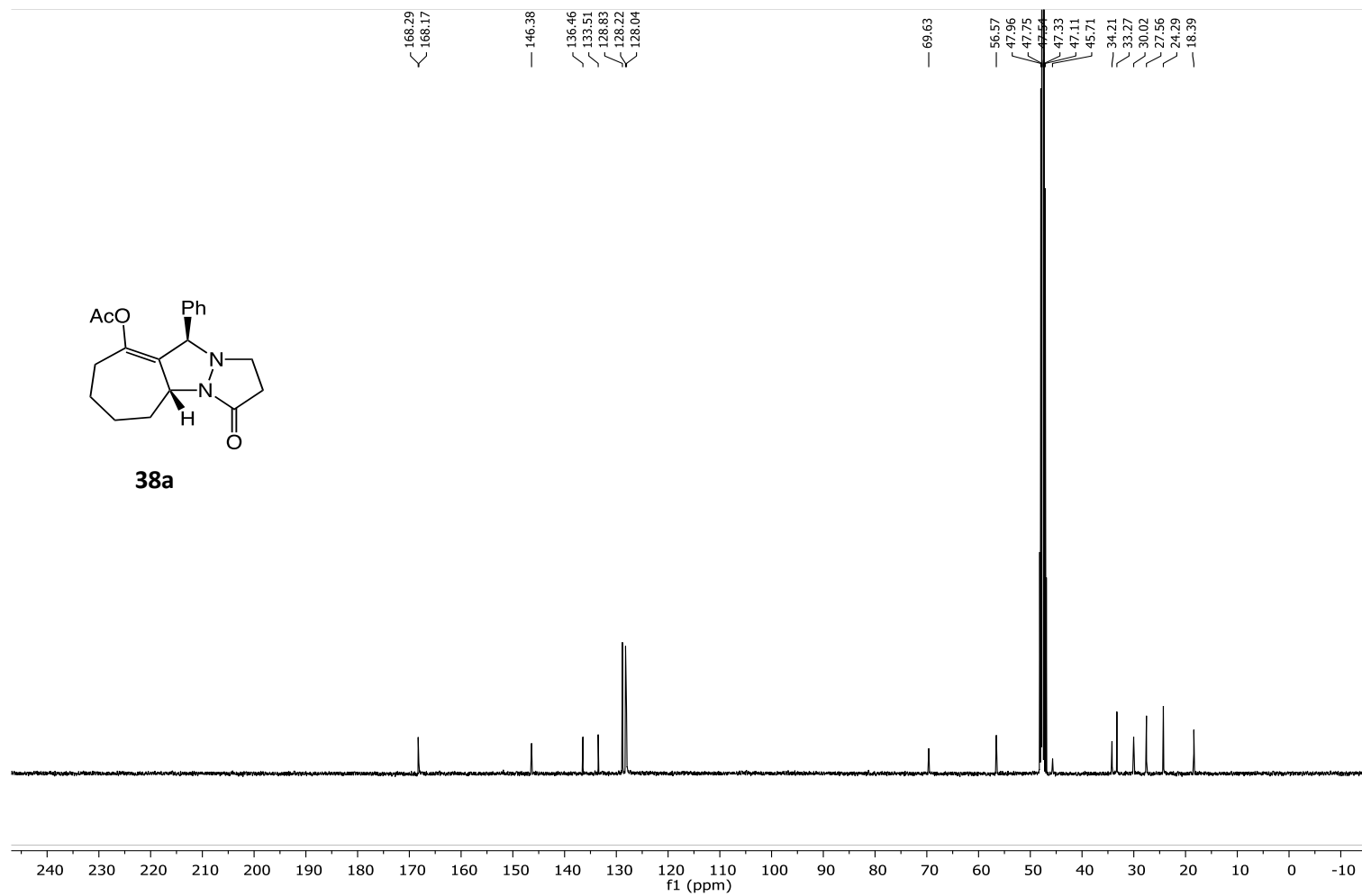
36

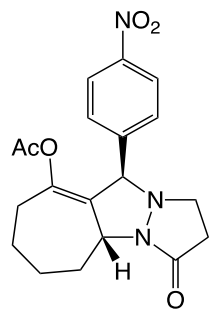




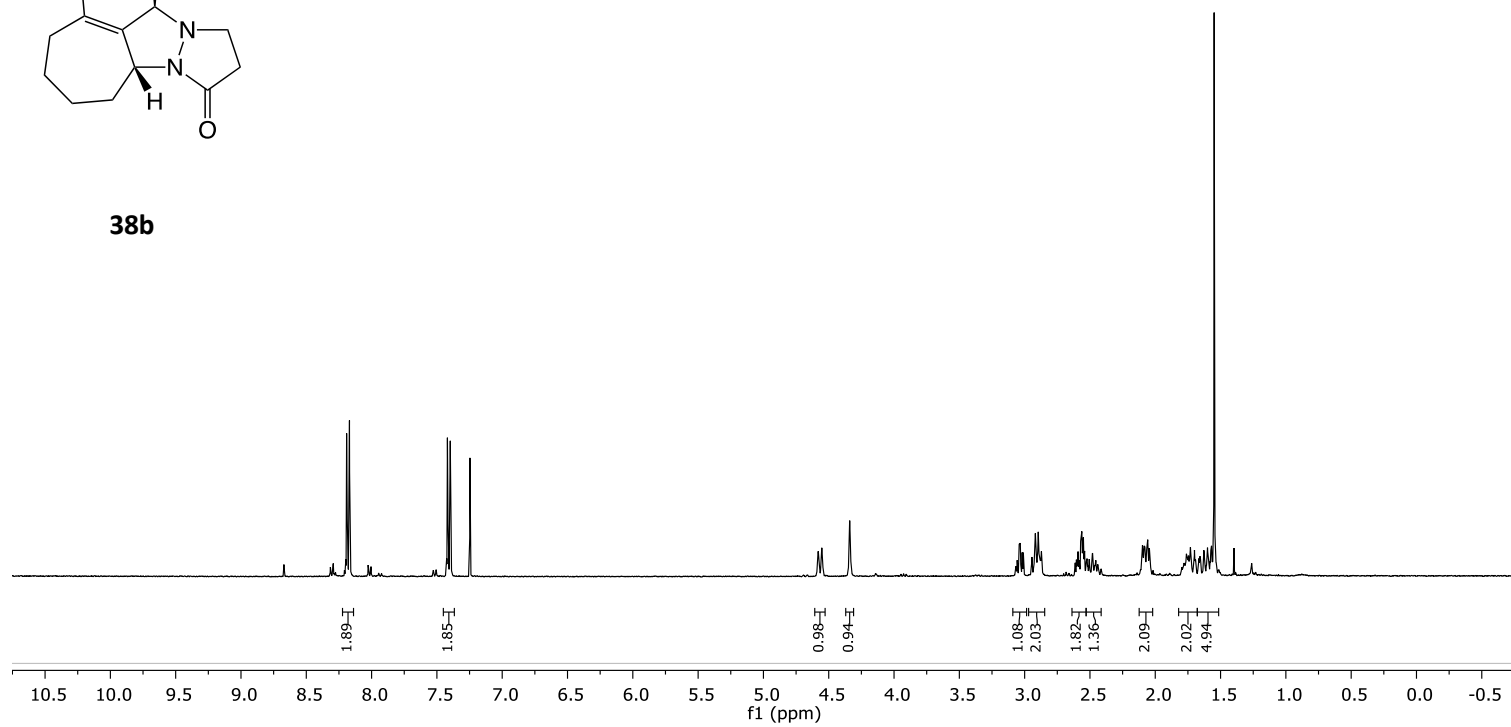
38a

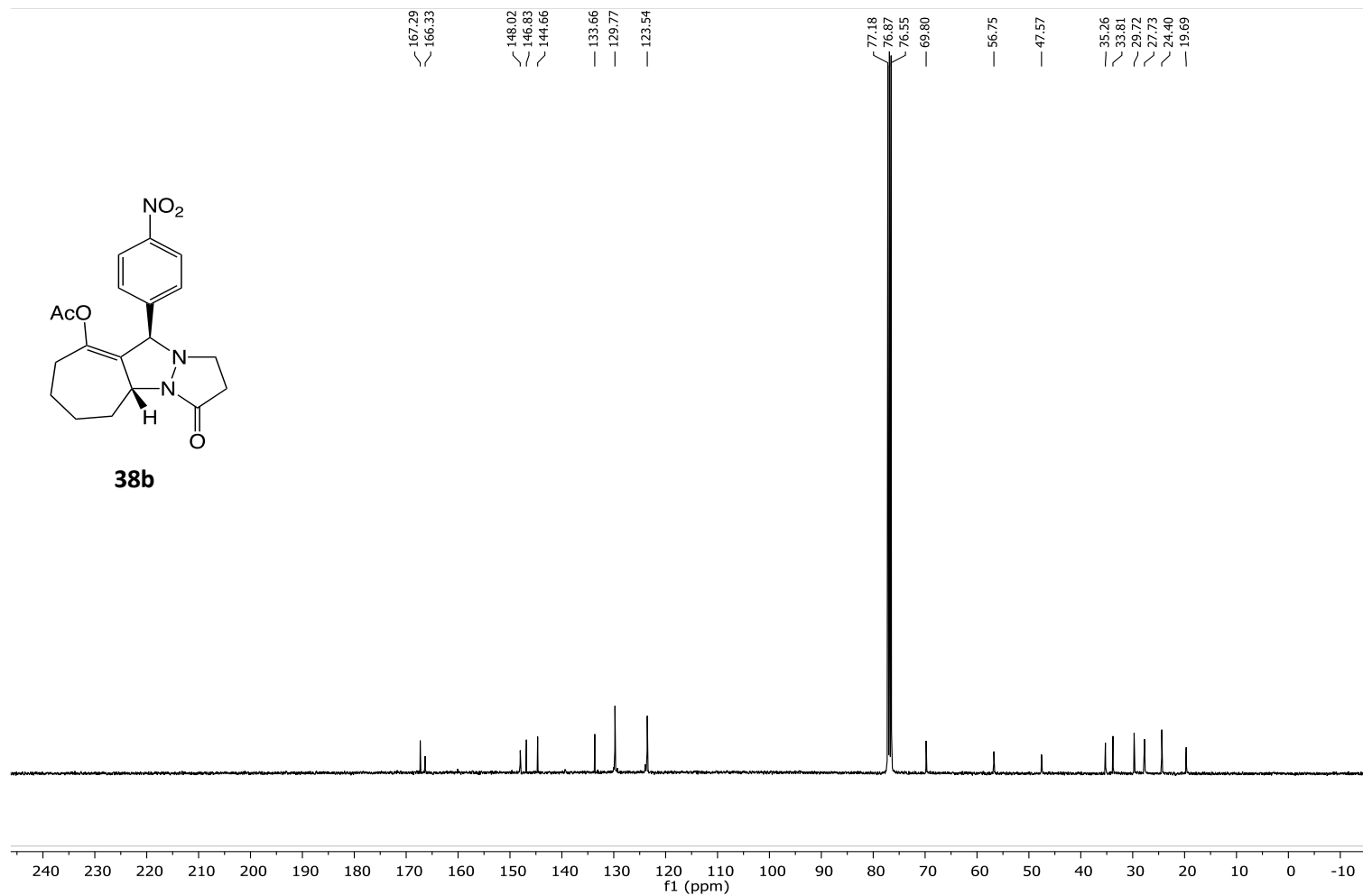


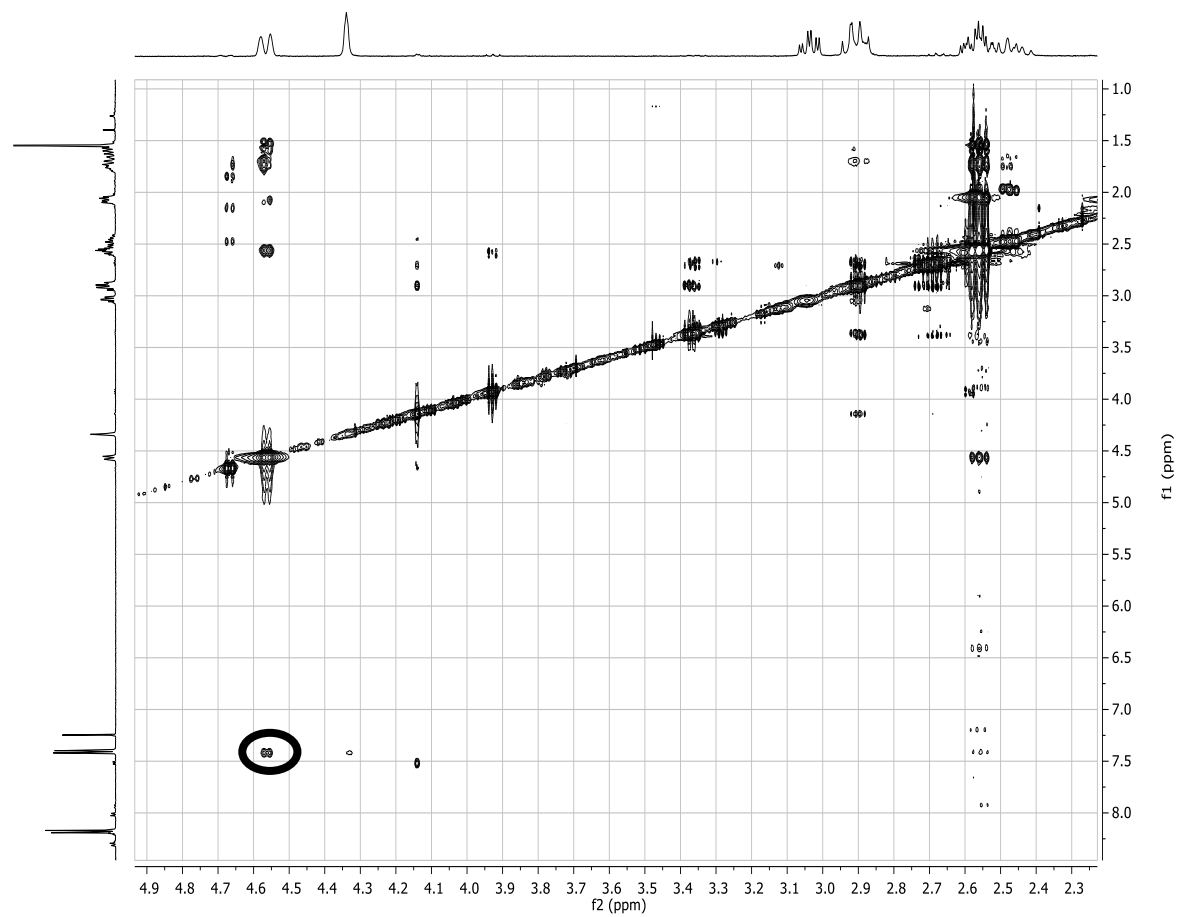
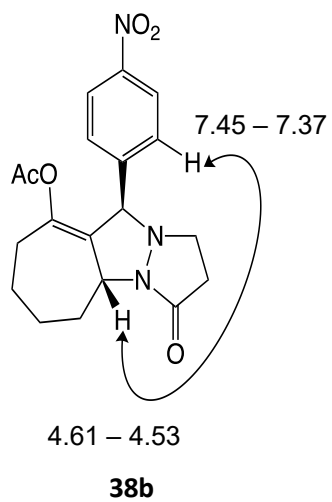


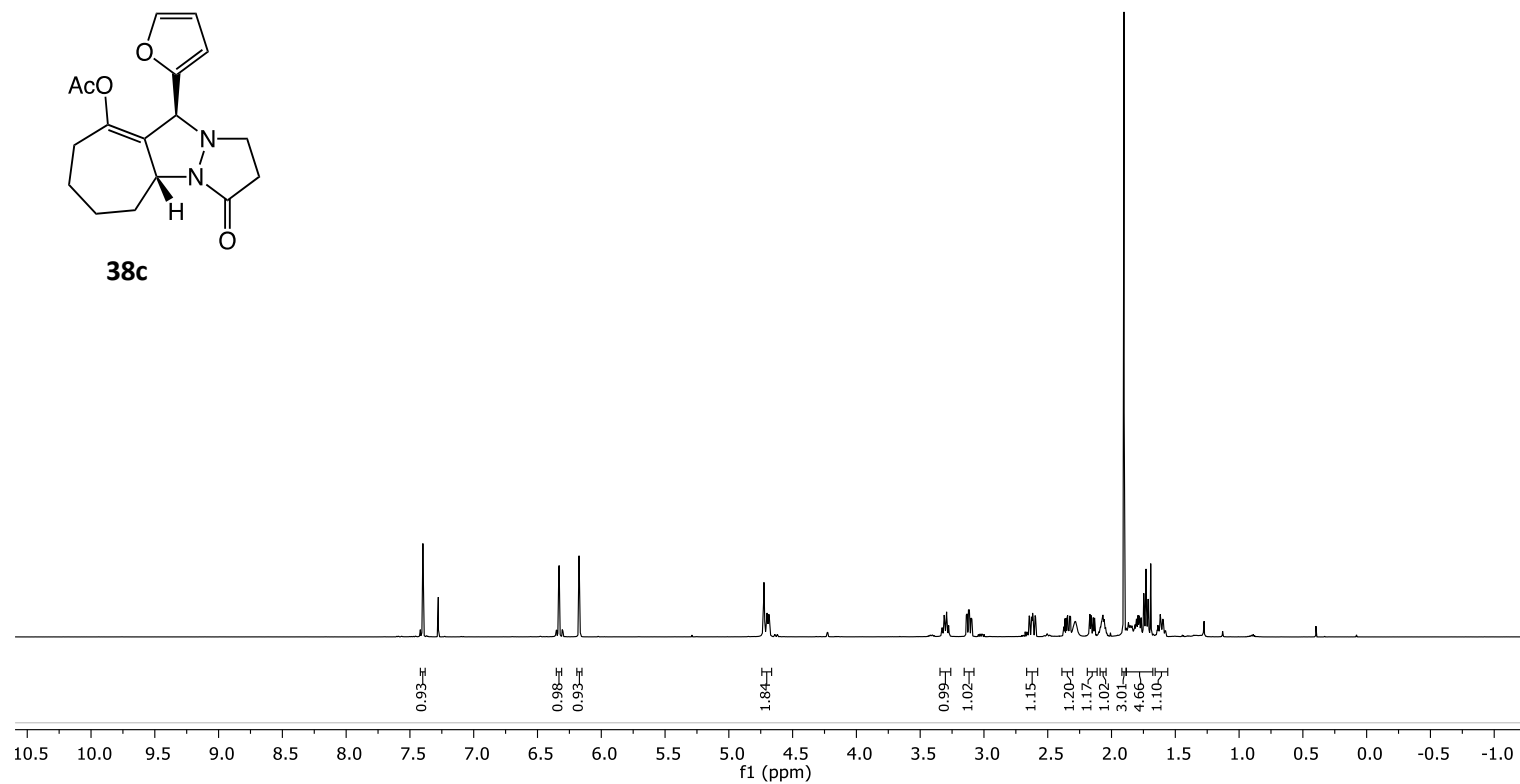
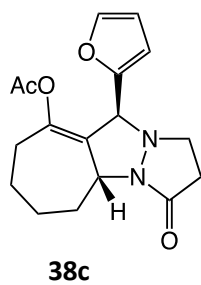


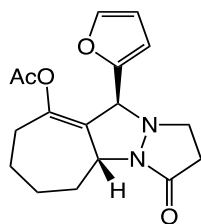
38b



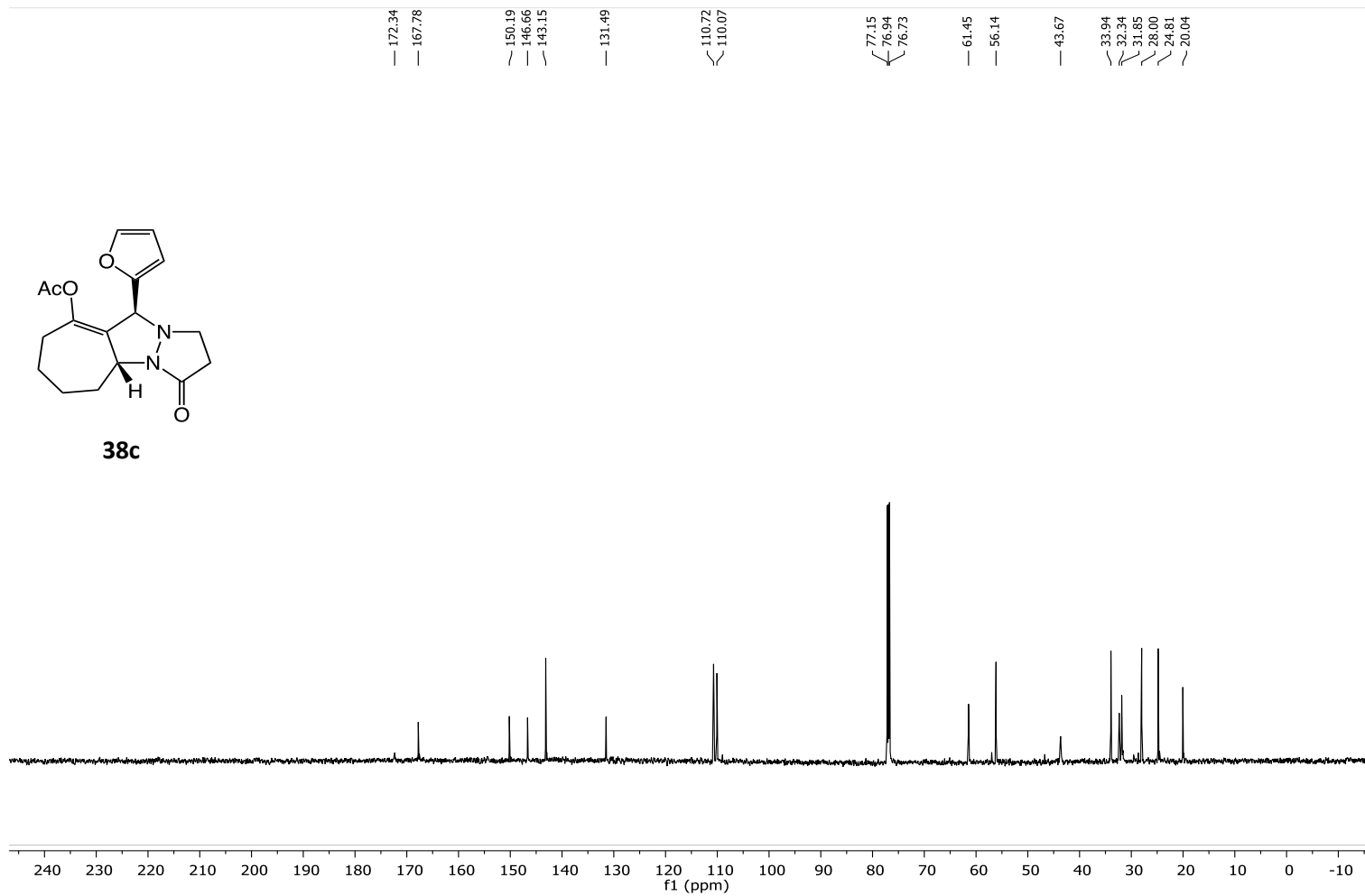


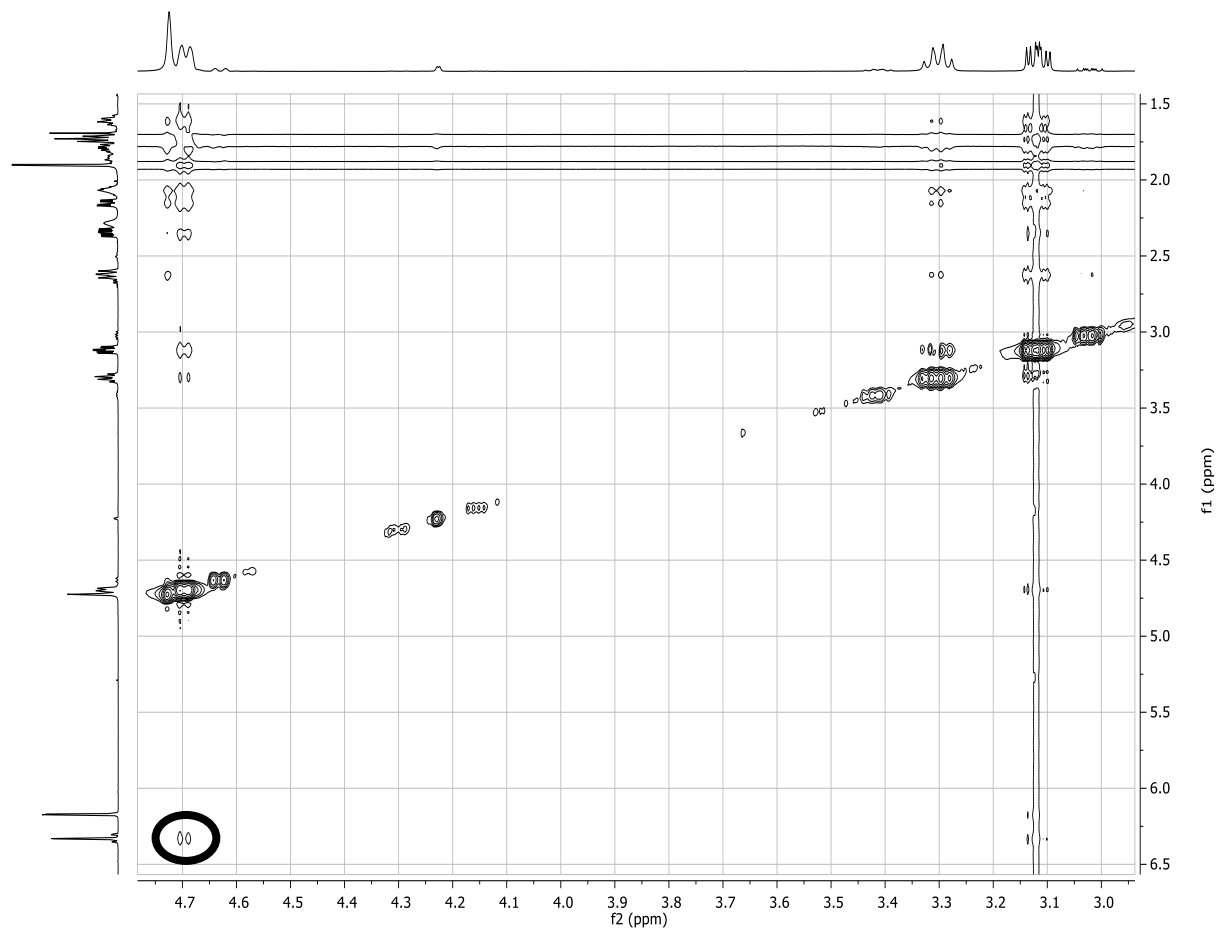
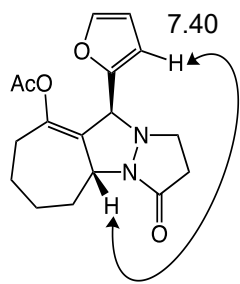


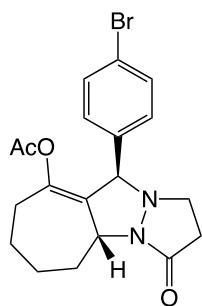




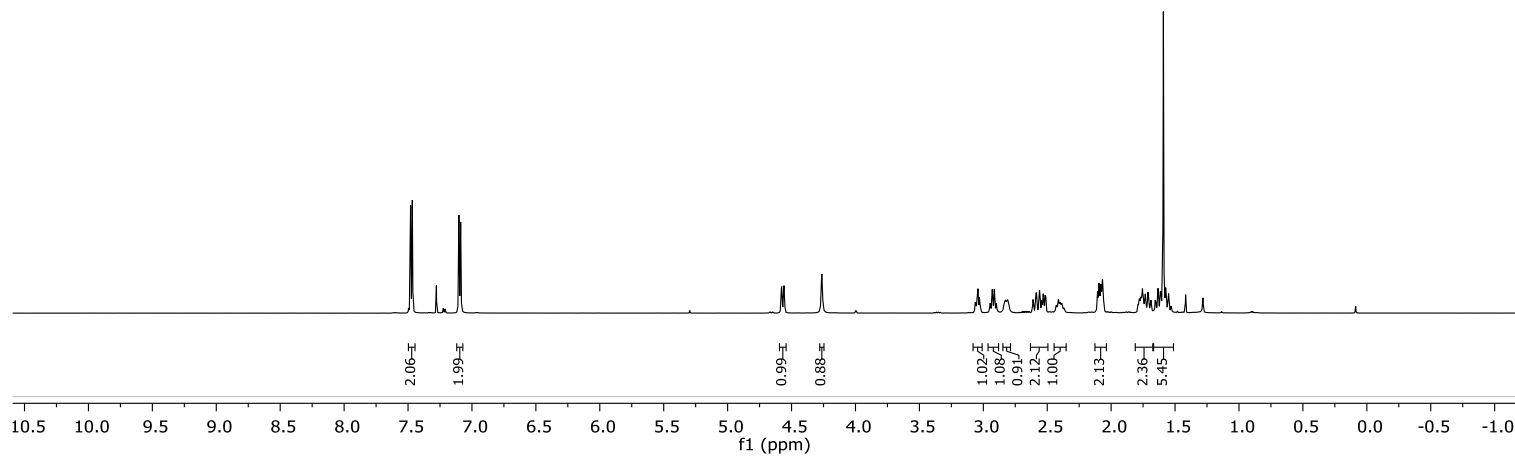
38c

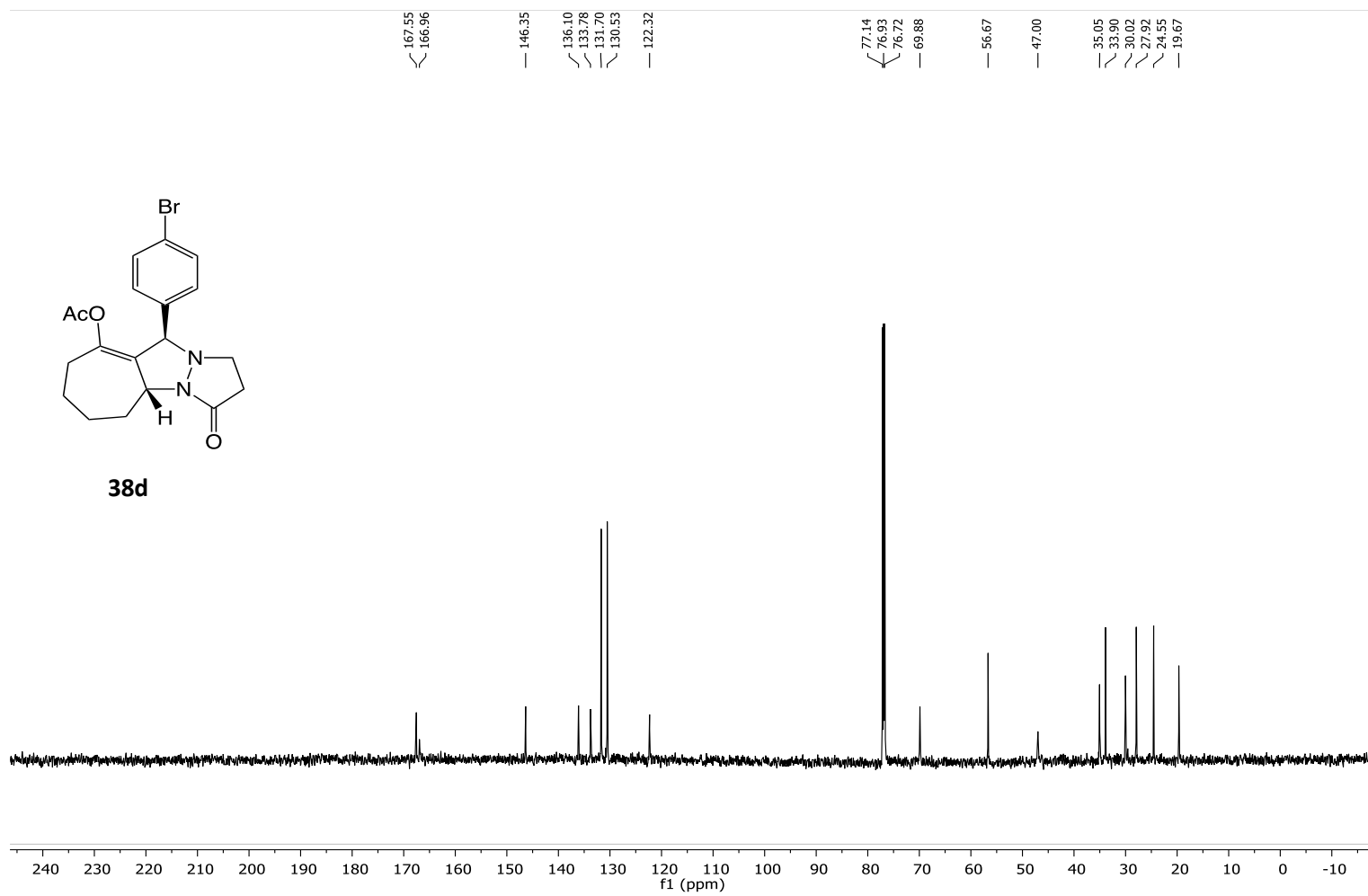


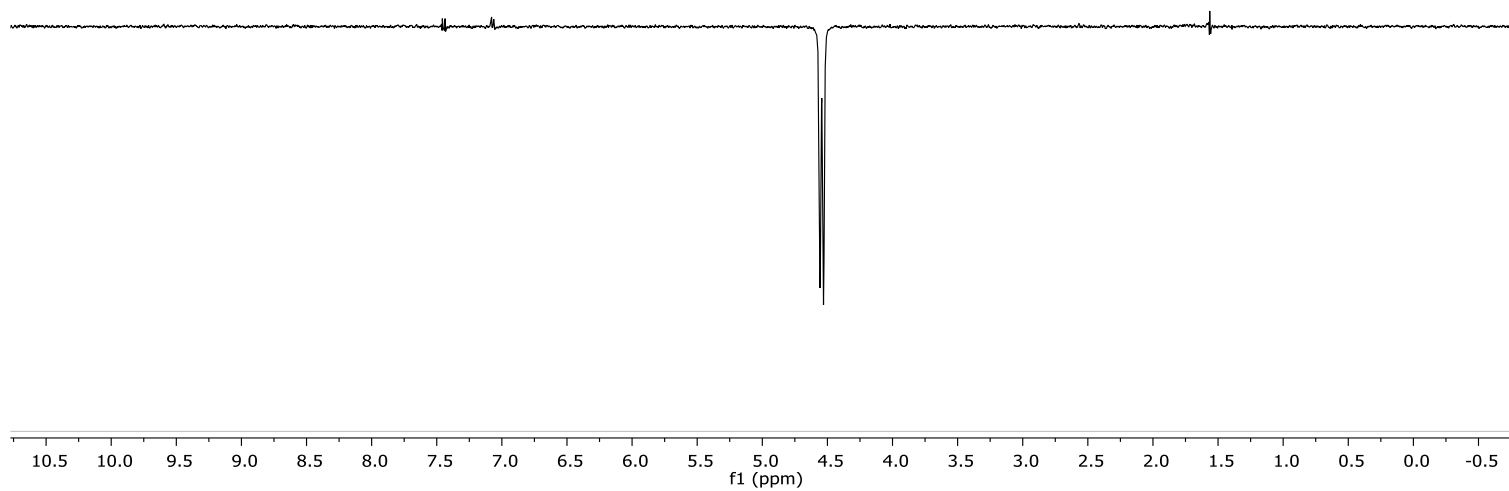
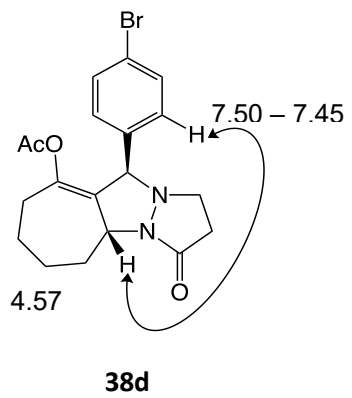


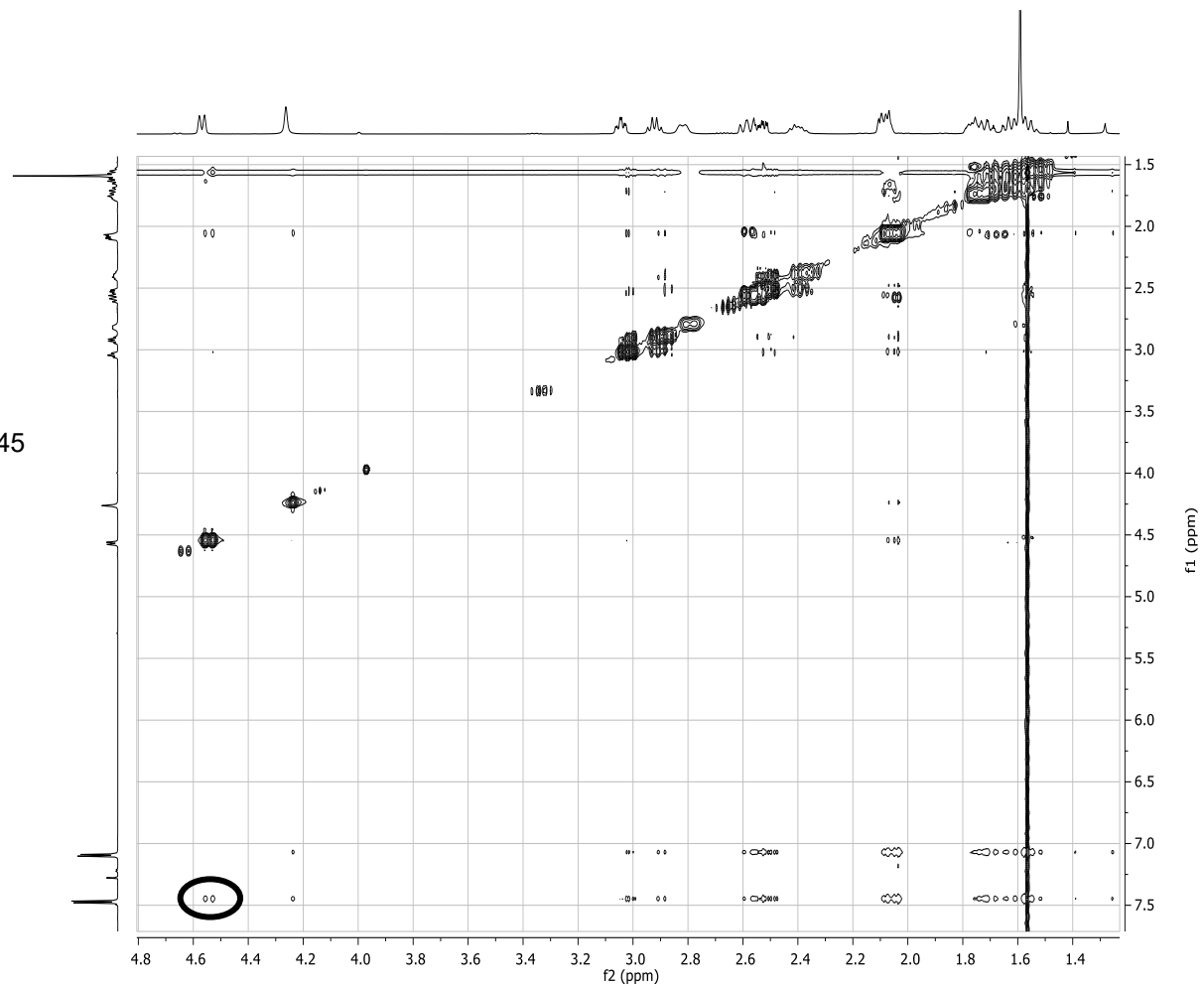
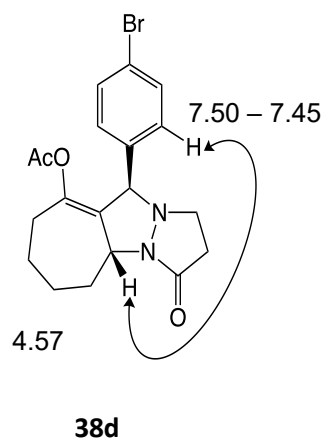


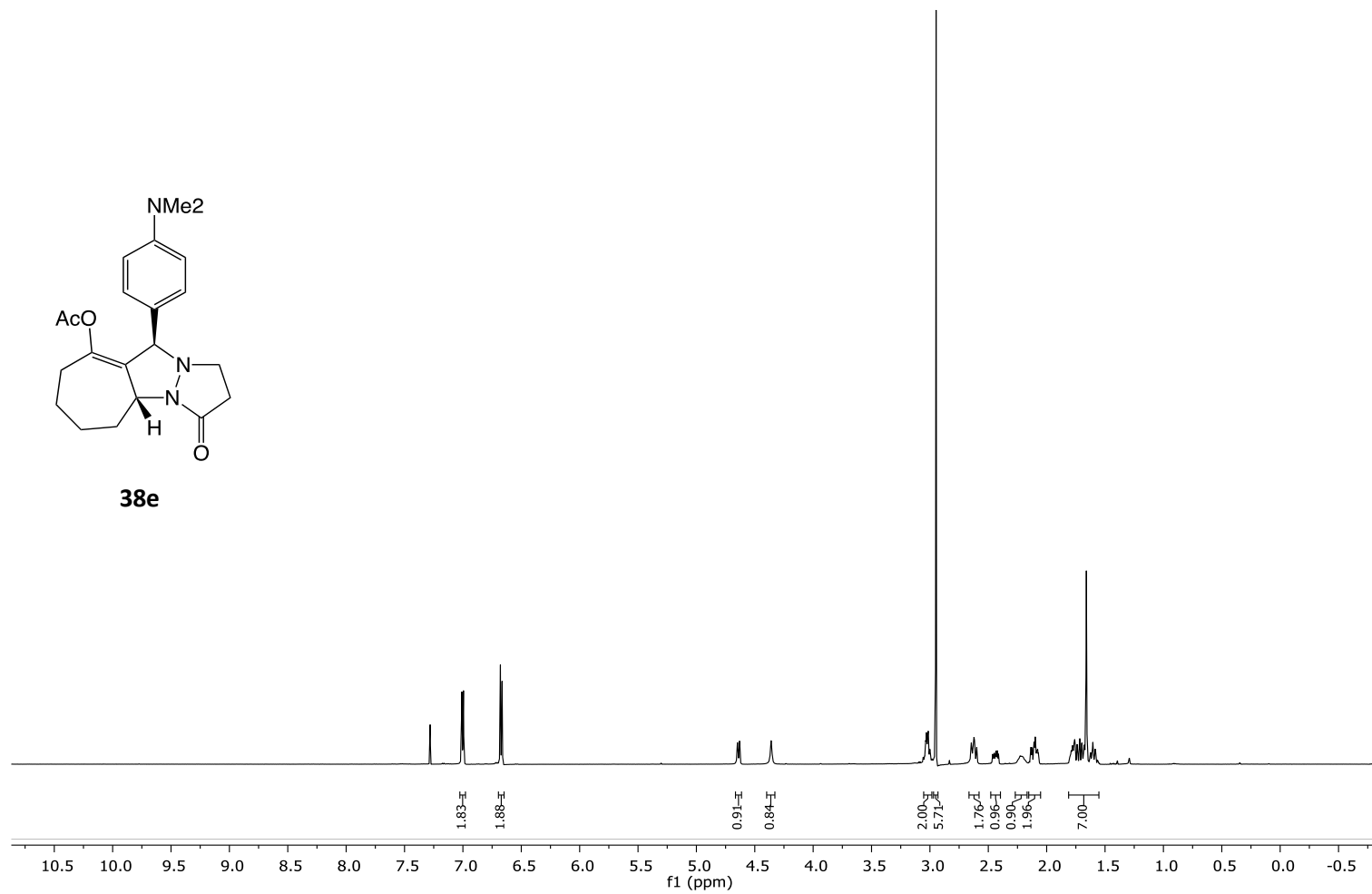
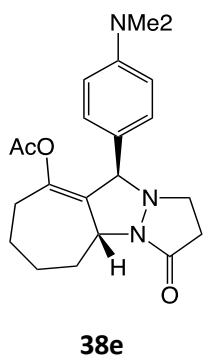
38d

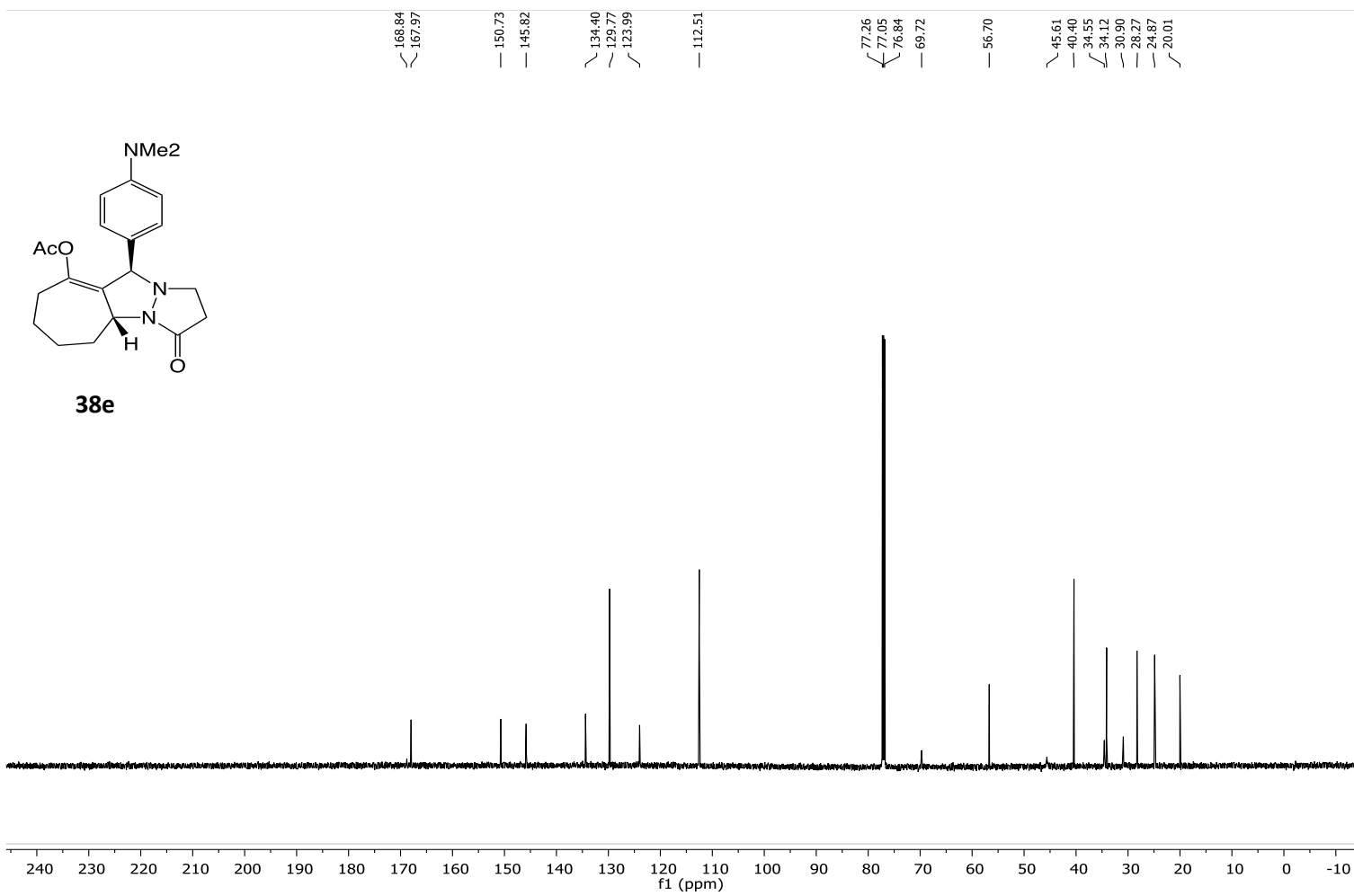


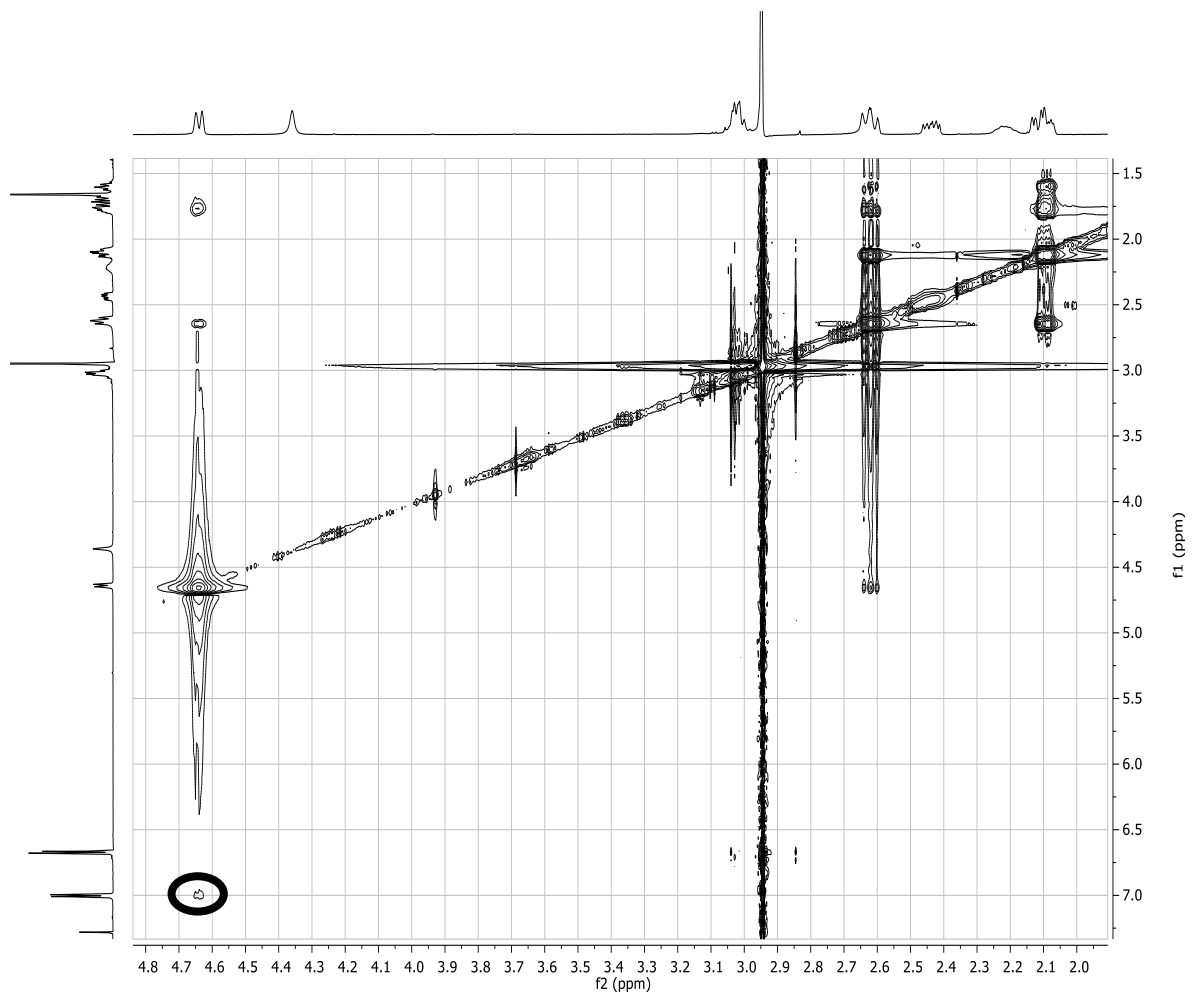
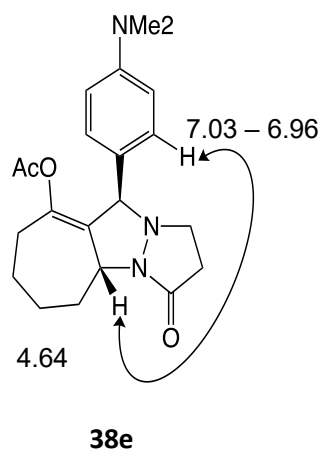


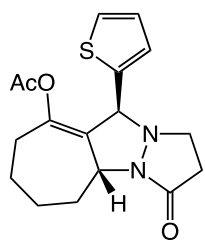




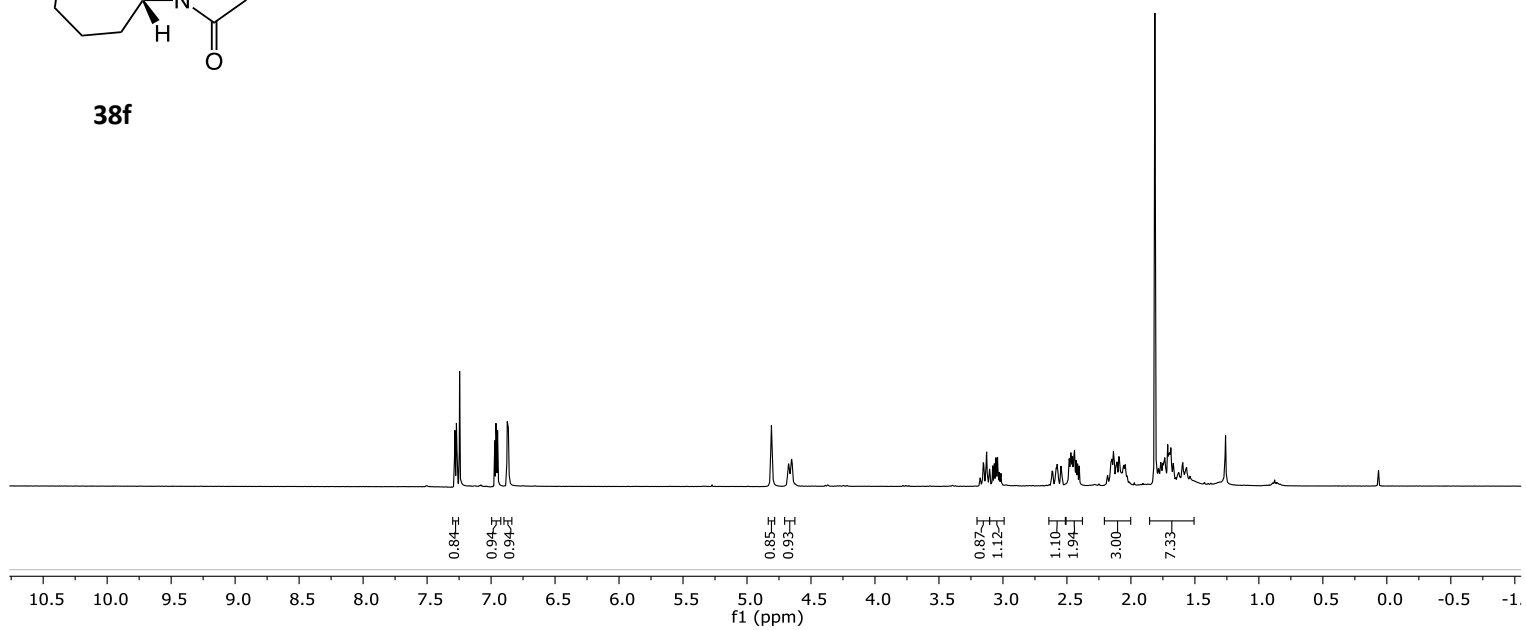


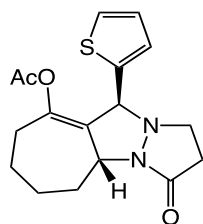




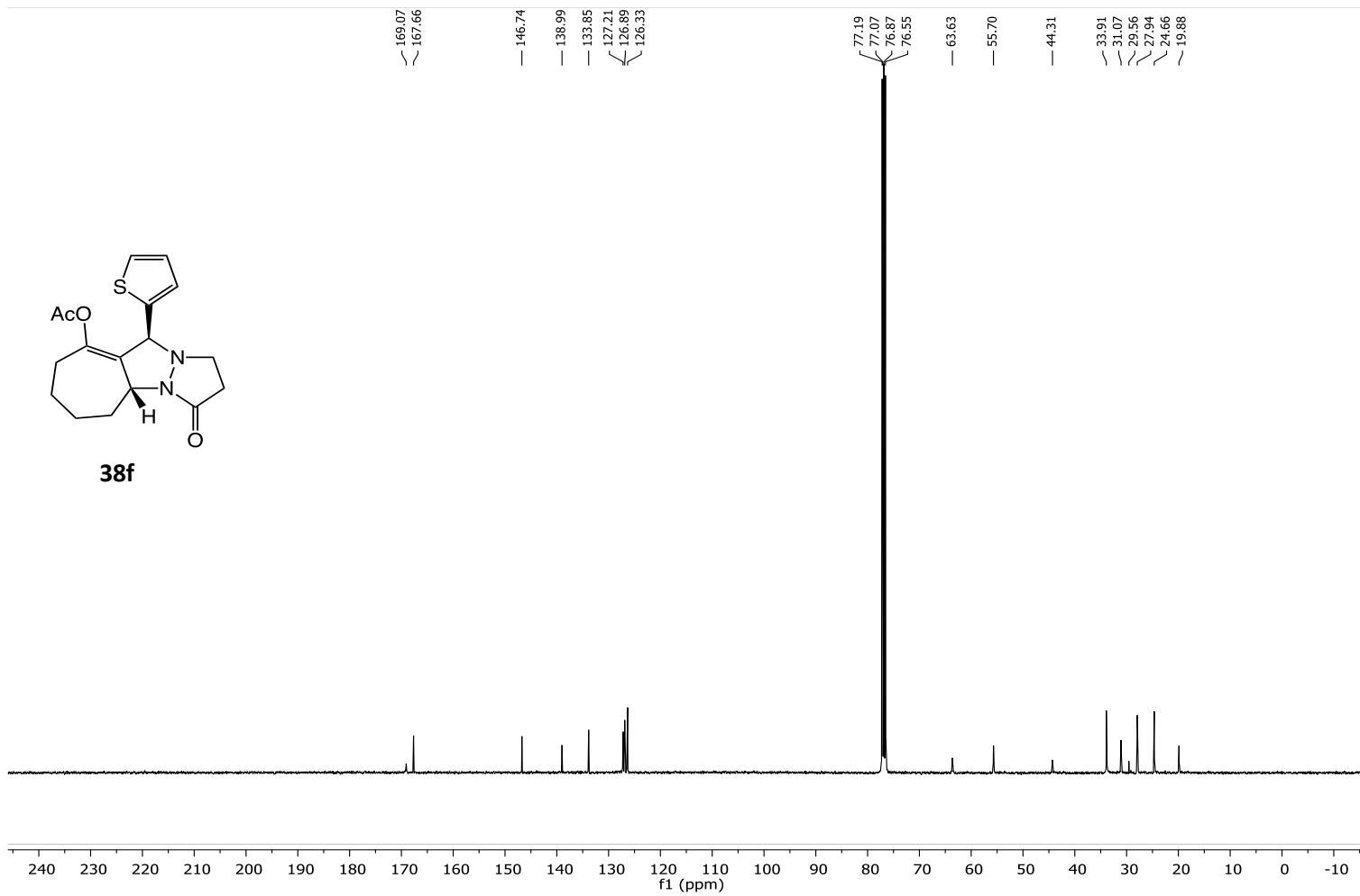


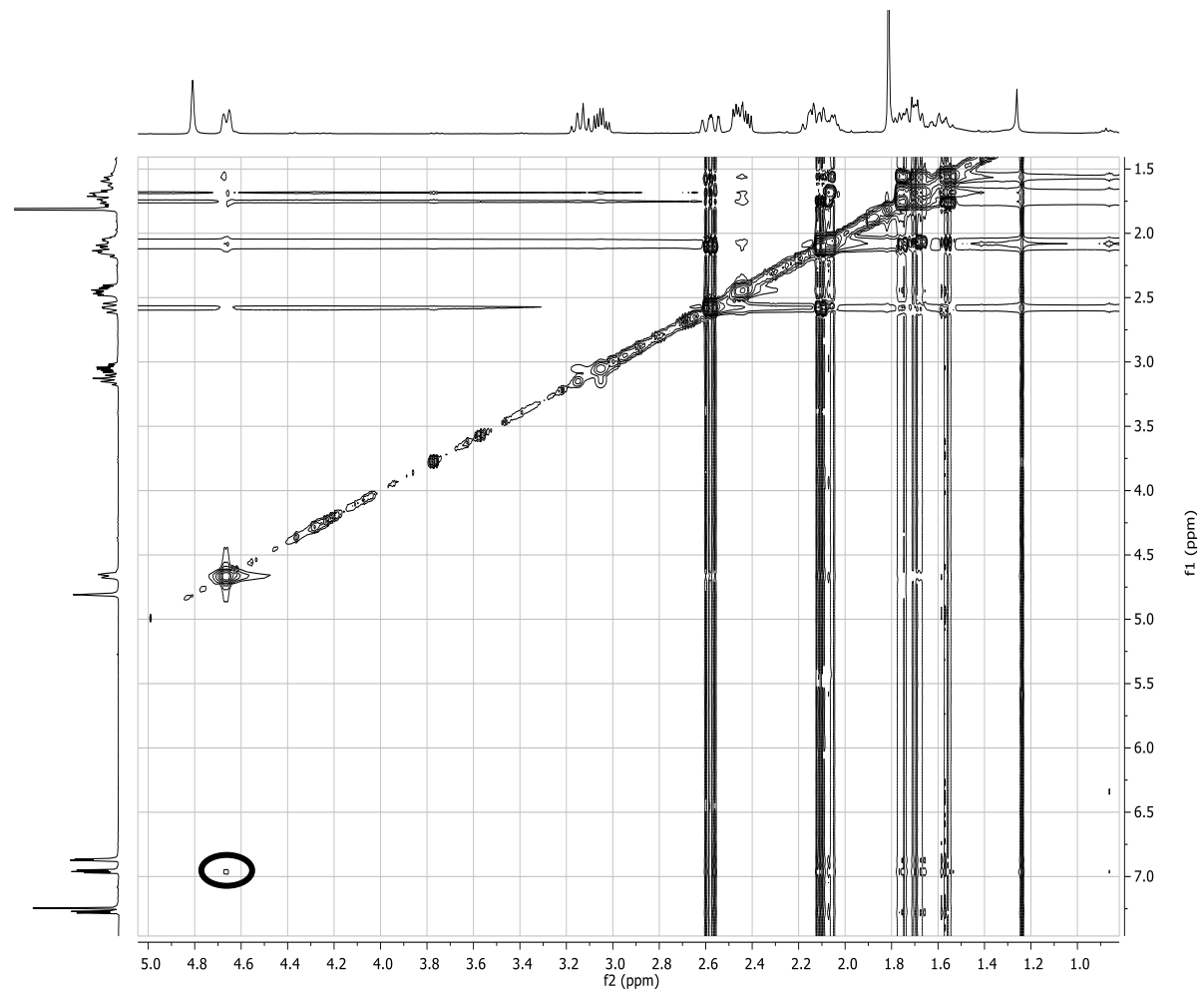
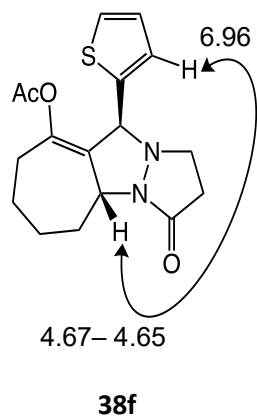
38f

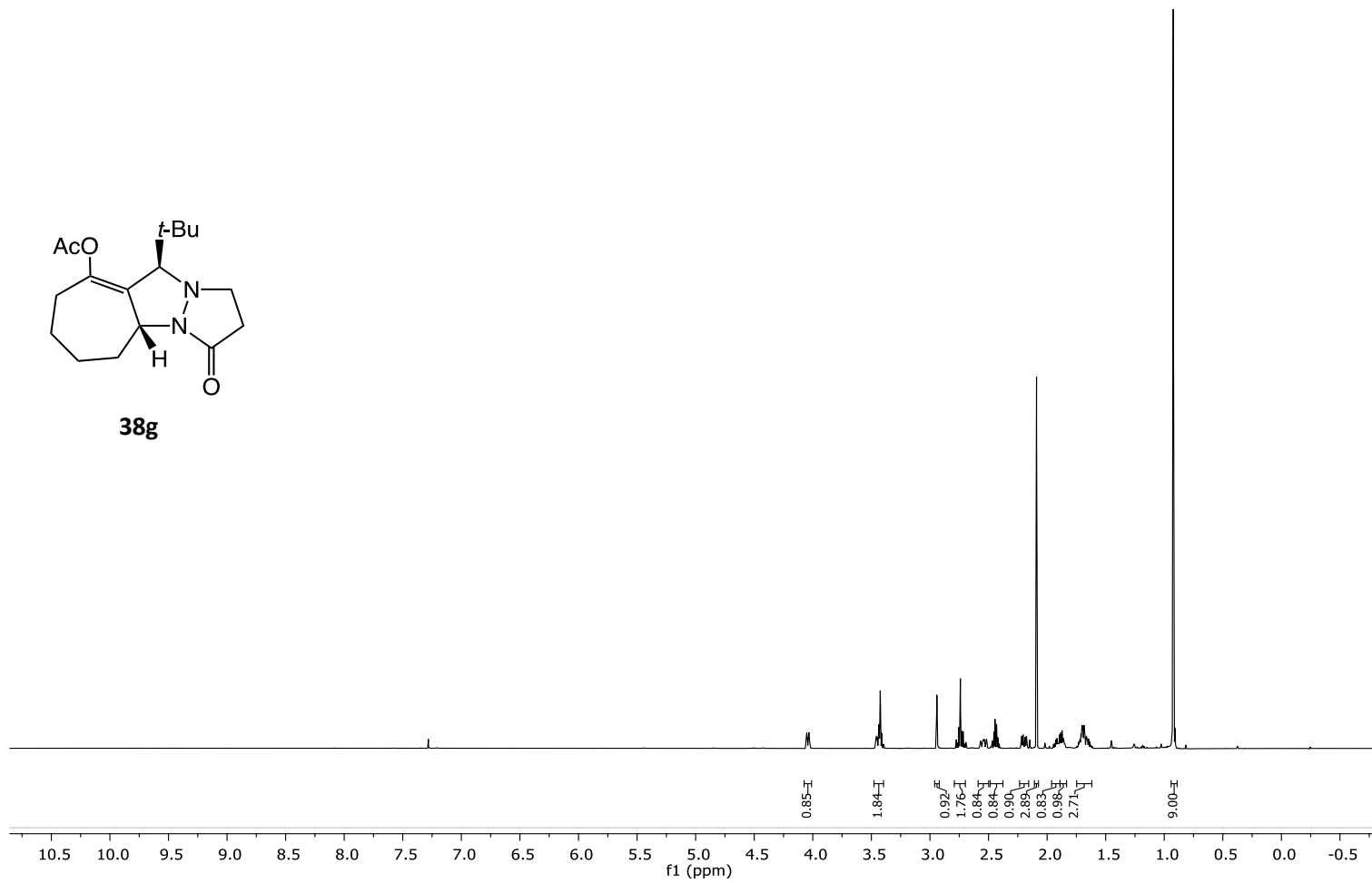
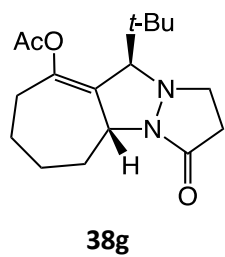


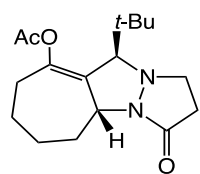


38f

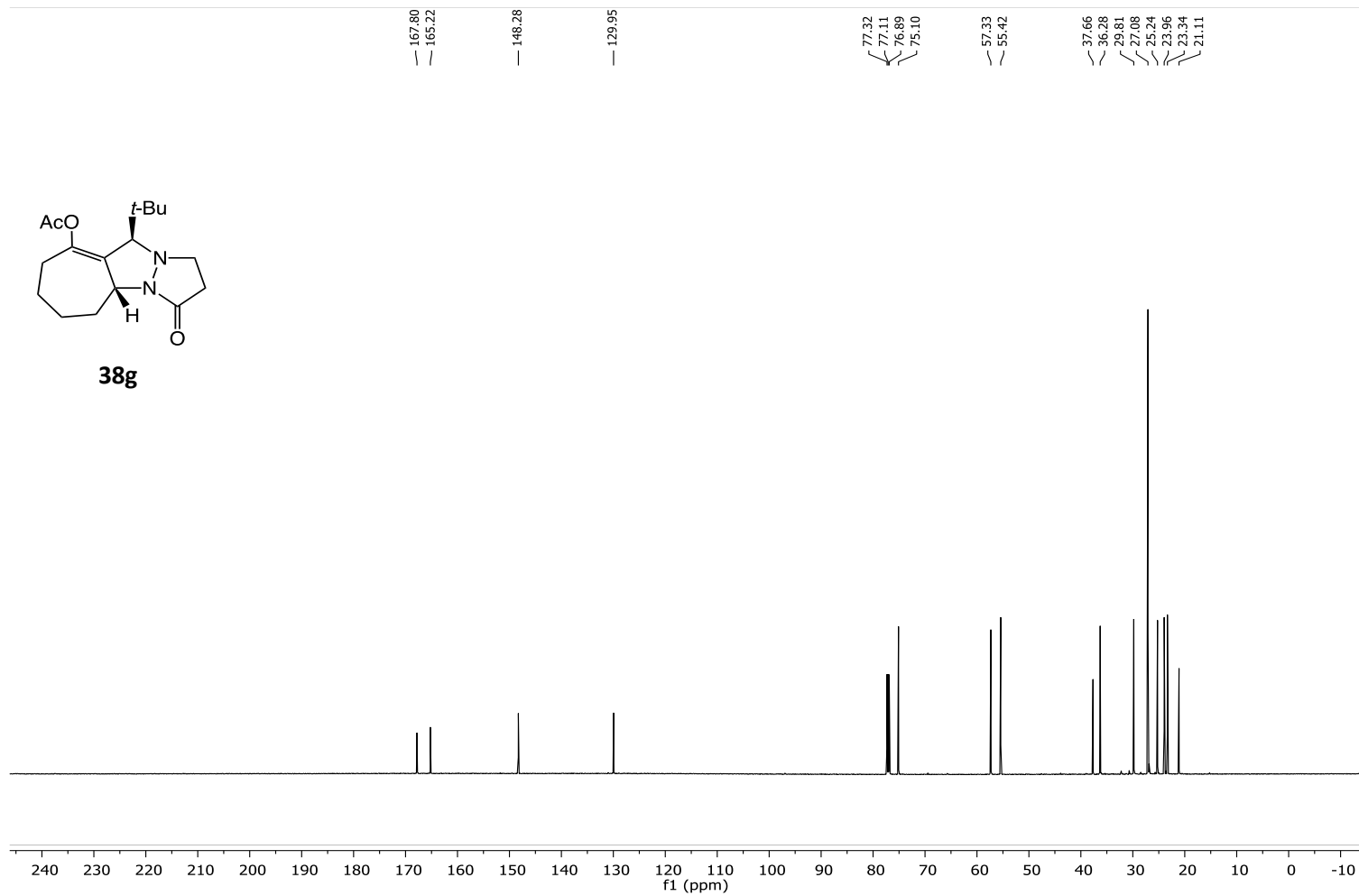


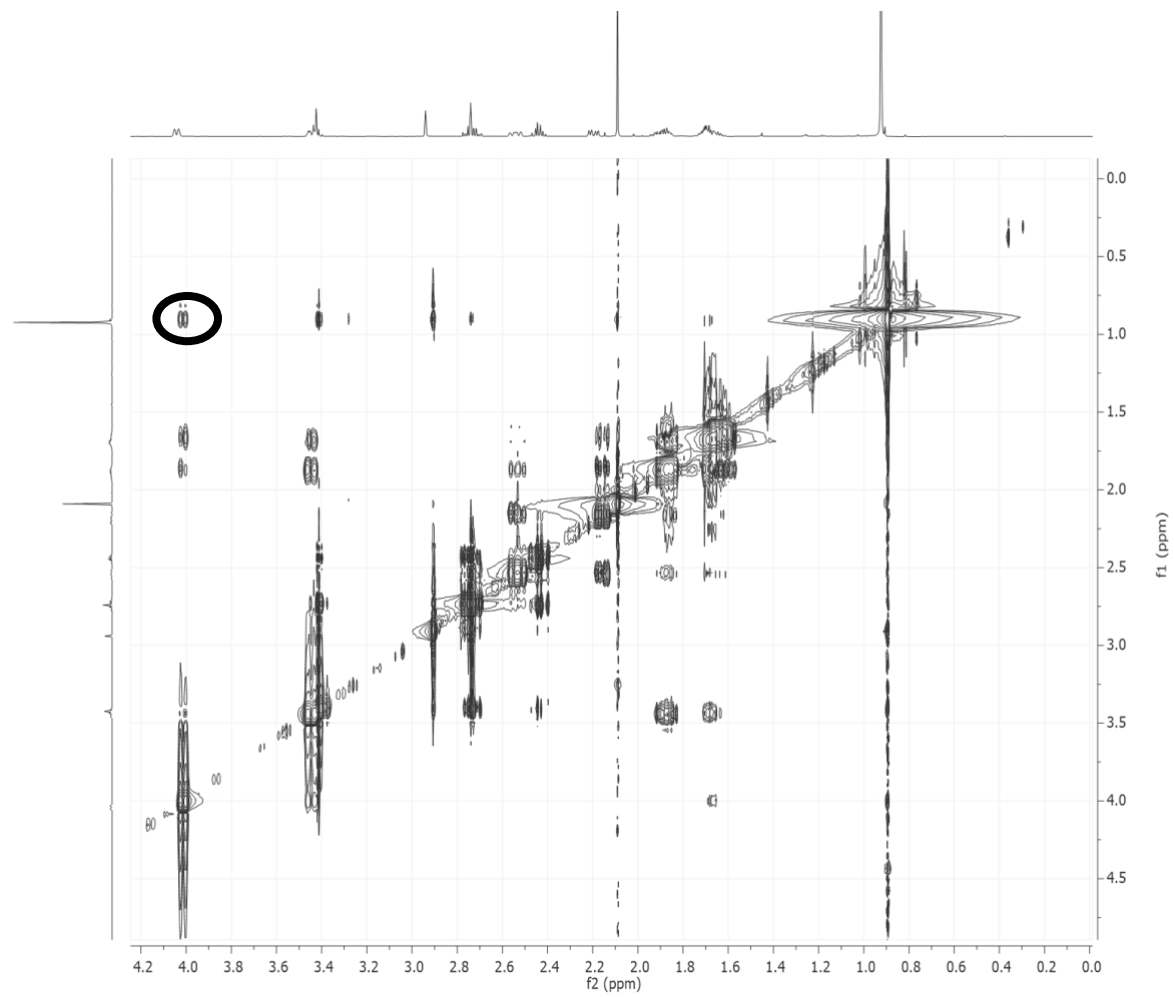
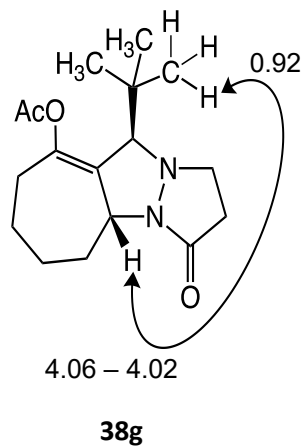


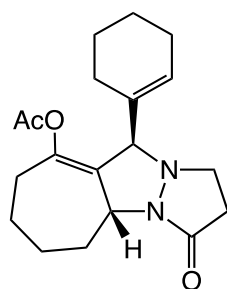




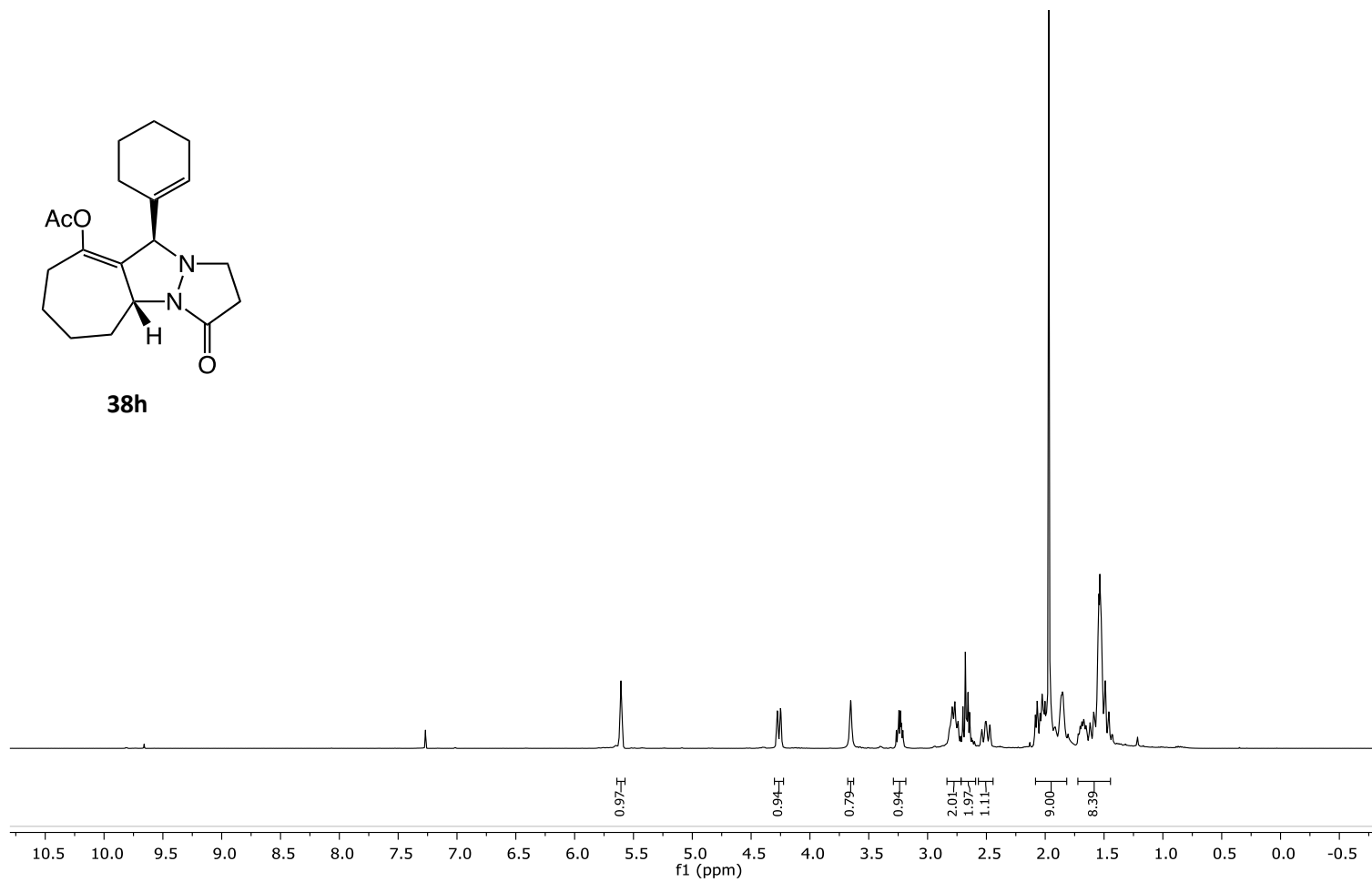
38g

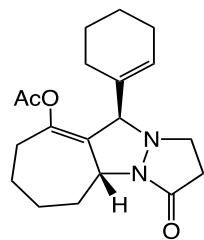




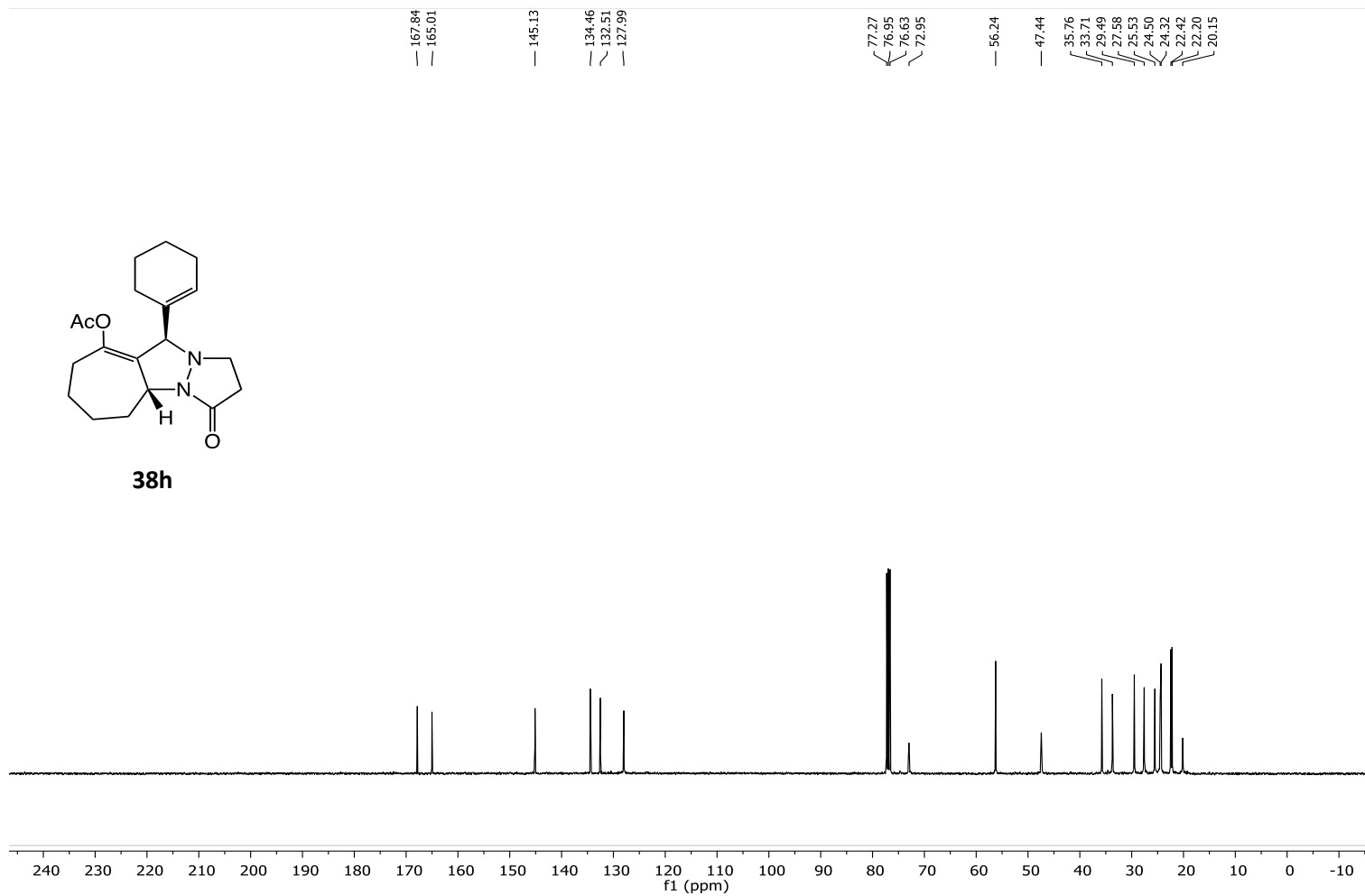


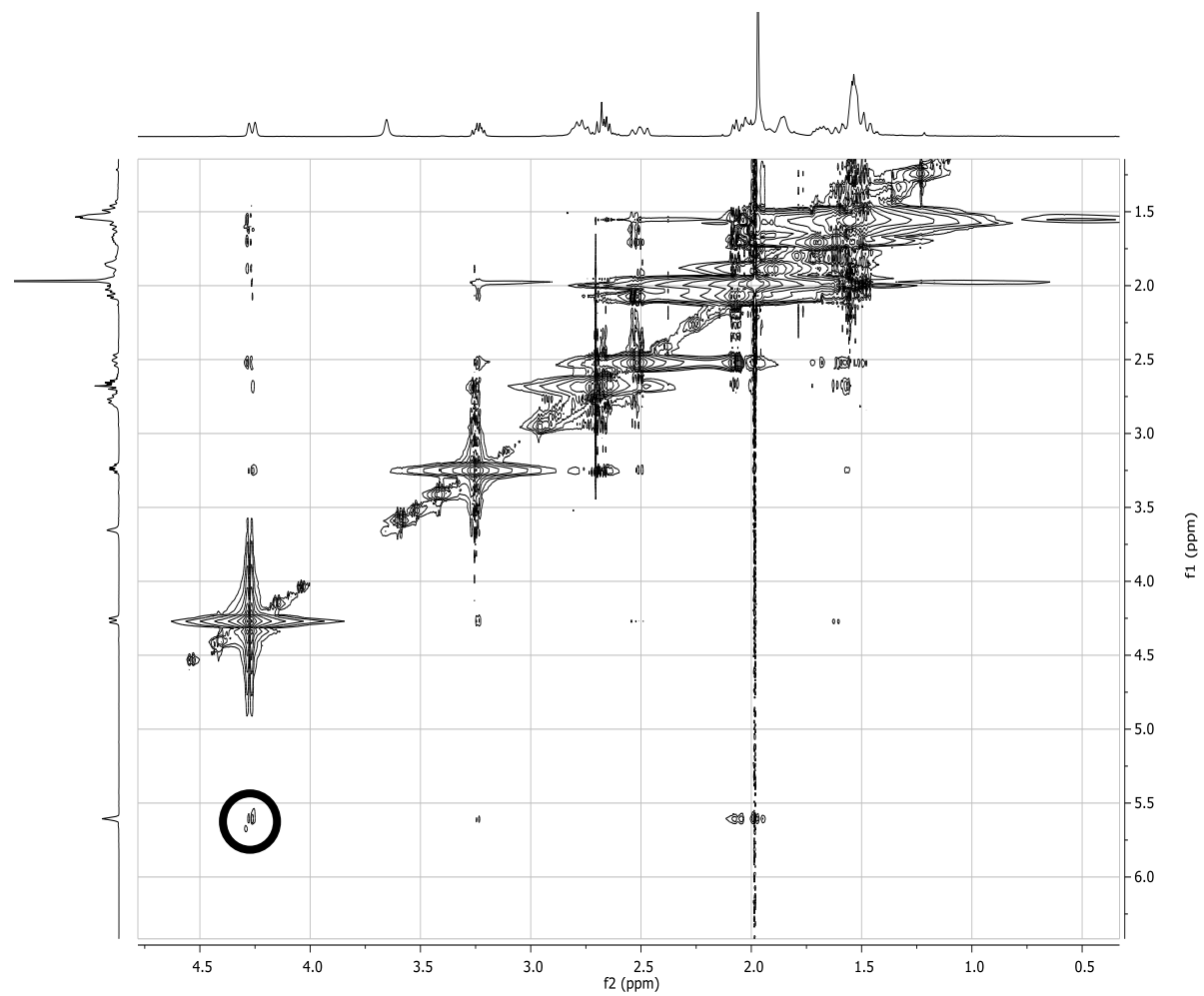
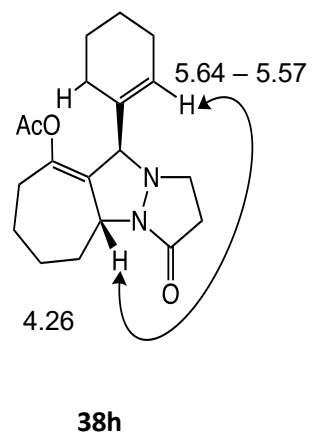
38h

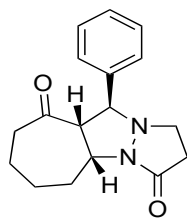




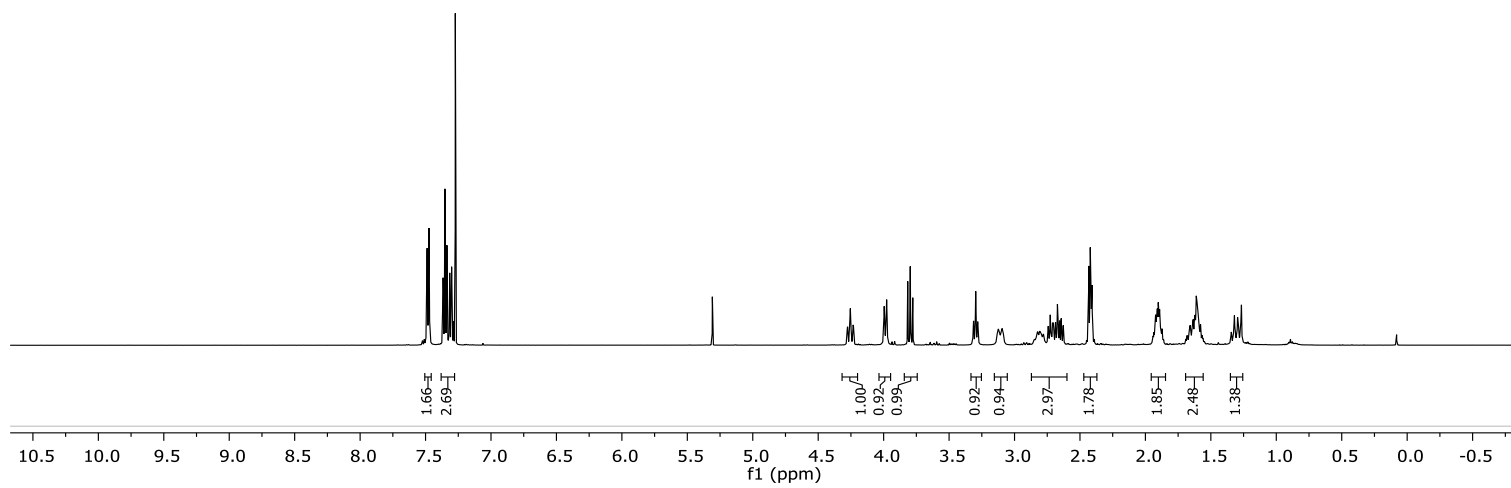
38h

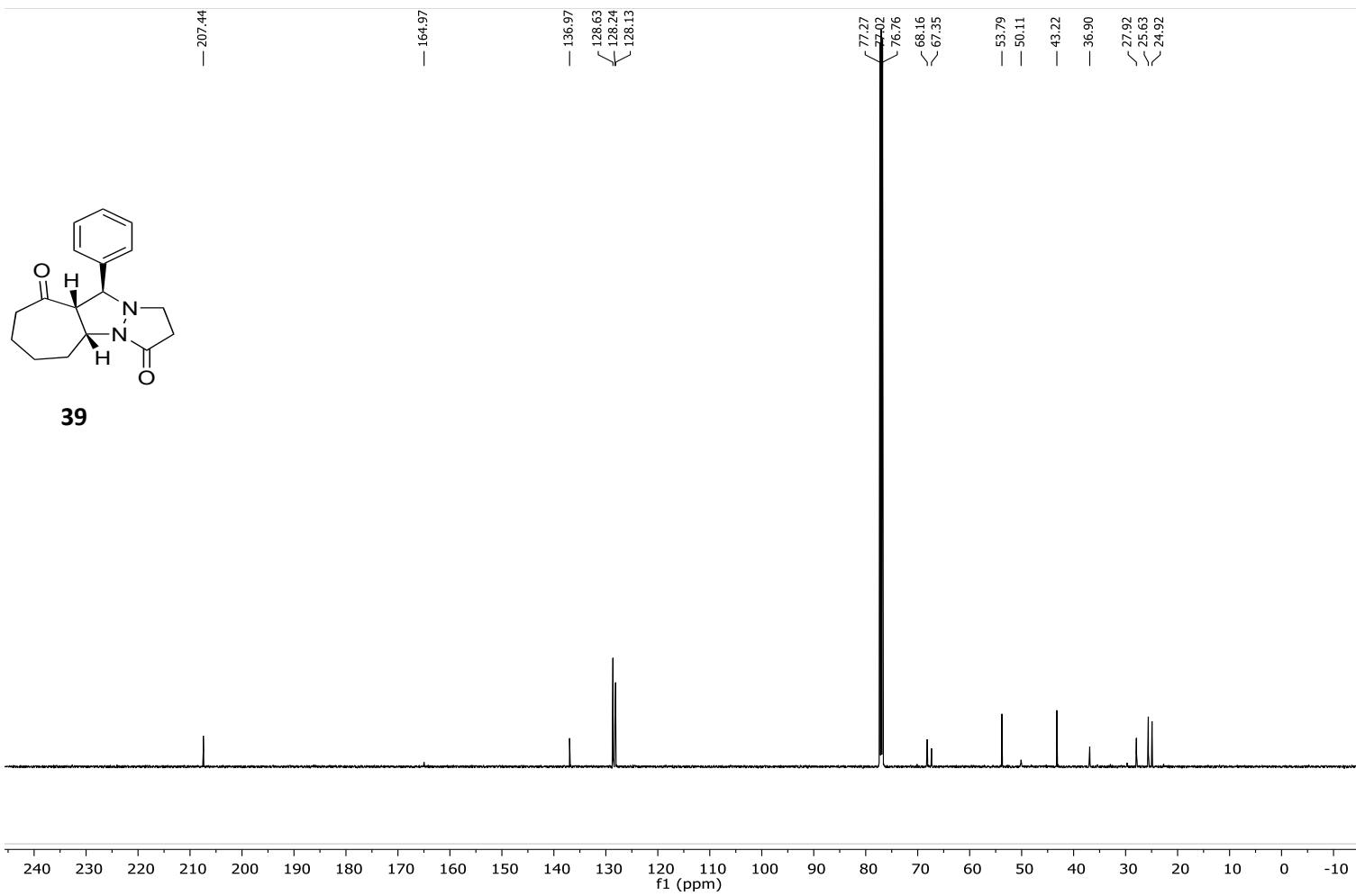


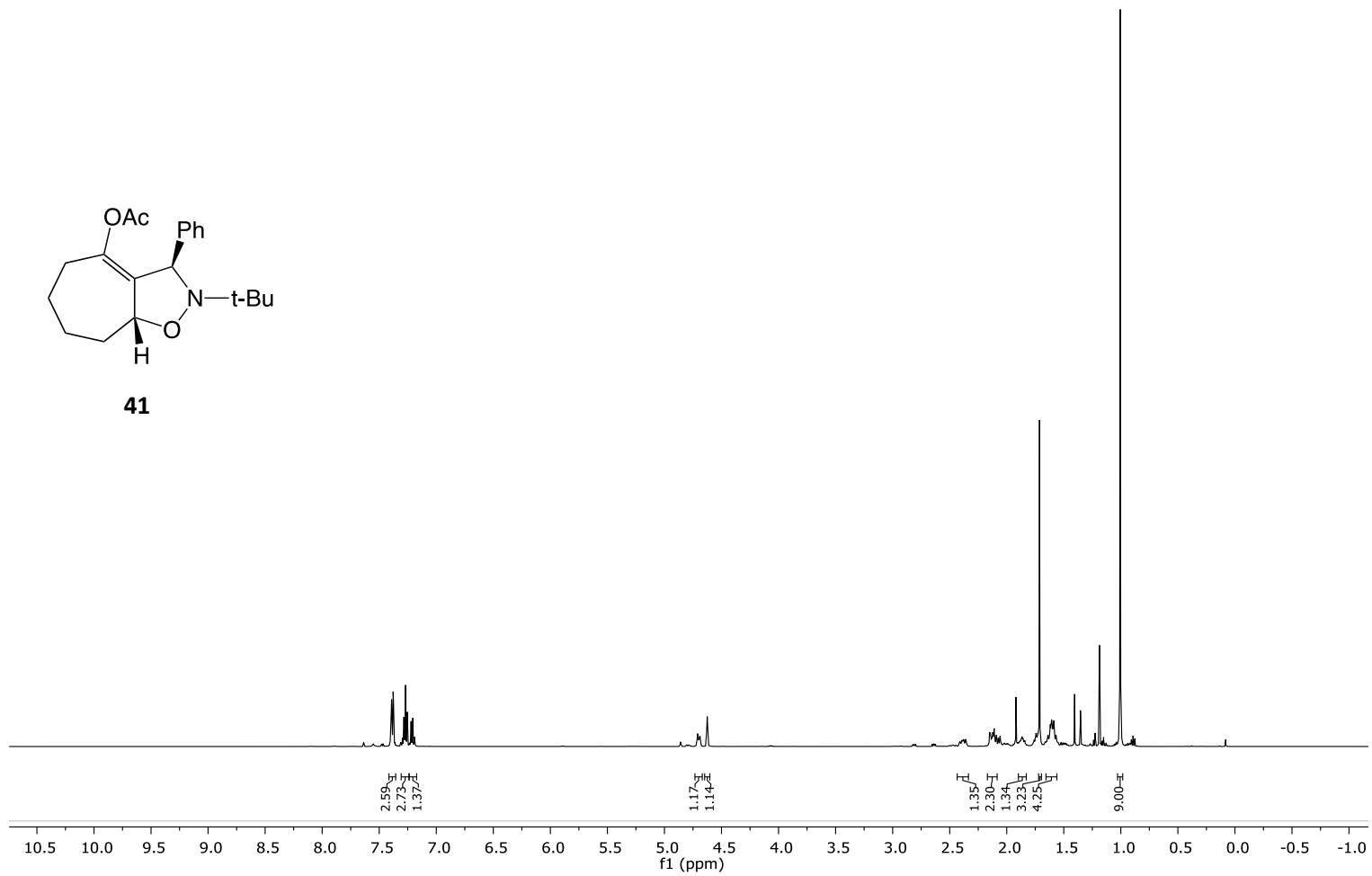
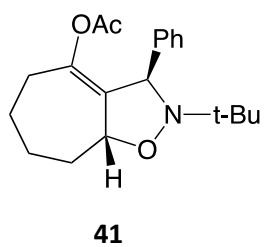


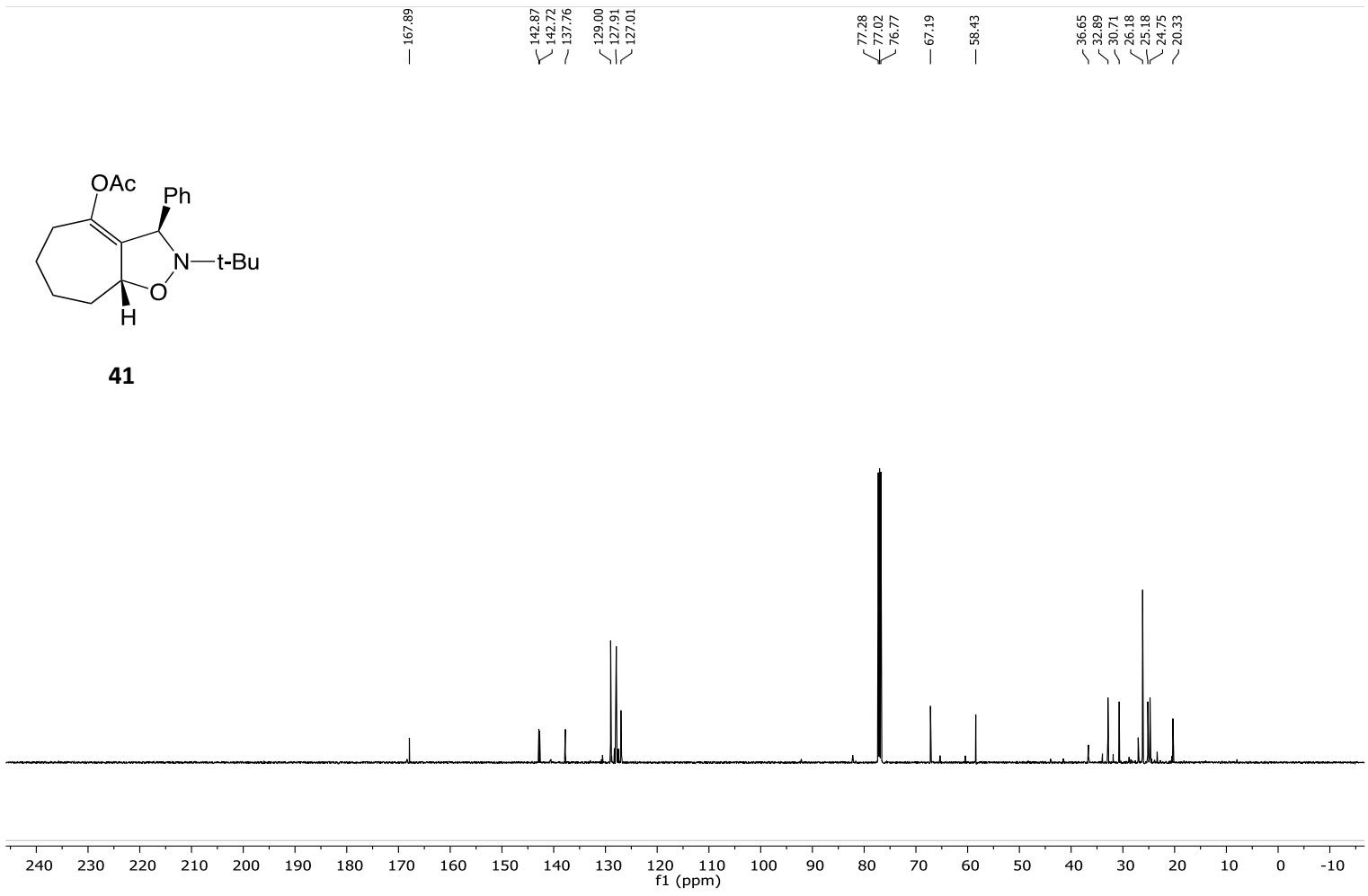


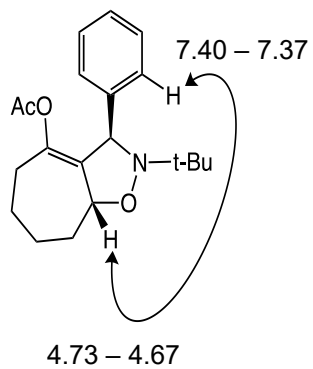
39



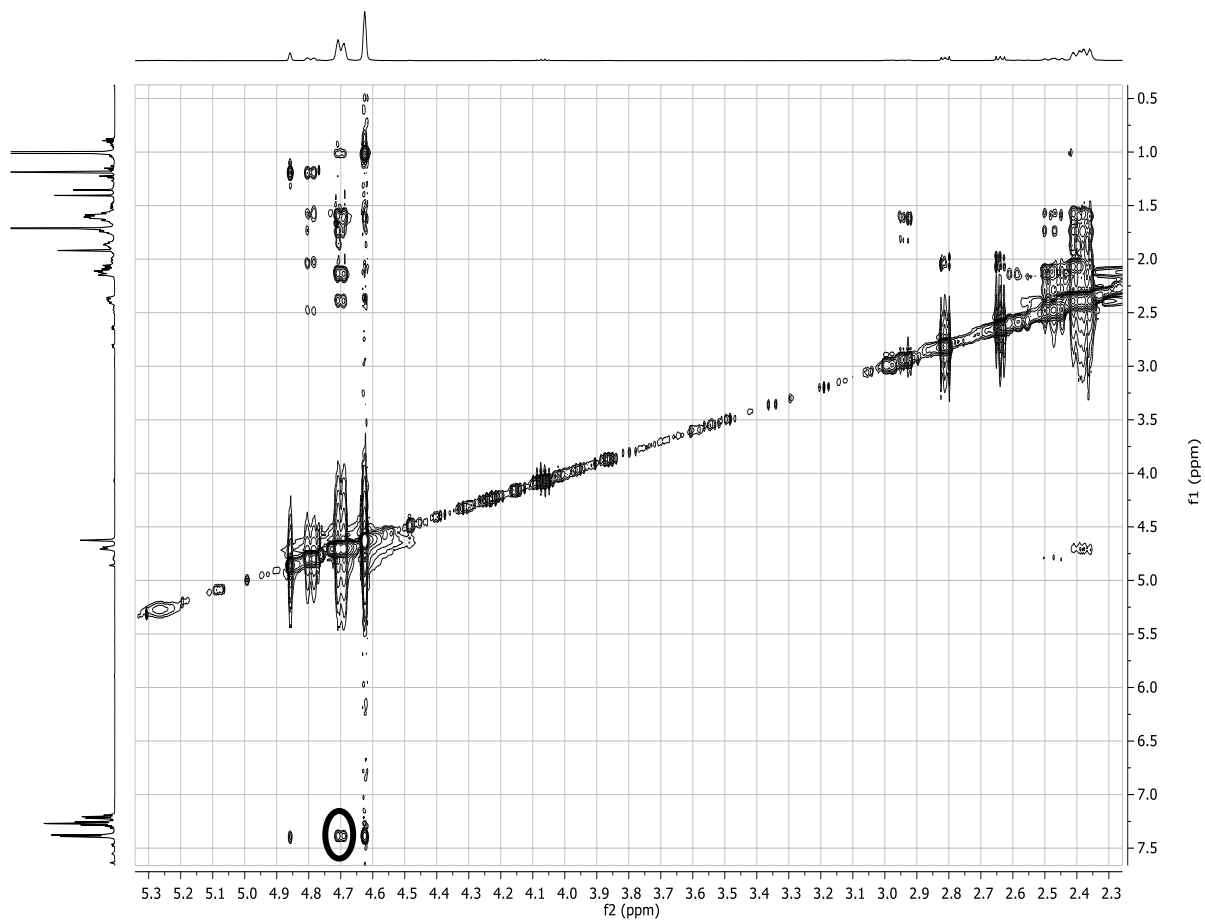


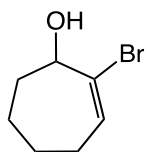




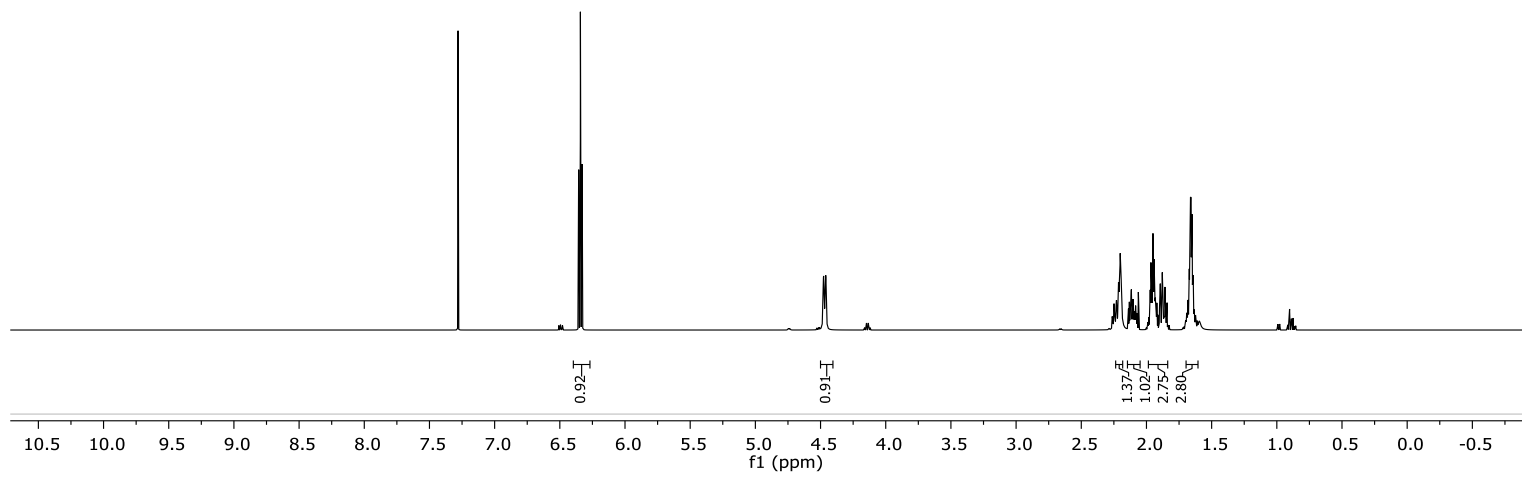


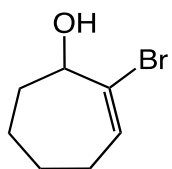
41



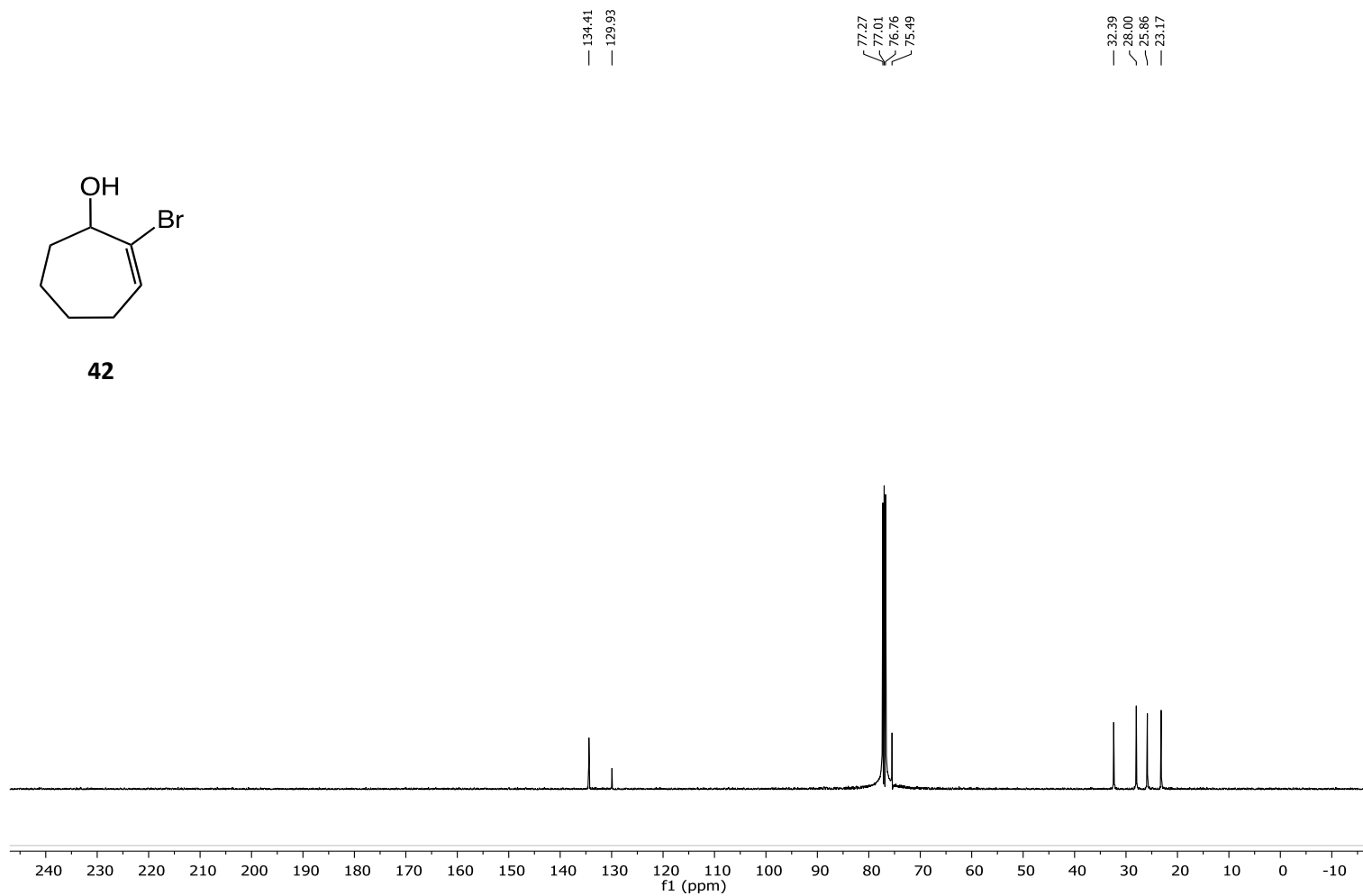


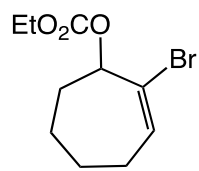
42



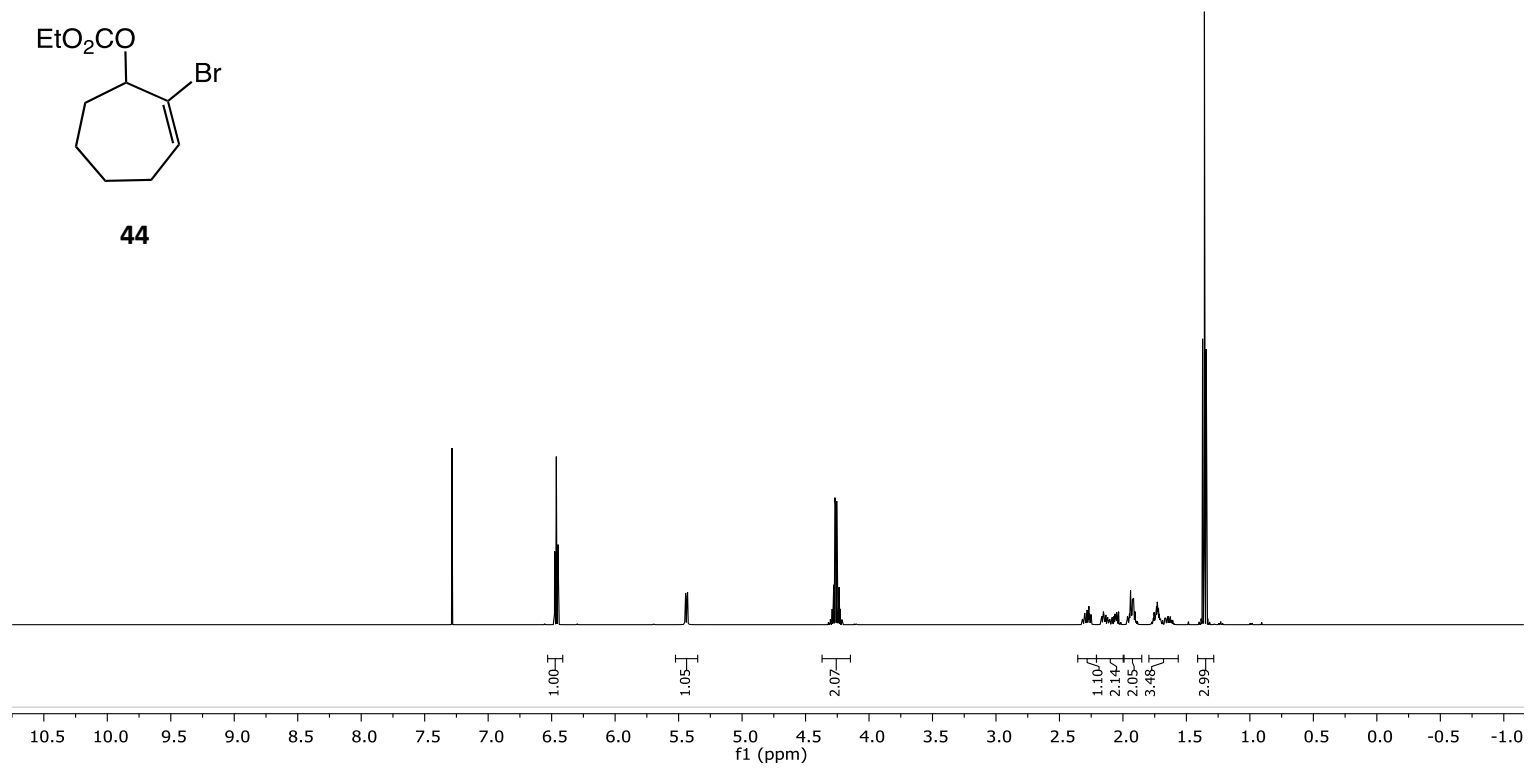


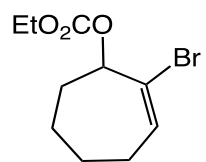
42



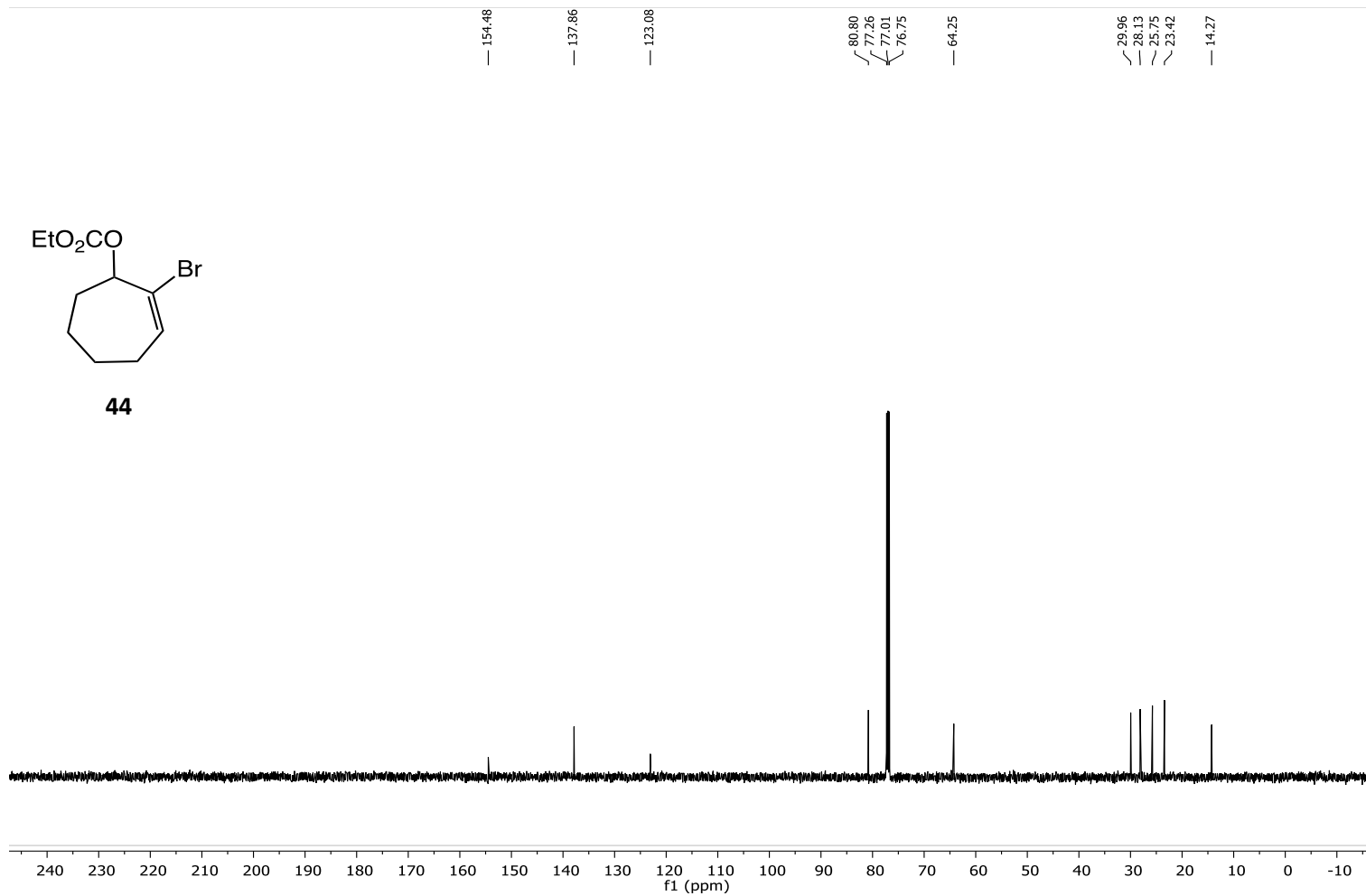


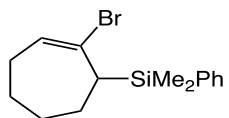
44



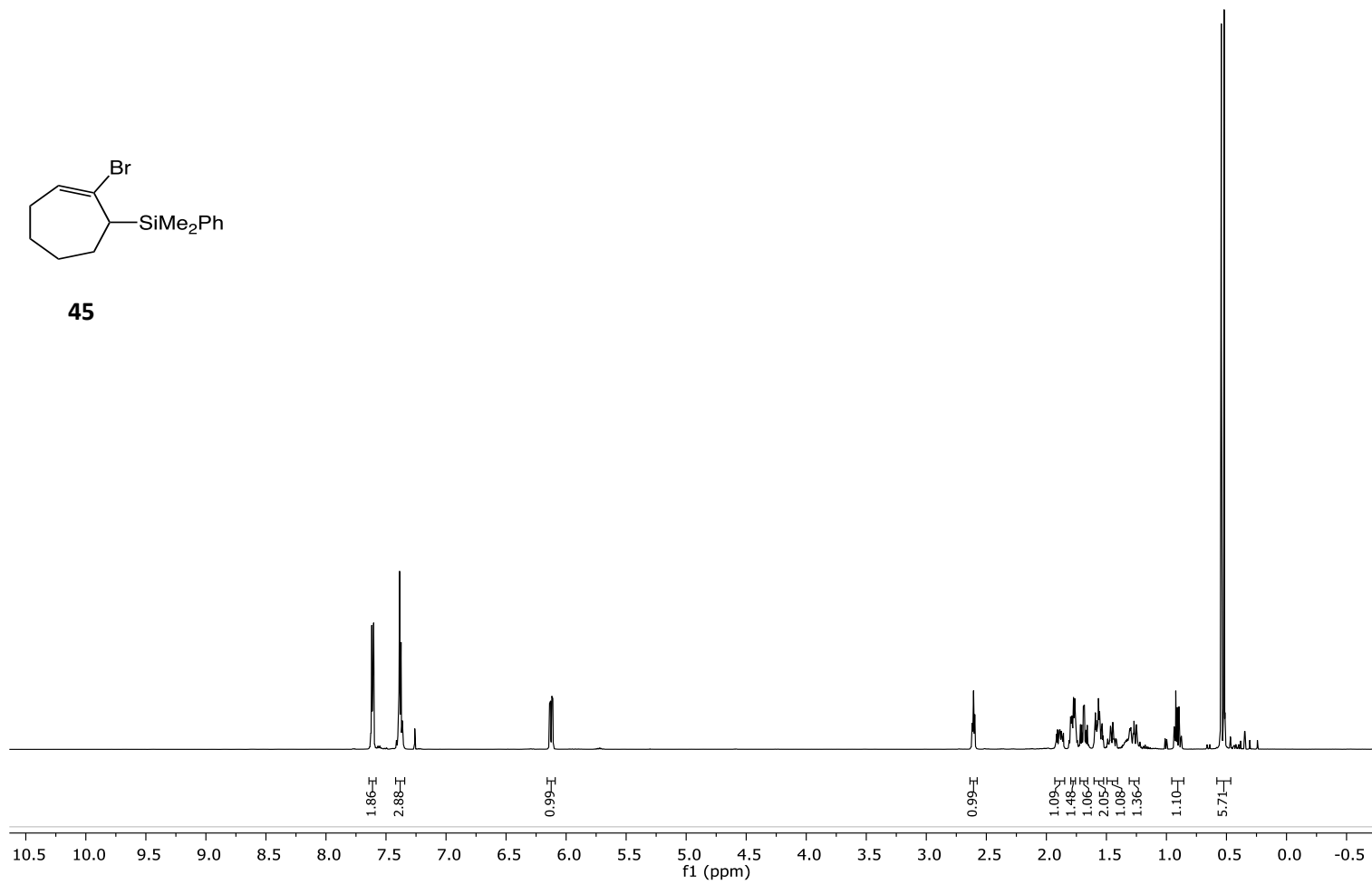


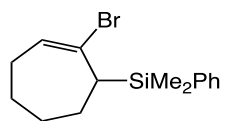
44



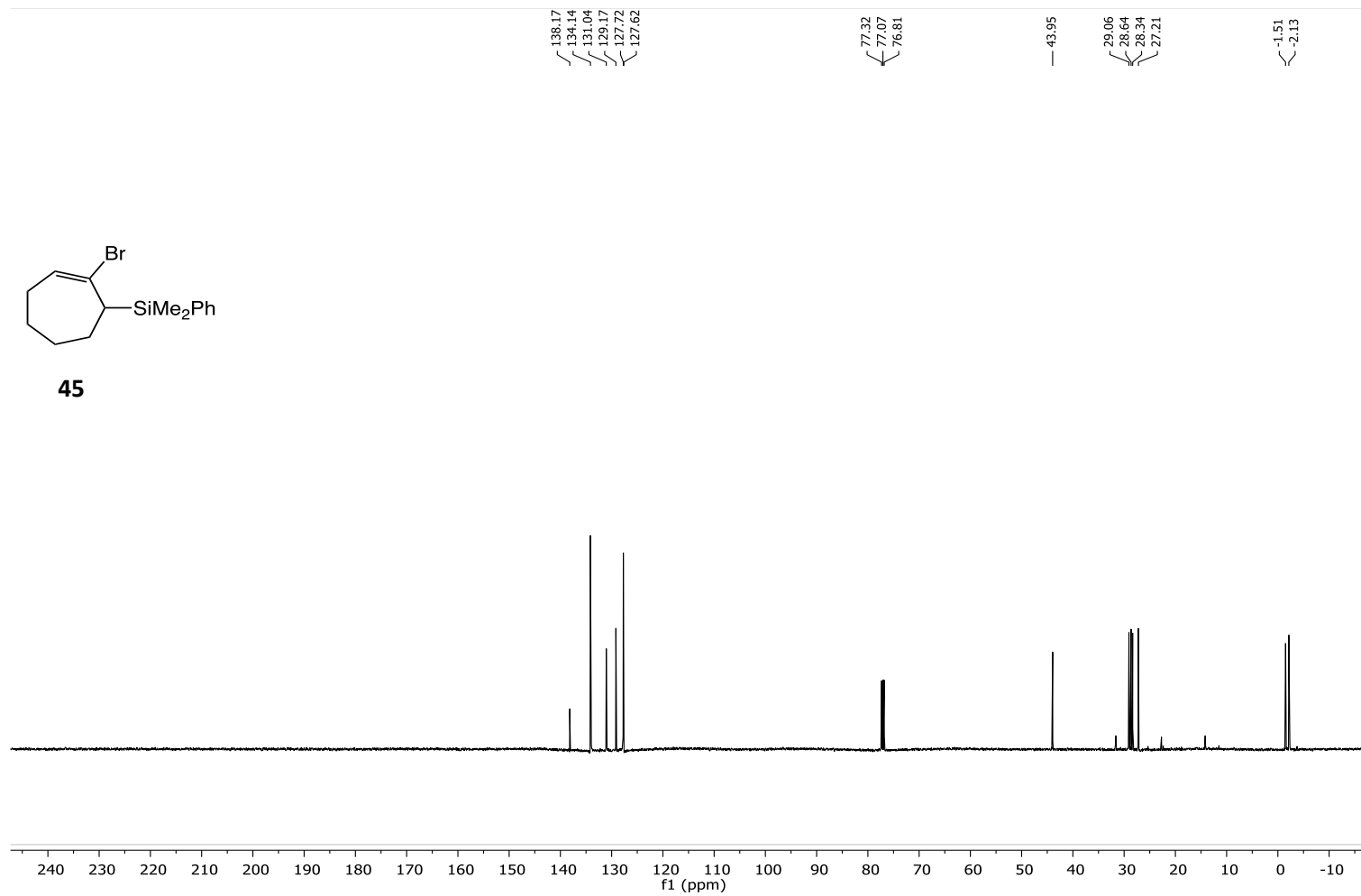


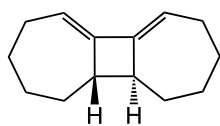
45



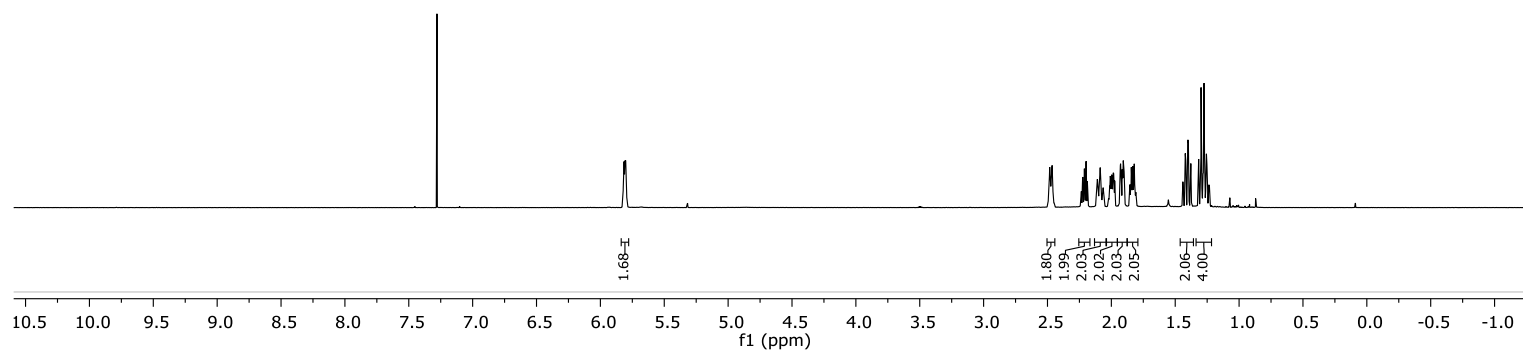


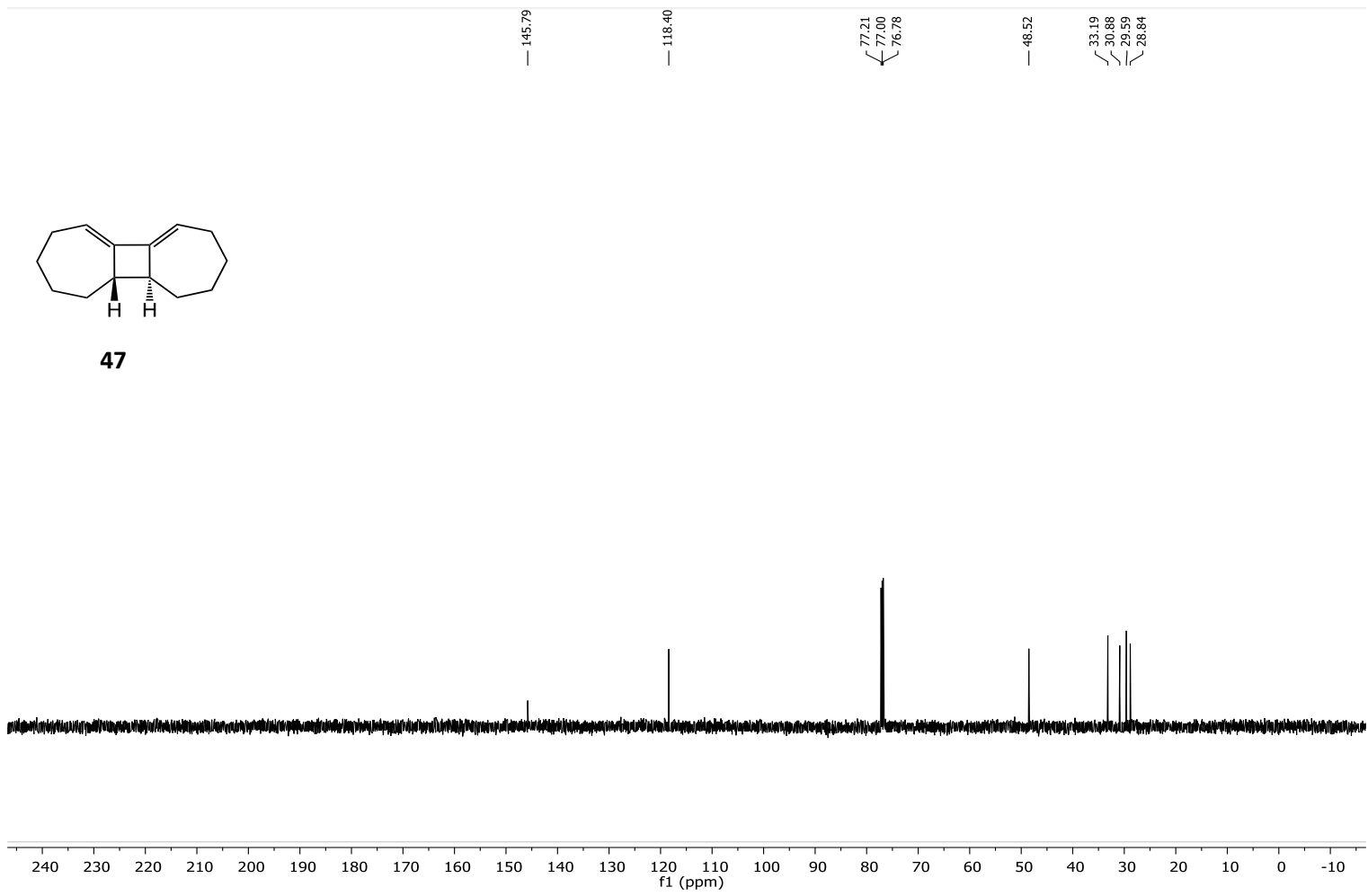
45

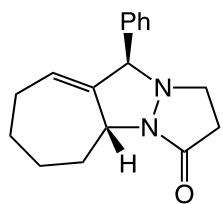




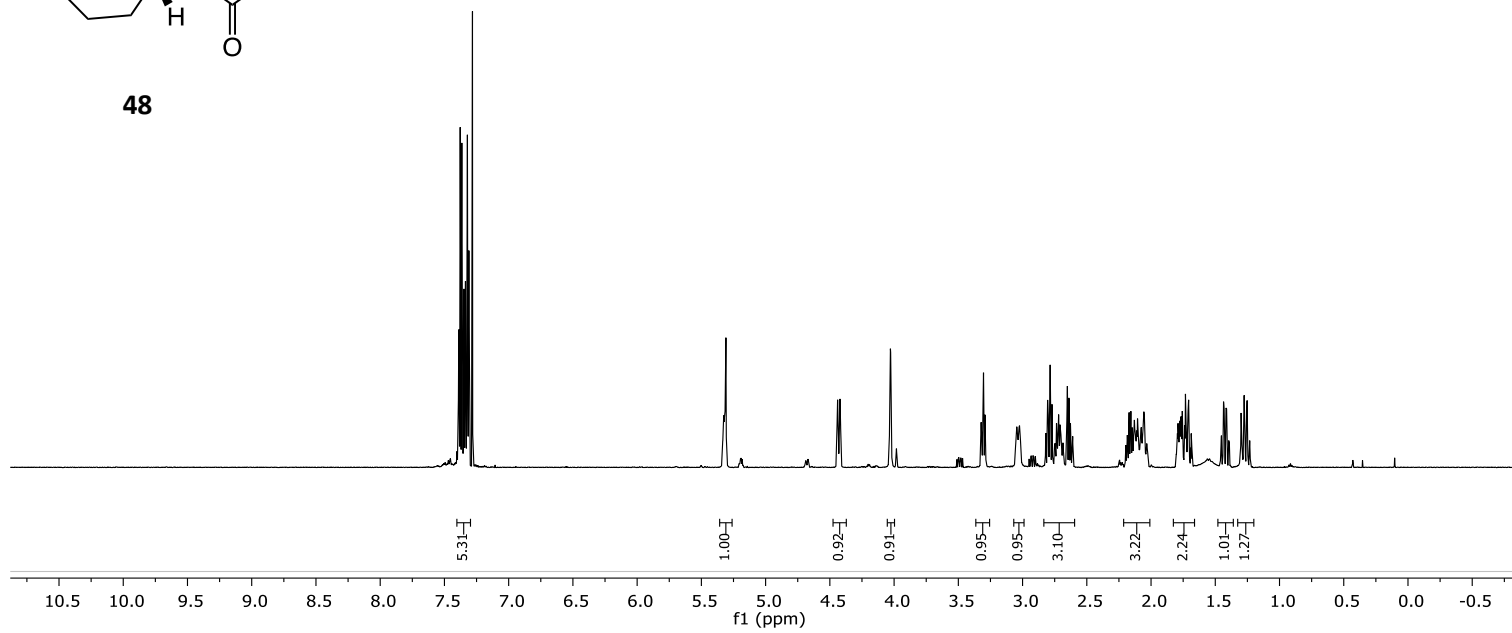
47

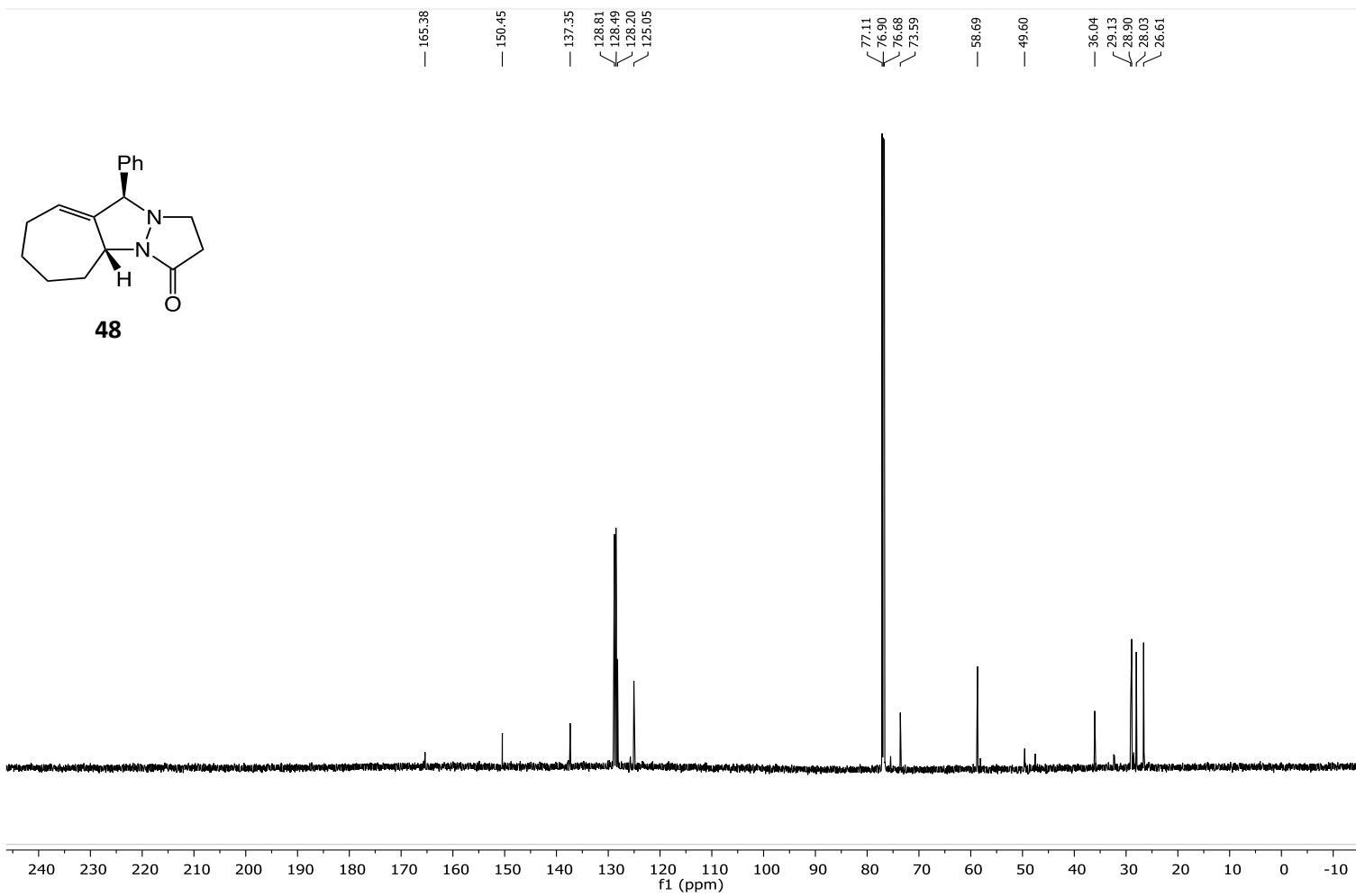


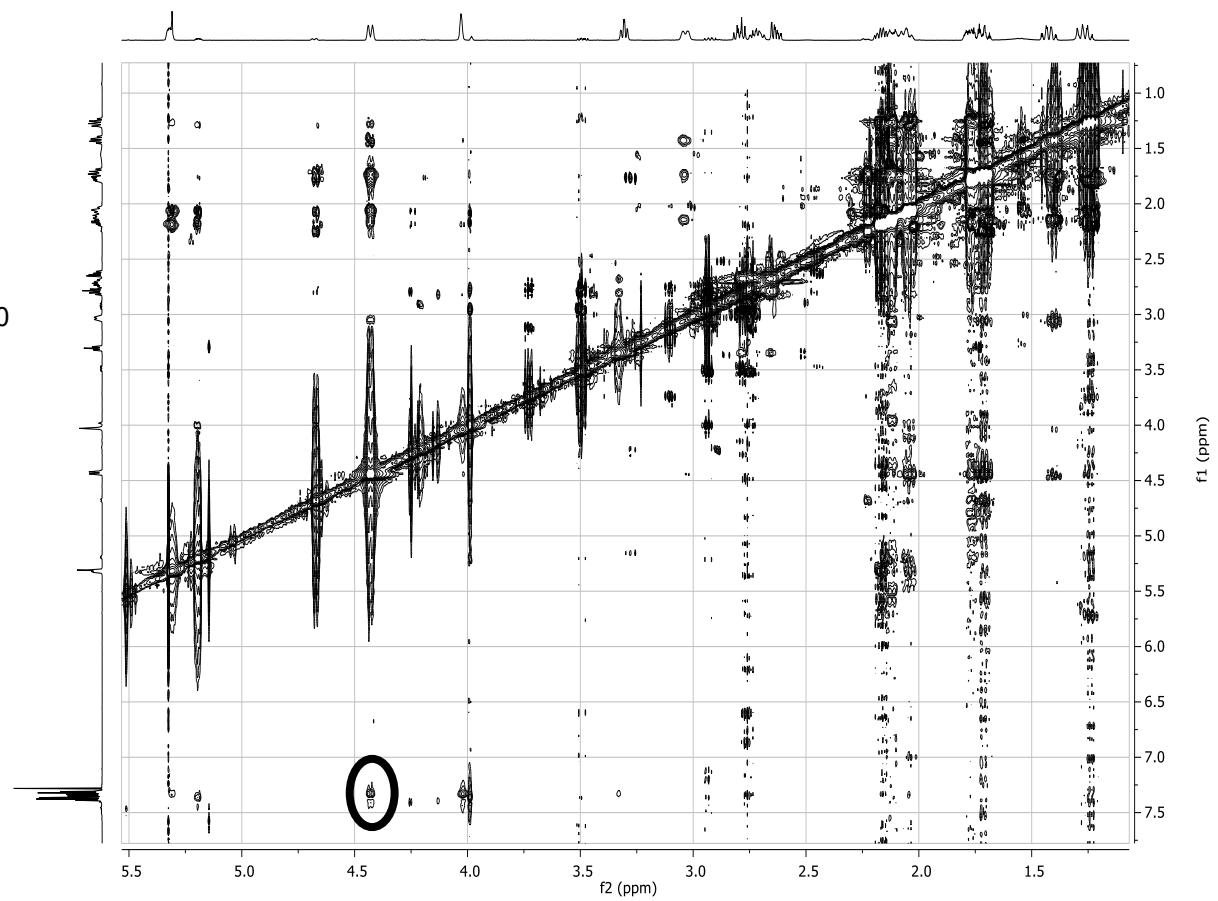
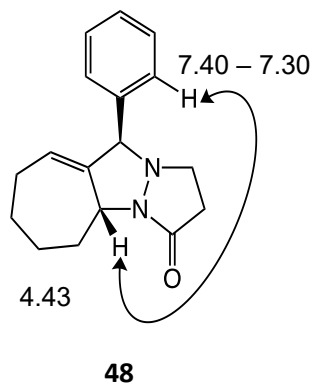




48







**Appendix II: X-ray Crystallographic Data for Compound
25 (Chapter 2)**

STRUCTURE REPORT

XCL Code: FGW1706

Date: 20 July 2017

Compound: Dodecahydrocyclobuta[1,2-*a*:3,4-*a'*]di[7]annulene-1,10-dione

Formula: C₁₄H₂₀O₂

Supervisor: F. G. West

Crystallographer: R.

McDonald

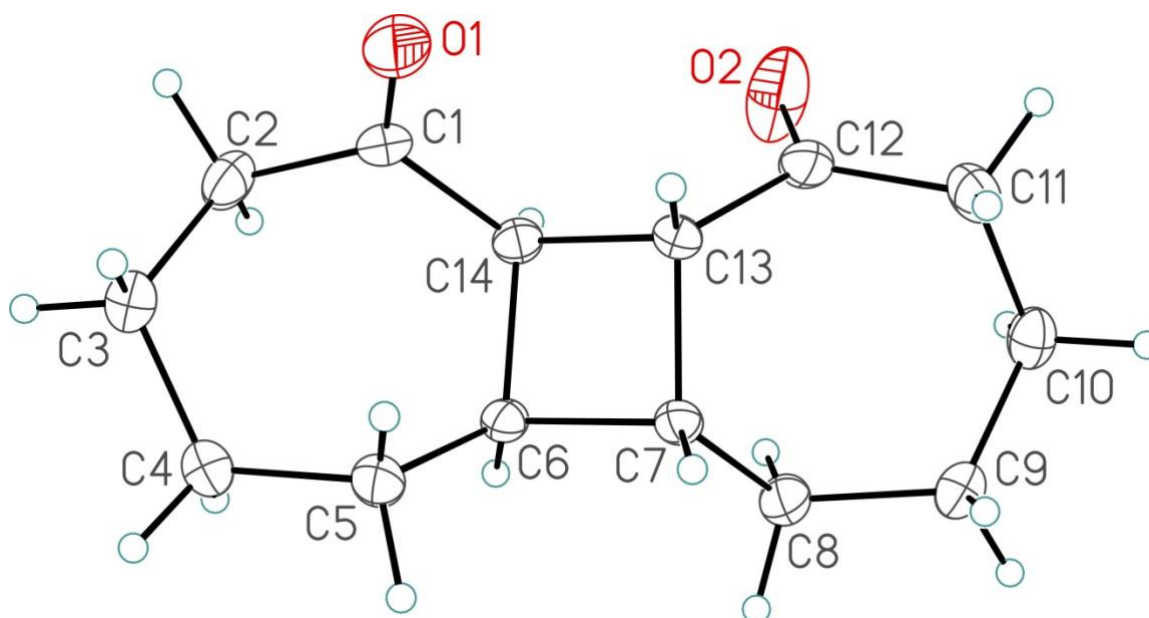
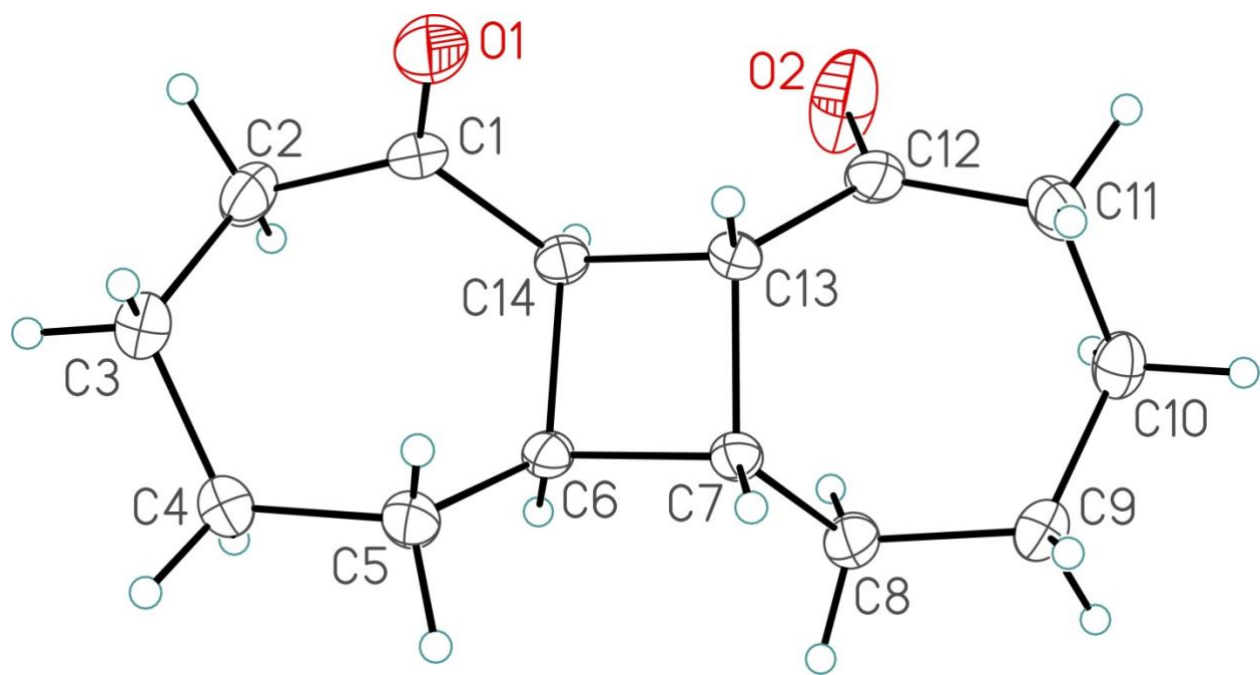
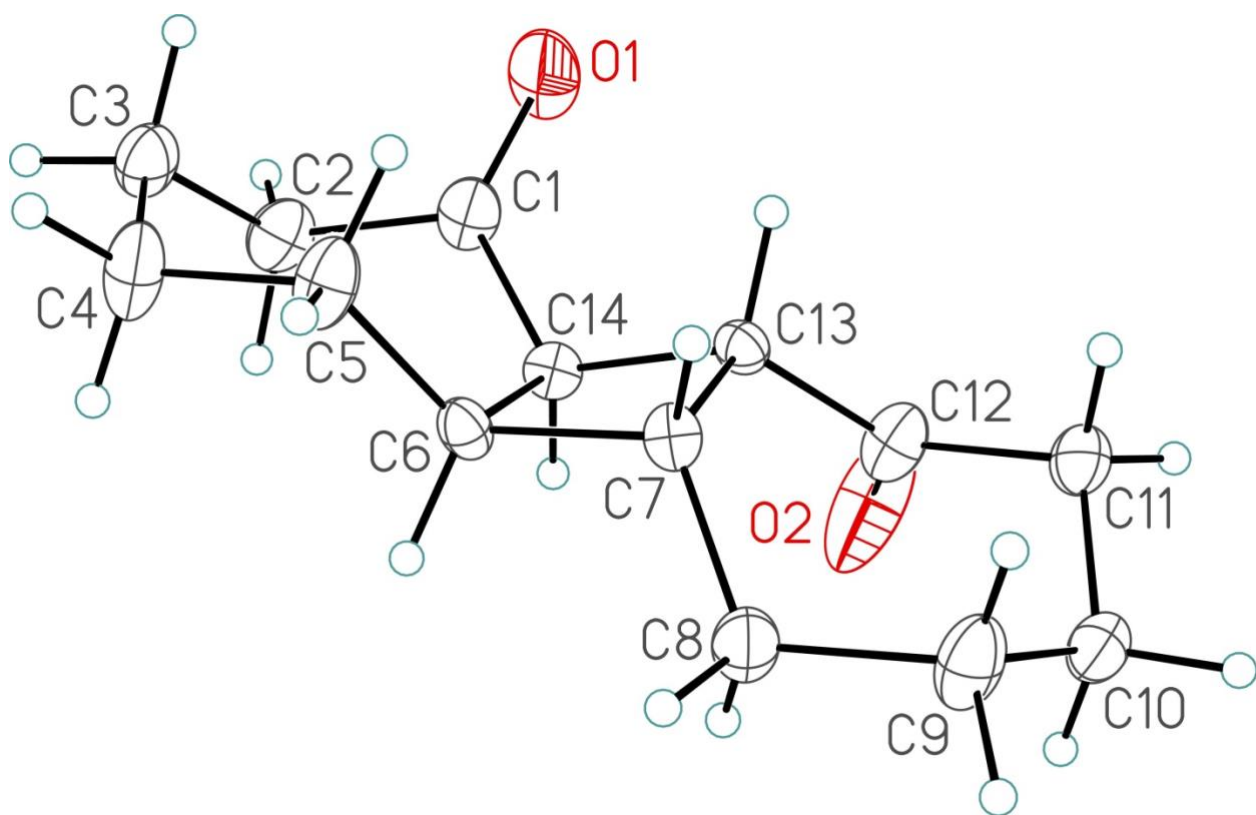


Figure Legends

Figure 1. Perspective view of the dodecahydrocyclobuta[1,2-*a*:3,4-*a'*]di[7]annulene-1,10-dione molecule showing the atom labelling scheme. Non-hydrogen atoms are represented by Gaussian ellipsoids at the 30% probability level. Hydrogen atoms are shown with arbitrarily small thermal parameters.

Figure 2. Alternate view of the molecule.





List of Tables

- Table 1.** Crystallographic Experimental Details
- Table 2.** Atomic Coordinates and Equivalent Isotropic Displacement Parameters
- Table 3.** Selected Interatomic Distances
- Table 4.** Selected Interatomic Angles
- Table 5.** Torsional Angles
- Table 6.** Anisotropic Displacement Parameters
- Table 7.** Derived Atomic Coordinates and Displacement Parameters for Hydrogen Atoms

Table 1. Crystallographic Experimental Details*A. Crystal Data*

formula	C ₁₄ H ₂₀ O ₂
formula weight	220.30
crystal dimensions (mm)	0.49 × 0.20 × 0.04
crystal system	monoclinic
space group	<i>I</i> 2/ <i>a</i> (an alternate setting of <i>C</i> 2/ <i>c</i> [No. 15])
unit cell parameters ^a	
<i>a</i> (Å)	9.4532 (2)
<i>b</i> (Å)	6.52438 (14)
<i>c</i> (Å)	40.1529 (9)
β (deg)	91.9285 (14)
<i>V</i> (Å ³)	2475.08 (9)
<i>Z</i>	8
ρ _{calcd} (g cm ⁻³)	1.182
μ (mm ⁻¹)	0.608

B. Data Collection and Refinement Conditions

diffractometer	Bruker D8/APEX II CCD ^b
radiation (λ [Å])	Cu Kα (1.54178) (microfocus source)
temperature (°C)	-100
scan type	ω and φ scans (1.0°) (5 s exposures)
data collection 2θ limit (deg)	147.87
total data collected	8286 (-11 ≤ <i>h</i> ≤ 11, -8 ≤ <i>k</i> ≤ 8, -47 ≤ <i>l</i> ≤ 49)
independent reflections	2428 (<i>R</i> _{int} = 0.0449)
number of observed reflections (<i>NO</i>)	2098 [<i>F</i> _o ² ≥ 2σ(<i>F</i> _o ²)]
structure solution method	direct methods/dual space (<i>SHELXD</i> ^c)
refinement method	full-matrix least-squares on <i>F</i> ² (<i>SHELXL-2014</i> ^e)
absorption correction method	Gaussian integration (face-indexed)
range of transmission factors	1.0000–0.6536
data/restraints/parameters	2428 / 0 / 145
goodness-of-fit (<i>S</i>) ^e [all data]	1.077
final <i>R</i> indices ^f	
<i>R</i> ₁ [<i>F</i> _o ² ≥ 2σ(<i>F</i> _o ²)]	0.0536
<i>wR</i> ₂ [all data]	0.1577
largest difference peak and hole	0.460 and -0.334 e Å ⁻³

^aObtained from least-squares refinement of 9869 reflections with 8.82° < 2θ < 147.34°.

^bPrograms for diffractometer operation, data collection, data reduction and absorption correction were those supplied by Bruker.

(continued)

Table 1. Crystallographic Experimental Details (continued)

^cSchneider, T. R.; Sheldrick, G. M. *Acta Crystallogr.* **2002**, *D58*, 1772-1779.

^dSheldrick, G. M. *Acta Crystallogr.* **2015**, *C71*, 3–8.

^e $S = [\sum w(F_o^2 - F_c^2)^2 / (n - p)]^{1/2}$ (n = number of data; p = number of parameters varied; $w = [\sigma^2(F_o^2) + (0.0841P)^2 + 1.4472P]^{-1}$ where $P = [\text{Max}(F_o^2, 0) + 2F_c^2]/3$).

^f $R_1 = \sum ||F_o| - |F_c|| / \sum |F_o|$; $wR_2 = [\sum w(F_o^2 - F_c^2)^2 / \sum w(F_o^4)]^{1/2}$.

Table 2. Atomic Coordinates and Equivalent Isotropic Displacement Parameters

Atom	<i>x</i>	<i>y</i>	<i>z</i>	$U_{\text{eq}}, \text{\AA}^2$
O1	0.0678(2)	-0.1230(2)	0.33402(4)	0.0827(6)*
O2	-0.12410(18)	0.0485(4)	0.42122(4)	0.1060(9)*
C1	0.0050(2)	0.0394(2)	0.33189(4)	0.0424(4)*
C2	-0.0555(2)	0.1162(3)	0.29886(4)	0.0464(4)*
C3	0.0599(2)	0.2144(3)	0.27864(4)	0.0461(4)*
C4	0.1197(3)	0.4130(3)	0.29375(4)	0.0558(5)*
C5	0.18660(19)	0.3912(3)	0.32877(4)	0.0454(4)*
C6	0.08304(16)	0.3866(2)	0.35662(4)	0.0300(3)*
C7	0.15004(14)	0.3516(2)	0.39200(3)	0.0294(3)*
C8	0.1040(2)	0.5054(3)	0.41785(4)	0.0453(4)*
C9	0.1583(2)	0.4610(3)	0.45356(4)	0.0524(5)*
C10	0.07570(17)	0.2988(3)	0.47189(4)	0.0397(4)*
C11	0.0804(2)	0.0859(3)	0.45593(4)	0.0430(4)*
C12	0.00042(19)	0.0838(3)	0.42298(4)	0.0439(4)*
C13	0.08075(14)	0.1348(2)	0.39258(3)	0.0278(3)*
C14	-0.00399(14)	0.1842(2)	0.36057(4)	0.0297(3)*

Anisotropically-refined atoms are marked with an asterisk (*). The form of the anisotropic displacement parameter is: $\exp[-2\pi^2(h^2a^*U_{11} + k^2b^*U_{22} + l^2c^*U_{33} + 2klb^*c^*U_{23} + 2hla^*c^*U_{13} + 2hka^*b^*U_{12})]$.

Table 3. Selected Interatomic Distances (Å)

Atom1	Atom2	Distance	Atom1	Atom2	Distance
O1	C1	1.216(2)	C6	C14	1.5668(19)
O2	C12	1.199(2)	C7	C8	1.518(2)
C1	C2	1.512(2)	C7	C13	1.5594(19)
C1	C14	1.494(2)	C8	C9	1.534(2)
C2	C3	1.523(3)	C9	C10	1.520(2)
C3	C4	1.531(3)	C10	C11	1.531(2)
C4	C5	1.529(2)	C11	C12	1.501(2)
C5	C6	1.511(2)	C12	C13	1.497(2)
C6	C7	1.5526(19)	C13	C14	1.5259(19)

Table 4. Selected Interatomic Angles (deg)

Atom1	Atom2	Atom3	Angle	Atom1	Atom2	Atom3	Angle
O1	C1	C2	121.33(16)	C7	C8	C9	114.81(15)
O1	C1	C14	122.48(16)	C8	C9	C10	114.99(15)
C2	C1	C14	115.89(14)	C9	C10	C11	113.99(14)
C1	C2	C3	110.51(15)	C10	C11	C12	110.89(14)
C2	C3	C4	113.96(15)	O2	C12	C11	121.16(16)
C3	C4	C5	114.93(16)	O2	C12	C13	121.25(17)
C4	C5	C6	115.10(15)	C11	C12	C13	117.55(14)
C5	C6	C7	115.19(12)	C7	C13	C12	116.03(12)
C5	C6	C14	116.56(12)	C7	C13	C14	90.27(10)
C7	C6	C14	89.02(10)	C12	C13	C14	117.88(13)
C6	C7	C8	114.26(12)	C1	C14	C6	114.30(12)
C6	C7	C13	89.34(10)	C1	C14	C13	118.29(13)
C8	C7	C13	117.33(12)	C6	C14	C13	90.04(10)

Table 5. Torsional Angles (deg)

Atom1	Atom2	Atom3	Atom4	Angle	Atom1	Atom2	Atom3	Atom4	Angle
O1	C1	C2	C3	-80.2(2)	C6	C7	C8	C9	174.56(14)
C14	C1	C2	C3	93.56(18)	C13	C7	C8	C9	71.93(19)
O1	C1	C14	C6	110.0(2)	C6	C7	C13	C12	-130.32(14)
O1	C1	C14	C13	5.9(2)	C6	C7	C13	C14	-8.81(10)
C2	C1	C14	C6	-63.68(18)	C8	C7	C13	C12	-13.15(19)
C2	C1	C14	C13	-167.80(13)	C8	C7	C13	C14	108.36(14)
C1	C2	C3	C4	-67.1(2)	C7	C8	C9	C10	-80.0(2)
C2	C3	C4	C5	59.6(2)	C8	C9	C10	C11	62.8(2)
C3	C4	C5	C6	-80.0(2)	C9	C10	C11	C12	-68.45(19)
C4	C5	C6	C7	176.54(14)	C10	C11	C12	O2	-88.0(2)
C4	C5	C6	C14	74.19(19)	C10	C11	C12	C13	89.80(18)
C5	C6	C7	C8	129.60(15)	O2	C12	C13	C7	117.7(2)
C5	C6	C7	C13	-110.51(13)	O2	C12	C13	C14	12.4(3)
C14	C6	C7	C8	-111.31(13)	C11	C12	C13	C7	-60.1(2)
C14	C6	C7	C13	8.58(10)	C11	C12	C13	C14	-165.40(14)
C5	C6	C14	C1	-12.26(19)	C7	C13	C14	C1	126.61(13)
C5	C6	C14	C13	109.09(14)	C7	C13	C14	C6	8.73(10)
C7	C6	C14	C1	-130.12(13)	C12	C13	C14	C1	-113.45(16)
C7	C6	C14	C13	-8.77(10)	C12	C13	C14	C6	128.66(13)

Table 6. Anisotropic Displacement Parameters (U_{ij} , Å²)

Atom	U_{11}	U_{22}	U_{33}	U_{23}	U_{13}	U_{12}
O1	0.1691(19)	0.0262(7)	0.0524(9)	-0.0048(6)	-0.0025(10)	0.0094(9)
O2	0.0720(11)	0.197(2)	0.0495(9)	-0.0046(11)	0.0093(8)	-0.0904(14)
C1	0.0604(10)	0.0276(8)	0.0390(9)	-0.0029(6)	0.0006(7)	-0.0147(7)
C2	0.0507(10)	0.0512(10)	0.0369(9)	-0.0104(7)	-0.0059(7)	-0.0104(8)
C3	0.0586(10)	0.0466(10)	0.0328(8)	-0.0032(7)	-0.0006(7)	-0.0040(8)
C4	0.0822(14)	0.0525(11)	0.0323(9)	0.0062(7)	-0.0019(9)	-0.0242(10)
C5	0.0499(10)	0.0522(10)	0.0341(9)	0.0028(7)	0.0013(7)	-0.0233(8)
C6	0.0367(7)	0.0225(7)	0.0304(7)	0.0018(5)	-0.0054(6)	-0.0010(5)
C7	0.0269(6)	0.0307(7)	0.0305(8)	0.0034(5)	-0.0017(5)	-0.0062(5)
C8	0.0705(12)	0.0299(8)	0.0352(9)	-0.0026(6)	-0.0042(8)	-0.0039(7)
C9	0.0702(12)	0.0529(11)	0.0336(9)	-0.0041(7)	-0.0061(8)	-0.0195(9)
C10	0.0354(8)	0.0532(10)	0.0304(8)	-0.0028(7)	0.0021(6)	0.0004(7)
C11	0.0521(10)	0.0435(9)	0.0339(9)	0.0073(6)	0.0091(7)	0.0001(7)
C12	0.0520(10)	0.0433(9)	0.0368(9)	-0.0008(7)	0.0069(7)	-0.0219(8)
C13	0.0293(7)	0.0235(7)	0.0306(7)	0.0021(5)	0.0017(5)	0.0005(5)
C14	0.0256(6)	0.0302(7)	0.0334(8)	-0.0009(5)	-0.0001(5)	-0.0035(5)

The form of the anisotropic displacement parameter is:

$$\exp[-2\pi^2(h^2a^2U_{11} + k^2b^2U_{22} + l^2c^2U_{33} + 2klb^*c^*U_{23} + 2hla^*c^*U_{13} + 2hka^*b^*U_{12})]$$

Table 7. Derived Atomic Coordinates and Displacement Parameters for Hydrogen Atoms

Atom	<i>x</i>	<i>y</i>	<i>z</i>	$U_{\text{eq}}, \text{\AA}^2$
H2A	-0.130762	0.218088	0.302817	0.056
H2B	-0.098434	0.000481	0.286179	0.056
H3A	0.020979	0.243737	0.255937	0.055
H3B	0.138188	0.114934	0.276511	0.055
H4A	0.191913	0.467668	0.278819	0.067
H4B	0.042338	0.515039	0.294490	0.067
H5A	0.242943	0.263333	0.329665	0.054
H5B	0.252763	0.506969	0.332749	0.054
H6	0.020030	0.509742	0.355995	0.036
H7	0.255526	0.342259	0.391438	0.035
H8A	-0.000739	0.509089	0.417580	0.054
H8B	0.137281	0.643078	0.411348	0.054
H9A	0.258346	0.416639	0.452828	0.063
H9B	0.156137	0.590038	0.466498	0.063
H10A	-0.024248	0.343118	0.472808	0.048
H10B	0.114074	0.289201	0.495079	0.048
H11A	0.180020	0.046323	0.452645	0.052
H11B	0.038380	-0.015654	0.471026	0.052
H13	0.152917	0.026569	0.388370	0.033
H14	-0.104846	0.215170	0.365395	0.036

**Appendix III: X-ray Crystallographic Data for Compound
27 (Chapter 2)**

STRUCTURE REPORT

XCL Code: FGW1801

Date: 6 February 2018

Compound: 5,11-diphenyl-7,8,9,10,10a,11-hexahydro-5*H*-5,11-epoxycyclohepta[b]naphthalen-6-yl acetate

Formula: C₂₉H₂₆O₃

Supervisor: F. G. West

Crystallographer: M. J. Ferguson

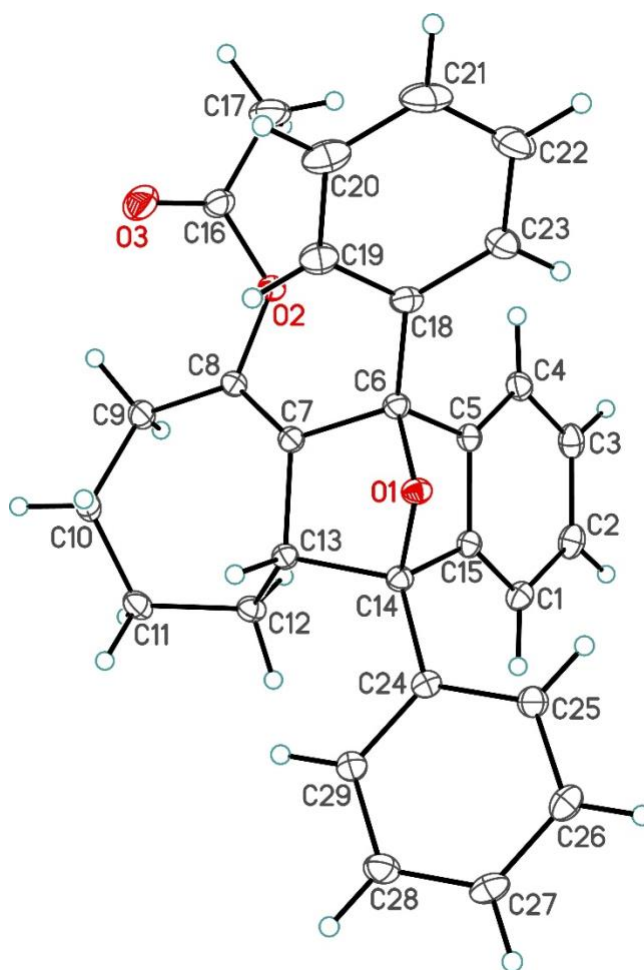
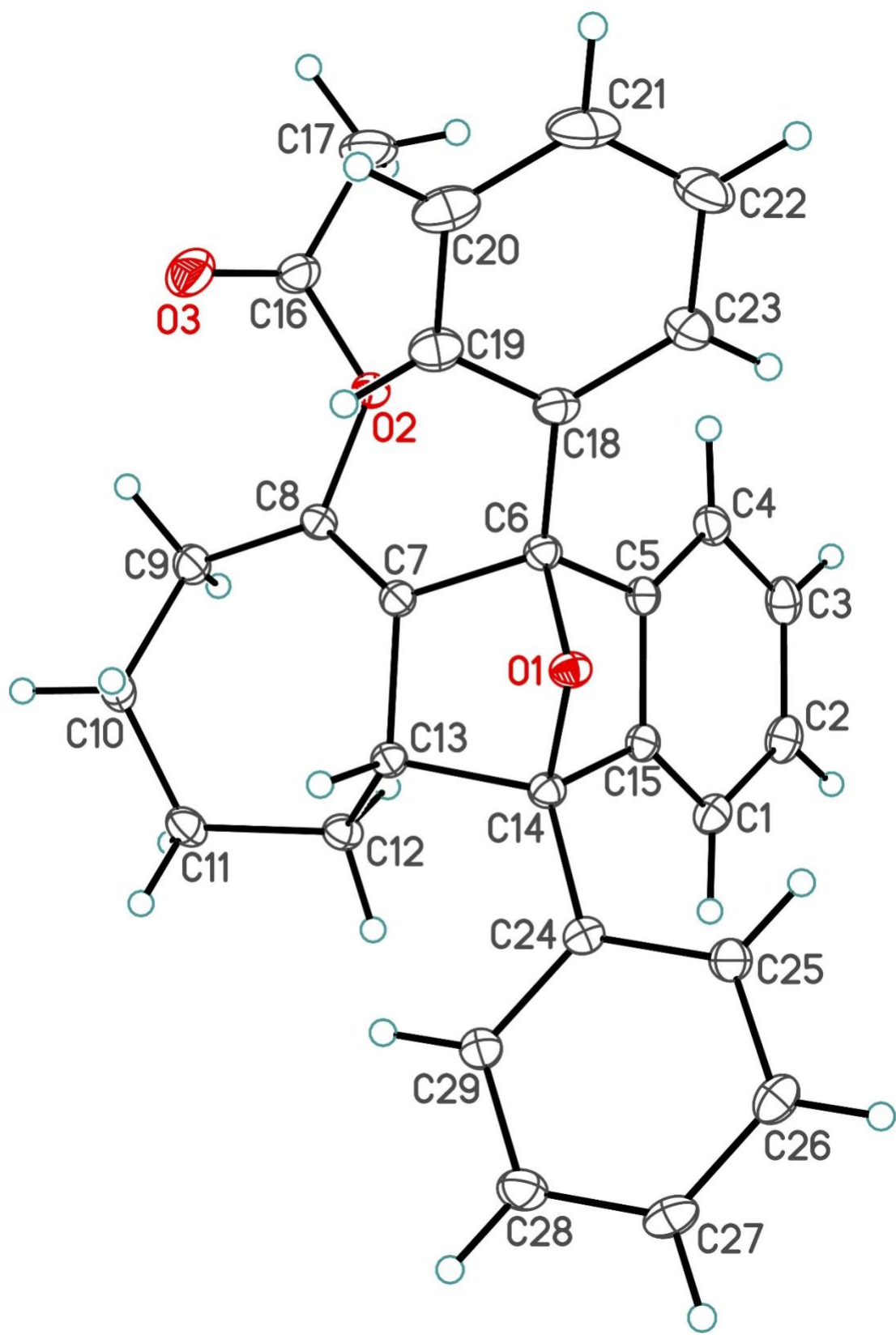
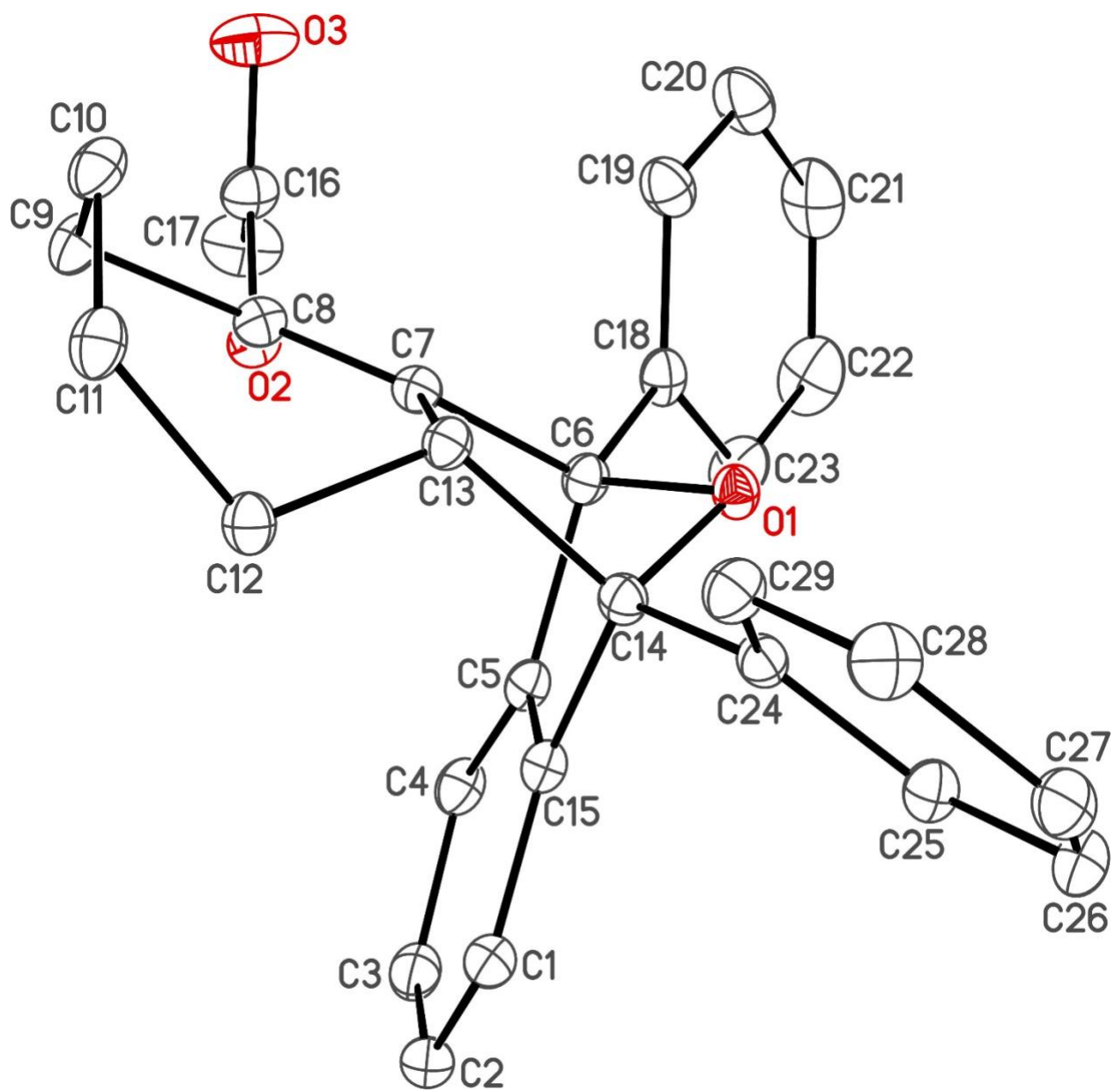


Figure Legends

Figure 1. Perspective view of the 5,11-diphenyl-7,8,9,10,10a,11-hexahydro-5*H*-5,11-epoxycyclohepta[*b*]naphthalen-6-yl acetate molecule showing the atom labelling scheme. Non-hydrogen atoms are represented by Gaussian ellipsoids at the 30% probability level. Hydrogen atoms are shown with arbitrarily small thermal parameters.

Figure 2. Alternate view of the molecule. Hydrogen atoms have been removed for clarity.





List of Tables

- Table 1.** Crystallographic Experimental Details
- Table 2.** Atomic Coordinates and Equivalent Isotropic Displacement Parameters
- Table 3.** Selected Interatomic Distances
- Table 4.** Selected Interatomic Angles
- Table 5.** Torsional Angles
- Table 6.** Anisotropic Displacement Parameters
- Table 7.** Derived Atomic Coordinates and Displacement Parameters for Hydrogen Atoms

Table 1. Crystallographic Experimental Details*A. Crystal Data*

formula	C ₂₉ H ₂₆ O ₃
formula weight	422.50
crystal dimensions (mm)	0.49 × 0.32 × 0.11
crystal system	monoclinic
space group	<i>P</i> 2 ₁ / <i>c</i> (No. 14)
unit cell parameters ^a	
<i>a</i> (Å)	10.4018(5)
<i>b</i> (Å)	19.7375(10)
<i>c</i> (Å)	11.6185(6)
β (deg)	109.9432(15)
<i>V</i> (Å ³)	2242.3(2)
<i>Z</i>	4
ρ _{calcd} (g cm ⁻³)	1.252
μ (mm ⁻¹)	0.631

B. Data Collection and Refinement Conditions

diffractometer	Bruker D8/APEX II CCD ^b
radiation (λ [Å])	Cu Kα (1.54178) (microfocus source)
temperature (°C)	-100
scan type	ω and φ scans (1.0°) (5 s exposures)
data collection 2θ limit (deg)	147.69
total data collected	15646 (-12 ≤ <i>h</i> ≤ 12, -24 ≤ <i>k</i> ≤ 23, -14 ≤ <i>l</i> ≤ 14)
independent reflections	4530 (<i>R</i> _{int} = 0.0191)
number of observed reflections (<i>NO</i>)	4365 [<i>F</i> _o ² ≥ 2σ(<i>F</i> _o ²)]
structure solution method	intrinsic phasing (<i>SHELXT-2014</i> ^c)
refinement method	full-matrix least-squares on <i>F</i> ² (<i>SHELXL-2016</i> ^d)
absorption correction method	Gaussian integration (face-indexed)
range of transmission factors	0.9424–0.8349
data/restraints/parameters	4530 / 0 / 290
goodness-of-fit (<i>S</i>) ^e [all data]	1.041
final <i>R</i> indices ^f	
<i>R</i> ₁ [<i>F</i> _o ² ≥ 2σ(<i>F</i> _o ²)]	0.0365
<i>wR</i> ₂ [all data]	0.0916
largest difference peak and hole	0.266 and -0.252 e Å ⁻³

^aObtained from least-squares refinement of 9242 reflections with 4.48° < 2θ < 147.64°.

^bPrograms for diffractometer operation, data collection, data reduction and absorption correction were those supplied by Bruker.

(continued)

Table 1. Crystallographic Experimental Details (continued)

^cSheldrick, G. M. *Acta Crystallogr.* **2015**, *A71*, 3–8. (*SHELXT-2014*)

^dSheldrick, G. M. *Acta Crystallogr.* **2015**, *C71*, 3–8. (*SHELXL-2016*)

$eS = [\Sigma w(F_o^2 - F_c^2)^2 / (n - p)]^{1/2}$ (n = number of data; p = number of parameters varied; $w = [\sigma^2(F_o^2) + (0.0427P)^2 + 0.7965P]^{-1}$ where $P = [\text{Max}(F_o^2, 0) + 2F_c^2] / 3$).

$fR_1 = \Sigma ||F_o| - |F_c|| / \Sigma |F_o|$; $wR_2 = [\Sigma w(F_o^2 - F_c^2)^2 / \Sigma w(F_o^4)]^{1/2}$.

Table 2. Atomic Coordinates and Equivalent Isotropic Displacement Parameters

Atom	<i>x</i>	<i>y</i>	<i>z</i>	$U_{eq}, \text{\AA}^2$
O1	0.60040(7)	0.28918(4)	0.75595(6)	0.02049(16)*
O2	0.34332(7)	0.45817(4)	0.62364(6)	0.02275(16)*
O3	0.12660(9)	0.42145(5)	0.53670(9)	0.0450(2)*
C1	0.87616(11)	0.40457(5)	0.77406(10)	0.0246(2)*
C2	0.90140(11)	0.46511(6)	0.84082(10)	0.0285(2)*
C3	0.80291(12)	0.49360(6)	0.88167(10)	0.0288(2)*
C4	0.67528(11)	0.46290(6)	0.85747(9)	0.0254(2)*
C5	0.65263(10)	0.40159(5)	0.79604(9)	0.0210(2)*
C6	0.53043(10)	0.35402(5)	0.74874(9)	0.0203(2)*
C7	0.48059(10)	0.36722(5)	0.60974(9)	0.0195(2)*
C8	0.39264(10)	0.41461(5)	0.55086(9)	0.0209(2)*
C9	0.34932(11)	0.43319(6)	0.41771(9)	0.0262(2)*
C10	0.37465(12)	0.37638(6)	0.33833(9)	0.0267(2)*
C11	0.52308(12)	0.36993(6)	0.34354(10)	0.0271(2)*
C12	0.62839(11)	0.36865(5)	0.47384(9)	0.0230(2)*
C13	0.57844(10)	0.32767(5)	0.56206(9)	0.0195(2)*
C14	0.68892(10)	0.30803(5)	0.68708(9)	0.0194(2)*
C15	0.75201(10)	0.37293(5)	0.75425(9)	0.0203(2)*
C16	0.20748(11)	0.45778(6)	0.60742(11)	0.0283(2)*
C17	0.17581(14)	0.50740(8)	0.69062(14)	0.0446(3)*
C18	0.42712(11)	0.34680(5)	0.81242(10)	0.0243(2)*
C19	0.30092(12)	0.31740(6)	0.75023(12)	0.0306(2)*
C20	0.20657(13)	0.30615(7)	0.80875(14)	0.0404(3)*
C21	0.23827(15)	0.32377(8)	0.93048(14)	0.0473(4)*
C22	0.36410(15)	0.35221(9)	0.99368(13)	0.0474(4)*
C23	0.45905(13)	0.36380(7)	0.93517(11)	0.0350(3)*
C24	0.78610(10)	0.25101(5)	0.69007(9)	0.0204(2)*
C25	0.87741(11)	0.23069(6)	0.80378(10)	0.0253(2)*
C26	0.96983(12)	0.17860(6)	0.81267(11)	0.0297(2)*
C27	0.97285(12)	0.14641(6)	0.70759(11)	0.0300(2)*
C28	0.88228(12)	0.16552(6)	0.59438(11)	0.0304(2)*
C29	0.78836(11)	0.21761(6)	0.58538(10)	0.0256(2)*

Anisotropically-refined atoms are marked with an asterisk (*). The form of the anisotropic displacement parameter is: $\exp[-2\pi^2(h^2a^*U_{11} + k^2b^*U_{22} + l^2c^*U_{33} + 2klb^*c^*U_{23} + 2hla^*c^*U_{13} + 2hka^*b^*U_{12})]$.

Table 3. Selected Interatomic Distances (Å)

Atom1	Atom2	Distance	Atom1	Atom2	Distance
O1	C6	1.4604(12)	C11	C12	1.5366(14)
O1	C14	1.4591(11)	C12	C13	1.5292(13)
O2	C8	1.4189(12)	C13	C14	1.5627(13)
O2	C16	1.3603(13)	C14	C15	1.5269(14)
O3	C16	1.1939(15)	C14	C24	1.5053(14)
C1	C2	1.3998(16)	C16	C17	1.4897(16)
C1	C15	1.3812(14)	C18	C19	1.3911(16)
C2	C3	1.3867(17)	C18	C23	1.3906(16)
C3	C4	1.3978(16)	C19	C20	1.3892(16)
C4	C5	1.3837(15)	C20	C21	1.383(2)
C5	C6	1.5240(14)	C21	C22	1.383(2)
C5	C15	1.4024(14)	C22	C23	1.3957(17)
C6	C7	1.5406(13)	C24	C25	1.3973(14)
C6	C18	1.5050(14)	C24	C29	1.3907(15)
C7	C8	1.3241(14)	C25	C26	1.3872(15)
C7	C13	1.5285(13)	C26	C27	1.3861(17)
C8	C9	1.5017(14)	C27	C28	1.3837(17)
C9	C10	1.5308(15)	C28	C29	1.3974(15)
C10	C11	1.5297(16)			

Table 4. Selected Interatomic Angles (deg)

Atom1	Atom2	Atom3	Angle	Atom1	Atom2	Atom3	Angle
C6	O1	C14	98.08(7)	O1	C14	C13	99.87(7)
C8	O2	C16	118.93(8)	O1	C14	C15	100.09(7)
C2	C1	C15	117.79(10)	O1	C14	C24	109.95(8)
C1	C2	C3	120.99(10)	C13	C14	C15	108.58(8)
C2	C3	C4	121.15(10)	C13	C14	C24	118.82(8)
C3	C4	C5	117.76(10)	C15	C14	C24	116.57(8)
C4	C5	C6	134.36(10)	C1	C15	C5	121.18(10)
C4	C5	C15	121.02(10)	C1	C15	C14	132.76(9)
C6	C5	C15	104.44(9)	C5	C15	C14	106.04(8)
O1	C6	C5	100.43(7)	O2	C16	O3	123.61(10)
O1	C6	C7	101.02(7)	O2	C16	C17	110.83(10)
O1	C6	C18	108.31(8)	O3	C16	C17	125.56(11)
C5	C6	C7	102.41(8)	C6	C18	C19	119.32(10)
C5	C6	C18	121.91(9)	C6	C18	C23	121.37(10)
C7	C6	C18	119.34(8)	C19	C18	C23	119.10(10)
C6	C7	C8	125.96(9)	C18	C19	C20	120.76(12)
C6	C7	C13	105.42(8)	C19	C20	C21	119.91(13)
C8	C7	C13	126.99(9)	C20	C21	C22	119.85(12)
O2	C8	C7	116.53(9)	C21	C22	C23	120.45(13)
O2	C8	C9	115.06(8)	C18	C23	C22	119.93(13)
C7	C8	C9	128.06(9)	C14	C24	C25	118.10(9)
C8	C9	C10	112.89(9)	C14	C24	C29	123.08(9)
C9	C10	C11	114.58(9)	C25	C24	C29	118.82(10)
C10	C11	C12	114.27(8)	C24	C25	C26	120.89(10)
C11	C12	C13	112.22(9)	C25	C26	C27	119.83(10)
C7	C13	C12	113.16(8)	C26	C27	C28	119.99(10)
C7	C13	C14	99.17(7)	C27	C28	C29	120.24(10)
C12	C13	C14	116.36(8)	C24	C29	C28	120.21(10)

Table 5. Torsional Angles (deg)

Atom1	Atom2	Atom3	Atom4	Angle	Atom1	Atom2	Atom3	Atom4	Angle
C14	O1	C6	C5	-52.75(8)	C6	C7	C8	C9	174.68(10)
C14	O1	C6	C7	52.24(8)	C13	C7	C8	O2	-161.42(9)
C14	O1	C6	C18	178.42(8)	C13	C7	C8	C9	11.38(18)
C6	O1	C14	C13	-59.92(8)	C6	C7	C13	C12	-134.19(9)
C6	O1	C14	C15	51.14(8)	C6	C7	C13	C14	-10.26(9)
C6	O1	C14	C24	174.37(8)	C8	C7	C13	C12	31.85(14)
C16	O2	C8	C7	-116.84(11)	C8	C7	C13	C14	155.78(10)
C16	O2	C8	C9	69.41(12)	O2	C8	C9	C10	-165.98(9)
C8	O2	C16	O3	1.79(17)	C7	C8	C9	C10	21.13(16)
C8	O2	C16	C17	-179.18(10)	C8	C9	C10	C11	-78.50(12)
C15	C1	C2	C3	-2.36(16)	C9	C10	C11	C12	49.24(13)
C2	C1	C15	C5	2.08(15)	C10	C11	C12	C13	39.20(12)
C2	C1	C15	C14	179.78(10)	C11	C12	C13	C7	-80.60(10)
C1	C2	C3	C4	-0.08(17)	C11	C12	C13	C14	165.49(8)
C2	C3	C4	C5	2.78(16)	C7	C13	C14	O1	42.37(8)
C3	C4	C5	C6	-177.28(10)	C7	C13	C14	C15	-61.87(9)
C3	C4	C5	C15	-3.07(15)	C7	C13	C14	C24	161.78(8)
C4	C5	C6	O1	-151.22(11)	C12	C13	C14	O1	164.01(8)
C4	C5	C6	C7	104.92(12)	C12	C13	C14	C15	59.76(11)
C4	C5	C6	C18	-31.81(17)	C12	C13	C14	C24	-76.58(11)
C15	C5	C6	O1	33.90(9)	O1	C14	C15	C1	151.28(11)
C15	C5	C6	C7	-69.96(9)	O1	C14	C15	C5	-30.77(9)
C15	C5	C6	C18	153.31(9)	C13	C14	C15	C1	-104.63(12)
C4	C5	C15	C1	0.66(15)	C13	C14	C15	C5	73.32(9)
C4	C5	C15	C14	-177.59(9)	C24	C14	C15	C1	32.82(15)
C6	C5	C15	C1	176.39(9)	C24	C14	C15	C5	-149.23(9)
C6	C5	C15	C14	-1.86(10)	O1	C14	C24	C25	-61.17(12)
O1	C6	C7	C8	168.83(10)	O1	C14	C24	C29	118.40(10)
O1	C6	C7	C13	-24.95(9)	C13	C14	C24	C25	-175.24(9)
C5	C6	C7	C8	-87.76(12)	C13	C14	C24	C29	4.33(14)
C5	C6	C7	C13	78.46(9)	C15	C14	C24	C25	51.78(12)
C18	C6	C7	C8	50.36(15)	C15	C14	C24	C29	-128.65(10)
C18	C6	C7	C13	-143.42(9)	C6	C18	C19	C20	175.98(11)
O1	C6	C18	C19	-81.24(11)	C23	C18	C19	C20	1.15(17)
O1	C6	C18	C23	93.47(12)	C6	C18	C23	C22	-175.67(12)
C5	C6	C18	C19	163.24(10)	C19	C18	C23	C22	-0.95(18)
C5	C6	C18	C23	-22.05(15)	C18	C19	C20	C21	-0.52(19)
C7	C6	C18	C19	33.41(14)	C19	C20	C21	C22	-0.3(2)
C7	C6	C18	C23	-151.88(11)	C20	C21	C22	C23	0.5(2)
C6	C7	C8	O2	1.88(15)	C21	C22	C23	C18	0.1(2)

Table 5. Torsional Angles (continued)

Atom1	Atom2	Atom3	Atom4	Angle	Atom1	Atom2	Atom3	Atom4	Angle
C14	C24	C25	C26	-179.80(10)	C24	C25	C26	C27	0.49(17)
C29	C24	C25	C26	0.62(16)	C25	C26	C27	C28	-1.06(17)
C14	C24	C29	C28	179.29(10)	C26	C27	C28	C29	0.54(18)
C25	C24	C29	C28	-1.14(16)	C27	C28	C29	C24	0.58(17)

Table 6. Anisotropic Displacement Parameters (U_{ij} , Å²)

Atom	U_{11}	U_{22}	U_{33}	U_{23}	U_{13}	U_{12}
O1	0.0211(3)	0.0200(3)	0.0227(3)	0.0036(3)	0.0105(3)	0.0026(3)
O2	0.0221(4)	0.0225(4)	0.0234(4)	-0.0034(3)	0.0075(3)	0.0032(3)
O3	0.0254(4)	0.0516(6)	0.0534(6)	-0.0203(5)	0.0077(4)	-0.0028(4)
C1	0.0218(5)	0.0258(5)	0.0251(5)	0.0040(4)	0.0066(4)	0.0007(4)
C2	0.0257(5)	0.0267(6)	0.0282(5)	0.0033(4)	0.0028(4)	-0.0048(4)
C3	0.0346(6)	0.0220(5)	0.0238(5)	-0.0009(4)	0.0023(4)	-0.0009(4)
C4	0.0292(5)	0.0248(5)	0.0204(5)	-0.0001(4)	0.0061(4)	0.0048(4)
C5	0.0218(5)	0.0230(5)	0.0171(4)	0.0027(4)	0.0055(4)	0.0023(4)
C6	0.0206(5)	0.0206(5)	0.0203(5)	0.0013(4)	0.0077(4)	0.0031(4)
C7	0.0192(5)	0.0201(5)	0.0195(5)	-0.0010(4)	0.0071(4)	-0.0015(4)
C8	0.0211(5)	0.0204(5)	0.0211(5)	-0.0033(4)	0.0070(4)	0.0010(4)
C9	0.0287(5)	0.0259(5)	0.0213(5)	0.0012(4)	0.0051(4)	0.0078(4)
C10	0.0315(6)	0.0263(5)	0.0186(5)	-0.0015(4)	0.0038(4)	0.0035(4)
C11	0.0358(6)	0.0268(5)	0.0202(5)	0.0010(4)	0.0112(4)	0.0053(4)
C12	0.0259(5)	0.0228(5)	0.0226(5)	0.0020(4)	0.0111(4)	0.0026(4)
C13	0.0201(5)	0.0186(5)	0.0194(5)	0.0004(4)	0.0064(4)	0.0020(4)
C14	0.0193(5)	0.0207(5)	0.0195(5)	0.0018(4)	0.0084(4)	0.0004(4)
C15	0.0214(5)	0.0207(5)	0.0177(4)	0.0027(4)	0.0054(4)	0.0023(4)
C16	0.0235(5)	0.0285(6)	0.0325(6)	-0.0016(5)	0.0090(4)	0.0043(4)
C17	0.0361(7)	0.0470(8)	0.0575(8)	-0.0172(7)	0.0247(6)	0.0025(6)
C18	0.0247(5)	0.0245(5)	0.0271(5)	0.0060(4)	0.0133(4)	0.0059(4)
C19	0.0298(6)	0.0280(6)	0.0381(6)	0.0032(5)	0.0171(5)	0.0001(4)
C20	0.0318(6)	0.0374(7)	0.0599(8)	0.0087(6)	0.0260(6)	0.0011(5)
C21	0.0454(8)	0.0543(9)	0.0589(9)	0.0156(7)	0.0396(7)	0.0104(6)
C22	0.0513(8)	0.0663(10)	0.0354(7)	0.0083(6)	0.0289(6)	0.0124(7)
C23	0.0337(6)	0.0475(7)	0.0274(6)	0.0040(5)	0.0153(5)	0.0065(5)
C24	0.0195(5)	0.0189(5)	0.0239(5)	0.0024(4)	0.0088(4)	0.0000(4)
C25	0.0266(5)	0.0258(5)	0.0239(5)	0.0027(4)	0.0091(4)	0.0023(4)
C26	0.0264(5)	0.0275(6)	0.0322(6)	0.0081(4)	0.0059(4)	0.0048(4)
C27	0.0260(5)	0.0211(5)	0.0437(7)	0.0026(5)	0.0128(5)	0.0058(4)
C28	0.0331(6)	0.0263(6)	0.0337(6)	-0.0045(4)	0.0137(5)	0.0039(5)
C29	0.0258(5)	0.0254(5)	0.0250(5)	-0.0005(4)	0.0079(4)	0.0032(4)

The form of the anisotropic displacement parameter is:

$$\exp[-2\pi^2(h^2a^2U_{11} + k^2b^2U_{22} + l^2c^2U_{33} + 2klb^*c^*U_{23} + 2hla^*c^*U_{13} + 2hka^*b^*U_{12})]$$

Table 7. Derived Atomic Coordinates and Displacement Parameters for Hydrogen Atoms

Atom	<i>x</i>	<i>y</i>	<i>z</i>	$U_{\text{eq}}, \text{\AA}^2$
H1	0.942223	0.385858	0.743397	0.029
H2	0.987310	0.487005	0.858398	0.034
H3	0.822513	0.534692	0.926893	0.035
H4	0.606410	0.483443	0.882352	0.030
H9A	0.400048	0.474113	0.408607	0.031
H9B	0.250677	0.444498	0.387973	0.031
H10A	0.346195	0.332851	0.364558	0.032
H10B	0.315982	0.384303	0.252281	0.032
H11A	0.544418	0.408435	0.298487	0.033
H11B	0.532451	0.327773	0.300903	0.033
H12A	0.714831	0.348767	0.471484	0.028
H12B	0.647698	0.415681	0.504511	0.028
H13	0.531840	0.285665	0.519939	0.023
H17A	0.076460	0.510959	0.669622	0.054
H17B	0.213255	0.551827	0.681422	0.054
H17C	0.216881	0.492058	0.775554	0.054
H19	0.278993	0.304870	0.666773	0.037
H20	0.120385	0.286381	0.765191	0.048
H21	0.173755	0.316345	0.970593	0.057
H22	0.386065	0.363948	1.077506	0.057
H23	0.545388	0.383279	0.979156	0.042
H25	0.876169	0.252843	0.875986	0.030
H26	1.030910	0.165017	0.890583	0.036
H27	1.037081	0.111243	0.713290	0.036
H28	0.883952	0.143147	0.522506	0.036
H29	0.725839	0.230247	0.507496	0.031

**Appendix IV: X-ray Crystallographic Data for Compound
38a (Chapter 2)**

STRUCTURE REPORT

XCL Code: FGW1805

Date: 14 May 2018

Compound: 3-oxo-10-phenyl-2,3,4a,5,6,7,8,10-octahydro-1*H*-cyclohepta[*c*]pyrazolo[1,2-*a*]pyrazol-9-yl acetate

Formula: C₁₉H₂₂N₂O₃

Supervisor: F. G. West

Crystallographer: M. J. Ferguson

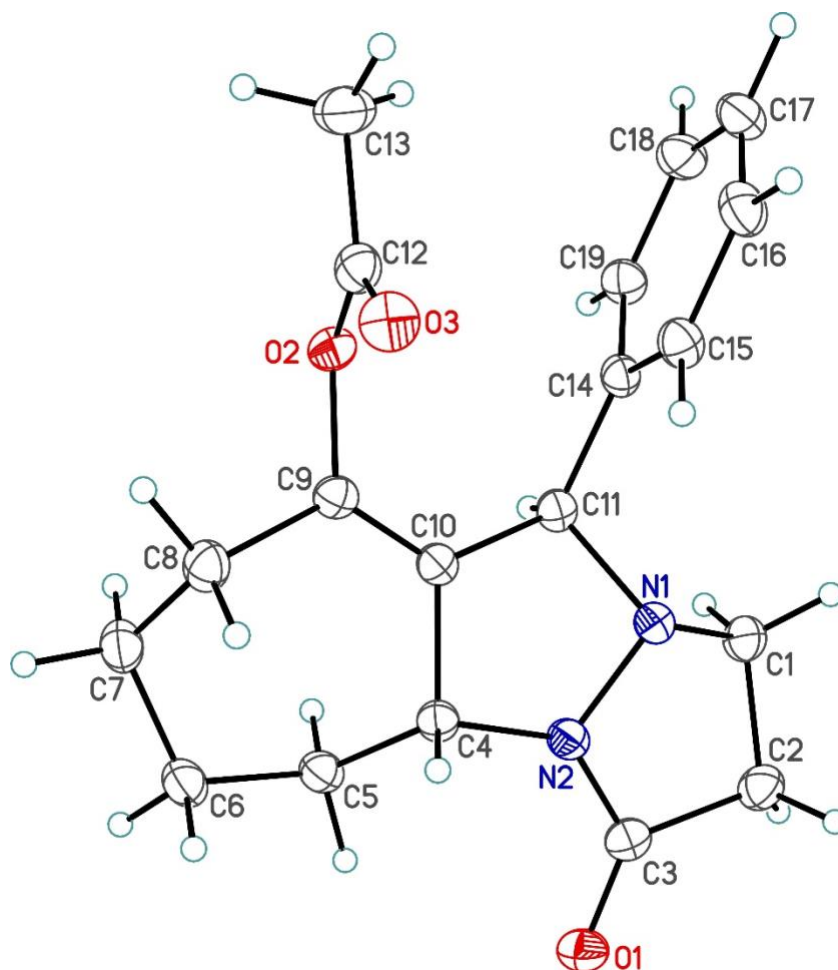
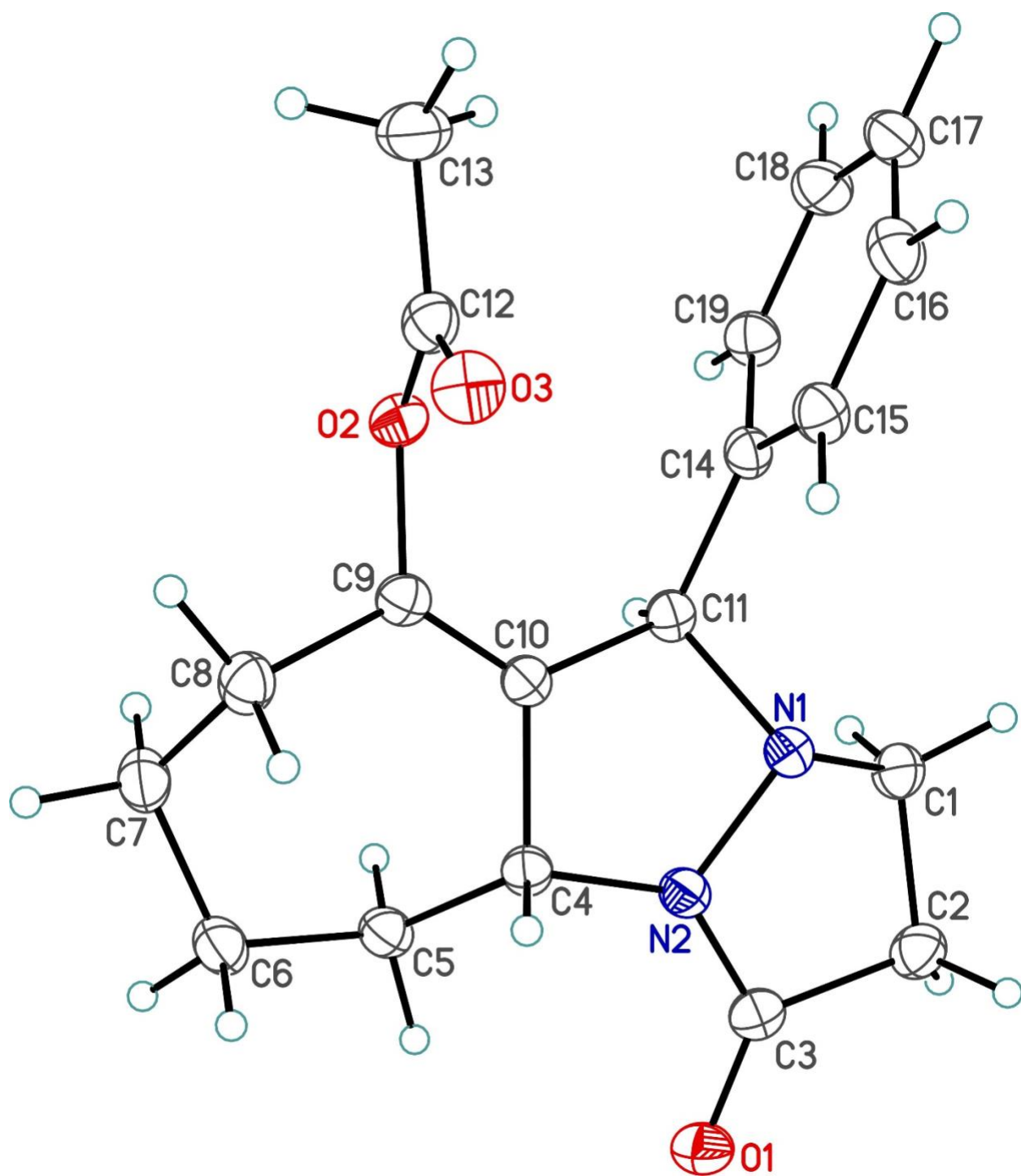
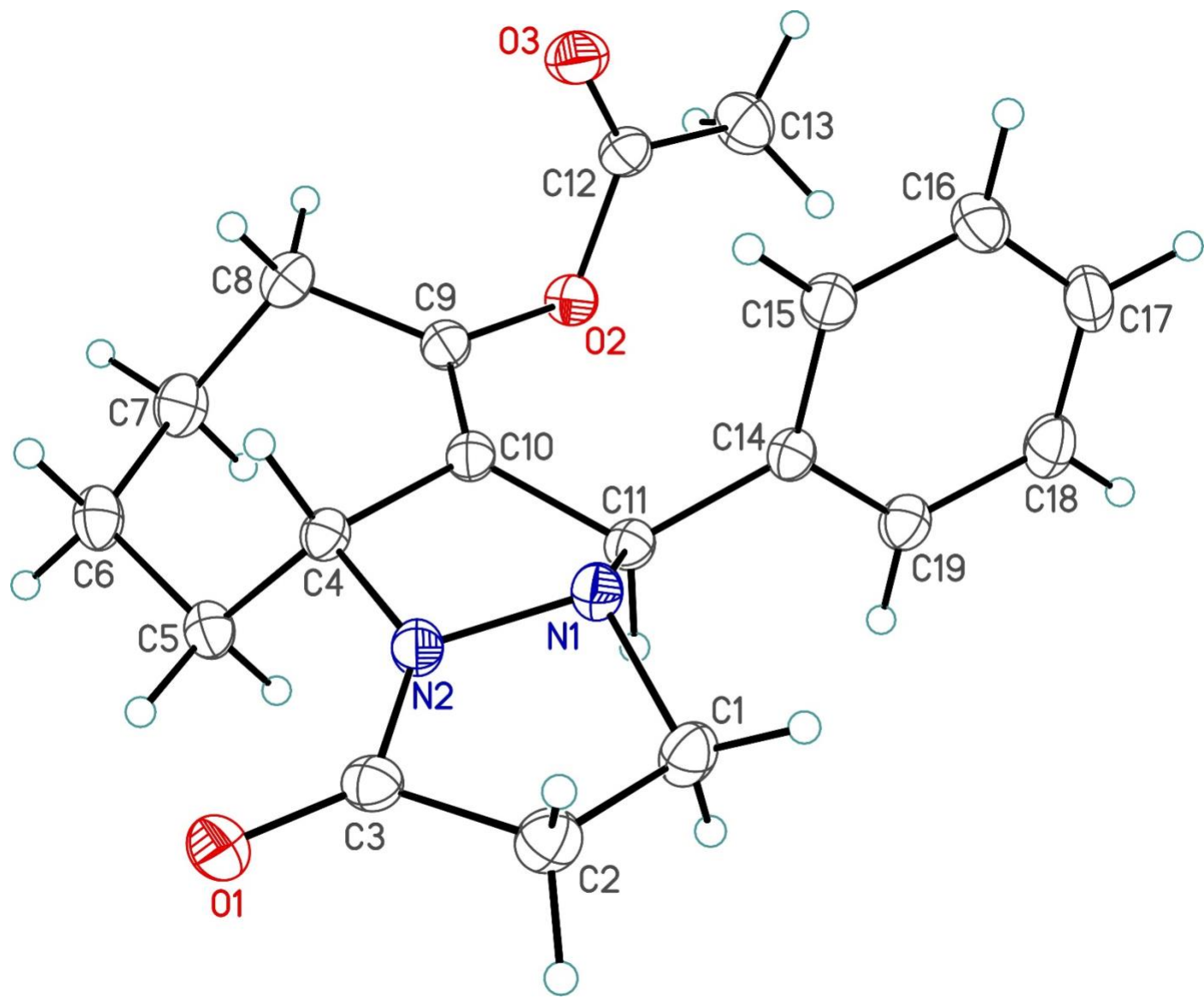


Figure Legends

Figure 1. Perspective view of the 3-oxo-10-phenyl-2,3,4a,5,6,7,8,10-octahydro-1*H*-cyclohepta[*c*]pyrazolo[1,2-*a*]pyrazol-9-yl acetate molecule showing the atom labelling scheme. Non-hydrogen atoms are represented by Gaussian ellipsoids at the 30% probability level. Hydrogen atoms are shown with arbitrarily small thermal parameters.

Figure 2. Alternate view of the molecule.





List of Tables

- Table 1.** Crystallographic Experimental Details
- Table 2.** Atomic Coordinates and Equivalent Isotropic Displacement Parameters
- Table 3.** Selected Interatomic Distances
- Table 4.** Selected Interatomic Angles
- Table 5.** Torsional Angles
- Table 6.** Anisotropic Displacement Parameters
- Table 7.** Derived Atomic Coordinates and Displacement Parameters for Hydrogen Atoms

Table 1. Crystallographic Experimental Details*A. Crystal Data*

formula	C ₁₉ H ₂₂ N ₂ O ₃
formula weight	326.38
crystal dimensions (mm)	0.35 × 0.04 × 0.03
crystal system	monoclinic
space group	<i>P</i> 2 ₁ / <i>c</i> (No. 14)
unit cell parameters ^a	
<i>a</i> (Å)	9.4347(4)
<i>b</i> (Å)	19.5106(7)
<i>c</i> (Å)	9.3179(4)
β (deg)	91.389(3)
<i>V</i> (Å ³)	1714.70(12)
<i>Z</i>	4
ρ _{calcd} (g cm ⁻³)	1.264
μ (mm ⁻¹)	0.695

B. Data Collection and Refinement Conditions

diffractometer	Bruker D8/APEX II CCD ^b
radiation (λ [Å])	Cu Kα (1.54178) (microfocus source)
temperature (°C)	-100
scan type	ω and φ scans (1.0°) (5-10-15 s exposures) ^c
data collection 2θ limit (deg)	144.73
total data collected	11846 (-11 ≤ <i>h</i> ≤ 11, -24 ≤ <i>k</i> ≤ 23, -11 ≤ <i>l</i> ≤ 11)
independent reflections	3393 (<i>R</i> _{int} = 0.0382)
number of observed reflections (<i>NO</i>)	2769 [<i>F</i> _o ² ≥ 2σ(<i>F</i> _o ²)]
structure solution method	intrinsic phasing (<i>SHELXT-2014</i> ^d)
refinement method	full-matrix least-squares on <i>F</i> ² (<i>SHELXL-2016</i> ^e)
absorption correction method	Gaussian integration (face-indexed)
range of transmission factors	1.0000–0.8289
data/restraints/parameters	3393 / 0 / 219
extinction coefficient (<i>x</i>) ^f	0.0013(3)
goodness-of-fit (<i>S</i>) ^g [all data]	1.043
final <i>R</i> indices ^h	
<i>R</i> ₁ [<i>F</i> _o ² ≥ 2σ(<i>F</i> _o ²)]	0.0386
<i>wR</i> ₂ [all data]	0.1028
largest difference peak and hole	0.207 and -0.210 e Å ⁻³

^aObtained from least-squares refinement of 6760 reflections with 9.06° < 2θ < 144.74°.

^bPrograms for diffractometer operation, data collection, data reduction and absorption correction were those supplied by Bruker.

(continued)

Table 1. Crystallographic Experimental Details (continued)

^cData were collected with the detector set at three different positions. Low-angle (detector $2\theta = -33^\circ$) data frames were collected using a scan time of 5 s, medium-angle (detector $2\theta = 75^\circ$) frames using a scan time of 10 s, and high-angle (detector $2\theta = 117^\circ$) frames using a scan time of 15 s.

^dSheldrick, G. M. *Acta Crystallogr.* **2015**, *A71*, 3–8. (*SHELXT-2014*)

^eSheldrick, G. M. *Acta Crystallogr.* **2015**, *C71*, 3–8. (*SHELXL-2016*)

^f $F_c^* = kF_c[1 + x\{0.001F_c^2\lambda^3/\sin(2\theta)\}]^{-1/4}$ where k is the overall scale factor.

^g $S = [\sum w(F_o^2 - F_c^2)^2/(n - p)]^{1/2}$ (n = number of data; p = number of parameters varied; $w = [\sigma^2(F_o^2) + (0.0126P)^2 + 0.4617P]^{-1}$ where $P = [\text{Max}(F_o^2, 0) + 2F_c^2]/3$).

^h $R_1 = \sum ||F_o| - |F_c||/\sum |F_o|$; $wR_2 = [\sum w(F_o^2 - F_c^2)^2/\sum w(F_o^4)]^{1/2}$.

Table 2. Atomic Coordinates and Equivalent Isotropic Displacement Parameters

Atom	<i>x</i>	<i>y</i>	<i>z</i>	$U_{\text{eq}}, \text{\AA}^2$
O1	0.63459(12)	0.17095(6)	0.51840(11)	0.0413(3)*
O2	0.08607(10)	0.33202(5)	0.17770(10)	0.0328(2)*
O3	-0.04966(12)	0.36712(6)	0.35838(12)	0.0435(3)*
N1	0.47278(12)	0.32746(6)	0.42430(12)	0.0306(3)*
N2	0.48131(13)	0.25369(6)	0.43202(12)	0.0314(3)*
C1	0.62361(15)	0.34720(8)	0.41427(17)	0.0382(3)*
C2	0.69636(17)	0.29368(8)	0.51079(17)	0.0396(4)*
C3	0.60515(15)	0.23070(8)	0.48781(14)	0.0330(3)*
C4	0.34460(14)	0.22287(7)	0.39285(14)	0.0286(3)*
C5	0.35980(16)	0.15841(7)	0.30132(14)	0.0338(3)*
C6	0.22193(18)	0.11793(8)	0.28809(16)	0.0398(3)*
C7	0.09760(18)	0.15376(8)	0.21092(17)	0.0416(4)*
C8	0.04403(16)	0.21848(8)	0.28582(16)	0.0370(3)*
C9	0.14031(15)	0.27892(7)	0.26664(13)	0.0297(3)*
C10	0.27347(14)	0.28244(7)	0.31267(13)	0.0277(3)*
C11	0.38406(14)	0.33796(7)	0.29280(13)	0.0286(3)*
C12	-0.01315(15)	0.37331(8)	0.23704(16)	0.0346(3)*
C13	-0.0664(2)	0.42513(9)	0.13127(19)	0.0501(4)*
C14	0.33741(14)	0.41158(7)	0.27841(14)	0.0292(3)*
C15	0.25930(16)	0.44406(8)	0.38363(15)	0.0354(3)*
C16	0.21821(17)	0.51194(8)	0.36600(18)	0.0420(4)*
C17	0.25597(18)	0.54786(8)	0.24465(19)	0.0439(4)*
C18	0.33476(18)	0.51638(8)	0.14056(18)	0.0424(4)*
C19	0.37550(16)	0.44834(8)	0.15748(15)	0.0356(3)*

Anisotropically-refined atoms are marked with an asterisk (*). The form of the anisotropic displacement parameter is: $\exp[-2\pi^2(h^2a^*U_{11} + k^2b^*U_{22} + l^2c^*U_{33} + 2klb^*c^*U_{23} + 2hla^*c^*U_{13} + 2hka^*b^*U_{12})]$.

Table 3. Selected Interatomic Distances (Å)

Atom1	Atom2	Distance	Atom1	Atom2	Distance
O1	C3	1.2303(18)	C6	C7	1.530(2)
O2	C9	1.4146(16)	C7	C8	1.534(2)
O2	C12	1.3624(18)	C8	C9	1.502(2)
O3	C12	1.1961(18)	C9	C10	1.3194(19)
N1	N2	1.4432(16)	C10	C11	1.5184(18)
N1	C1	1.4794(18)	C11	C14	1.5073(18)
N1	C11	1.4813(16)	C12	C13	1.490(2)
N2	C3	1.3443(18)	C14	C15	1.3931(19)
N2	C4	1.4614(17)	C14	C19	1.3903(19)
C1	C2	1.530(2)	C15	C16	1.389(2)
C2	C3	1.513(2)	C16	C17	1.384(2)
C4	C5	1.5282(18)	C17	C18	1.380(2)
C4	C10	1.5280(18)	C18	C19	1.390(2)
C5	C6	1.524(2)			

Table 4. Selected Interatomic Angles (deg)

Atom1	Atom2	Atom3	Angle	Atom1	Atom2	Atom3	Angle
C9	O2	C12	115.95(10)	O2	C9	C10	118.71(12)
N2	N1	C1	102.14(11)	C8	C9	C10	125.17(13)
N2	N1	C11	102.06(10)	C4	C10	C9	121.52(12)
C1	N1	C11	115.91(11)	C4	C10	C11	107.90(11)
N1	N2	C3	113.52(11)	C9	C10	C11	130.47(12)
N1	N2	C4	110.49(10)	N1	C11	C10	100.18(10)
C3	N2	C4	135.46(12)	N1	C11	C14	111.30(11)
N1	C1	C2	101.75(12)	C10	C11	C14	119.38(11)
C1	C2	C3	103.05(12)	O2	C12	O3	122.71(13)
O1	C3	N2	126.52(14)	O2	C12	C13	110.88(13)
O1	C3	C2	127.78(13)	O3	C12	C13	126.40(15)
N2	C3	C2	105.65(12)	C11	C14	C15	121.95(12)
N2	C4	C5	112.57(11)	C11	C14	C19	118.88(12)
N2	C4	C10	100.58(11)	C15	C14	C19	119.16(13)
C5	C4	C10	113.52(11)	C14	C15	C16	120.10(14)
C4	C5	C6	112.34(12)	C15	C16	C17	120.19(15)
C5	C6	C7	116.38(13)	C16	C17	C18	120.15(15)
C6	C7	C8	114.80(12)	C17	C18	C19	119.83(14)
C7	C8	C9	112.66(12)	C14	C19	C18	120.56(14)
O2	C9	C8	115.69(12)				

Table 5. Torsional Angles (deg)

Atom1	Atom2	Atom3	Atom4	Angle	Atom1	Atom2	Atom3	Atom4	Angle
C12	O2	C9	C8	75.91(15)	N2	C4	C10	C11	8.79(13)
C12	O2	C9	C10	-111.21(14)	C5	C4	C10	C9	64.92(17)
C9	O2	C12	O3	2.5(2)	C5	C4	C10	C11	-111.68(12)
C9	O2	C12	C13	-177.58(12)	C4	C5	C6	C7	63.95(17)
C1	N1	N2	C3	26.70(14)	C5	C6	C7	C8	-63.74(18)
C1	N1	N2	C4	-160.32(11)	C6	C7	C8	C9	75.77(17)
C11	N1	N2	C3	146.89(11)	C7	C8	C9	O2	110.24(14)
C11	N1	N2	C4	-40.13(13)	C7	C8	C9	C10	-62.12(18)
N2	N1	C1	C2	-35.78(13)	O2	C9	C10	C4	-172.12(11)
C11	N1	C1	C2	-145.78(12)	O2	C9	C10	C11	3.6(2)
N2	N1	C11	C10	41.87(12)	C8	C9	C10	C4	0.0(2)
N2	N1	C11	C14	169.10(10)	C8	C9	C10	C11	175.77(13)
C1	N1	C11	C10	151.92(12)	C4	C10	C11	N1	-31.74(12)
C1	N1	C11	C14	-80.85(14)	C4	C10	C11	C14	-153.38(11)
N1	N2	C3	O1	172.79(13)	C9	C10	C11	N1	152.07(14)
N1	N2	C3	C2	-4.69(15)	C9	C10	C11	C14	30.4(2)
C4	N2	C3	O1	2.2(3)	N1	C11	C14	C15	-58.47(17)
C4	N2	C3	C2	-175.30(14)	N1	C11	C14	C19	120.52(13)
N1	N2	C4	C5	140.18(11)	C10	C11	C14	C15	57.46(17)
N1	N2	C4	C10	19.03(13)	C10	C11	C14	C19	-123.56(14)
C3	N2	C4	C5	-49.0(2)	C11	C14	C15	C16	-179.88(13)
C3	N2	C4	C10	-170.16(14)	C19	C14	C15	C16	1.1(2)
N1	C1	C2	C3	33.70(15)	C11	C14	C19	C18	-179.85(13)
C1	C2	C3	O1	164.02(14)	C15	C14	C19	C18	-0.8(2)
C1	C2	C3	N2	-18.54(15)	C14	C15	C16	C17	-0.7(2)
N2	C4	C5	C6	167.50(11)	C15	C16	C17	C18	0.0(2)
C10	C4	C5	C6	-79.06(15)	C16	C17	C18	C19	0.4(2)
N2	C4	C10	C9	-174.61(12)	C17	C18	C19	C14	0.1(2)

Table 6. Anisotropic Displacement Parameters (U_{ij} , Å²)

Atom	U_{11}	U_{22}	U_{33}	U_{23}	U_{13}	U_{12}
O1	0.0410(6)	0.0382(6)	0.0445(6)	0.0058(5)	-0.0009(4)	0.0059(5)
O2	0.0337(5)	0.0362(5)	0.0285(4)	0.0027(4)	-0.0001(4)	0.0027(4)
O3	0.0395(6)	0.0488(7)	0.0426(6)	-0.0007(5)	0.0089(5)	0.0017(5)
N1	0.0317(6)	0.0277(6)	0.0324(6)	0.0012(4)	-0.0013(4)	-0.0023(5)
N2	0.0312(6)	0.0276(6)	0.0354(6)	0.0021(5)	-0.0006(4)	-0.0012(5)
C1	0.0326(8)	0.0386(8)	0.0432(8)	0.0043(6)	-0.0041(6)	-0.0075(6)
C2	0.0335(8)	0.0444(9)	0.0406(8)	0.0039(6)	-0.0040(6)	-0.0019(7)
C3	0.0325(7)	0.0377(8)	0.0289(6)	0.0017(5)	0.0034(5)	0.0028(6)
C4	0.0305(7)	0.0291(7)	0.0262(6)	0.0014(5)	0.0020(5)	-0.0017(5)
C5	0.0418(8)	0.0290(7)	0.0308(6)	0.0000(5)	0.0017(5)	0.0008(6)
C6	0.0515(9)	0.0297(7)	0.0382(7)	-0.0018(6)	-0.0002(6)	-0.0051(7)
C7	0.0463(9)	0.0376(8)	0.0407(8)	-0.0040(6)	-0.0038(6)	-0.0093(7)
C8	0.0350(8)	0.0399(8)	0.0360(7)	0.0016(6)	0.0009(6)	-0.0068(6)
C9	0.0334(7)	0.0306(7)	0.0253(6)	0.0009(5)	0.0027(5)	0.0009(6)
C10	0.0320(7)	0.0273(6)	0.0239(6)	-0.0007(5)	0.0032(5)	-0.0009(5)
C11	0.0308(7)	0.0300(7)	0.0252(6)	-0.0005(5)	0.0029(5)	-0.0020(5)
C12	0.0278(7)	0.0365(8)	0.0395(7)	-0.0012(6)	0.0006(5)	-0.0020(6)
C13	0.0492(10)	0.0460(9)	0.0547(10)	0.0081(8)	-0.0046(8)	0.0094(8)
C14	0.0299(7)	0.0280(7)	0.0296(6)	-0.0006(5)	0.0000(5)	-0.0035(5)
C15	0.0391(8)	0.0342(7)	0.0331(7)	-0.0019(5)	0.0041(6)	-0.0030(6)
C16	0.0420(9)	0.0350(8)	0.0492(8)	-0.0099(6)	0.0027(7)	0.0005(7)
C17	0.0447(9)	0.0272(7)	0.0596(10)	0.0013(7)	-0.0046(7)	-0.0009(6)
C18	0.0451(9)	0.0363(8)	0.0458(8)	0.0107(6)	-0.0001(7)	-0.0057(7)
C19	0.0383(8)	0.0353(7)	0.0333(7)	0.0032(6)	0.0037(6)	-0.0034(6)

The form of the anisotropic displacement parameter is:

$$\exp[-2\pi^2(h^2a^2U_{11} + k^2b^2U_{22} + l^2c^2U_{33} + 2klb^*c^*U_{23} + 2hla^*c^*U_{13} + 2hka^*b^*U_{12})]$$

Table 7. Derived Atomic Coordinates and Displacement Parameters for Hydrogen Atoms

Atom	<i>x</i>	<i>y</i>	<i>z</i>	$U_{\text{eq}}, \text{\AA}^2$
H1A	0.640335	0.394237	0.450781	0.046
H1B	0.656290	0.344056	0.314325	0.046
H2A	0.794931	0.285264	0.481246	0.048
H2B	0.697328	0.308252	0.612585	0.048
H4	0.291170	0.211957	0.481379	0.034
H5A	0.390266	0.171687	0.204272	0.041
H5B	0.434448	0.128789	0.344760	0.041
H6A	0.192141	0.105595	0.385911	0.048
H6B	0.241493	0.074660	0.236732	0.048
H7A	0.018052	0.120867	0.201050	0.050
H7B	0.126803	0.166267	0.113010	0.050
H8A	-0.051567	0.229973	0.246791	0.044
H8B	0.035468	0.209016	0.389637	0.044
H11	0.441601	0.325894	0.207685	0.034
H13A	0.014222	0.447978	0.087210	0.060
H13B	-0.124158	0.459178	0.180388	0.060
H13C	-0.124118	0.402292	0.056656	0.060
H15	0.234108	0.419728	0.467559	0.042
H16	0.164035	0.533786	0.437436	0.050
H17	0.227591	0.594289	0.232977	0.053
H18	0.361066	0.541154	0.057570	0.051
H19	0.429840	0.426771	0.085809	0.043

**Appendix V: X-ray Crystallographic Data for Compound
38a (Chapter 2)**

STRUCTURE REPORT

XCL Code: FGW1811

Date: 7 December 2018

Compound: 10-phenylhexahydro-1H-cyclohepta[c]pyrazolo[1,2-*a*]pyrazole-3,9(2H,4*a*H)-dione

Formula: C₁₇H₂₀N₂O₂

Supervisor: F. G. West

Crystallographer: M. J. Ferguson

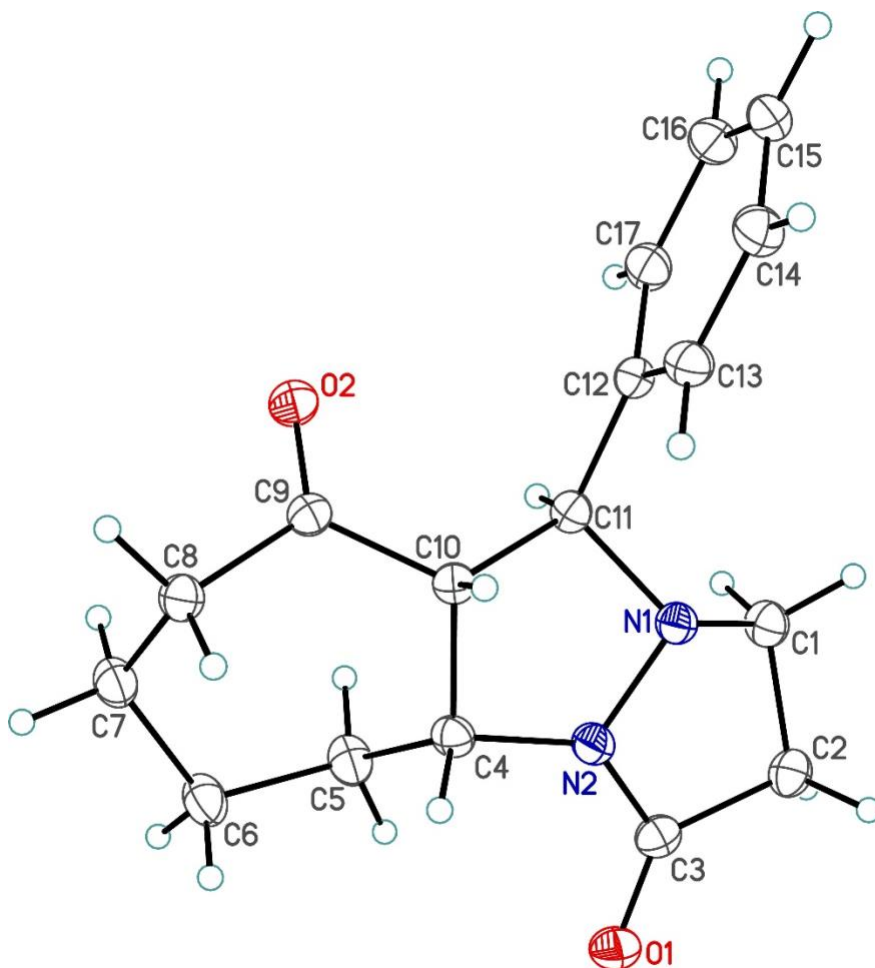
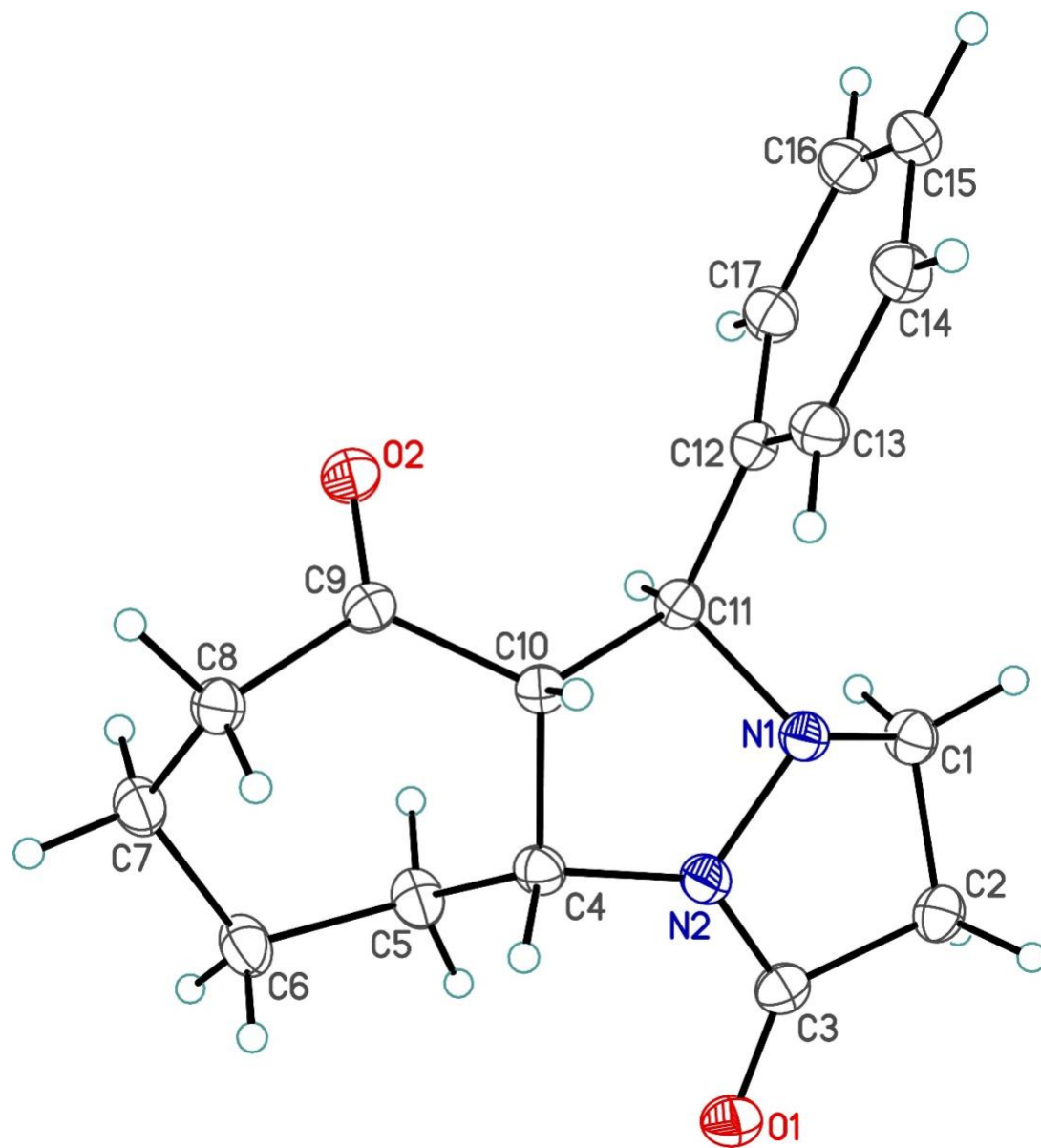
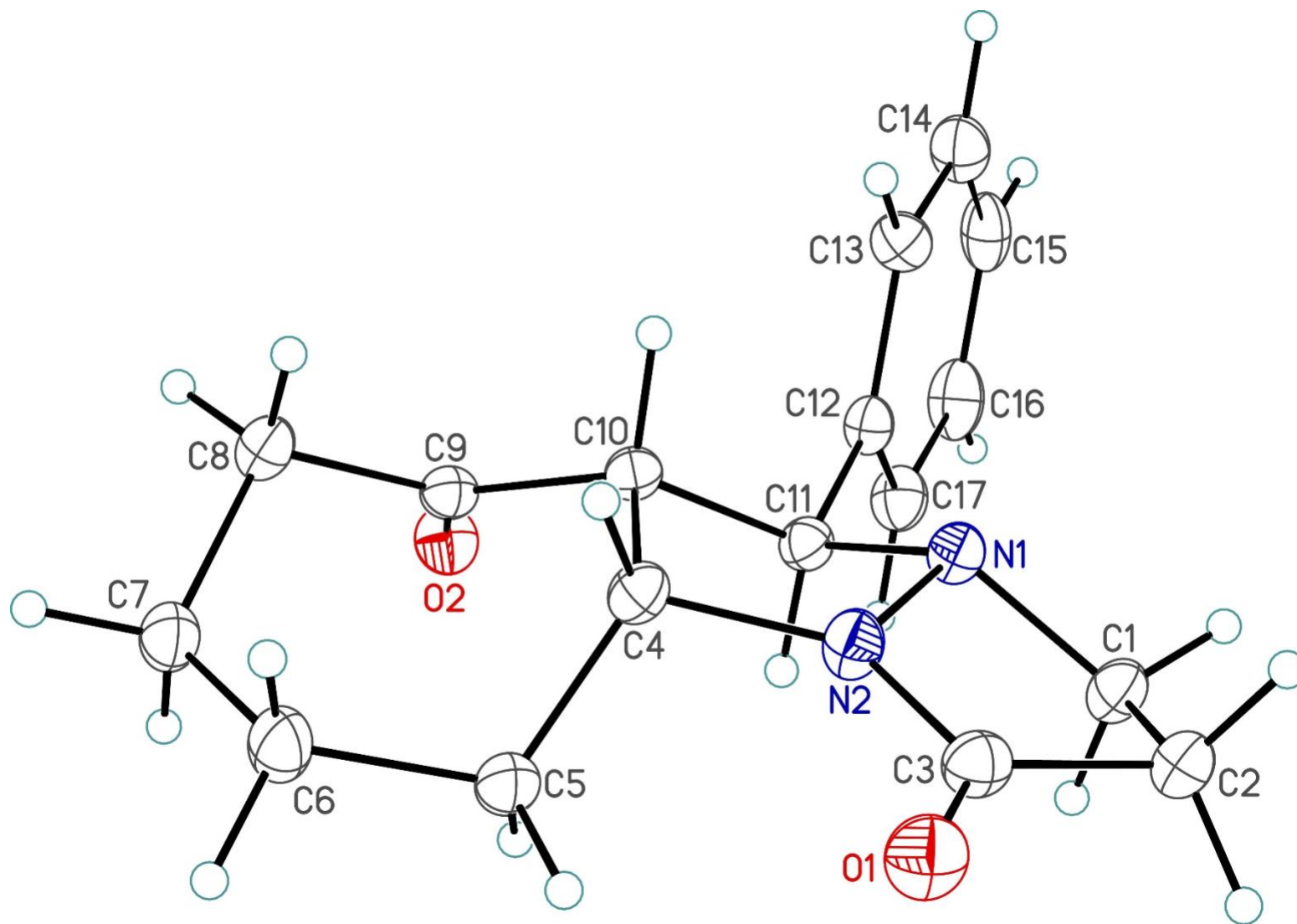


Figure Legends

Figure 1. Perspective view of the 10-phenylhexahydro-1H-cyclohepta[*c*]pyrazolo[1,2-*a*]pyrazole-3,9(2H,4*a*H)-dione molecule showing the atom labelling scheme. Non-hydrogen atoms are represented by Gaussian ellipsoids at the 30% probability level. Hydrogen atoms are shown with arbitrarily small thermal parameters.

Figure 2. Alternate view of the molecule.





List of Tables

- Table 1.** Crystallographic Experimental Details
- Table 2.** Atomic Coordinates and Equivalent Isotropic Displacement Parameters
- Table 3.** Selected Interatomic Distances
- Table 4.** Selected Interatomic Angles
- Table 5.** Torsional Angles
- Table 6.** Anisotropic Displacement Parameters
- Table 7.** Derived Atomic Coordinates and Displacement Parameters for Hydrogen Atoms

Table 1. Crystallographic Experimental Details*A. Crystal Data*

formula	C ₁₇ H ₂₀ N ₂ O ₂
formula weight	284.35
crystal dimensions (mm)	0.18 × 0.07 × 0.05
crystal system	monoclinic
space group	<i>C2/c</i> (No. 15)
unit cell parameters ^a	
<i>a</i> (Å)	21.9967(8)
<i>b</i> (Å)	5.3193(2)
<i>c</i> (Å)	25.8361(9)
β (deg)	103.876(3)
<i>V</i> (Å ³)	2934.79(19)
<i>Z</i>	8
ρ _{calcd} (g cm ⁻³)	1.287
μ (mm ⁻¹)	0.680

B. Data Collection and Refinement Conditions

diffractometer	Bruker D8/APEX II CCD ^b
radiation (λ [Å])	Cu Kα (1.54178) (microfocus source)
temperature (°C)	-100
scan type	ω and φ scans (1.0°) (5 s exposures)
data collection 2θ limit (deg)	148.31
total data collected	7384 (-27 ≤ <i>h</i> ≤ 27, -6 ≤ <i>k</i> ≤ 6, -32 ≤ <i>l</i> ≤ 32)
independent reflections	2943 (<i>R</i> _{int} = 0.0389)
number of observed reflections (<i>NO</i>)	2224 [<i>F</i> _o ² ≥ 2σ(<i>F</i> _o ²)]
structure solution method	intrinsic phasing (<i>SHELXT-2014</i> ^c)
refinement method	full-matrix least-squares on <i>F</i> ² (<i>SHELXL-2017</i> ^d)
absorption correction method	Gaussian integration (face-indexed)
range of transmission factors	0.9493–0.8022
data/restraints/parameters	2943 / 0 / 190
goodness-of-fit (<i>S</i>) ^e [all data]	1.063
final <i>R</i> indices ^f	
<i>R</i> ₁ [<i>F</i> _o ² ≥ 2σ(<i>F</i> _o ²)]	0.0442
<i>wR</i> ₂ [all data]	0.1210
largest difference peak and hole	0.157 and -0.244 e Å ⁻³

^aObtained from least-squares refinement of 2233 reflections with 8.28° < 2θ < 145.98°.

^bPrograms for diffractometer operation, data collection, data reduction and absorption correction were those supplied by Bruker.

(continued)

Table 1. Crystallographic Experimental Details (continued)

^cSheldrick, G. M. *Acta Crystallogr.* **2015**, *A71*, 3–8. (*SHELXT-2014*)

^dSheldrick, G. M. *Acta Crystallogr.* **2015**, *C71*, 3–8. (*SHELXL-2017*)

$eS = [\Sigma w(F_o^2 - F_c^2)^2 / (n - p)]^{1/2}$ (n = number of data; p = number of parameters varied; $w = [\sigma^2(F_o^2) + (0.0586P)^2 + 0.1196P]^{-1}$ where $P = [\text{Max}(F_o^2, 0) + 2F_c^2]/3$).

$fR_1 = \Sigma ||F_o| - |F_c|| / \Sigma |F_o|$; $wR_2 = [\Sigma w(F_o^2 - F_c^2)^2 / \Sigma w(F_o^4)]^{1/2}$.

Table 2. Atomic Coordinates and Equivalent Isotropic Displacement Parameters

Atom	<i>x</i>	<i>y</i>	<i>z</i>	$U_{eq}, \text{\AA}^2$
O1	0.75445(6)	-0.0699(2)	0.69588(5)	0.0427(3)*
O2	0.54925(6)	0.6475(2)	0.55317(5)	0.0384(3)*
N1	0.59460(6)	0.0780(3)	0.67110(5)	0.0289(3)*
N2	0.65504(6)	0.0675(3)	0.65860(5)	0.0324(3)*
C1	0.61215(8)	0.1084(3)	0.72955(6)	0.0345(4)*
C2	0.67116(8)	-0.0529(3)	0.74553(6)	0.0351(4)*
C3	0.70057(8)	-0.0212(3)	0.69864(7)	0.0333(4)*
C4	0.65338(7)	0.1537(3)	0.60480(6)	0.0289(4)*
C5	0.70272(8)	0.3562(4)	0.60543(7)	0.0370(4)*
C6	0.71788(9)	0.3941(4)	0.55096(7)	0.0423(5)*
C7	0.66815(8)	0.5296(4)	0.50883(7)	0.0371(4)*
C8	0.60254(8)	0.4141(3)	0.49881(6)	0.0330(4)*
C9	0.57540(7)	0.4533(3)	0.54681(6)	0.0281(3)*
C10	0.58375(7)	0.2404(3)	0.58638(6)	0.0260(3)*
C11	0.56465(7)	0.2933(3)	0.63880(6)	0.0271(3)*
C12	0.49576(7)	0.2970(3)	0.63649(6)	0.0283(3)*
C13	0.45686(8)	0.1011(3)	0.61265(7)	0.0339(4)*
C14	0.39393(8)	0.1013(4)	0.61254(7)	0.0416(4)*
C15	0.36864(9)	0.2952(4)	0.63626(7)	0.0445(5)*
C16	0.40663(10)	0.4896(4)	0.65988(8)	0.0464(5)*
C17	0.47008(9)	0.4907(3)	0.66013(7)	0.0375(4)*

Anisotropically-refined atoms are marked with an asterisk (*). The form of the anisotropic displacement parameter is: $\exp[-2\pi^2(h^2a^*{}^2U_{11} + k^2b^*{}^2U_{22} + l^2c^*{}^2U_{33} + 2klb^*c^*U_{23} + 2hla^*c^*U_{13} + 2hka^*b^*U_{12})]$.

Table 3. Selected Interatomic Distances (Å)

Atom1	Atom2	Distance	Atom1	Atom2	Distance
O1	C3	1.2317(19)	C6	C7	1.526(2)
O2	C9	1.2127(18)	C7	C8	1.532(2)
N1	N2	1.4425(17)	C8	C9	1.514(2)
N1	C1	1.4750(19)	C9	C10	1.507(2)
N1	C11	1.4758(19)	C10	C11	1.5371(19)
N2	C3	1.341(2)	C11	C12	1.502(2)
N2	C4	1.4557(19)	C12	C13	1.395(2)
C1	C2	1.528(2)	C12	C17	1.385(2)
C2	C3	1.513(2)	C13	C14	1.384(2)
C4	C5	1.526(2)	C14	C15	1.383(3)
C4	C10	1.561(2)	C15	C16	1.377(3)
C5	C6	1.535(2)	C16	C17	1.394(3)

Table 4. Selected Interatomic Angles (deg)

Atom1	Atom2	Atom3	Angle	Atom1	Atom2	Atom3	Angle
N2	N1	C1	101.81(12)	O2	C9	C8	121.40(15)
N2	N1	C11	102.35(12)	O2	C9	C10	122.20(14)
C1	N1	C11	117.74(13)	C8	C9	C10	116.38(13)
N1	N2	C3	113.49(13)	C4	C10	C9	112.33(12)
N1	N2	C4	112.84(12)	C4	C10	C11	103.95(12)
C3	N2	C4	133.66(14)	C9	C10	C11	116.46(13)
N1	C1	C2	102.24(13)	N1	C11	C10	100.19(12)
C1	C2	C3	102.69(13)	N1	C11	C12	110.00(12)
O1	C3	N2	125.45(16)	C10	C11	C12	116.97(12)
O1	C3	C2	128.68(15)	C11	C12	C13	120.93(14)
N2	C3	C2	105.85(14)	C11	C12	C17	120.42(16)
N2	C4	C5	110.92(13)	C13	C12	C17	118.59(16)
N2	C4	C10	100.50(12)	C12	C13	C14	120.52(17)
C5	C4	C10	115.98(14)	C13	C14	C15	120.57(19)
C4	C5	C6	113.13(14)	C14	C15	C16	119.38(17)
C5	C6	C7	116.07(15)	C15	C16	C17	120.39(18)
C6	C7	C8	114.59(15)	C12	C17	C16	120.55(19)
C7	C8	C9	110.29(13)				

Table 5. Torsional Angles (deg)

Atom1	Atom2	Atom3	Atom4	Angle	Atom1	Atom2	Atom3	Atom4	Angle
C1	N1	N2	C3	27.50(18)	C5	C4	C10	C11	-96.56(15)
C1	N1	N2	C4	-153.03(13)	C4	C5	C6	C7	73.6(2)
C11	N1	N2	C3	149.68(14)	C5	C6	C7	C8	-53.7(2)
C11	N1	N2	C4	-30.85(16)	C6	C7	C8	C9	68.87(19)
N2	N1	C1	C2	-36.05(16)	C7	C8	C9	O2	83.78(19)
C11	N1	C1	C2	-146.95(14)	C7	C8	C9	C10	-95.17(17)
N2	N1	C11	C10	42.96(14)	O2	C9	C10	C4	-126.98(16)
N2	N1	C11	C12	166.73(12)	O2	C9	C10	C11	-7.3(2)
C1	N1	C11	C10	153.56(13)	C8	C9	C10	C4	51.95(18)
C1	N1	C11	C12	-82.67(17)	C8	C9	C10	C11	171.67(13)
N1	N2	C3	O1	172.76(16)	C4	C10	C11	N1	-41.37(14)
N1	N2	C3	C2	-5.82(19)	C4	C10	C11	C12	-160.15(13)
C4	N2	C3	O1	-6.6(3)	C9	C10	C11	N1	-165.50(13)
C4	N2	C3	C2	174.85(17)	C9	C10	C11	C12	75.72(18)
N1	N2	C4	C5	127.39(15)	N1	C11	C12	C13	-63.28(18)
N1	N2	C4	C10	4.17(17)	N1	C11	C12	C17	113.92(16)
C3	N2	C4	C5	-53.3(2)	C10	C11	C12	C13	50.1(2)
C3	N2	C4	C10	-176.49(18)	C10	C11	C12	C17	-132.72(16)
N1	C1	C2	C3	33.32(17)	C11	C12	C13	C14	177.47(15)
C1	C2	C3	O1	163.94(18)	C17	C12	C13	C14	0.2(2)
C1	C2	C3	N2	-17.54(18)	C11	C12	C17	C16	-177.45(15)
N2	C4	C5	C6	161.58(14)	C13	C12	C17	C16	-0.2(2)
C10	C4	C5	C6	-84.63(18)	C12	C13	C14	C15	-0.3(3)
N2	C4	C10	C9	149.82(13)	C13	C14	C15	C16	0.3(3)
N2	C4	C10	C11	23.06(15)	C14	C15	C16	C17	-0.3(3)
C5	C4	C10	C9	30.20(18)	C15	C16	C17	C12	0.2(3)

Table 6. Anisotropic Displacement Parameters (U_{ij} , Å²)

Atom	U_{11}	U_{22}	U_{33}	U_{23}	U_{13}	U_{12}
O1	0.0319(7)	0.0493(8)	0.0458(7)	0.0056(6)	0.0071(6)	0.0089(6)
O2	0.0432(7)	0.0309(7)	0.0431(7)	0.0015(5)	0.0144(6)	0.0062(5)
N1	0.0282(7)	0.0323(7)	0.0264(6)	0.0011(5)	0.0068(6)	0.0020(6)
N2	0.0284(7)	0.0402(8)	0.0294(7)	0.0043(6)	0.0083(6)	0.0043(6)
C1	0.0366(10)	0.0409(10)	0.0255(8)	-0.0011(7)	0.0067(7)	0.0006(7)
C2	0.0371(9)	0.0378(10)	0.0280(8)	0.0028(7)	0.0030(7)	-0.0009(8)
C3	0.0313(9)	0.0326(9)	0.0341(9)	0.0006(7)	0.0041(7)	0.0018(7)
C4	0.0297(8)	0.0325(9)	0.0249(7)	-0.0027(6)	0.0072(6)	0.0024(6)
C5	0.0294(9)	0.0504(11)	0.0298(8)	0.0009(8)	0.0042(7)	-0.0065(8)
C6	0.0303(9)	0.0633(13)	0.0343(9)	0.0069(9)	0.0096(8)	-0.0024(8)
C7	0.0360(10)	0.0456(11)	0.0314(8)	0.0014(7)	0.0114(7)	-0.0014(8)
C8	0.0338(9)	0.0391(10)	0.0257(8)	0.0005(7)	0.0063(7)	0.0029(7)
C9	0.0264(8)	0.0283(8)	0.0284(8)	-0.0007(6)	0.0040(6)	-0.0007(6)
C10	0.0266(8)	0.0250(8)	0.0261(7)	-0.0021(6)	0.0057(6)	-0.0002(6)
C11	0.0293(8)	0.0267(8)	0.0252(7)	-0.0011(6)	0.0061(6)	-0.0001(6)
C12	0.0286(8)	0.0308(8)	0.0259(7)	0.0044(6)	0.0076(6)	0.0036(6)
C13	0.0286(9)	0.0353(9)	0.0375(8)	0.0010(7)	0.0077(7)	0.0012(7)
C14	0.0305(9)	0.0522(12)	0.0419(10)	0.0089(9)	0.0080(8)	-0.0004(8)
C15	0.0335(10)	0.0621(13)	0.0424(10)	0.0201(9)	0.0180(8)	0.0109(9)
C16	0.0507(12)	0.0524(12)	0.0443(10)	0.0088(9)	0.0275(10)	0.0185(10)
C17	0.0442(11)	0.0365(10)	0.0351(8)	-0.0007(7)	0.0163(8)	0.0050(8)

The form of the anisotropic displacement parameter is:

$$\exp[-2\pi^2(h^2a^2U_{11} + k^2b^2U_{22} + l^2c^2U_{33} + 2klb*c*U_{23} + 2hla*c*U_{13} + 2hka*b*U_{12})]$$

Table 7. Derived Atomic Coordinates and Displacement Parameters for Hydrogen Atoms

Atom	<i>x</i>	<i>y</i>	<i>z</i>	$U_{eq}, \text{\AA}^2$
H1A	0.578791	0.045596	0.745995	0.041
H1B	0.621089	0.286425	0.739737	0.041
H2A	0.699318	0.009047	0.778920	0.042
H2B	0.660625	-0.231086	0.750222	0.042
H4	0.660820	0.008567	0.582497	0.035
H5A	0.741597	0.309579	0.631911	0.044
H5B	0.687631	0.517207	0.616974	0.044
H6A	0.757458	0.490149	0.556444	0.051
H6B	0.725311	0.226976	0.536759	0.051
H7A	0.681511	0.530163	0.474871	0.045
H7B	0.665872	0.706670	0.520005	0.045
H8A	0.574920	0.493411	0.467078	0.040
H8B	0.604850	0.231975	0.491657	0.040
H10	0.558478	0.094521	0.568599	0.031
H11	0.584335	0.453627	0.654810	0.033
H13	0.473703	-0.033569	0.596359	0.041
H14	0.367880	-0.032823	0.596023	0.050
H15	0.325447	0.294196	0.636253	0.053
H16	0.389502	0.623696	0.676111	0.056
H17	0.495915	0.625459	0.676655	0.045